Strategies for Neuroprotection and Intraocular Pressure Modulation in Experimental Models of Glaucoma

by

Elizabeth Anne Cairns

Submitted in partial fulfilment of the requirements
for the degree of Doctor of Philosophy

at

Dalhousie University
Halifax, Nova Scotia
December 2017

This thesis is dedicated in the memory of three people of whom were perhaps my biggest supporters in pursuing a PhD, and of whom would have been so excited to read the final product

Prof. Owen C. Sharkey (1922 – 2014)

Dr. Thompson T. Wright (1919 – 2016)

Marlene A. Cairns (1958 – 2017)

TABLE OF CONTENTS

LIST OF TABLES

LIST OF FIGURES

ABSTRACT

Glaucoma is a blinding eye disease caused by death of retinal ganglion cells (RGCs). Intraocular pressure (IOP) is the only modifiable risk factor, and is the target of all current glaucoma therapeutics. However, IOP modification does not always successfully prevent further RGC loss. Therefore, therapies directly targeting RGC death may be additionally beneficial. The inflammatory cytokine tumor necrosis factor α (TNFα) is upregulated in glaucoma; however, how TNFα contributes to RGC death remains unclear. Recently, TNFα was suggested to promote calcium-permeable AMPA receptor (cpAMPAR) expression in experimental glaucoma, and was associated with excitotoxic RGC death. Furthermore, aside from IOP-lowering effects, cannabinoid receptor 1 (CB_1) modulation is suggested to be neuroprotective in experimental glaucoma, likely through multiple mechanisms of action. In other neurons, CB_1 modulation can inhibit TNFα-mediated increases in cpAMPAR expression; therefore, CB_1-mediated neuroprotection in experimental glaucoma could include manipulation of this pathway. However, there are several disadvantages of direct CB_1 orthosteric modulators, which may limit usefulness as clinically-relevant therapeutics. Recently, a new class of CB_1 modulators have been developed, CB_1 positive allosteric modulators (PAMs), which have the potential to modulate CB_1, while limiting some disadvantages. Therefore, the aims of my thesis were to investigate TNFα-induced changes in cpAMPAR expression and modulation of this mechanism by CB_1, and to investigate the ability of CB_1 PAMs to decrease IOP and provide RGC neuroprotection in experimental glaucoma. IOP was assessed using rebound tonometry, and RGC density by Brn3a immunohistochemistry. Functional expression of cpAMPARs was evaluated through calcium imaging in *ex vivo* isolated retina. The data presented here demonstrate that: (1) TNFα incubation increases AMPA-induced changes in calcium dynamics, consistent with an increase in cpAMPARs observed in at least one model of experimental glaucoma; (2) CB_1 PAMs can reduce IOP acutely; (3) chronic administration was not neuroprotective in two models of experimental glaucoma. Taken together, my work demonstrates that while TNFα-induced increases in cpAMPAR expression may contribute to RGC death, and CB_1 modulation may be a therapeutic target in modifying this pathway, the CB_1 PAMs explored here were insufficient in preventing RGC death when administered in experimental glaucoma.

LIST OF ABBREVIATIONS USED

2-AG	2-arachydonyl glycerol
ABHD	α/β-hydrolase domain
ACEA	Arachidonyl-2-chloroethylamide
ADAR2	Adenosine deaminases acting on RNA 2
AEA	*N*-arachidonoyl ethanolamine; anandamide
Akt	Protein kinase B
ANOVA	Analysis of variance
AM251	*N*-(Piperidin-1-yl)-5-(4-iodophenyl)-1-(2,4-dichlorophenyl)-4-methyl-1*H*-pyrazole-3-carboxamide
AM630	6-Iodo-2-methyl-1-[2-(4-morpholinyl)ethyl]-1*H*-indol-3-yl](4-methoxyphenyl)methanone
AMPA	α-amino-3-hydroxyl-5-methy-4-isoxazolepropronate
ATP	Adenosine triphosphate
Brn3a	Brain-specific homeobox/POU domain protein 3a
cAMP	Cyclic adenosine monophosphate
CB	Ciliary body
CB_1	Cannabinoid receptor 1
CB_2	Cannabinoid receptor 2
CBD	Cannabidiol
CNS	Central nervous system
COX-2	Cyclooxygenase 2
CP55,940	(-)-*cis*-3-[2-Hydroxy-4-(1,1-dimethylheptyl)phenyl]-*trans*-4-(3-hydroxypropyl)cyclohexanol
cpAMPAR	Calcium-permeable AMPA receptor
DAG	Diacyl glycerol
DAGL	DAG lipase
DMSO	Dimethyl sulfoxide
DNA	Deoxyribonucleic acid
ECS	Endocannabinoid system
ERK	Extracellular signal-related kinase
FAAH	Fatty acid amide hydrolase

FHTS	Frank-Ter Haar syndrome
GAT211	3-(2-Nitro-1-phenylethyl)-2-phenyl-1*H*-indole
GAT228	(R)-3-(2-Nitro-1-phenylethyl)-2-phenyl-1*H*-indole
GAT229	(S)-3-(2-Nitro-1-phenylethyl)-2-phenyl-1*H*-indole
GCL	Ganglion cell layer
GPR18	G protein-coupled receptor 18
GPR55	G protein-coupled receptor 55
GPR119	G protein-coupled receptor 119
HBSS	Hank's balanced salt solution
HEPES	4-(2-hydroxyethyl)-1-piperazineethanesulfonic acid
HU210	(6a*R*)-*trans*-3-(1,1-Dimethylheptyl)-6a,7,10,10a-tetrahydro-1-hydroxy-6,6-dimethyl-6*H*-dibenzo[*b*,*d*]pyran-9-methanol
HU308	4-[4-(1,1-Dimethylheptyl)-2,6-dimethoxyphenyl]-6,6-dimethylbicyclo[3.1.1]hept-2-ene-2-methanol
IEM1460	*N*,*N*,*H*,-Trimethyl-5-[(tricyclo[3.3.1.13,7]dec-1-ylmethyl)amino]-1-pentanaminiumbromide hydrobromide
iGluR	Ionotropic glutamate receptor
IL	Interleukin
INL	Inner nuclear layer
i.p.	Intraperitoneal
IPL	Inner plexiform layer
IOP	Intraocular pressure
JZL184	4-[*Bis*(1,3-benzodioxol-5-yl)hydroxymethyl]-1-piperidinecarboxylic acid 4-nitrophenyl ester
KML29	4-[*Bis*(1,3-benzodioxol-5-yl)hydroxymethyl]-1-piperidinecarboxylic acid 2,2,2-trifluoro-1-(trifluoromethyl)ethyl ester
KO	Knockout
LPS	Lipopolysaccharide
LY2183240	5-[(1,1'-Biphenyl]-4-yl)methyl]-*N*,*N*-dimethyl-1*H*-tetrazole-1-carboxamide
MAGL	Monoacylglycerol lipase
metAEA	Methanandamide
mGluR	Metabotropic glutamate receptor

MK801	(5*S*,10*R*)-(+)-5-Methyl-10,11-dihydro-5*H*-dibenzo[*a*,*d*]cyclohepten-5,10-imine maleate
mRNA	Messenger ribonucleic acid
NAAA	N-acylethanolamine-hydrolyzing acid amidase
NADA	N-arachidonoyl dopamine
NAGly	N-arachidoyl glycine
NAPE	*N*-acyl phosphatidylethanolamine
NAPE-PLD	NAPE-specific phospholipase D
NMDA	*N*-methyl-D-aspartate
NFL	Nerve fibre layer
OEA	Oleylethanolamide
OHT	Ocular hypertension
ONH	Optic nerve head
ONL	Outer nuclear layer
ONT	Optic nerve transection
OPL	Outer plexiform layer
ORG27569	5-Chloro-3-ethyl-*N*-[2-[4-(1-piperidinyl)phenyl]ethyl-1*H*-indole-2-carboxamide
PAM	Positive allosteric modulator
PBS	Phosphate buffered saline
PEA	Palmitoylethanolamide
PI3K	Phosphoinositide 3-kinase
PSNCBAM-1	*N*-(4-Chlorophenyl)-*N*'-[3-[6-(1-pyrrolidinyl)-2-pyridinyl]phenyl]urea
PPARα	Peroxisome proliferator activated receptor α
POAG	Primary open-angle glaucoma
RGC	Retinal ganglion cell
ROS	Reactive oxygen species
SC	Schlemm's canal
SR141716A	Rimonabant; *N*-(Piperidin-1-yl)-5-(4-chlorophenyl)-1-(2,4-dichlorophenyl)-4-methyl-1*H*-pyrazole-3-carboxamide hydrochloride
SR144528	5-(4-Chloro-3-methylphenyl)-1-[(4-methylphenyl)methyl]-*N*-[(1*S*,2*S*,4*R*)-1,3,3-trimethylbicyclo[2.2.1]hept-2-yl]-1*H*-pyrazole-3-carboxamide

THC	Tetrahydrocannabinol
TM	Trabecular meshwork
TNFα	Tumor necrosis factor α
TNFR	TNFα receptor
TRPV1	Transient vanilloid receptor 1
URB597	Cyclohexylcarbamic acid 3'-(Aminocarbonyl)-[1,1'-biphenyl]-3-yl ester
WIN	WIN55,212-2; (*R*)-(+)-[2,3-Dihydro-5-methyl-3-(4-morpholinylmethyl)pyrrolo[1,2,3-*de*]-1,4-benzoxazin-6-yl]-1-naphthalenylmethanone mesylate
WT	Wildtype
ZCZ011	6-Methyl-3-(2-nitro-1-(thiophen-2-yl)ethyl)-2-phenyl-1*H*-indole)

ACKNOWLEDGMENTS

This thesis would not have been possible without the help of so many.

Huge thanks go to:

Retina Lab & Co.: Spring, for always having the answer, or at least knowing where to find it. Michele, for teaching me just some of your many skills. Janette, for helping to take care of the colony. Bryan, for inspiring me from so early on, being very patient, teaching me the ways of the calcium rig, and still giving me advice in my final year. Ross, for walking through a snow storm to give my mice drugs so that my experiment wouldn't go to waste. Anna, for accepting me as one of your lab children, and for your endless support in so many different ways. Tom, Jordan, Ben, and Andrea for lending an ear and being in it with me. Steve, for the late night and weekend lab chats that gave me clarity and kept me going. Bill, for always coming to my rescue. To Mel, for believing in me, putting up with me, and teaching me your ways of getting things done; sometimes it can get a little scary of how much I've picked up from you.

Mallory, Jenn, Jen, Fiona, Chris, Mitch, Colin, Leo, Thor, Sarah, Stephanie, Owen, and Crystal, this journey has been filled with so many ups and downs. You were always the shoulder, the escape, or the breath of fresh air I so desperately needed to keep me standing. You all mean so much to me.

The Marsh and Cogdon families, particularly Sue and Mike, thank you for taking me in with open arms, feeding me, comforting me, and continuing to inspire me as to just how much one can accomplish.

To my dad, with your boundless enthusiasm about learning and sharing that knowledge with others, thank you for getting me excited about exploring and asking questions from such an early age, it's the reason why I do what I do today.

Chapter 1: INTRODUCTION

1.1 THE EYE

The eye is an organ responsible for the generation of vision. Proper vision requires a number of ocular tissues working in tandem, and without proper functioning of any one of these tissues, deficits can occur. Changes in vision can result in profound implications in the ability to carry out every day tasks, and lead to major detriments in quality of life (Vu, Keeffe, McCarty, & Taylor, 2005).

The transmission of a visual stimulus begins with light entering the eye. Light passes through the cornea, which is focused by the lens onto the retina, at the back of the eye. Cells of the retina convert this light stimulus to an electrochemical signal, which then passed to the brain for higher processing (**Fig. 1.1;** Kolb, 2003).

The retina is a multi-layered tissue comprising of three neuronal layers and two plexiform layers (**Fig. 1.2**). The first neuronal layer, the outer nuclear layer (ONL), is comprised of the rod and cone photoreceptors, which synapse within the outer plexiform layer (OPL) onto the horizontal and bipolar cells. The soma of these two cells, along with the soma of some amacrine cells, are contained within the inner nuclear layer (INL). Bipolar cells project onto dendrites of amacrine cells and retinal ganglion cells (RGCs) within the inner plexiform layer (IPL). The innermost layer of the retina is the ganglion cell layer (GCL), which contains the soma of RGCs, but also of "displaced" amacrine cells, which can comprise up to half of the soma in this layer, depending on the animal. The axons of the RGCs extend through the nerve fibre layer, bundling together forming the optic nerve. The optic nerve exits the back of the eye, at the optic nerve head (ONH), projecting to the superior colliculus and the lateral geniculate nucleus (Euler, Haverkamp, Schubert, & Baden, 2014; Kolb, 2003; Masland, 2012; Sanes & Zipursky, 2010).

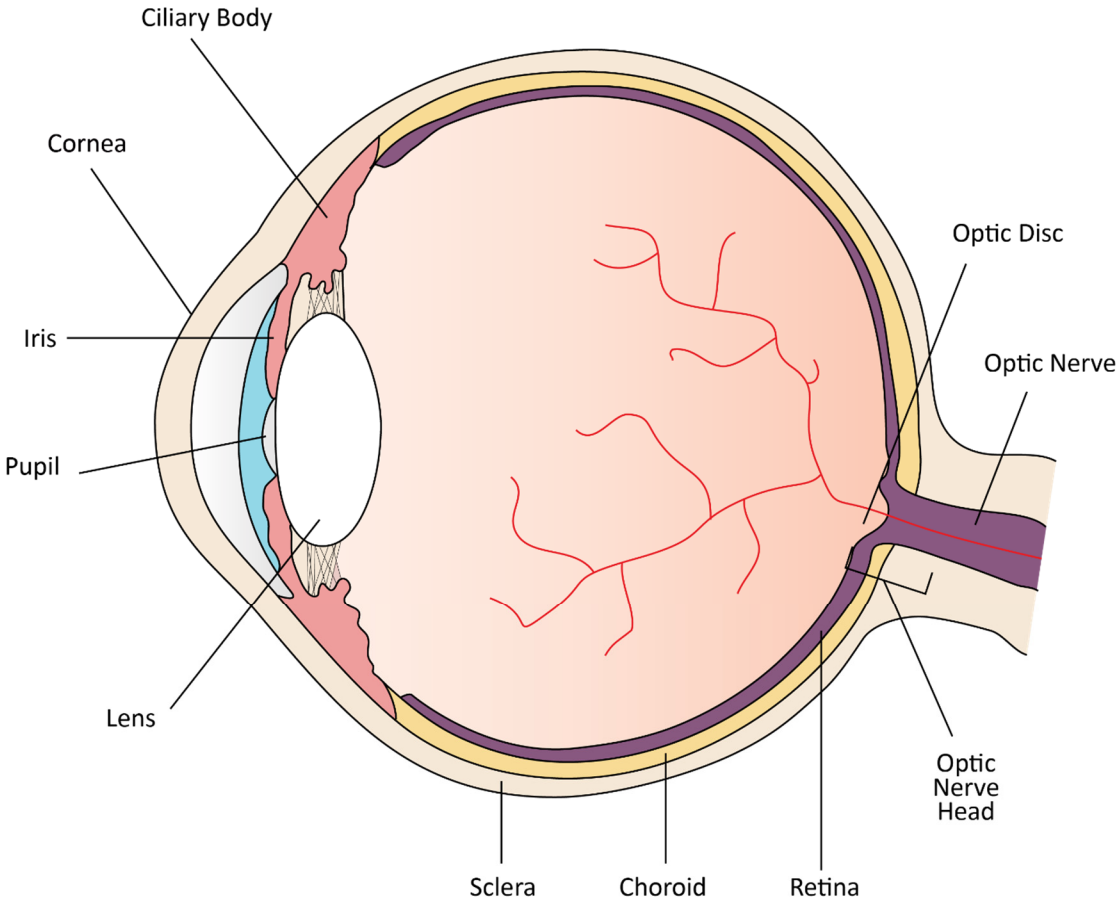

Figure 1.1 - The gross anatomy of the eye

Figure 1.2 - The retina. Schematic cross section of the retina, showing the outer nuclear layer (ONL), outer plexiform layer (OPL), inner nuclear layer (INL), inner plexiform layer (IPL), ganglion cell layer (GCL), and nerve fibre layer (NFL). Rod and cone photoreceptors synapse onto horizontal and bipolar cells. Bipolar cells then synapse onto amacrine and retinal ganglion cells (RGCs), whose nerves bundle come together to form the optic nerve. The retina also contains three glia types: astrocytes (not shown), microglia (not shown), and Müller glia, which span the length of the retina. Modified from Euler et al., 2014.

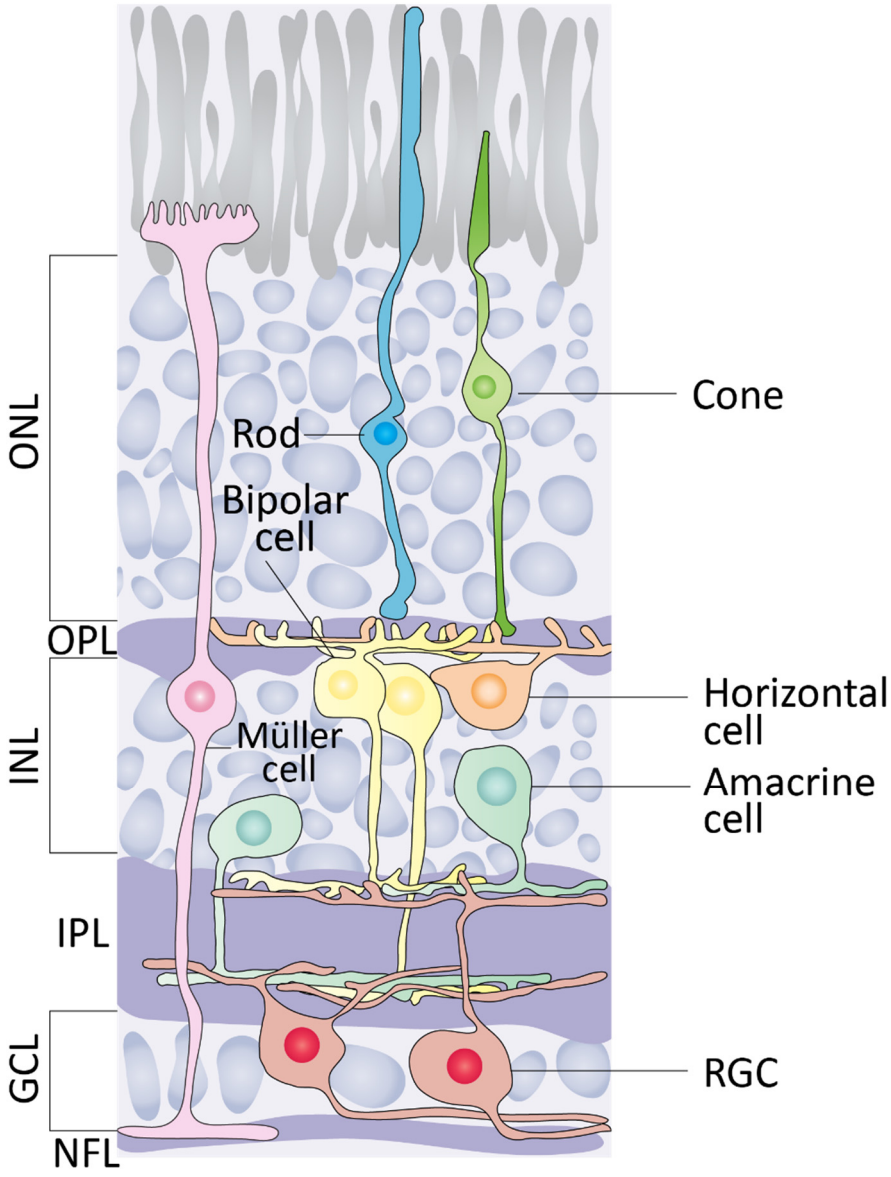
ONL
OPL
INL
IPL
GCL
NFL
Rod
Cone
Bipolar cell
Horizontal cell
Müller cell
Amacrine cell
RGC

In general, retinal processing mainly occurs via the vertical pathway, comprising of the photoreceptors, bipolar cells, and RGCs, and is typically propagated using the excitatory neurotransmitter glutamate. Lateral pathways, involving horizontal and amacrine cells, are responsible for modulation of the visual signal, which is mediated through the release of various excitatory and inhibitory neurotransmitters, including glycine and GABA. Presynaptic glutamatergic signals are received and processed on postsynaptic neurons via slower metabotropic glutamate receptors (mGluRs), or faster ionotropic receptors (iGluRs), depending on the cell type (Euler et al., 2014; Masland, 2012).

Aside from the neurons described above, the retina also contains three main resident glial cell types: Müller glia, astrocytes, and microglia. Müller glia are the primary glia in the retina. Müller soma are located within the INL, but have two main radial processes which span the retina. These processes terminate with end feet forming the outer and inner limiting membranes, above and below the ONL and GCL, respectively. Additionally, Müller glia also have several secondary processes which extend from the main trunk. Together, these processes interact with all the main neuron types in the retina, as well as the retina vasculature. Retinal astrocytes are highly associated with retinal blood vessels in the OPL and GCL, but also project processes which associate with the unmyelinated RGC axons in the nerve fibre layer (NFL). Microglia are the smallest glia in the retina, and are highly expressed in both plexiform layers. Müllers, astrocytes and microglia play important roles in retinal homeostasis, including initiation and regulation of the immune response, maintenance of the blood-retinal barrier, and buffering of the retinal extracellular environment. As such, retinal glial are important contributors to synaptic regulation through the buffering of ions and neurotransmitters (Chong & Martin, 2015; Mac Nair & Nickells, 2015; Vecino, Rodriguez, Ruzafa, Pereiro, & Sharma, 2016).

Other than the retina, several other highly specialized ocular tissues aid in the production of the visual signal. Aqueous humor is a clear liquid produced by the eye that serves two main purposes: to help maintain the shape of the eye globe, ensuring proper optics; and to serve as a modified circulatory system delivering oxygen and nutrients to tissues in avascular areas (including the lens and cornea) while also clearing solutes. Thus, the intraocular pressure (IOP) of the eye globe is maintained through dynamic regulation the aqueous humor production (inflow) and drainage (outflow; Civan, 2008).

Aqueous humor is produced by the active transport of solutes across the cells of the ciliary body, from the pigmented epithelial cells to the non-pigmented epithelial cells (**Fig. 1.3**). Following production, secreted aqueous humor moves from the posterior chamber, through the pupil, into the anterior chamber. From the anterior chamber, aqueous humor exits the eye through either the trabecular meshwork, the so called "conventional pathway," and/or through the uveoscleral route. Conventional drainage runs from the irideocorneal angle through the trabecular meshwork and juxtacanalicular tissue, into the Schlemm's canal, and then out through the episcleral vessels. In the uveoscleral route, aqueous humor is drained from the angle, but diffuses between the ciliary muscle bundles, through the supraciliary and suprachoroidal spaces, where it drains into the lymph vessels and/or ciliary body capillaries (Alm & Nilsson, 2009; Civan, 2008; Tamm, Braunger, & Fuchshofer, 2015; Toris, 2008; Yucel & Gupta, 2015). Unlike the active process of aqueous humor production, pressure in collection vessels is lower than the surrounding areas, creating a passive gradient for flow (McLaren, 2010).

The contribution of conventional and uveoscleral outflow pathways to total aqueous humor outflow varies by animal, but also with age. The uveoscleral outflow route in mice is responsible for approximately 80% of total outflow in mice, and 4-60% in humans (Alm &

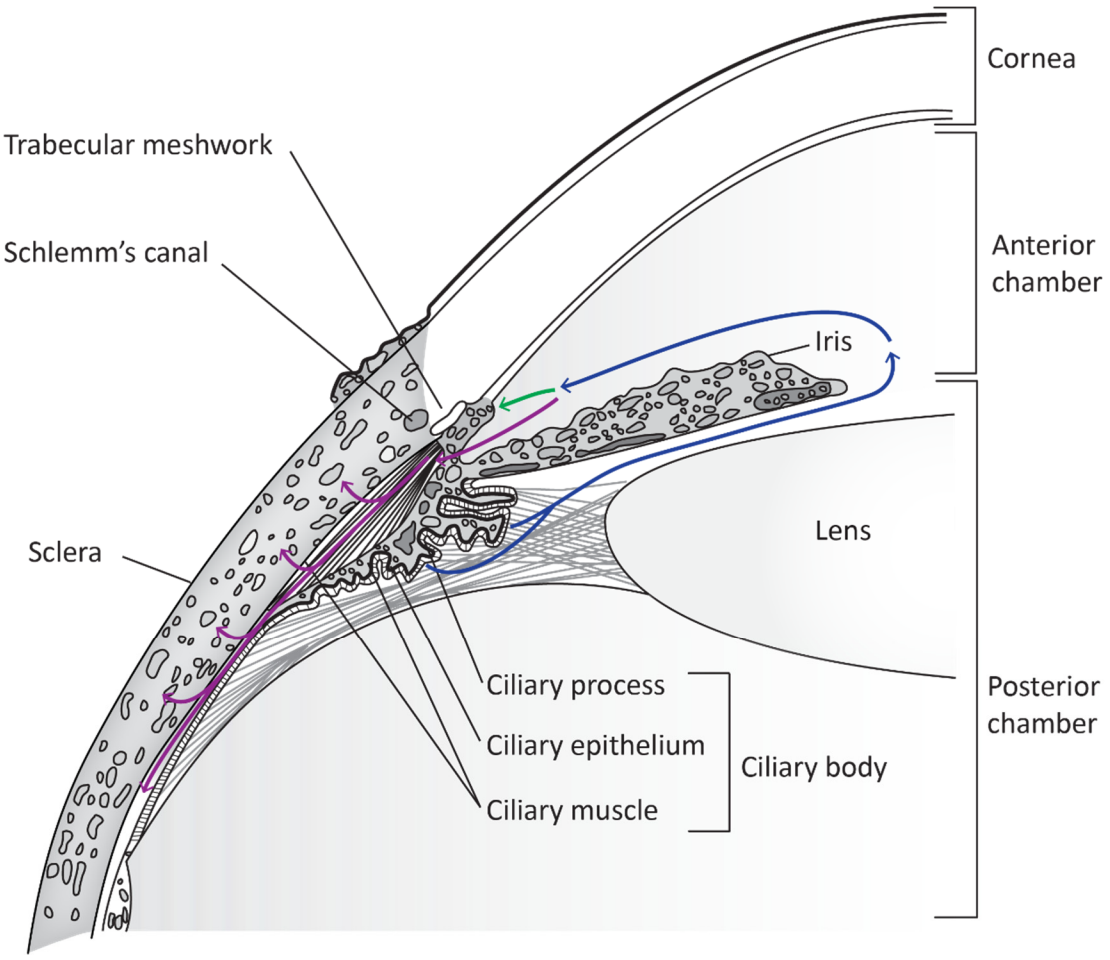

Figure 1.3 - Ocular structures associated with aqueous humor inflow and outflow. Aqueous humor is produced by the ciliary body, and flows from the posterior chamber through the pupil to the anterior chamber (blue). Aqueous humor flow out of the eye either through the conventional pathway (green) via the Schlemm's canal, or through the uveoscleral pathway (purple). Modified from Cairns, Baldridge, and Kelly, 2016a; and Riordan-Eva, 2011.

Nilsson, 2009; Toris, 2008). In monkeys, approximately 45-70% of aqueous humor drainage occurs through the uveoscleral route, which is reduced by about half with ageing (Toris, 2008). With age, the trabecular meshwork also undergoes several changes, including cell loss and increased stiffness, which is purported to contribute to increased resistance to aqueous humor outflow over time (Fautsch & Johnson, 2006; M. Johnson, 2006).

IOP is dynamic; it changes throughout the day, but also reactively in response to local stimuli. While diurnal changes are a result of differences in aqueous humor production, smaller reactive changes can occur by modification of outflow through the conventional, but not uveoscleral, route (Civan, 2008; Fautsch & Johnson, 2006). Diurnal variation of IOP typically ranges from 2-5 mmHg in humans (Civan, 2008). However, much wider fluctuations have been noted in pathology (Harasymowycz et al., 2016; Konstas et al., 2016; Sacca et al., 1998; Toris, 2008).

1.2 GLAUCOMA

Glaucoma is a progressive eye disease which is defined by selective RGC loss, leading to optic nerve head cupping, due to loss of RGC axons, and remodeling of the optic nerve head (Harasymowycz et al., 2016; Weinreb, Aung, & Medeiros, 2014; Weinreb et al., 2016). Over time, glaucoma can lead to vision loss, significantly impacting quality of life (Medeiros et al., 2015; Parrish et al., 1997). There are several risk factors which can contribute to the development of glaucoma, including thin central cornea, age, and ocular hypertension (Sena & Lindsley, 2017). Even though ocular hypertension is frequently associated with glaucoma, it is not synonymous with the disease, and is not required for diagnosis (Weinreb et al., 2016).

Approximately 54,000 Canadians are blind as a result of glaucoma (Harasymowycz et al., 2016), and it is the leading cause of irreversible blindness worldwide (King, Azuara-Blanco, & Tuulonen, 2013; Sena & Lindsley, 2017). Because of an increase in the ageing population, the global prevalence of glaucoma is also increasing, with notable rises estimated in Asia and Africa (Tham et al., 2014).

Glaucoma can be categorized into two main types: open angle glaucoma and angle-closure glaucoma. While these types are different anatomically, they both share the characteristic RGC loss leading to vision loss (Canadian Ophthalmological Society Glaucoma Clinical Practice Guideline Expert Committee & Canadian Ophthalmological Society, 2009; Harasymowycz et al., 2016). Both types of glaucoma can be primary or secondary. Secondary cases are defined as cases occurring due to a known cause of IOP increase or angle closure (for example, occurring as a side effect of an unrelated medication), while primary cases are of unknown etiology (Canadian Ophthalmological Society Glaucoma Clinical Practice Guideline Expert Committee & Canadian Ophthalmological Society, 2009; Harasymowycz et al., 2016).

1.2.1 Angle-Closure Glaucoma

While not as common as open angle glaucoma, angle-closure glaucoma is the cause of 50% of all glaucoma-induced blindness (Harasymowycz et al., 2016). Angle-closure glaucoma occurs where flow of aqueous humor through the outflow pathways is blocked. This can arise as a result of pupillary block and/or plateau-iris configuration, for example (Harasymowycz et al., 2016). Secondary to this, IOP can increase significantly, occurring slowly, or in 33% of presenting angle-closure cases, very rapidly, resulting in ocular emergency (Sun et al., 2017).

Persons of Inuit and Asian decent are at greater risk for angle-closure glaucoma, due to anatomical differences in the eye including shallowed anterior chambers (Harasymowycz et al., 2016; Sun et al., 2017). It is estimated that 76.7% of all cases of primary angle-closure glaucoma are in Asia, where it affects approximately 1.09% of the population, compared with 0.50% worldwide (Tham et al., 2014).

In the past, gonioscopy was the main technique used to diagnose angle-closure. However, recent advances in imaging technology have enabled use of optical coherence tomography and ultrasound bioscopy as important diagnostic tools, enabling a better view of the anterior chamber, including the iridiocorneal angle and associated structures (Sun et al., 2017).

1.2.2 Open Angle Glaucoma

Open angle glaucoma describes a glaucoma where the iridiocorneal angle is open. Increased resistance to aqueous humor outflow has been suggested as one causative mechanism, potentially a result of stiffening of the trabecular meshwork cells (Tamm et al., 2015). However, open angle glaucoma can occur with or without the presence of ocular hypertension; half of newly diagnosed open angle glaucoma cases have IOP which is considered “normal” (10-20 mmHg), at least initially (Shih & Calkins, 2012; Weinreb et al., 2016). Primary open angle glaucoma (POAG) is the most common type of glaucoma in most countries, comprising 80% of the cases in the US (Weinreb et al., 2014), and is most prevalent in populations of African descent (Harasymowycz et al., 2016; Kapetanakis et al., 2016; Tham et al., 2014).

1.2.2.1 Normal Tension Glaucoma

One subtype of open-angle glaucoma occurs where there is vision loss while IOP is within a "normal" range (< 21 mmHg; Harasymowycz et al., 2016). Although, there is question as to whether or not normal tension glaucoma is its own class, or whether it simply is an "early" form of glaucoma. However, other factors have been suggested to be involved which may refute this hypothesis (e.g., some cases of what appears to be an auto-immune-type pathology; Harsymowycz et al., 2016; Weinreb et al., 2016).

1.2.3 Current Therapies for the Treatment of Glaucoma

Glaucoma resulting in vision loss can have detrimental effects on quality of life (Medeiros et al., 2015; Parrish et al., 1997). Early intervention in diagnosis and treatment is therefore essential. However, glaucoma is relatively asymptomatic before becoming severe. In fact, it is estimated that 50% of all glaucoma cases are undiagnosed, and therefore not being properly managed (Harasymowycz et al., 2016). Self-reported changes in visual field may not be detectible until 30-50% of RGCs have been lost (Weinreb et al., 2014), making regular examinations of the optic nerve head and IOP monitoring key in early detection (Harasymowycz et al., 2016; Weinreb et al., 2016).

Prior to detectible visual field deficits, as self-reported or measured through automated perimetry testing (Harasymowycz et al., 2016), an increasing cup-to-disc ratio and/or cup-to-disc asymmetry may be used to diagnose glaucoma, as assessed through fundus examination (Weinreb et al., 2014). Loss of RGC axons results in a decrease of the neuroretinal rim size, and, therefore, increased optic cup size (Burgoyne, 2015).

Currently, the only strategy to manage glaucoma is directed at modifying intraocular pressure (even in normal tension glaucoma; (Harasymowycz et al., 2016; Weinreb et al.,

2014; Weinreb et al., 2016). For every mmHg reduction in IOP, there is a 30% reduced risk of progression (Heijl et al., 2002). There are currently two main strategies for IOP management, pharmacologic (either modifying aqueous humor inflow or outflow, or both), and surgical. The type of therapy depends the type of glaucoma, patient ability to adhere to drug administration regimes, amount of IOP modification required, and accessibility and feasibility of drugs, as assessed by the managing practitioner (Harasymowycz et al., 2016; Weinreb et al., 2016).

1.2.3.1 Successes and Failures in Managing Glaucoma

Successful management of glaucoma is currently defined as reducing IOP to a point which is thought to slow or prevent further optic disc deterioration and vision loss (Harasymowycz et al., 2016). However, the amount of IOP lowering required to achieve this is difficult to predict (Harasymowycz et al., 2016). The aggressiveness of treatment depends on the severity of the disease (estimated through assessment of the optic nerve and visual field loss/progression, as well as taking into consideration other risk factors), tolerability of the intervention, and life expectancy (Harasymowycz et al., 2016; Weinreb et al., 2014; Weinreb et al., 2016). Furthermore, intended IOP targets need to be continuously revaluated based on actual outcomes, as RGC loss can progress despite apparent IOP control. A trial investigating POAG, the Early Manifest Glaucoma Trial, demonstrated that while risk of visual field progression was half in treated eyes, 45% of treated eyes still had progressive visual field loss after 6 years, compared with 62% of untreated eyes (Heijl et al., 2002; Weinreb et al., 2014).

IOP modification can also be difficult to achieve. Results from the Ocular Hypertensive Treatment Study found that at 5 years, 49% of patients with ocular hypertension required two or more topical medications to successfully manage pressure

(Kass et al., 2002). This is furthered by difficulties in patient adherence (in both proper application and adherence to schedules), which has been estimated to affect up to 80% of patients (Harasymowycz et al., 2016).

There are five main types of approved glaucoma therapeutics: α_2-adrenergic agonists, cholinergic agonists, β-adrenergic antagonists (β-blockers), carbonic anhydrase inhibitors, and prostaglandin analogues (see **Table 1.1**; Harasymowycz et al., 2016; Schmidl, Schmetterer, Garhofer, & Popa-Cherecheanu, 2015). These drugs either decrease aqueous humor production, or increase aqueous humor outflow through either the conventional or uveoscleral route, and may be given alone or in combination. Prostaglandin analogues, such as latanoprost, bimatoprost, travoprost, and tafluprost, are typically used as first-line therapeutics. These drugs are advantageous over other types of ocular hypotensives in that they have a much longer duration of action, which is effective independent of the time of day, and are generally well tolerated (Harasymowycz et al., 2016).

In certain cases of POAG, and in most cases of angle-closure glaucoma, surgical intervention is required (Harasymowycz et al., 2016). These interventions involve either creating new routes for aqueous humor outflow (for example, trabeculectomy, used in POAG, or peripheral laser iridotomy, used to relieve iris block in angle-closure glaucoma), or stimulating remodeling of trabecular meshwork cells (laser trabeculoplasty, used in POAG; Weinreb et al., 2014; Weinreb et al., 2016). In acute angle-closure glaucoma, laser iridotomy alone can be sufficient to abort further increases in IOP, with one study reporting no increases in IOP on follow-up in 42% of eyes treated (Aung, Ang, Chan, & Chew, 2001; Weinreb et al., 2014). Trabeculectomy also produces favourable outcomes, with stable IOP reductions, without additional medical intervention, in 57% of patients on a 20 year follow-up (Landers, Martin, Sarkies, Bourne, & Watson, 2012). However, surgical intervention (even through laser therapy) poses significant risk of complications, including cataract

Table 1.1 - Current Pharmacological Tools for the Treatment of Glaucoma

	Examples	**Primary MOA**
Prostaglandin analogues	Latanoprost, bimatoprost, travoprost, and tafluprost	Increase uveoscleral outflow
α_2-agonists	Brimonidine and apraclonidine	Decrease aqueous humor production
Cholinergic agonists	Pilocarpine and carbachol	Constrict pupil, opening trabecular meshwork, and thus increasing conventional outflow
β-blockers	Timolol, betaxolol, metipranolol, carteolol, and levobunolol	Decrease aqueous humor production
Carbonic anhydrase inhibitors	Dorzolamide, brinzolamide, acetazolamide, and methazolamide	Decrease aqueous humor production

formation and inflammation (including endophthalmitis), and IOP can still increase over time (Harasymowycz et al., 2016; Weinreb et al., 2016).

1.3 Neuroprotective Therapies for Glaucoma

Since IOP modification is not always effective at deceasing the progression of glaucoma, therapies which directly target RGC loss are of significant interest (Tamm, Schmetterer, & Grehn, 2013). Such an approach could be combined with an IOP-lowering therapy to improve outcomes in a greater number of patients (Levin, Crowe, Quigley, & Lasker/IRRF Initiative on Astrocytes and Glaucomatous Neurodegeneration Participants, 2017). However, despite many decades of research, so far, no drug with the primary intent of neuroprotection has been successfully developed. There are many reasons contributing to this apparent lack of progress, including a lack of clinically available biomarkers to measure progress in glaucoma, but also perhaps reflects an incomplete understanding of glaucoma pathogenesis (Khatib & Martin, 2017; Levin et al., 2017; Quigley, 2012; Tamm et al., 2013).

RGC loss in glaucoma is complex, stemming from mechanical, vascular, and/or biochemical injury (Krizaj et al., 2014; Levkovitch-Verbin, 2015; Nickells, Howell, Soto, & John, 2012; Weinreb et al., 2016). The multiplicity of pathways involved in this disorder is highlighted by the fact that RGC axonal degeneration and RGC soma loss occur by temporally and mechanistically distinct pathways, with axon degeneration occurring prior to soma loss (Howell, Soto, Libby, & John, 2013; Li, Schlamp, Poulsen, & Nickells, 2000; Libby et al., 2005b; Maes, Schlamp, & Nickells, 2017; Nickells et al., 2012). However, it is now well established, that glaucomatous RGC death ultimately occurs by apoptosis, a form of programmed cell death (Levkovitch-Verbin, 2015; Maes et al., 2017; Quigley et al., 1995). Apoptosis involves activation of proteolytic caspases, which induce irreversible damage

once initiated (Qu, Wang, & Grosskreutz, 2010). Apoptosis is initiated via signals from either the extracellular environment (the extrinsic pathway), or from within the cell (the intrinsic pathway, Howell et al., 2013; Levkovitch-Verbin, 2015; Maes et al., 2017; Thomas, Berry, Logan, Blanch, & Ahmed, 2017). Involvement of both intrinsic and extrinsic apoptotic cascades have been implicated in glaucomatous RGC injury (Howell et al., 2013; Maes et al., 2017; Nickells et al., 2012; Qu et al., 2010; Thomas et al., 2017).

Several mechanisms have been proposed as mediators glaucomatous RGC damage, including: loss of neurotrophic support, inflammation, mitochondrial dysfunction and oxidative stress, and excitotoxicity (Almasieh, Wilson, Morquette, Cueva Vargas, & Di Polo, 2012; Tamm et al., 2013; Weinreb et al., 2016). The complex nature of these mechanisms reflects the heterogeneity of glaucomatous pathology – not all glaucomas present and progress in the same manner. It is also possible that more than one mechanism may contribute to RGC death, and that this contribution may vary throughout the progressive course of the pathology (Tamm et al., 2013). The following paragraphs summarize these proposed mechanisms in more detail.

Structurally, the optic nerve head is the weakest part of the wall of the eye. Therefore, any changes in IOP and/or with the flexibility of the posterior sclera can result in mechanical stress on the optic nerve head, resulting in significant changes to the lamina and direct stress on the axons of the optic nerve (Burgoyne, 2015; Khatib & Martin, 2017; T. D. Nguyen & Ethier, 2015; Nickells et al., 2012). Pressure-induced strain on the optic nerve disrupts both anterograde and retrograde transport along RGC axons, and has lead to the hypothesis of loss of neurotrophic support as a mechanism of glaucomatous injury (Almasieh et al., 2012). This has been furthered by research showing that increasing pro-survival neurotrophins, such as brain-derived neurotrophic factor and nerve growth factor,

pharmacologically or genetically, can delay the onset of glaucomatous injury (Almasieh et al., 2012; Weber, 2013).

Mitochondria are the "power houses" of the cell, producing adenosine triphosphate (ATP) through oxidative phosphorylation. RGCs have a high metabolic demand due to their long, partially unmyelinated axons; thus, slight changes in mitochondrial function or oxygen availability (as a result of changes in vascular perfusion and ischemia) can have profound effects on RGC function. If severe enough, oxidative stress and mitochondrial dysfunction result in energy crises, which can ultimately result in initiation of intrinsic apoptosis (Pinazo-Duran, Zanon-Moreno, Gallego-Pinazo, & Garcia-Medina, 2015). Markers indicating oxidative stress have been reported in models of glaucoma, including elevation of reactive oxygen species (ROS; Pinazo-Duran et al., 2015). ROS is a normal biproduct of the electron transport chain; however, accumulation is associated with cellular damage, as it is known to induce DNA mutations and disrupt membrane phospholipids. Additionally, markers of mitochondrial dysfunction have also been reported in glaucoma, including increased mutations in mitochondrial DNA isolated from patients with POAG compared with age-matched controls (Abu-Amero, Morales, & Bosley, 2006; Pinazo-Duran et al., 2015).

Excitotoxicity is a common mechanism of neuronal cell death, and is implicated in neuronal loss in models of neuronal injury (e.g., traumatic brain and spinal cord injuries) and neurodegenerative disease (e.g., Alzheimer's disease; Almasieh et al., 2012). Excitotoxicity involves excess excitatory activation, leading to increased membrane depolarization due to increased cation influx, including Ca^{2+}. Ca^{2+} is an important second messenger, of which intracellular concentrations are normally very tightly regulated. However, excessive intracellular Ca^{2+} can result in the activation of a variety of pathways, including activation of calcium-dependent caspases, and apoptosis (Casson, 2006).

Glutamate is the primary excitatory neurotransmitter in the CNS, including the retina (**section 1.1**), and binds to both mGluRs (G protein-coupled receptors) and iGluRs (ligand-gated cation channels). There are three types of iGluRs in the retina: *N*-methyl-D-aspartate (NMDA), α-amino-3-hydroxyl-5-methy-4-isoxazolepropronate (AMPA), and kainate receptors. While all three iGluRs are permeable to Na^+ and K^+, only NMDA receptors, and some types of AMPA and kainate receptors are permeable to Ca^{2+}. Consistently, intraocular injection of iGluR agonists produces robust RGC death (Almasieh et al., 2012).

The findings from studies of excitotoxicity in glaucomatous RGC death been controversial, mainly due to the inconsistencies in reports of increased glutamate in models of glaucoma as well as from tissues taken from humans with glaucoma, and the uncovering of scientific fraud (Almasieh et al., 2012; Osborne, 2009; Salt & Cordeiro, 2006). Yet, glutamate receptor blockers have showed promise in pre-clinical trials, and memantine, an NMDA receptor antagonist, was even investigated in a large-scale clinical randomized control trial (though, did not meet outcomes, and the trial was discontinued; Almasieh et al., 2012; Weinreb et al., 2016). However, recent evidence suggesting that blocking calcium-permeable AMPA receptors may provide neuroprotection against glaucomatous RGC loss has renewed interest in this area (Almasieh et al., 2012; Cueva Vargas et al., 2015; Cueva Vargas & Di Polo, 2016; Lebrun-Julien et al., 2009).

While much of the early research on glaucoma focused solely on RGCs, glia have been found to be important contributors to the development of the glaucomatous pathology. Changes in the reactivity of glia, including Müllers, microglia, and astrocytes, occurs early in the pathogenesis of glaucoma, often prior to detectible RGC damage (Almasieh et al., 2012; Bosco, Steele, & Vetter, 2011; Nakazawa et al., 2006). In models of RGC injury, inhibition of gliosis reduces or delays RGC death (Baptiste et al., 2005; Cueva Vargas, Belforte, & Di Polo, 2016; Ganesh & Chintala, 2011; Howell et al., 2012; Livne-Bar et

al., 2016; H. Yin et al., 2016). However, with evidence of contributions to both pro-survival and pro-apoptotic pathways, the role of glial in glaucomatous pathology is not completely clear (Mac Nair & Nickells, 2015).

Astrocytes at the optic neve head become reactive shortly after injury in models of glaucoma, and along with reactive microglia, have been found to release neurotoxic factors such as endothelins, which can alter vascular perfusion, therefore contributing to oxidative stress (Mac Nair, Fernandes, Schlamp, Libby, & Nickells, 2014; Tezel, 2008). Astrocytes can also release extracellular matrix degrading enzymes, which may be responsible for remodeling of the optic nerve head following injury, and play a role in the disruption of axonal transport (Mac Nair & Nickells, 2015; Vohra, Tsai, & Kolko, 2013).

Following RGC soma loss, retinal glia become active, and are involved in clearing the remaining debris (Mac Nair & Nickells, 2015). However, proinflammatory cytokines released by these activated retinal glia also give rise to secondary RGC death (Levkovitch-Verbin et al., 2001). Tumor necrosis factor alpha (TNFα, a proinflammatory cytokine) has been identified as a potentially important player in the development of glaucomatous RGC death (Nucci et al., 2016). Among the many functions of TNFα, it is an initiator of extrinsic apoptotic pathways, but has also been suggested to be able to modify AMPA receptor expression, and could therefore promote excitotoxicity (Cueva Vargas et al., 2015; Cueva Vargas & Di Polo, 2016). Consistently, TNFα antagonism or TNFα genetic deletion increases RGC survival in rodent models of glaucoma (Mac Nair & Nickells, 2015; Nakazawa et al., 2006; Roh et al., 2012).

While the understanding of the mechanisms contributing to glaucoma have extensively progressed in the last few decades, there are still many unknowns, especially pertaining to possible dynamic interactions between these pathways. These unknowns may

contribute to the lack of success in developing a neuroprotective therapy for the treatment of glaucoma (Levin et al., 2017; Tamm et al., 2013). Several prospective drugs targeting these pathways have produced promising results *in vitro* and/or pre-clinical study; however, as of yet, none have successfully translated to an approved clinical therapeutic (Khatib & Martin, 2017; Levin et al., 2017). In many cases, manipulation of these pathways has lead to delayed or minimally reduced RGC death, rather than complete neuroprotection (Almasieh et al., 2012; Nucci et al., 2016).

One strategy to increase efficacy in reducing glaucomatous RGC loss may be through targeting multiple pathways simultaneously; for instance, combining therapies which modulate both inflammation and excitotoxicity (Levin et al., 2017). Use of cannabinoids, a group of compounds which modulate the endocannabinoid system (ECS), may be able to provide such a multi-modal approach. Components of the ECS are present throughout the eye, including both the anterior chamber and the retina (Cairns, Baldridge, & Kelly, 2016a; Cairns, Toguri, Porter, Szczesniak, & Kelly, 2016b; Schwitzer, Schwan, Angioi-Duprez, Giersch, & Laprevote, 2016). While much of the early work with cannabinoids in the eye focused on IOP modification, several cannabinoids have also shown promise as immune modulators, as well as possessing the ability to modulate neuronal excitability (Cairns et al., 2016a; Cairns et al., 2016b). Consistent with this, administration of cannabinoids in several animal models of experimental glaucoma has been associated with reduced RGC loss, but by mechanisms which have yet to be fully elucidated (Cairns et al., 2016a; Cairns et al., 2016b; Nucci et al., 2016). However, there are several disadvantages associated with cannabinoids that may hinder their usefulness as clinically-relevant therapeutics, including possible psychotropic side effects and loss of effect with repeated administration (Pacher & Kunos, 2013; Pertwee, 2009; Pertwee, 2012). The development of newer classes cannabinoid modulators, such as allosteric modulators, may provide new opportunities to provide

similar neuroprotection, while increasing potential clinical utility (Janero & Thakur, 2016; Pacher & Kunos, 2013; Pertwee, 2009; Pertwee, 2012).

1.4 PROJECT RATIONALE

The overall objective of this work was to identify strategies to manipulate mechanisms leading to RGC death, with the aim of investigating therapeutics which may improve RGC survival in models of glaucoma. Given evidence suggesting that a successful glaucoma therapeutic may need to target multiple mechanisms of injury, I investigated the potential of modulation at the intersection of inflammation and excitotoxicity, two mechanisms that have independently been associated with glaucomatous RGC death. However, to do so, I required a model of glaucomatous injury where a novel potential therapeutic could be used chronically. As many of the currently available models are of acute injury, require repeated manipulations to achieve persistent ocular hypertension, or are significantly delayed, I began this work by investigating a new potential model.

Specifically, in **Chapter 2**, I investigated the nee mouse, a new potential experimental model of glaucoma. I investigated the time course of the development of pathology through measuring changes in IOP and RGC density. Additionally, I investigated the outcome this loss had on vision through testing with the visual water box. In **Chapter 3**, I investigated the hypothesis that increased TNFα in experimental models of glaucoma can promote excitotoxicity through promotion of changes in calcium-permeable AMPA receptors. To investigate this, I used Ca^{2+}-imaging on *ex vivo* retinas, from normotensive and ocular hypertensive mice and rats. Finally, in **Chapter 4**, I built on the work from the previous chapter, and investigated if cannabinoid-modulation could directly modulate TNFα-induced changes in calcium-permeable AMPA receptor expression. Additionally, I investigated if a novel cannabinoid modulator (a positive allosteric modulator of cannabinoid receptor 1)

could reduce IOP in normotensive and ocular hypertensive mice, and increase RGC survival in two models of RGC damage.

Chapter 2: MATERIALS AND METHODS

Note: Fig. 2.5A was previously published as part of Cairns et al., 2017 .

2.1 ANIMALS

Experiments were performed in accordance to ethical guidelines set out by the Canadian Council on Animal Care, and the ARVO statement for the Use of Animals in Ophthalmic and Vision Research. Additionally, experimental procedures were approved by Dalhousie's University Committee on Laboratory Animals.

Male Brown Norway rats (250-300g) were acquired from Charles River Laboratories (Wilmington, MA). Male C57Bl/6J (25g), and male and female *Sh3pxd2b* heterozygous mice were acquired from Jackson Research Laboratories (Bar Harbour, ME). Animals were fed *ad libitum* on a standard diet, and kept on a 12-hour light/dark cycle (07:00-19:00), unless otherwise specified. Prior to experimental manipulation, animals not derived through the colony were allowed to acclimatize to the animal care facility for at least one week.

2.2 STATISTICAL ANALYSIS

Data gathered from experiments were analyzed using the statistical software GraphPad Prism (version 6.0, GraphPad Software Inc., La Jolla, CA). Data are presented as means ± S.E.M. Unless otherwise stated, analysis between two groups was performed using t-tests, while analysis between groups of three or more was performed using one-way analysis of variance (ANOVA), with *post-hoc* tests as defined per experimental summary. A *P* value of less than 0.05 was considered significant.

2.3 INTRAOCULAR PRESSURE

Intraocular pressure (IOP) measurements were carried out as previously published (Caldwell et al., 2013; Hudson, Beazley, Szczesniak, Straiker, & Kelly, 2011). In order to reduce IOP variability due to time of day, all IOP measurements were initiated at 9:30 AM

unless otherwise indicated (Aihara, Lindsey, & Weinreb, 2003; Dalvin & Fautsch, 2015; Konstas, Mantziris, Cate, & Stewart, 1997). The protocol for measurements between mice and rats varied slightly, as described below.

Mice were restrained by hand and anesthetized using 3% isoflurane with a flow rate of 1 mL/min. Following induction of anesthesia, indicated by the disappearance of the pedal reflex, isoflurane was reduced to 1.5% for maintenance of sedation. Mice were then placed in a prone position, and 10 recordings were taken in each eye using a handheld rebound tonometer (Tonolab, Icare, Finland) using the mouse setting. The average of these 10 recordings was used for data analysis. Mice were then returned to their cage and allowed to recover.

Rat IOP measurements were carried out, similar to that described for mice, using the Tonolab on the rat setting, except that measurements were performed on awake animals, held (but not restrained) by a second researcher. Rats were handled frequently prior to recordings in order to acclimatize them to the researcher, as well as to minimize stress on the animal.

To monitor effects of drug administration on IOP, IOP measurements were carried out throughout the day. The IOP of mice, like in humans, varies diurnally over a 24 hr period (Aihara et al., 2003; Dalvin & Fautsch, 2015; Hudson et al., 2011); therefore, changes in IOP from baseline is expected in vehicle-treated animals throughout the day. Consistent with these reports, IOP in C57Bl/6 mice was significantly higher at 10 pm versus 1 pm ($P < 0.05$, 16.5± 0.4 and 14.9 ± 0.5 mmHg, respectively, $N = 30$, unpaired t-test; **Fig. 2.1A**). I investigated if these diurnal changes in IOP were consistent between eyes, and found that there was no significant difference between IOP in left and right eyes at either time ($N = 15$

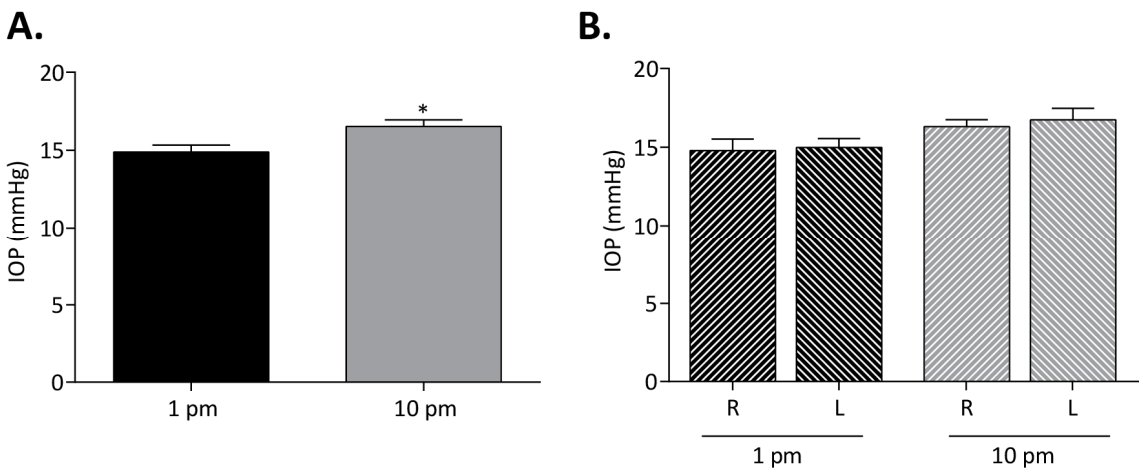

Figure 2.1 - Effect of time of day on IOP. (**A**) IOPs in normotensive C57Bl/6 mice are significantly higher at night (10 pm, grey), than during the day (1 pm, black, t-test). (**B**) However, at neither time point are left and right eyes significantly different from each other (paired t-test). N = 15 mice, 30 eyes. * = $P < 0.05$

pairs at each time point; **Fig. 2.1B**). As there is no difference between left and right eyes, comparing change in IOP over time within mice was deemed appropriate.

2.4 Retinal Ganglion Cell Survival

Retinal ganglion cell (RGC) survival was assessed by investigation of RGC density in naïve, vehicle, or drug-treated animals. RGC density was assessed using immunohistochemistry with a brain-specific homeobox/POU domain protein 3a (Brn3a) antibody. Brn3a is a nuclear protein, expressed in 80-95% of adult RGCs (Nuschke, Farrell, Levesque, & Chauhan, 2015).

Animals were euthanized by i.p. injection of 240 mg/ml sodium pentobarbital (McGill University, Montreal, QC). Enucleated were eyes fixed overnight in 4% paraformaldehyde, and then kept in phosphate buffered saline (PBS) containing Ca^{2+} and Mg^{+} (Sigma Aldrich, Oakville, ON) for up to 2 months. Isolated retinas were then permeabilized with a solution containing 0.5% Triton X-100 at -80^{o}C for 13 mins at room temperature. After thawing, retinas were rinsed in fresh permeabilizing solution for 10 mins, followed by an overnight incubation in a blocking buffer (1% Triton X-100 and 2% bovine serum albumin) containing 1:100 donkey anti-Brn3a (Santa Cruz Biotechnology Inc., Santa Cruz, CA), with gentle mixing at 4^{o}C. Retinas were then rinsed 3 times (15 mins/wash) in fresh PBS. Next, retinas were incubated in the secondary antibody (1:200 Alexa 488 donkey anti-goat antibody in blocking buffer; Jackson ImmunoResearch Laboratories, West Grove, PA) for 2 hours at room temperature, and then washed again in fresh PBS for 1 hour. Retinas were then flat-mounted on glass slides with thin coverslips using Fluoromount™ (Sigma Aldrich) to reduce loss of fluorescent signal over time.

Retinas were imaged using either a Nikon (E800; Nikon Canada Inc., Mississauga, ON) or Zeiss confocal system (LSM 510; Zeiss, Thornwood, NY). Twelve images of the ganglion cell layer were captured as a representative proportion of total population of RGCs, including 4 images each from center, middle, and peripheral regions from optic nerve head (approximately 0.336, 1.176, and 1.848 mm from the optic nerve head; **Fig. 2.2**). All images were saved offline, and labeled in such a way to blind the animal and/or treatment. RGCs were manually counted using Cell Counter on Image J. RGC densities were calculated in Excel per acquisition area, either 0.10 or 0.11 mm^2, depending on the system used.

2.5 EXPERIMENTAL MODELS OF GLAUCOMA

Several models of experimental glaucoma are currently available, including genetic models, such as the DBA/2J mouse, and surgically-induced models of ocular hypertension. There are several different types of surgically-induced models, such as bead models and transient high IOP ischemia/reperfusion models, as well as models of IOP-independent RGC death, like optic nerve transection (ONT; T. V. Johnson & Tomarev, 2010; Morgan & Tribble, 2015; Morrison, Cepurna Ying Guo, & Johnson, 2011). Each of these models poses several limitations, including variability in the degree and duration of pathology, and questions regarding the similarities in pathology to that observed in humans (T. V. Johnson & Tomarev, 2010; Morgan & Tribble, 2015; Morrison et al., 2011).

For my thesis studies, I used three different models of experimental glaucoma: a genetic model of angle-closure glaucoma, the nee mouse; a surgical model of open angle glaucoma, the bead model in rat; and an IOP-independent model of optic neuropathy, ONT in mouse. All three models offered distinct advantages for studying the mechanisms contributing to glaucomatous RGC damage as well as providing an opportunity to examine potential therapeutic interventions to decrease RGC loss.

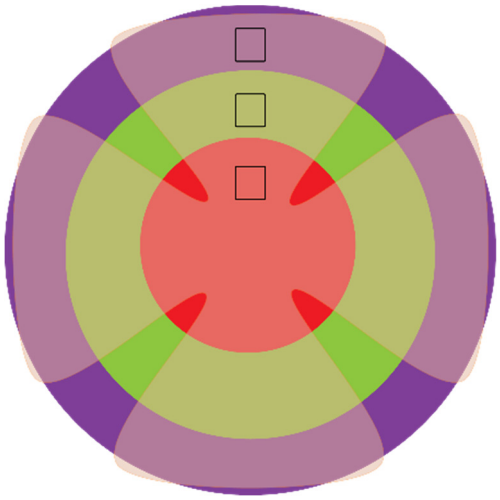

Figure 2.2 - Retinal sampling for RGC counts. Prior to flatmount, four cuts were made in the retina to enable flattening. Twelve images were taken from each retina as a population sample, one picture from center (red), middle (green), and peripheral retina (purple), in each of the four quadrants created. Images from the center, middle, and peripheral retina corresponds with distances of approximately 0.336, 1.176, and 1.848 mm from the optic nerve head. Each picture was 0.10 or 0.11 mm^2, depending on the system used.

2.5.1 THE NEE MOUSE MODEL OF GLAUCOMA

The nee mouse (short for nose, eyes, and ears) was generated following spontaneous mutation in a line of mice at the Jackson Laboratory (M. Anderson, personal communication). This mouse was identified phenotypically based on its small size, domed head, short nose, and large eyes and ears. Genetic analysis revealed that this mouse displayed a one base-pair deletion in the *Sh3pxd2b* gene, coding for the protein tyrosine kinase substrate 4, a podosome adaptor protein, resulting in a premature stop codon, which produces a truncated protein. While mice heterozygous for this mutation (*Sh3pxd2b*$^{+/nee}$) do not appear different from wildtype (*Sh3pxd2b*$^{+/+}$), carrying two copies of the mutated gene produces a visible phenotype (*Sh3pxd2b*$^{nee/nee}$, "nee"; Mao et al., 2009). The involvement of podosomes in adhesion to, and remodeling of, the extracellular matrix is consistent with the abnormal bone and tissue formation in nee mice, including decreased bone density, shortened skulls, and very little white adipose tissue (Mao et al., 2009).

Initial slit lamp analysis by Mao et al. (2009) revealed that adult nee mice had increased anterior chamber depths, perhaps a result of the peripheral anterior synechia that was also observed at 17 days post-natal (p17; Mao et al., 2009; Mao, Hedberg-Buenz, Koehn, John, & Anderson, 2011). This was subsequently found to be associated with significant increases in IOP, ganglion cell layer thinning, optic nerve loss, and optic nerve head excavation at 3 months (Mao et al., 2011). In humans, mutations in *SH3PXD2B* underlie congenital Frank-Ter Haar Syndrome (FTHS). Humans with FTHS exhibit many of the same symptoms as nee mice, but importantly, frequently display "prominent eyes," and congenital glaucoma (Aktas et al., 2014; Iqbal et al., 2010).

When I began my research, little was known about the time course of the development of pathology in nee mice, let alone potential of being used to investigate novel

therapeutics. Therefore, one of my first tasks prior to using this model in my studies was to investigate and characterize the glaucomatous pathology in this mouse, and validate nee as an experimental model of glaucoma, as described in the following sections.

2.5.1.1 Genotyping of Nee

As nee mice are infertile, the colony was maintained through breeding of heterozygotes. Nee mutants could be identified visually; however, genotyping of heterozygotes was required, as they appear otherwise as normal. Genotyping followed a protocol modified from Mao et al. (2009). Briefly, digested ear punch tissue (AccuStart II PCR Genotyping Kit, QuantaBio, Beverly, MA) was amplified using polymerase chain reaction (Piko 24 Thermal Cycler, Thermo Scientific, Waltham, MA). The forward (5' AGGCTCAGTTGCCCTGAATGTA 3') and reverse (5' TTCTCAGCGGGAACTTGCTCTT 3') primers (as per Mao et al., 2009) flanked the base pair deletion. The amplified product was then digested using the restriction enzyme *RsaI* (ThermoFisher Scientific, Waltham, MA), chosen as it cuts directly at the deletion site. Cutting of the wildtype results in two DNA products which are 546 and 167 base pairs, while mutant DNA is resistant to cutting, and maintains the full 713 base pair product. Therefore, heterozygotes were identified based on the presence of all three products.

2.5.1.2 Visual Water Box

Mao and colleagues (2011) had previously described significant RGC loss in nee mice at 3 months; however, it was unknown what type of effect this loss would have on vision. Therefore, in order to determine the degree of decrement in visual function in these mice, 3.5 month-old male and female nee mice underwent evaluation using the visual water box, a two-choice visual discrimination task, following a protocol from Wong and Brown (2006). Wildtype littermates were used as control.

Mice were switched to a reverse light cycle (lights on 7:00 pm and off at 7:00 am), and allowed to acclimatize for 3 days, allowing for testing during their active cycle. The water box is a trapezoidal box filled with 15 cm of room temperature (approximately 22^0C) water (**Fig. 2.3A**). At the narrow end of the box, plexiglass walls form a release chute, while the other end consists of a midline divider between two 17-inch monitors (Accu Synch 70 NEC 3) outside of a plexiglass wall. A plexiglass escape platform was placed in the water, below one of the two computer screens, which was moved back and forth depending on the stimulus. Reflections from the computer screens on the water made this platform invisible from water level.

The computer monitors were connected to a computer running a custom-made computer program based on a Vista program used in Prusky et al., 2000. This program controlled the visual stimuli, which consisted of a homogenous grey screen (negative stimulus), or black and white vertical stripes (approximately 4 cm wide, positive stimulus; **Fig 2.3B**). Testing occurred in a dark room, with the exception of light coming from the stimuli on the computer screens, and a bulb above the holding cages (as described below). A digital camera (Panasonic) was hung from the ceiling, and used to videotape trials so offline analysis of swimming patterns could be performed. A correct trial was defined as a swimming pattern that did not enter the side displaying the negative stimulus beyond the midline divider (the "choice line"). If the mouse entered this side, the trial was defined as an error. If the mouse failed to find the hidden platform within 60 second of release from the chute, the trial was considered incorrect, and the mouse was led to the platform using the plastic bucket. Following either an error or incorrect trial, mice were immediately released from the chute again to perform an error trial.

Figure 2.3 - The visual water box. (**A**) The visual water box apparatus is a trapezoidal box filled with 15 cm deep room temperature water. Mice are trained that when released from the chute at the smaller end of the trapezoid to swim towards the opposite end of the box towards the computer screen displaying the vertical grating (positive stimulus). The mice learn that the vertical grating depicts the location of a hidden platform, enabling escape from the water. (**B**) The location of the hidden platform varies by trial, alternating between the left and right, in a pre-defined manner. Mice who cross the "choice line" on the side displaying the grey screen (negative stimulus) are scored as incorrect. Images adapted from Wong and Brown (2007) and Prusky, West, & Douglas (2000).

A.

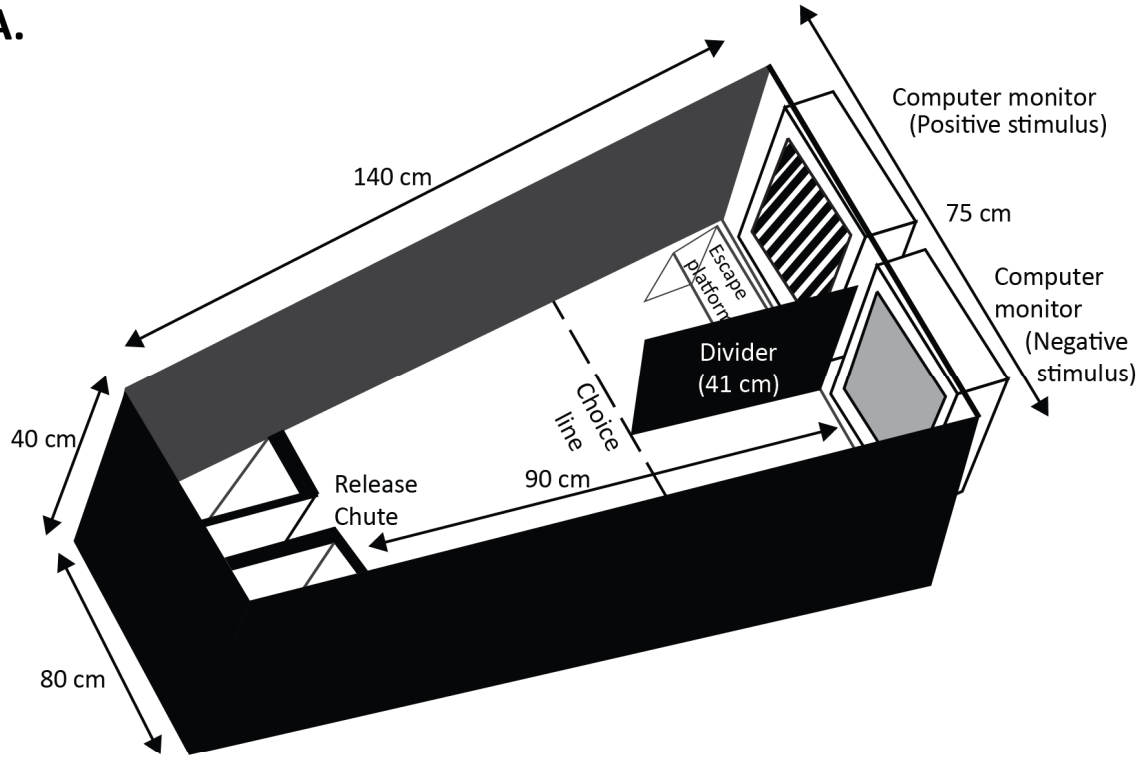
140 cm
Computer monitor
(Positive stimulus)
75 cm
Computer
monitor
(Negative
stimulus)
Escape
platform
Divider
(41 cm)
Choice
line
40 cm
Release
Chute
90 cm
80 cm

B.

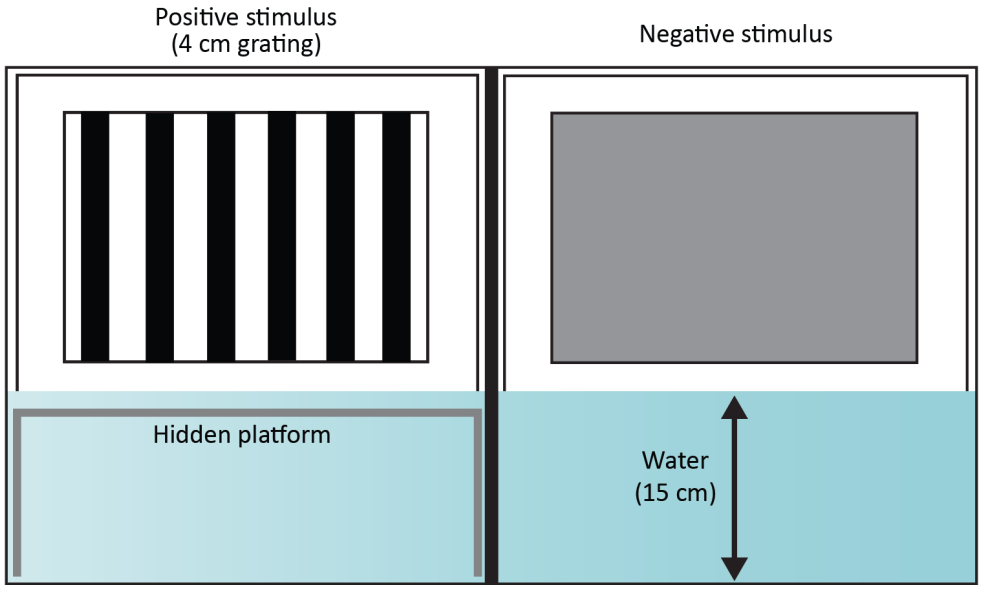
Positive stimulus
(4 cm grating)
Negative stimulus
Hidden platform
Water
(15 cm)

During training and testing, mice were placed into housing cages lined with paper towel. To limit fatigue, trials occurred with a minimum of 5 minutes between trials. The housing cages were also placed on a heating pad, and under a 60-W heating lamp to aid in maintenance of body temperature.

Prior to testing, mice underwent training for 1 day to familiarize the mice with the plastic container used to move mice from the housing cage to the water box, the layout of the water box, and to facilitate association of the positive stimulus with the location of the hidden platform. This occurred over a series of 6 trials, where mice were released from increasing distances of the hidden platform, with alternating positive stimulus positions (outlined in **Table 2.1**). Testing occurred over 8 trials for 8 days. The positive stimulus alternated between left and right in the same pattern for the first 4 days (LRLLRLRR), and reversed for the last 4 days (RRLRLLRL). Visual detection was defined when a mouse reached 70% accuracy over 8 testing days.

Wildtype mice undergoing testing reached criteria for visual detection at day 4, and maintained above 70% accuracy for the remaining 4 days (N = 7; **Fig. 2.4A**). Nee mice, on the other hand, did not reach criteria for visual detection throughout any of the 8 days of testing (N = 4). One means to assess if the inability to reach threshold for accuracy is because of anxiety or learning impairment is to analyze latency to reach the platform. If latency decreases over time, this would suggest that the mice are able to learn the task, regardless of visual ability (Wong and Brown, 2006). Wildtype mice had an average latency of 20.5 ± 3.8 seconds on day 1, that decreased over time and resulted in a day 8 latency of 6.8 ± 0.8 seconds ($P < 0.05$; **Fig. 2.4B**). Nee mice were slower on the first day compared to wildtype ($P < 0.05$, 39.4 ± 6.5 seconds), but decreased in time to reach the platform over the 8 days of testing (18.62 ± 3.8 seconds on day 8, $P < 0.05$). This indicates that while nee mice are unable to reach criteria for visual detection, this does not appear to be due to a learning

Table 2.1 - Training Phase Protocol

Trial	Grating position	Place released
1	Left	Released on platform (held for 60 s)
2	Left	Released from midline divider on left side (maximum 60 seconds to find platform)
3	Right	Released on platform (held for 60 s)
4	Right	Released from midline divider on right side (maximum 60 seconds to find platform)
5	Left	Released from chute (maximum 60 seconds to find platform)
6	Right	Released from chute (maximum 60 seconds to find platform)

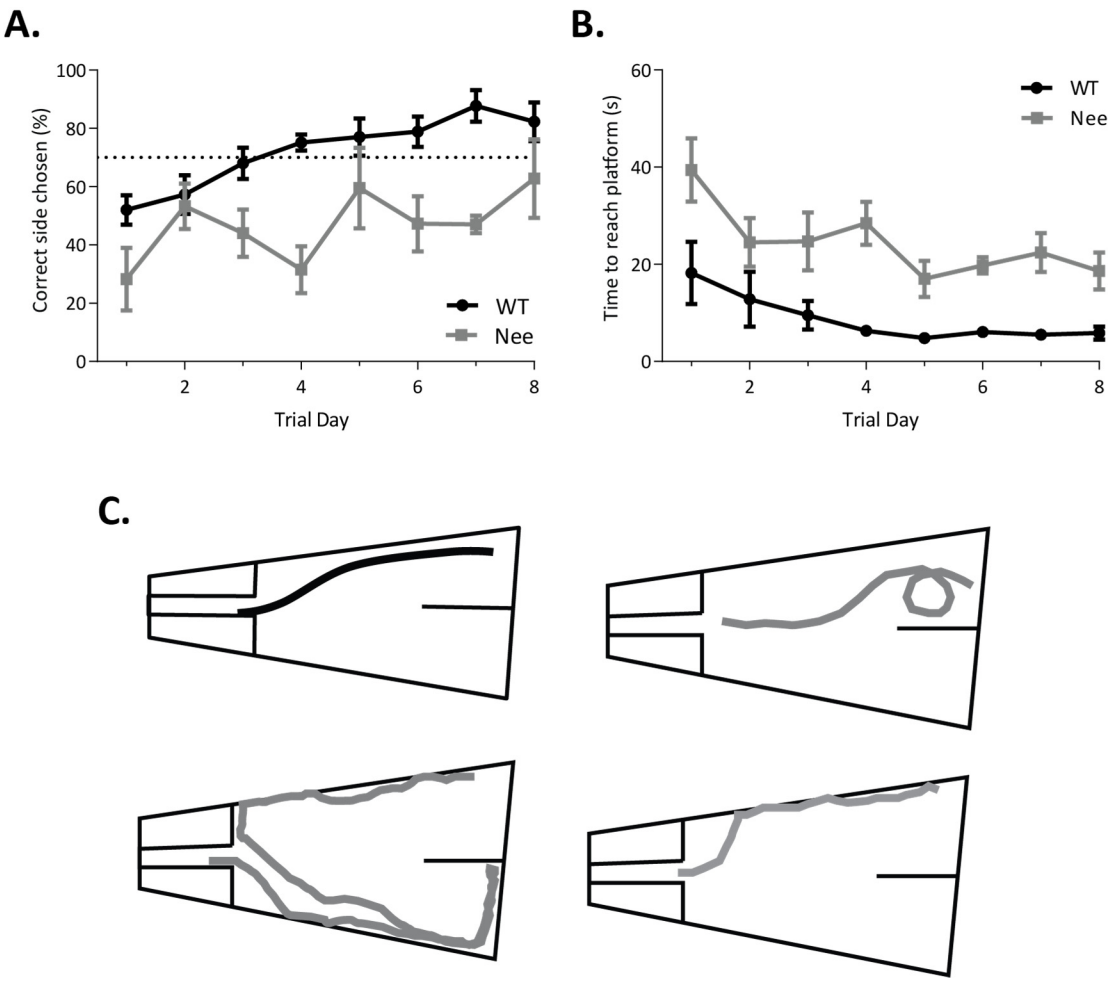

Figure 2.4 - Nee mice lack functional vision. (**A**) Nee mice (*N* = 4) failed to meet criterion for visual detection (70% accuracy, dotted line) throughout the 8 days of trial, while wildtype (WT) mice (*N* = 7) passed the threshold on day 4. (**B**) Both, nee and WT mice displayed decreased latency to reach the platform over the course of 8 days of testing, suggesting that the mice were able to learn the task. (**C**) Representative paths from the 8th day of testing, demonstrate that nee mice (grey paths) developed swimming patterns associated with non-visual location strategies, while WT mice (black path) did not.

impairment or anxious behaviour. In fact, the swim paths exhibited by nee mice on the last day of testing were similar to those reported by Wong and Brown (2006) as being a learned non-visual strategy to platform location – swimming along the perimeter of the water box until the platform is reached (**Fig. 2.4C**). Taken together, these results indicate that nee mice are visually impaired, which is consistent with the ganglion cell layer thinning and axon loss previously described (Mao et al., 2011).

2.5.1.3 Nee IOP and RGC Loss Over Time

The time course of ocular hypertension development and RGC loss in nee mice was also investigated. Daytime IOPs (3pm) were measured in male and female nee mice, and were compared to wildtype littermates (**Fig. 2.5A**). At p16, IOP was elevated in nee compared with wildtype ($P < 0.05$, 17.6 ± 1.8 and 12.6 ± 0.4 mmHg, $N = 6$ and 5, respectively). This ocular hypertension persisted over the lifetime of the mice, as IOP at p28, p37, and at approximately 3 months of age was also elevated ($P < 0.05$, mean difference 6.8 ± 2.4, 11.3 ± 2.3, and 10.6 ± 2.2 mmHg, respectively, N = 8-19).

RGC densities also declined in nee mice over time (**Fig. 2.5B**). At p16, RGC densities in nee mice were similar to wildtype littermates (3617 ± 91 and 3810 ±179 RGCs/mm^2, N = 6 and 4, respectively). At p28, RGC density had declined ($P < 0.05$, mean difference 1714 ± 324 RGCs/mm^2 from wildtype littermates, $N = 14$ and 6), which further continued at p37 ($P < 0.05$, mean difference RGCs/mm^2 from wildtype littermates, $N = 11$ and 9). By approximately 3 months of age, there were very few RGCs remaining, which made analysis difficult (**Fig 2.6**). Therefore, nee mice undergo significant RGC loss with an onset sometime between p16 and p28, which continues throughout the life of the mouse.

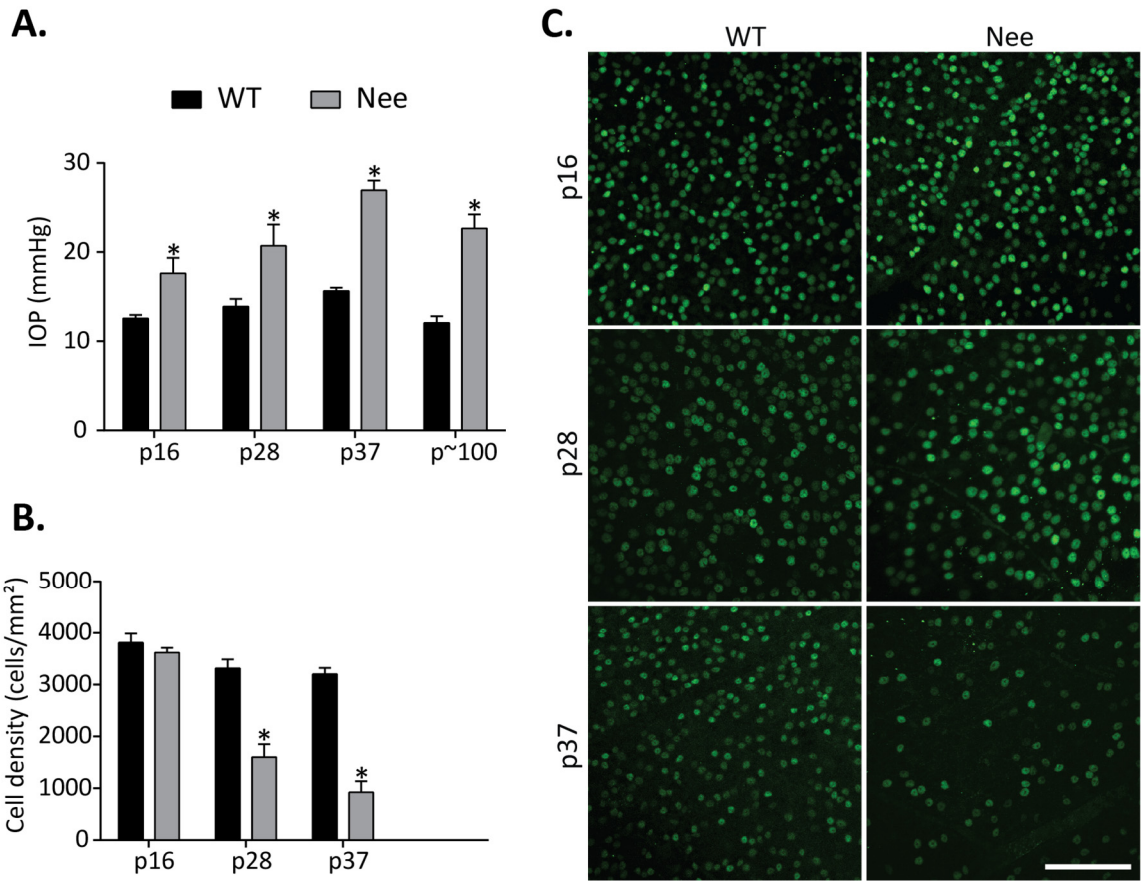

Figure 2.5 - Nee mice develop ocular hypertension and progressive RGC loss. (**A**) Nee mice (grey) have significantly greater IOP compared with wildtype littermates (WT; black) at p16, p28, p37, and at approximately p100. (**B**) RGC densities in nee mice are not significantly different at p16, but are at p28 and p37, from WT, as seen in the representative Brn3a images in **C**. *N* = 5-14, t-tests, * = *P* < 0.05 compared to WT at the given age. Scale bar 100 µm.

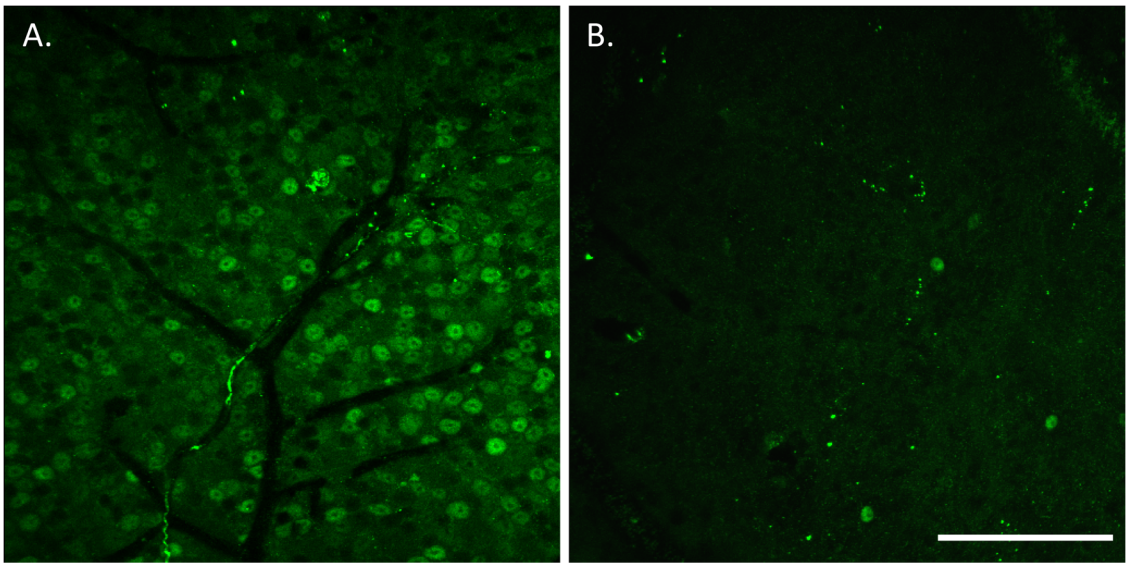

Figure 2.6 - Representative images of retinas from adult mice (p100). (**A**) Retina from an approximately 3 month-old wildtype mouse shows RGC normal density, which is comparable to RGC densities from younger wildtype mice. (**B**) Retina from an aged-matched nee mouse shows dramatic loss of RGCs, with only few cells remaining**.** Scale bar 100 µm.

2.5.1.4 Summary

Taken together, these results suggest that nee mice are an advantageous model for the investigation of glaucoma. Their rapid and consistent onset of pathology makes them an attractive model compared with others available models, including the DBA/2J mouse and the ocular hypertensive bead models.

2.5.2 Ocular Hypertensive Bead Rat Model

This model uses beads to provide resistance to aqueous humor outflow in the anterior chamber, generating an increase in IOP, and resultant RGC loss. As such, the bead model reflects the increased resistance seen in patients with primary open-angle glaucoma (M. Johnson, 2006; Weinreb et al., 2014; Weinreb et al., 2016).

Ocular hypertension was induced in one eye of male Brown Norway rats following a protocol modified from Sappington et al. (2010) and Cone et al. (2010), and was carried out by a technician in the Retina Lab, Michele Hooper. Briefly, rats were anesthetized with isoflurane, and eyes were dilated with 1% tropicamide (Bausch & Lomb, Tampa, FL). A small glass needle (World Precision Instruments, Sarasota, FL; previously pulled with an electrode puller to an approximate diameter of 100 μm; Sutter Instruments Co., Novato, CA) was fitted to a Hamilton syringe (Hamilton Company, Franklin, MA) using polyethylene tubing filled with sterile saline. The needle was then filled with a 10 μL solution containing approximately 3 x 10^7 10 μm polystyrene microbeads (Polysciences Inc., Warrington, PA) suspended in sterile PBS. Once filled, the needle was carefully inserted into the anterior chamber of the eye, and the solution was injected. The needle was held in place following injection for approximately 1 minute to allow the solution to settle prior to removal.

Subsequent monitoring of IOP occurred using the Tonolab handheld tonometer, on awake and unrestrained rats. These recordings were acquired at regular intervals following the induction of ocular hypertension, beginning 3-5 days following injection, and at least every 7 days thereafter.

2.5.3 Optic Nerve Transection

The ONT model was used as a model of IOP-independent RGC death. Axotomies were performed by Dr. Anna-Maria Szczesniak following a protocol adapted from Berkelaar et al. (1994), with animal husbandry and drug administration carried out by myself. Male C57Bl/6 mice were anesthetized using 3% isoflurane at 1 L/min, and then maintained at 2% isoflurane. Once the pedal reflex disappeared, the optic nerve was exposed by creating an incision above the eye between the bone and periocular space. Using fine microscissors, the optic nerve was then cut, avoiding the nearby highly vascularized lacrimal glands, which if touched can lead to significant blood loss. The main incision was then closed by suture, and mice were recovered. Post-operatively, mice received buprenorphine and Lactated Ringer's solution, in order to provide pain relief and fluid resuscitation, respectively. Axotomized mice were kept for 7 days prior to sacrifice.

Chapter 3: THE CONTRIBUTION OF TNFα-INDUCED EXPRESSION OF CPAMPARS IN GLAUCOMATOUS RGC DEATH

3.1 INTRODUCTION

Inflammation is a defence mechanism activated following injury or infection. While in acute settings inflammation aids in restoring homeostasis, chronic activation can be damaging, resulting in cell death and loss of function. There is now significant data supporting glaucoma as a neuroinflammatory disorder, including evidence of “hallmarks" of inflammation, such as reactive gliosis, leukocyte transendothelial migration, complement activation, and cytokine signalling (Mac Nair & Nickells, 2015; Vohra et al., 2013). As the eye is immune privileged, resident glial cells, including Müller glia, astrocytes, and microglia, play an important role in the immune response. Müller glia span the retina, with endfeet in the ganglion cell layer, and in the outer nuclear layer, but make connections with all the neurons through the retina, as well as retinal vessels. Astrocytes are present in the nerve fiber layer, interacting with the vasculature and the unmyelinated axons of retinal ganglion cells (RGCs). Microglia are present primarily in the inner plexiform layer, but are also present in the outer plexiform layer (Mac Nair & Nickells, 2015; Vecino et al., 2016).

Astrocytes, microglia, and Müller glia become activated throughout the course of glaucomatous pathology. However, the contribution of these cells to the developing pathology is not yet fully clear (Mac Nair & Nickells, 2015; Son et al., 2010; Vecino et al., 2016; R. Wang, Seifert, & Jakobs, 2017). Initially, activation of glia appears beneficial, aiding phagocytosis of potentially neurotoxic cellular debris. However, glia can also release proinflammatory cytokines, which can both directly and indirectly contribute to RGC apoptosis (Mac Nair & Nickells, 2015; Vohra et al., 2013). Inhibition of reactive gliosis pharmacologically, through high dose irradiation, or through transcorneal electrical stimulation, can delay and/or reduce RGC death in various models of glaucoma (Baptiste et al., 2005; Bosco et al., 2011; Cueva Vargas et al., 2016; Ganesh & Chintala, 2011; Howell et

al., 2012; Levkovitch-Verbin, Kalev-Landoy, Habot-Wilner, & Melamed, 2006; Livne-Bar et al., 2016; H. Yin et al., 2016).

Data demonstrating that axonal injury can occur independently of retinal glial activation has lead to the hypothesis that retinal glial-mediated apoptosis occurs as a second wave of glaucomatous neurodegeneration (Fitzgerald, Bartlett, Harvey, & Dunlop, 2010; Levkovitch-Verbin et al., 2001; Mac Nair & Nickells, 2015). Initial axonal injury caused by mechanical or ischemic insult results in early reactive gliosis and monocyte infiltration within the axon and optic nerve head. This results in early oligodendrocyte loss, RGC axonal retraction and death, which is later followed by RGC soma loss (Mac Nair et al., 2014; Nakazawa et al., 2006; but see Son et al., 2010). Signals from dying RGC somas (e.g., neurotransmitters, reactive oxygen species [ROS], heat shock proteins, cytokines, and ATP) are then thought to activate retinal glial cells (Krizaj et al., 2014; Mac Nair, Schlamp, Montgomery, Shestopalov, & Nickells, 2016). Upon activation, retinal glia further release cytokines, resulting in potentiation of the inflammatory response, and a second wave of RGC death (Mac Nair & Nickells, 2015; Weber, 2013). Therefore, modulating the inflammatory response may be a possible target to reduce RGC death in the treatment of glaucoma (Mac Nair & Nickells, 2015; Vohra et al., 2013).

3.1.1 The Role of TNFα in Glaucoma

Tumor necrosis factor alpha (TNFα) is a cytokine upregulated in animal models of glaucoma, as well as in humans with glaucoma (Berger et al., 2008; Fontaine et al., 2002; Nakazawa et al., 2006; Roh et al., 2012; Tezel & Wax, 2000; Yang et al., 2011). Polymorphisms in the promotor for TNF, which result in increased TNFα production, are associated with open angle, but not normal tension, glaucoma (Almasieh et al., 2012; Bozkurt et al., 2012; Cueva Vargas & Di Polo, 2016; Fan et al., 2010; Xin, Gao, Wu, & Sun,

2013). As such, TNFα has been increasingly investigated for it's contribution to glaucomatous RGC loss, with hopes of establishing a new therapeutic target.

TNFα promotes either pro-survival or pro-apoptotic pathways, depending on the type of TNFα protein expressed and the receptor (Probert, 2015; Tezel, 2008). TNFα is initially expressed as a transmembrane protein, but can undergo enzymatic cleavage, resulting in a smaller soluble form. Soluble TNFα preferentially binds to TNFα receptor 1 (TNFR1), which is classically associated with initiating extrinsic apoptosis. The membrane bound form of TNFα preferentially binds to TNFR2, which is associated with promoting survival and inflammation, and innate immune responses (Almasieh et al., 2012; Cueva Vargas & Di Polo, 2016; Probert, 2015; Tezel, 2008). Both TNFR1 and TNFR2 are also upregulated in models of glaucoma (Fontaine et al., 2002; Tezel & Wax, 2000; Tezel, 2008).

In the retina, TNFα is produced by Müller cells, astrocytes, and microglia (Cueva Vargas et al., 2016; Lebrun-Julien et al., 2010; Roh et al., 2012; H. Yin et al., 2016). Retinal TNFα from these sources is associated with activation of several signalling cascades, resulting in increased activity of messenger signalling kinases, including c-Jun N-terminal kinases, nuclear factor κ B, and p38-mitogen-activated protein kinases (Dvoriantchikova & Ivanov, 2014; C. Harada et al., 2010; Lebrun-Julien et al., 2009; Nakazawa et al., 2006). Manipulating ocular TNFα, either pharmacologically or genetically, has been associated with both RGC apoptosis and survival, as reviewed below.

A single intravitreal injection of TNFα in otherwise healthy rats and mice leads to delayed RGC death (approximately 8 weeks), preceded by early oligodendrocyte loss (1 week, Kitaoka et al., 2006; Nakazawa et al., 2006). Injection of TNFα also exacerbated ischemic damage and RGC loss (Berger et al., 2008). Further, compared with wildtype mice, TNFα knockout mice (KO) exhibit increased oligodendrocyte and RGC survival in models of

ocular hypertension (Lebrun-Julien et al., 2009; Nakazawa et al., 2006). Consistent with this, administration of a TNFα neutralizing antibody, or block with the TNFα fusion protein etanercept, increased RGC survival following excitotoxic injury (Lebrun-Julien et al., 2009), ocular hypertension (Nakazawa et al., 2006; Roh et al., 2012), and ischemic injury (Berger et al., 2008; Tezel & Wax, 2000). In models of RGC damage, upstream regulation of TNFα expression has also provided neuroprotection, including blockage of membrane-bound Fas ligand (Gregory et al., 2011), apoptosis signal-regulating kinase 1 (C. Harada et al., 2010), and the p75 neurotrophin receptor (Lebrun-Julien et al., 2010), as well as APJ receptor activation (Ishimaru et al., 2017). Transcorneal electrical stimulation following ONT was also associated with reduced TNFα expression, and increased RGC survival (H. Yin et al., 2016).

TNFα-induced mechanisms of glaucomatous RGC death could include direct activation of apoptosis (e.g., by activation of extrinsic apoptotic pathways), or promotion of indirect pathways, including activation of intrinsic apoptotic pathways, downregulation of pro-survival transcription factors, and/or promoting excitotoxicity (Tezel, 2008). Extrinsic activation of apoptosis involves activation of "death receptors," including TNFR1, leading to direct activation of initiator caspase 8. Caspase 8 activation can then lead to either direct activation of executioner caspases (such as caspase 3), or contribute to intrinsic apoptosis through activation of proteins affecting mitochondrial permeability, such as Bid (Thomas et al., 2017). Intrinsic pathways can be initiated by several mechanisms, but ultimately lead to loss of mitochondrial membrane potential, release of cytochrome C, apoptosome formation, and activation of effector caspases and/or apoptosis-inducing factor (Levkovitch-Verbin, 2015; Thomas et al., 2017). TNFα-induced changes in transcription factors, such as nuclear factor κ B, have also been observed, and can promote RGC death (Dvoriantchikova & Ivanov, 2014; Thomas et al., 2017).

Direct activation of caspase 3 through extrinsic activation as is likely not a primary mechanism of glaucomatous RGC loss, as injection of TNFα results in delayed (approximately 8 weeks), rather than immediate death of RGCs (Kitaoka et al., 2006). On the other hand, non-selective inhibition of caspases leads to an approximate 25% increase in cultured RGC survival following TNFα incubation (Tezel & Yang, 2004). Interestingly, survival was increased in this model when combined with a ROS inhibitor, suggesting that TNFα-mediated RGC death may also occur by caspase-independent mechanisms (Tezel & Yang, 2004).

TNFα may also be prompting ocular damage through promotion of excitotoxicity, that is, toxicity caused by improper excitatory signalling (Tezel, 2008). Aberrant excitatory signalling results in neuronal depolarization, and importantly, excessive Ca^{2+} influx. Excessive intracellular Ca^{2+} is cytotoxic, generating damage to mitochondria, leading to release of ROS, and causing activation of calpains and caspases. Although the severe effects of acute excitotoxicity are readily apparent in shellfish poisoning caused by domoic acid, an agonist at excitatory glutamate receptors, excitotoxicity may also contribute to more prolonged neurodegenerative damage in ischemia, trauma (such as spinal cord injury and/or traumatic brain injury), amyotrophic lateral sclerosis, and glaucoma (Almasieh et al., 2012; Casson, 2006; Weiss, 2011).

Research on excitotoxic neurodegeneration has focused on glutamate, the most common excitatory transmitter in the central nervous system (CNS), and its corresponding receptors (Almasieh et al., 2012; Casson, 2006; Weiss, 2011). There are two classes of glutamate receptors, the metabotropic glutamate receptors and the ionotropic glutamate receptors, the latter of which is more commonly investigated in excitotoxic research due to it's ubiquitous CNS expression, ionic permeability to cations, and involvement in fast excitatory neurotransmission(Casson, 2006). Ionotropic glutamate receptors, named after

their respective glutamate-analogue agonists, include *N*-methyl-D-aspartate (NMDA), α-amino-3-hydroxyl-5-methy-4-isoxazolepropronate (AMPA), and kainate receptors. All three receptor types pass Na^+ and K^+, but NMDA and only some types of AMPA and kainate receptors are permeable to Ca^{2+} (Brandstatter, Koulen, & Wassle, 1998; Thoreson & Witkovsky, 1999).

TNFα-induced excitotoxic damage could conceivably be achieved by manipulating pathways that would lead to increased excitatory activity. That is, by increasing excitatory glutamate receptor expression, enhanced glutamate release, and/or by reducing glutamate clearance (Cueva Vargas & Di Polo, 2016). Evidence exists supporting this connection in neuronal tissues outside the eye. For example, TNFα can promote release of glial glutamate (Vesce, Rossi, Brambilla, & Volterra, 2007), but can also increase surface glutamate receptor expression (Leonoudakis, Braithwaite, Beattie, & Beattie, 2004). In the eye, TNFα and excitotoxicity have independently been subject to extensive research for their contributions to glaucomatous RGC loss (Almasieh et al., 2012); however, specific investigation of the general relationship between TNFα and excitotoxicity in glaucoma to date is limited. The following section will describe evidence supporting excitotoxicity separate from TNFα, and conclude by speculating one possible link between these two systems in glaucoma.

3.1.2 Excitotoxicity and Glaucomatous RGC Death

In the eye, intravitreal injection of NMDA leads to rapid and robust RGC apoptosis (Almasieh et al., 2012). As such, increased glutamate release was thought to be a plausible mechanism of glaucomatous RGC loss (Casson, 2006). However, while some studies reported that glutamate is increased in the vitreous of patients with glaucoma, and in some models of glaucoma, repeated experiments were unable to replicate initial reported findings (Almasieh et al., 2012; Osborne, 2009; Salt & Cordeiro, 2006).

Instead, Müller clearance of glutamate was hypothesized to be impaired. Mice which lack functional glutamate transporters have spontaneous RGC damage in the absence of altered intraocular pressure (IOP, T. Harada et al., 2007). Additionally, reduced glutamate transporter expression was associated with RGC death in both the DBA/2J mouse and in ONT (Almasieh et al., 2012). However, Hartwick and colleagues (2005) found that glutamate clearance did not appear impaired in a model of ocular hypertension. Additionally, population studies have revealed that those with polymorphisms in glutamate transporter mechanisms were not associated with normotension glaucoma (Yasumura et al., 2011).

Conceivably, changes in glutamate receptor expression could, therefore, cause excitotoxic damage without requiring a change in glutamate concentration. Changes in glutamate receptor expression has been in noted in models of glaucoma, including upregulation of NMDA receptor mRNA and protein in a rodent model of chronic ocular hypertension (J. H. Kim, Lee, Jung, & Park, 2007). Regardless of whether there is increased glutamate release, reduced glutamate clearance, or changes in glutamate receptor expression, blocking glutamate receptors, and thus prevention of Ca^{2+} entry into RGCs, should provide protection against excitotoxic damage (Almasieh et al., 2012; Casson, 2006).

The NMDA receptor is a non-selective cation channel that is voltage-dependent (extracellularly blocked by Mg^{2+}or Zn^{2+}), but which also requires co-activation by either glycine or D-serine. Much of the initial excitotoxic investigation has focused on NMDA due to its permeability to Ca^{2+}. But while pre-clinical investigation of the NMDA receptor antagonist memantine had promising results, clinical trials using this compound for the treatment of glaucoma did not progress beyond the third phase (Almasieh et al., 2012; Weinreb et al., 2016).

Instead, some studies have suggested that blockade of AMPA and kainate receptors may be more protective than NMDA block in pathologies such as ischemic injury (A. M. Buchan et al., 1993; Gerace et al., 2014; Weiss, 2011). Since excitotoxicity is thought to involve an excess of Ca^{2+}, likely not solely from intracellular stores, attention has recently focused towards investigation of AMPA receptors which are calcium-permeable as a source of this Ca^{2+} (Kwak & Weiss, 2006; Weiss, 2011).

AMPA receptors are tetramers comprised of combinations of four subunits (GluA1-GluA4). Each subunit contains 3 transmembrane regions (M1, M3, andM4), and a hairpin loop (M2), which only partially crosses the membrane. Calcium-permeable AMPA receptors (cpAMPARs) are different from AMPA receptors in either one of two ways, either completely lacking the GluA2 subunit, or by expressing the unedited form of the GluA2 subunit (Fig. 3.1, Diamond, 2011; Henley & Wilkinson, 2016; Weiss, 2011; Wright & Vissel, 2012). In the adult brain, >99% of the GluA2 subunit mRNA undergoes post-transcriptional modification in the M2 region at the "Q/R" site (Wright & Vissel, 2012). This editing replaces adenosine in the 607th codon (C**A**G), coding for glutamine (Q), with inosine, which codes for arginine (R). While glutamine is neutral, arginine is positively charged, causing electrostatic repulsion within the channel pore. Receptors containing edited GluA2 therefore display impermeability to divalent cations, such as Ca^{2+}, but remain permeable to Na^{+} and K^{+} (Hume, Dingledine, & Heinemann, 1991; Wright & Vissel, 2012). As the remaining subunits contain only glutamine at this site, AMPA receptors not containing the GluA2 subunit also have a negative core, and therefore are also Ca^{2+}-permeable (Diamond, 2011; Henley & Wilkinson, 2016; Weiss, 2011; Wright & Vissel, 2012).

Basal expression of cpAMPARs varies by cell type (Henley & Wilkinson, 2016; Weiss, 2011). In general, cpAMPAR expression is more prominent in early post-natal neurons than in adult (Henley & Wilkinson, 2016). However, there are exceptions; some neural cell types

Figure 3.1 - The permeability of AMPA receptors is determined by the GluA2 subunit. AMPA receptors are tetramers made up of various combinations of its subunits (GluA1-4). However, the status of the GluA2 subunit determines calcium permeability. **(A)** In the brain, >99% of GluA2-containing AMPA receptors are edited at the "Q/R" site on the transmembrane region. **(B**) A post-transcriptional modification which results in a neutrally charged glutamine (Q), in place of a positively charged arginine (R), creating electrostatic repulsion of divalent cations within the receptor pore. Calcium-permeable AMPA receptors either express unedited GluA2, or lack the GluA2 subunit.

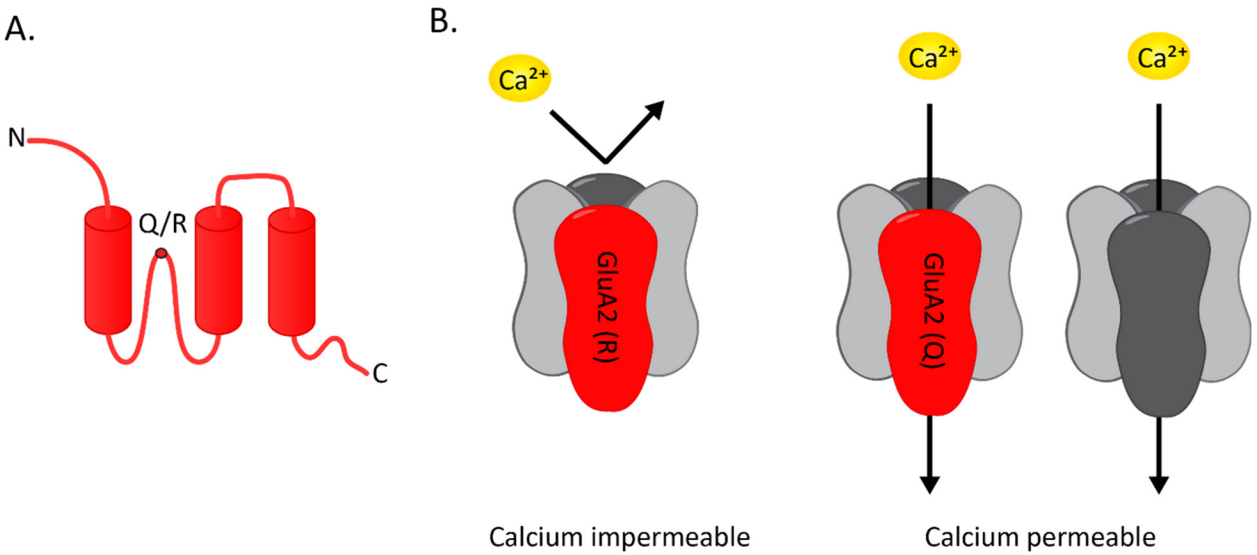
A.
N
Q/R
C
B.
Ca2+
GluA2 (R)
Ca2+
Ca2+
GluA2 (Q)
Calcium impermeable
Calcium permeable

retain populations throughout adulthood, though very limited in comparison to the population of calcium-impermeable AMPA receptors. For example, GABAergic inhibitory interneurons retain a significant population of cpAMPARs throughout adulthood. On the other hand, while hippocampal pyramidal cells express high levels of cpAMPARs during development, expression in adults is reduced (Henley & Wilkinson, 2016).

Having proportionally limited expression does not mean that the receptor is not functionally important. Accumulating evidence has demonstrated that GluA2 lacking cpAMPARs, in particular, may be involved in synaptic plasticity and in long-term potentiation, and have been suggested to be involved with addiction and fear conditioning (Conrad et al., 2008; Henley & Wilkinson, 2016; Scheyer et al., 2016; Stellwagen & Malenka, 2006; Weiss, 2011; Werner et al., 2017; Wolf & Tseng, 2012)

Congruent with a proposed important role of AMPA receptors in retinal excitotoxic damage, increases in cpAMPAR surface expression have also been found in some injury and/or disease models, including ischemia, spinal cord injury, traumatic brain injury, ALS, and Alzheimer's disease - diseases known to have excitotoxic components (Gerace et al., 2014; Henley & Wilkinson, 2016; Noh et al., 2005; Weiss, 2011; Wright & Vissel, 2012). Further, inhibiting cpAMPARs directly or indirectly in some cases has been associated with increased neuronal survival in these models (Gerace et al., 2014; Y. Liu et al., 2013; Noh et al., 2005; Weiss, 2011; Wright & Vissel, 2012; H. Z. Yin et al., 2012).

3.1.3 A Link Between TNFα and Excitotoxicity

The relationship between TNFα and AMPA receptors was first demonstrated by Beattie and colleagues in 2002. They reported that a 15 minute TNFα application significantly increased AMPA expression in co-cultured hippocampal neurons, and

increased frequency, but not amplitude, of miniature excitatory post synaptic currents. Interestingly, sequestration of TNFα, by addition of soluble TNFR1 in the absence of added TNFα, decreased AMPA receptor expression, suggesting a mechanism of constitutive regulation of receptor expression (Beattie et al., 2002). Soon after, Stellwagen and colleagues (2005) published a follow up study demonstrating TNFα administration in hippocampal neurons increased GluA1, but not GluA2 surface expression, through the activation of TNFR1. However, Ogoshi et al. (2005) found that in their hippocampal cultures, both surface expression of GluA1 and GluA2 was increased following TNFα application. Of note, this paper also reported an increase in AMPA-induced changes in intracellular Ca^{2+} following TNFα exposure, suggestive of an increase in cpAMPAR expression (Ogoshi et al., 2005). This provided the first functional evidence that TNFα can increase intracellular Ca^{2+}, potentially leading to excitotoxic neuronal loss, by increasing cpAMPAR expression (Ogoshi et al., 2005).

Following these initial studies, several groups have reported similar relationships between TNFα and cpAMPAR expression in cortical neurons (J. H. Hu et al., 2010; Leonoudakis et al., 2004; Steinmetz & Turrigiano, 2010), dorsal horn neurons (Han & Whelan, 2010; Wigerblad et al., 2017), and spinal motor neurons (H. Z. Yin et al., 2012). Additionally, this mechanism has been implicated with evidence of neuronal loss in some injury and disease models, such as spinal cord trauma (Ferguson et al., 2008), as well as excitotoxicity-induced loss of motor neurons (H. Z. Yin et al., 2012) and hippocampal neurons (Leonoudakis, Zhao, & Beattie, 2008). For example, nanoinjection of TNFα into the spinal cord caused an increase in GluA1 surface expression on motor neurons, similar to the effect observed following induction of a contusion spinal cord injury (Ferguson et al., 2008). Correspondingly, use of a soluble TNFα receptor decoy following injury was associated with a decrease in GluA1 surface expression, as well as a decrease in neuronal loss (Ferguson et

al., 2008). As TNFα-mediated increases in cpAMPARs could possibly play a role in excitotoxic injury in other models of neuronal degeneration, it is possible that this mechanism could be involved in glaucomatous RGC loss.

In the adult retina, cpAMPARs are expressed in the outer plexiform layer, inner nuclear layer, and inner plexiform layer, corresponding with expression in horizontal and amacrine cells (Diamond, 2011; Osswald, Galan, & Bowie, 2007). However, as discovered in other neuronal types (Henley & Wilkinson, 2016; Wright & Vissel, 2012), cpAMPAR expression in the retina also changes throughout development. In neonates, cpAMPARs are also expressed in rat ganglion cell layer, potentially corresponding with either displaced amacrine cells or RGCs, but this expression appears to decrease following eye opening (Osswald et al., 2007). However, ON-RGCs (an RGC subtype), at least, may contain cpAMPARs into adulthood (Jones, Carroll, & Nawy, 2012; Xia, Carroll, & Nawy, 2006; Xia, Nawy, & Carroll, 2007). Further, following eye opening, the type of cpAMPARs expressed also changes in horizontal and amacrine cells. While GluA2-lacking cpAMPARs (and therefore assumed cpAMPARs containing unedited GluA2) predominate prior to eye opening, following eye opening they are replaced with GluA2-containing cpAMPARs. As the retina matures, the cpAMPAR population in amacrine cells partially reverts to GluA2-lacking, while horizontal cells remain primarily GluA2-containting (Osswald et al., 2007).

A few studies have provided evidence that AMPA receptor expression, and/or specifically cpAMPAR expression, is altered in models of RGC injury. Primary evidence here comes from models of retinal hypoxia (Park et al., 2016; Sivakumar, Foulds, Luu, Ling, & Kaur, 2013), excitotoxicity (Challenor et al., 2015; Lebrun-Julien et al., 2009; Park, Mueller, McGrady, Ma, & Yorio, 2015), and ocular hypertension (Dong et al., 2015; A. L. Wang, Carroll, & Nawy, 2014). Similarly, blocking AMPA receptors has been protective in retinal culture models of hypoxia (Sivakumar et al., 2013), oxygen-glucose deprivation (Park et al.,

2016), and excitotoxicity (Lebrun-Julien et al., 2009; Park et al., 2015; A. L. Wang et al., 2014). Further, specific evidence of the neuroprotective effects of blocking cpAMPARs has been demonstrated in an ocular excitotoxic model (Lebrun-Julien et al., 2009), in an *in vivo* model of RGC death where GluA2 expression was decreased (Dong et al., 2015), and in a model of chronic ocular hypertension (Cueva Vargas et al., 2015).

However, there are difficulties in both measuring and interpreting cpAMPAR expression and contributions. Simply measuring AMPA receptor expression, either in general or per subunits, cannot always be generalized to cpAMPAR expression. Even still, even small changes in expression may have significant functional impact that may not be readily detectible by analysis of mRNA or protein expression (Wright & Vissel, 2012). Instead, direct measurement of cpAMPARs using selective probes, antagonists, and/or functional measurements (such as Ca^{2+} dynamics) are essential for measuring expression and contribution of these receptors to cellular function and pathology.

Ca^{2+} imaging of live neurons allows simultaneous measurement of calcium dynamics in multiple living cells. Such a technique can be used both in culture, to isolate specific responses, but also *in situ*, with the cells remaining within their normal circuit. Fura-2 pentapotassium salt, a ratiometric calcium indicator dye, can be loaded into living retinal RGCs by a technique that was adapted by a former trainee in the Retina Lab, Dr. Bryan Daniels (Daniels, 2011). This technique was based on a protocol developed for spinal cord, where electroporation is routinely used to load viral vectors for gene transfer. Electroporation allows for relatively consistent, immediate, and stable loading of freshly isolated retina. This enables investigation of tissue that has not been outside its natural environment for an extended period, and therefore potentially reducing changes in protein expression (that has been noted previously, including with ONT itself; Agudo et al., 2008; Agudo et al., 2009). How electroporation facilitates loading of cells is unknown; however, it

is thought that the electrical field may transiently disrupt the lipid membranes, creating temporary pores that enable diffusion into the cytoplasm (Daniels, 2011). Electroporation is also advantageous in that it's stable loading allows for measurement of changes in calcium dynamics after pharmacological manipulation not only between experiments, but depending on the protocol, also within the same cell.

3.1.4 OBJECTIVES

As most of the prior investigation of cpAMPARs has occurred either in cell cultures that do not fully reflect the dynamic nature of the retina, or have relied on methods of investigation that may limit the meaningfulness of the data due to lack of functional testing, I sought to employ functional measurements in order to acquire a better understanding of these changes. Therefore, the first objective of this chapter was to investigate the hypothesis that cpAMPARs are upregulated in glaucoma by demonstrating the difference in functional contribution (calcium dynamics) of cpAMPARs in RGCs in naïve animals compared with models of ocular hypertension.

Further, the direct connection between TNFα and cpAMPARs in RGCs has yet to be demonstrated functionally. Therefore, the second objective of this chapter was to investigate the hypothesis that direct application of TNFα can increase cpAMPAR expression in *ex vivo* retina.

3.2 MATERIALS AND METHODS

3.2.1 DRUGS AND REAGENTS

AMPA, MK801, and IEM1460 were acquired from Tocris (Bio-Techne, Minneapolis, MN). Recombinant mouse TNFα was purchased from R&D systems (Minneapolis, MN).

Unless otherwise indicated, all other drugs were acquired from Sigma Aldrich (Oakville, ON).

3.2.2 Ca^{2+} IMAGING

To assess contributions of cpAMPARs to changes in intracellular Ca^{2+} in RGCs, Ca^{2+} imaging was carried out *ex vivo* on live, isolated retinas, adapted from a protocol by Daniels (2011). Following sacrifice with sodium pentobarbital, eyes were enucleated and placed in 100% O_2 bubbled Hank's Balanced Salt Solution (HBSS, Sigma Aldrich) buffered with 10 mM HEPES (pH 7.4) made the day of the experiment. RGCs were loaded with fura-2 pentapotasium salt (fura-2, Invitrogen, Burlington, ON), a ratiometric Ca^{2+} indicator dye. Daniels (2011) previously reported 66.7 ± 7.3% colocalization of fura-2 positive cells in the ganglion cell layer of rats with retrograde labelled RGCs via rhodamine dextran from the superior colliculus. Additionally, while the majority of cells labelled via this method are RGCs, some fura-2 positive cells did not colocalize with the retrograde label, and therefore the presence of displaced amacrine cells within the sampled population cannot be ruled out (Daniels, 2011).

In mice, a small hole was made through the optic nerve using a 30G needle, followed by injection of 750 nL of 20 mM fura-2. The eye was then electroporated using Tweezertrodes™ (BTX, Holliston, MA), placed with the anode on the anterior pole and cathode on the posterior pole, and was subject to 5 square 10 ms 30 V 1 Hz pulses (ECM 830 electroporation system, BTX). The retina was then quickly isolated and mounted ganglion cell layer up on black filter paper (Millipore, Bedford, MA). The retina was then allowed to recover for at least 30 minutes in 100% O_2-bubbled HBSS in low light. A similar protocol was followed for rat eyes, except for the following: 4 µL of 30 mM of fura-2 was

administered with cathodes were placed in reverse polarity, and eyes were subject to 50 ms 40 V pulses.

For imaging, mounted retinas were placed in a superfused chamber with a flow rate of 1 mL/minute, and held in place using a circular harp made from platinum wire. All drugs were made the day of the experiment by dilution with HBSS. Drug treatments occurred by bath application by manually switching the input of the superfuser from the HBSS to the drug solution for 30 seconds (unless otherwise indicated). All drugs were administered in the presence of the NMDA receptor blocker MK801 (10 μM in mice, 20 μM in rats), to prevent secondary influx of Ca^{2+} as a result of RGC depolarization by NMDA receptor activation. Following each drug treatment, retinas were recovered for 10 minutes.

To acquire images and control shutter switching, Imaging Workbench 4 (Molecular Devices, Sunnyvale, CA) was used. Retinas were excited at 340 and 380 nm, and fura-2 image pairs were acquired at 540 nm with a 400 ms exposure. Images were acquired using a CCD camera (Sensicam, PCO, Germany), every 20 s in the absence of drug, and every 5 s following drug-induced stimulation. All recordings were saved for offline analysis.

A response was measured in a manually defined region of interest as the difference between the baseline fura-2 ratio (340/380 nm) signal prior to drug treatment and the maximum response within 180 s following drug treatment. Changes in the fura-2 ratio indicate changes in intracellular Ca^{2+}. However, as a corresponding Ca^{2+} concentrations were not calculated, changes in fura-2 ratio are referred to as simply "calcium responses." Ca^{2+} responses from each retina were averaged, with each *N* corresponding to the number of individual experiments, rather than the number of sampled cells.

3.3 RESULTS

3.3.1 cpAMPAR CONTRIBUTIONS TO AMPA-INDUCED CALCIUM DYNAMICS IN NAÏVE MICE AND RATS

In order to assess cpAMPAR contributions to calcium dynamics in naïve mice and rat retinas, I first began by investigating calcium responses with the AMPA receptor selective agonist AMPA. Fura-2 loaded retinas were subjected to varying doses of AMPA. AMPA administration in naïve adult male C57Bl/6 mice (1-100 μM) produced a dose-dependent increase in calcium responses (**Fig. 3.2A**). EC_{50} was calculated by using a 3 parameter non-linear fit, and was estimated as $\log EC_{50}$ -5.496 ± 0.3892 (3.189 μM). Similarly, AMPA administration in naïve male Brown Norway rats (1-250 μM) also produced a dose-dependent increase in calcium response (**Fig. 3.2B**). EC_{50} for the AMPA response in rat was estimated as $\log EC_{50}$ -4.75 ± 0.3594 (17.80 μM). Doses of AMPA greater than the EC_{50} were chosen for study going forward, e.g., 10 μM in mice and 50 μM in rats.

At the present time, there is no agonist that is selective for cpAMPARs. However, IEM1460 is a selective antagonist for GluA2-lacking cpAMPARs. Therefore, the contribution of cpAMPARs to AMPA-induced changes in intracellular Ca^{2+} were assessed by comparing the calcium response in the absence, and then the presence of IEM1460 (Daniels, 2011). To facilitate cpAMPAR antagonism, following recovery from an initial AMPA application, retinas were bath applied with 100 μM IEM1460 for 5 minutes, followed by a 30 s dose of 100 μM IEM1460 with the appropriate dose of AMPA. The dose of IEM1460 (100 μM) was based on previous reports *in vitro* (Tikhonov et al., 2000), and *in vivo* (Lebrun Julien et al., 2009). While this protocol involves repeated dosing in one population, Daniels (2011) previously reported that there was little variability within ganglion cell layer neurons in response given three consecutive administrations of either kainate or potassium. Therefore,

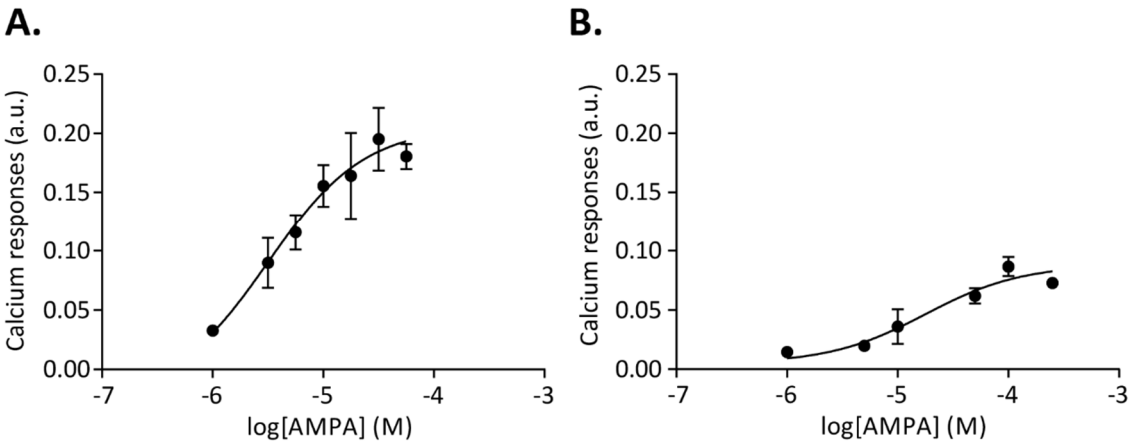

Figure 3.2 - Calcium dynamics in mouse and rat ganglion cell layer neurons with increasing doses of AMPA. Ganglion cell layer neurons loaded with the ratiometric Ca^{2+}-indicator dye fura-2 pentapotassium salt via electroporation display AMPA dose-dependent increases in calcium responses in both naïve mouse (**A**) and rat (**B**) retinas. *N* = 2-10 experiments per dose.

any changes in calcium dynamic observed should be only a result of pharmacological manipulation. Responses in each cell were normalized to the initial response (100%) prior to analysis to reduce variation due to differences in absolute response size between cells, with Tukey's repeated measures one-way ANOVA used for analysis.

In p28 wildtype mice, the calcium response produced by administration of IEM1460 with AMPA produced a slight, but not significantly different response from the response produced by AMPA alone ($P > 0.05$, mean difference 14.11 ± 6.56%, $N = 6$ experiments; **Fig. 3.3A,C**). Following washout, a recovery dose of AMPA produced a response which was also not significantly different from the initial response ($P > 0.05$, mean difference -3.71 ± 6.56%), indicating that no run-down of the response occurred. Similarly, in naïve rats, IEM1460 administration also did not result in a significant change in the AMPA-induced calcium response ($P > 0.05$, mean difference 14.30 ± 16.14%, $N = 6$ experiments; **Fig. 3.3B, D**). Washout did not produce a significant effect ($P > 0.05$, mean difference -11.52 ± 16.14%). Taken together, these results suggest that cpAMPARs do not significantly contribute to AMPA-induced calcium responses in naïve mice and rats.

3.3.2 cpAMPAR Contribution to AMPA-Induced Calcium Dynamics is Altered in Nee Mice

Potential changes in cpAMPAR expression was then investigated in a mouse model of ocular hypertension, the nee mouse. Nee mice display significantly elevated IOP and RGC loss, which persists throughout their lifespan (**Chapter 2**). As TNFα upregulation occurs early but appears transient, at least in some models of glaucoma (Roh et al., 2012), I chose the earliest time point where mice had significant RGC loss. At 16 post-natal days (p16), RGC densities in nee were not significantly different than control. However, at p28, nee mice had a mean RGC loss of 51.7 ± 9.6% (**Fig. 2.5B**).

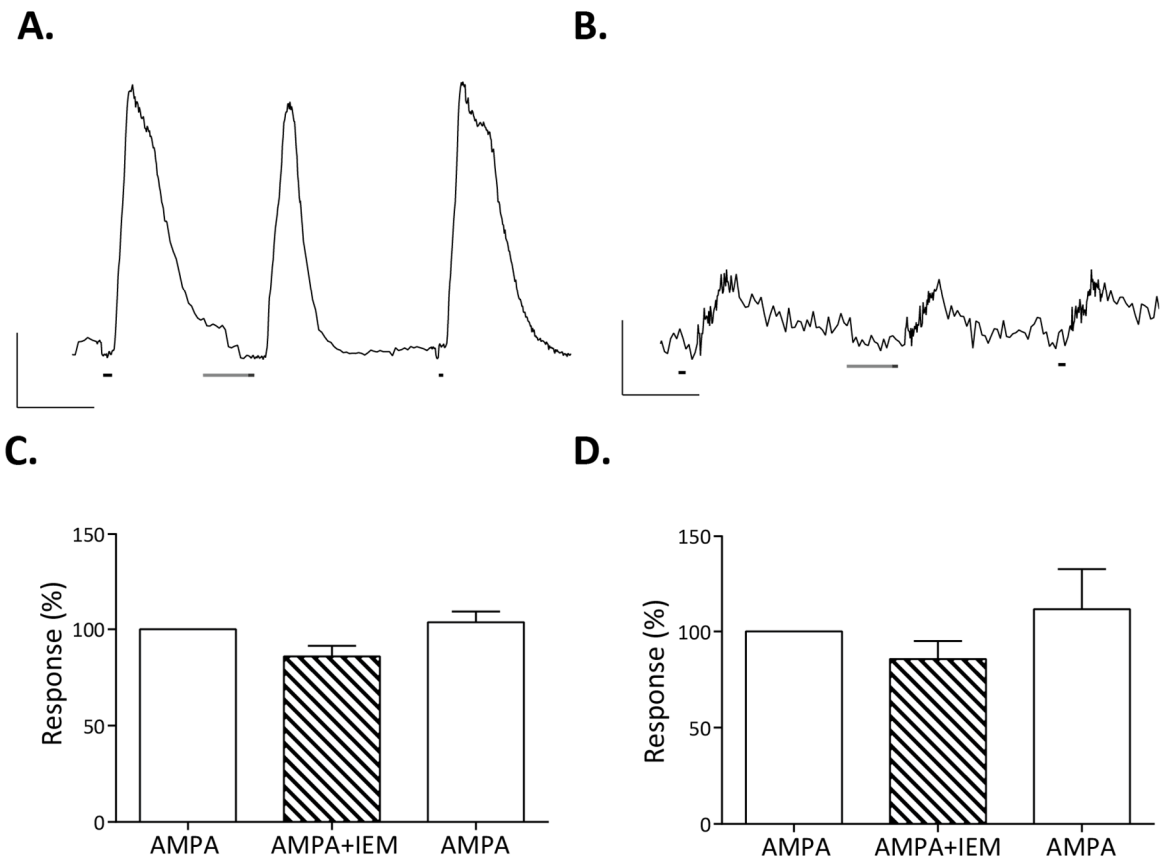

Figure 3.3- Calcium-permeable AMPA receptors do not contribute to AMPA-induced calcium responses in naïve mouse and rat ganglion cell layer neurons. (**A**) Example traces from a p28 wildtype mouse and (**B**) adult rat ganglion cell layer neuron showing similar calcium responses in the presence and absence of the cpAMPAR antagonist IEM1460. AMPA was first administered alone (30s, 10 μM in mouse and 50 μM in rat, first peak), followed by 5 min incubation with IEM1460 alone (100 μM), then a combined dose of AMPA and IEM1460 (30s, second peak), followed by another 30s administration of AMPA alone (third peak). Summary graphs from (**C**) p28 wildtype mice and (**D**) adult rat, normalized to the initial AMPA response, show no significant difference between AMPA responses in the presence of IEM1460. Black bars indicate AMPA application, grey bar indicates IEM1460 administration. *N* = 6 retinas in each group. Tukey's repeated one-way ANOVA. Scale bars represent 500 s on x-axis, 0.1 fura-2 arbitrary units on the y-axis.

Co-administration of IEM1460 and AMPA in male and female p28 nee mice resulted in a significant reduction in the AMPA-induced calcium response ($P < 0.0001$, mean difference 26.23 ± 4.66%, $N = 14$ experiments; **Fig. 3.4**). This effect was recovered with the washout AMPA application ($P < 0.01$, mean difference -18.96 ± 4.66% compared with IEM1460 + AMPA), and was not significantly different from the initial AMPA response ($P > 0.05$, mean difference 7.40 ± 4.66%).

In comparison to naïve wildtype mice, the IEM1460-sensitive response was significantly greater in nee mice ($P < 0.05$, mean difference 12.25 ± 5.59%; **Fig. 3.5**), suggesting that cpAMPAR contribution to the AMPA-induced calcium response is greater in these mice. These data are consistent with an increase in TNFα resulting in an increase in cpAMPARs, similar to observations in other models of RGC injury (Lebrun-Julien et al., 2009; Roh et al., 2012; Cueva Vargas et al., 2015).

3.3.3 cpAMPAR Contributions are not Significantly Altered in Bead Rats

To verify these findings in another model, cpAMPAR contribution to AMPA-induced calcium responses was investigated in a rat model of ocular hypertension (OHT). Intraocular bead administration in rats (**Fig. 3.6A**) reduces aqueous humor outflow by occluding the anterior chamber angle, producing an increase in IOP, typically becoming significantly elevated approximately 1 week post-injection. Approximate RGC damage was assessed by tracking the integral of the difference in IOP between control and ocular hypertensive eyes (ΔIOP) by the number of days post-injection. Integral values of 1000-2000 mmHg-days (e.g., ΔIOP 20 mmHg for 50-100 days) has been previously demonstrated to be associated with significant RGC axonal damage (Chauhan et al., 2002).

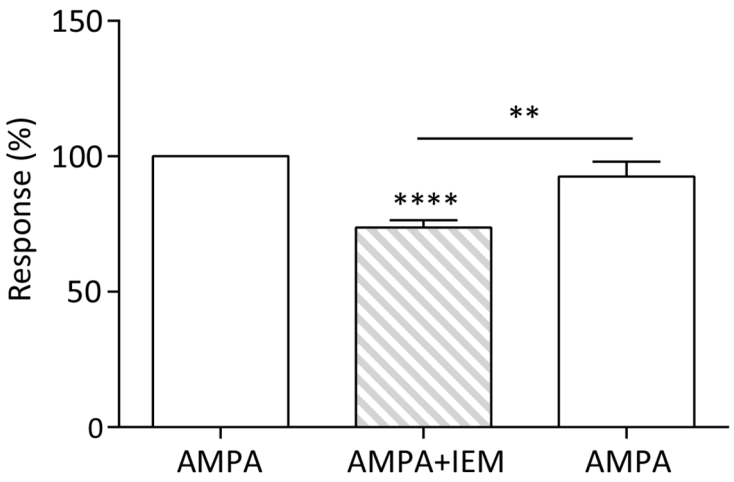

Figure 3.4 - Calcium-permeable AMPA receptors contribute to AMPA-induced calcium responses in nee ganglion cell layer neurons. Mean AMPA responses in the presence of IEM1460 are significantly less than the AMPA response alone, either prior to or following IEM1460 administration. *N* = 14 retinas. Tukey's repeated one-way ANOVA. ** = $P < 0.01$, **** = $P < 0.0001$.

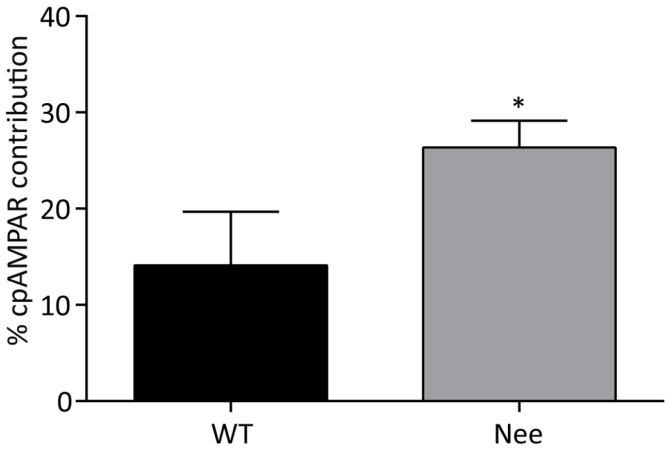

Figure 3.5 - Calcium-permeable AMPAR contribution to AMPA-induced calcium responses in p28 mice . The IEM1460-sensitive AMPA-induced calcium response is greater in nee mice (grey) compared to wildtype littermates (WT; black). *N* = 14 and 6 retinas, respectively. T-test. * = $P < 0.05$.

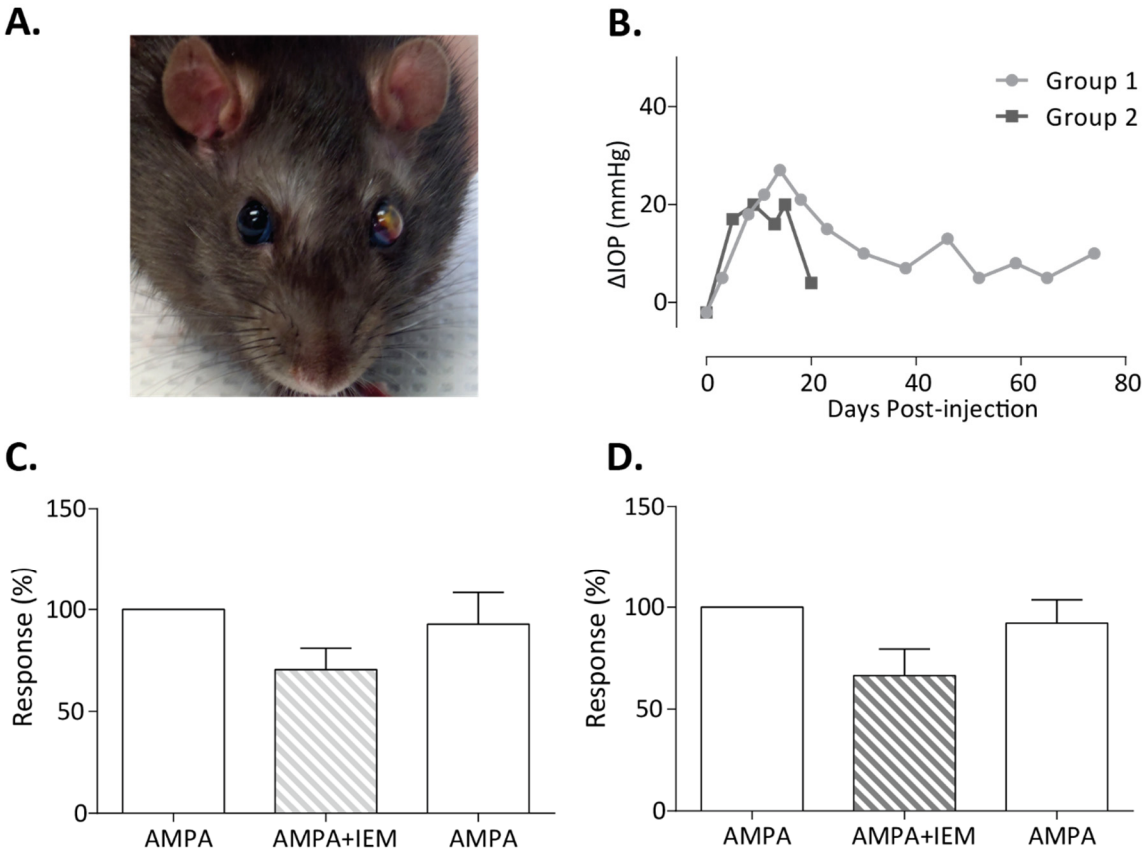

Figure 3.6 - Calcium-permeable AMPA receptors do not contribute to AMPA-induced calcium responses in ocular hypertensive rat. (**A**) Ocular hypertension (OHT) was induced in the left eye of Brown Norway rats by injection of polystyrene beads into the anterior chamber. (**B**) Transient increases in IOP, as shown in two representative IOP time courses, in the OHT model. Two groups of OHT rats were used, the first with a mean damage integral of 785 ± 94 mmHg-days (>65 days post-injection; Group 1, light grey), and the second having a mean damage integral of 322 ± 76 mmHg-days (21-36 days post injection, Group 2, dark grey). The mean normalized responses of Group 1 (**C**) and Group 2 (**D**), ganglion cell layer neurons show non-significant changes in AMPA response (50 μM) in the presence of IEM1460 (100 μM). *N* = 5 retinas in each group. Tukey's repeated one-way ANOVA.

The first group of rats investigated had an average integral of 785 ± 94 mmHg-days and were more than 65 days post-injection (range 66-89, **Fig. 3.6B**, "OHT – Group 1"), which corresponded with approximately 80% RGC axon loss (Chauhan et al., 2002). Combined AMPA and IEM1460 administration in this group of rats did not produce a significantly different calcium response than AMPA alone ($P > 0.05$, mean difference 29.46 ± 11.50%, $N = 5$ experiments; **Fig. 3.6C**). A third AMPA dose following recovery was also not significantly different from the initial response ($P > 0.05$, mean difference 7.18 ± 11.50%). These results suggest that, like naïve rats, cpAMPARs did not significantly contribute to the AMPA-induced calcium response measured at this time point (>65 days post-injection) in this model of ocular hypertension.

Given that there is a significant lag in time prior to significant observable RGC loss in the rat bead-induced OHT model, it is possible that early changes following induction of OHT may result in early transient changes in cpAMPAR expression which are not observed as the pathology progresses. This is supported by studies showing early gliosis, prior to RGC degeneration (reviewed in Almasieh et al., 2012; Mac Nair and Nickells, 2015). Therefore, IEM1460-sensitive AMPA-induced calcium responses were investigated in bead rats 21-36 days post-injection (average integral 322 ± 76 mmHg-days, **Fig. 3.6B**, "OHT – group 2"), corresponding with an approximate 32.5% loss of RGC axons (Chauhan et al., 2002). As seen in retinas with the higher integral, IEM1460 combined with AMPA did not produce a significantly different response than AMPA alone ($P > 0.05$, mean difference 33.56 ± 13.13%, $N = 5$ experiments; **Fig. 3.6D**). The third AMPA administration also did not result in a significantly different effect (mean difference 7.86 ± 13.13%).

Compared to naïve rats, IEM1460-sensitive contributions to AMPA-induced calcium responses were not significantly different in either ocular hypertensive rat group (mean difference -15.16 ± 15.31% in the higher integral group and -19.26 ± 15.31% in the earlier

group; **Fig. 3.7**). Taken together, these results suggest that there is no difference cpAMPAR contribution to AMPA-induced calcium responses in naïve and ocular hypertensive rats.

3.3.4 Bath Application of TNFα Alters Calcium Dynamics in Naïve Mouse

Next, the effects of administration of TNFα on AMPA-induced calcium responses were examined in naïve mouse retinas. Since TNFα may also modulate the activity of other ionotropic receptors, including on other retinal cells aside from RGCs (Cueva Vargas et al., 2015; Stellwagen & Malenka, 2006), working solutions for these experiments also included picrotoxin and strychnine, in order to block inhibitory synaptic input to RGCs via glycine and GABA receptors, respectively. This should reduce any depolarization-induced suppression of excitation though modulation of receptors on retinal cells upstream from RGCs, aiding in isolation of responses from RGCs themselves (Daniels, 2011).

Following an initial AMPA administration and recovery, naïve mouse retinas were subjected to varying lengths of bath applied TNFα (10^{-3} μg/μL, chosen based on previous *in vivo* studies in the eye, and *in vitro* studies in isolated neurons; Leonoudakis et al., 2008; Nakazawa et al., 2006; Ogoshi et al., 2005; Zhao, Leonoudakis, Abood, & Beattie, 2010). In order to do so, the tubes feeding the bathing apparatus were closed, forming a loop so that the TNFα could be recirculated through the system during incubation, rather than having fresh bath solution continuously running through. AMPA-induced calcium responses were then investigated immediately following bath application (and re-opening the bathing apparatus circuit), and 15 and 30 minutes later. Because such a closed-system may result in release of retinal factors which may affect cellular function, these experiments were analyzed in comparison to vehicle-treated retinas (unpaired t-test at each time point), rather than to the initial response.

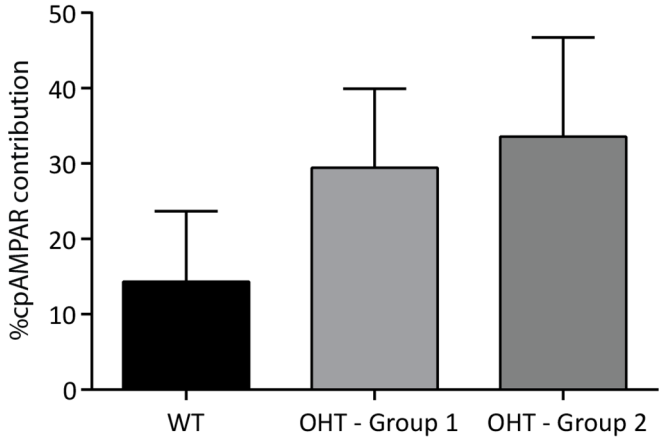

Figure 3.7 - Calcium-permeable AMPAR contribution to AMPA-induced calcium responses is not significantly different in ocular hypertensive rat. While the mean IEM1460-sensitive AMPA response in ocular hypertensive rat (grey bars, N = 5 retinas in each group) appears greater than in normotensive rat (WT, black, N = 6 retinas), there is no significant difference. Dunnett's one-way ANOVA compared with normotensive rat.

Following 15 minutes of bath administered 10^{-3} µg/µL TNFα, compared with control retinas receiving vehicle, there was no significant difference in AMPA-induced calcium responses immediately following application (mean difference 16.21 ± 24.63%, *N* = 5-6; **Fig 3.8A-B**), or 15 or 30 minutes thereafter (mean difference 49.50 ± 25.60% and -14.86 ± 46.19%, respectively). Similarly, bath application of TNFα for 30 minutes did not produce a significant effect on AMPA-induced calcium responses immediately following TNFα (mean difference 4.24 ± 15.66%), but resulted in a significant reduction 15 minutes thereafter (mean difference -27.62 ± 9.14%), which was recovered 15 minutes later (30 minutes following incubation, mean difference 0.35 ± 17.58%, *N* = 4-5; **Fig 3.8C-D**). However, 45 min bath application significantly increased AMPA-induced calcium responses compared with control ($P < 0.001$, mean difference 75.45 ± 10.86%, *N* = 4-6; **Fig 3.8E-F**), and this increase was sustained at 15 ($P < 0.0001$, mean difference 65.34 ± 8.50%) and 30 minutes thereafter ($P < 0.05$, mean difference 48.68 ± 18.52%). These results suggest that 45 minute incubation of TNFα induces a rapid increase in cpAMPARs, similar to previous observation in cultured hippocampal neurons (Leonoudakis et al., 2008; Ogoshi et al., 2005).

3.4 DISCUSSION

In this chapter, I have demonstrated that AMPA administration invokes a dose-dependent increase in calcium responses in both naïve mice and rat isolated retinas. However, cpAMPARs do not appear to be significantly contributing to these responses in naïve rat and mouse. In nee mice, on the other hand, cpAMPARs played a greater contribution to AMPA-induced calcium responses; though, this contribution was not replicated at the time points investigated in ocular hypertensive bead rat. Additionally, I have demonstrated that bath application of TNFα on isolated retinas can increase AMPA-induced calcium responses in naïve mouse ganglion cell layer neurons. These findings

Figure 3.8 - TNFα alters calcium dynamics in naïve mouse ganglion cell layer neurons. Representative traces of TNFα-incubated retinas (**A, C, E**), and mean normalized responses (to the initial AMPA response; 10 μM, **B, D, F**) following AMPA administration in the absence (black) or presence (grey) of 10^{-3} μg/μL TNFα (second peak) for either 15 (**A**,**B**), 30 (**C**,**D**), or 45 mins (**E**,**F**), followed by two additional AMPA responses 15 and 30 mins later (third and fourth peaks). (**A,B**) A 15 min incubation in TNFα did not alter AMPA responses. (**C,D**) However, a 30 min TNFα incubation resulted in a small, but significant, decrease in the third AMPA response (15 minutes following recovery from TNFα incubation. **E,F**). Forty-five min incubation with TNFα resulted in significantly increased in AMPA-induced calcium responses immediately following incubation, but also 15 and 30 mins later. *N* = 4-6 experiments per group. T-tests. * = $P < 0.05$, *** = $P < 0.001$, **** = $P < 0.0001$. Scale bars represent 500 s on x-axis, 0.1 fura-2 arbitrary units on the y-axis.

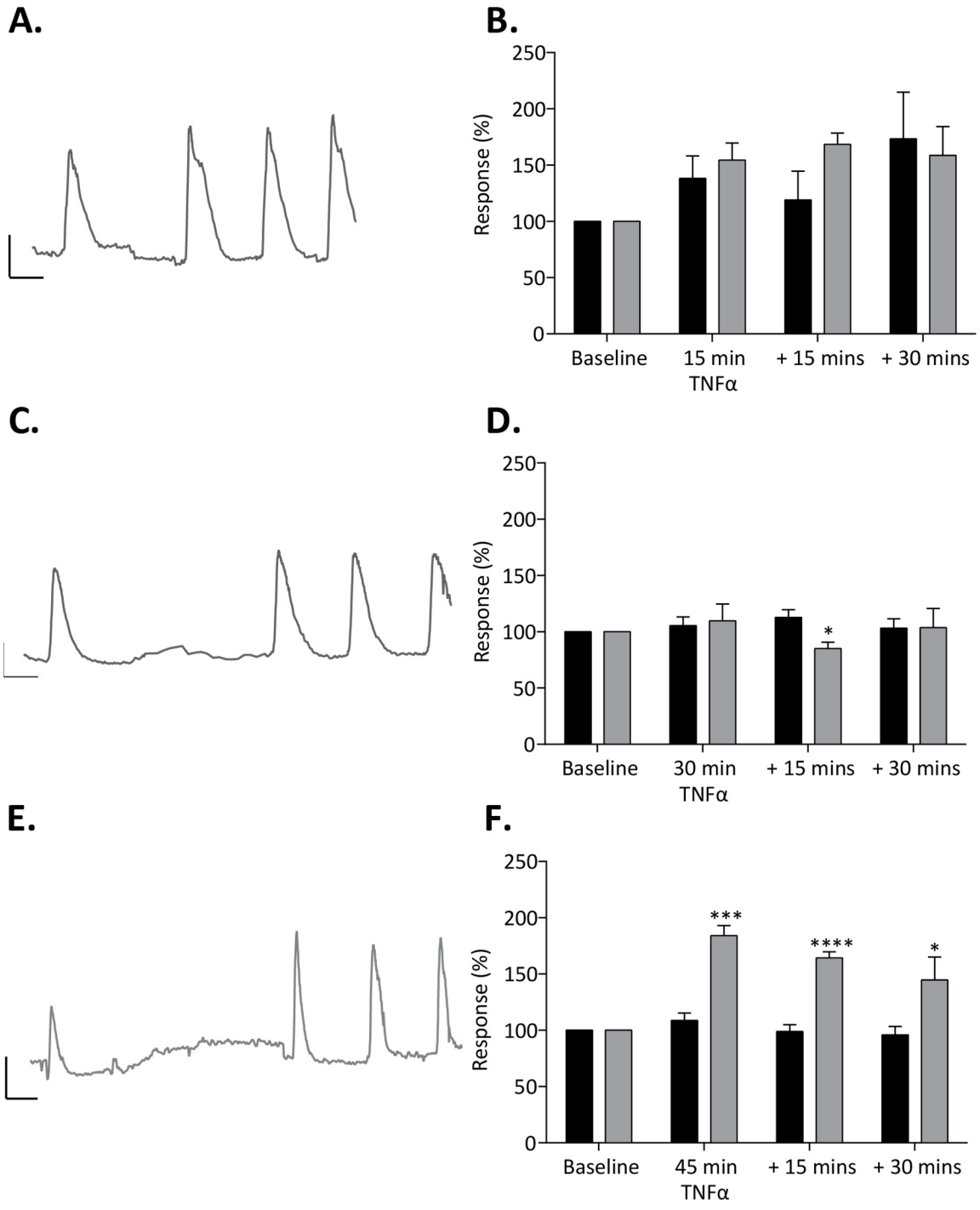
A.
B.
250
200
150
100
50
0
Response (%)
Baseline
15 min TNFα
+ 15 mins
+ 30 mins
C.
D.
250
200
150
100
50
0
Response (%)
*
Baseline
30 min TNFα
+ 15 mins
+ 30 mins
E.
F.
250
200
150
100
50
0
Response (%)
***
****
*
Baseline
45 min TNFα
+ 15 mins
+ 30 mins

suggest that cpAMPARs, through increased release of TNFα, may be significantly contributing to glutamatergic excitatory death by altering calcium dynamics (**Fig. 3.9**).

While studies investigating changes in cpAMPAR expression in ocular hypertensive bead rat did not achieve significance, the effect size compared with nee mice was similar. In naïve mice and rats, the cpAMPAR contribution to the AMPA-induced calcium response was 14.11 ± 6.56% and 14.30 ± 16.14%, respectively. In nee mice and ocular hypertensive rat, the apparent increase in cpAMPAR contribution from the respective naïve control was 26.23 ± 4.66%, and 29.46 ± 11.50% (OHT – group 1) and 33.56 ± 13.13% (OHT – group 2). The lack of significance in rat may be explained by the larger variability in the rat data. This may be due to differences in experimental protocol, which result in differences in fura-2 loading. As can be seen in **Fig. 3.2**, the range of calcium responses was greater in mice than in rats. Therefore, any observable effect may be much more difficult to detect in rats in comparison to mice. Additionally, the number of cells used for analysis per experiment (based on field of view) in mice was much larger than in rats. In mice, the number of ganglion cell layer neurons used per experiment ranged from 10-93 (median 45), where in rat, the number of cells used ranged from 4-44 (median 18).

Compared to the rapid and severe pathology of nee mice, IOP increases in the bead model, at least in our hands, are transient, and RGC loss is slow to occur. In bead rats, it takes several months to achieve the same level of RGC death which occurs in nee mice within a few days (Chauhan et al., 2002). Therefore, it is likely that while nee mice exhibit a greater number of RGCs simultaneously undergoing pathology and death, this number is lower in our bead model, and is in turn more difficult to capture. One way to investigate this hypothesis could be to measure TNFα levels in bead rats versus nee mice. If TNFα was less in ocular hypertensive bead rat compared with nee mice, this might suggest a lesser effect on cpAMPAR expression.

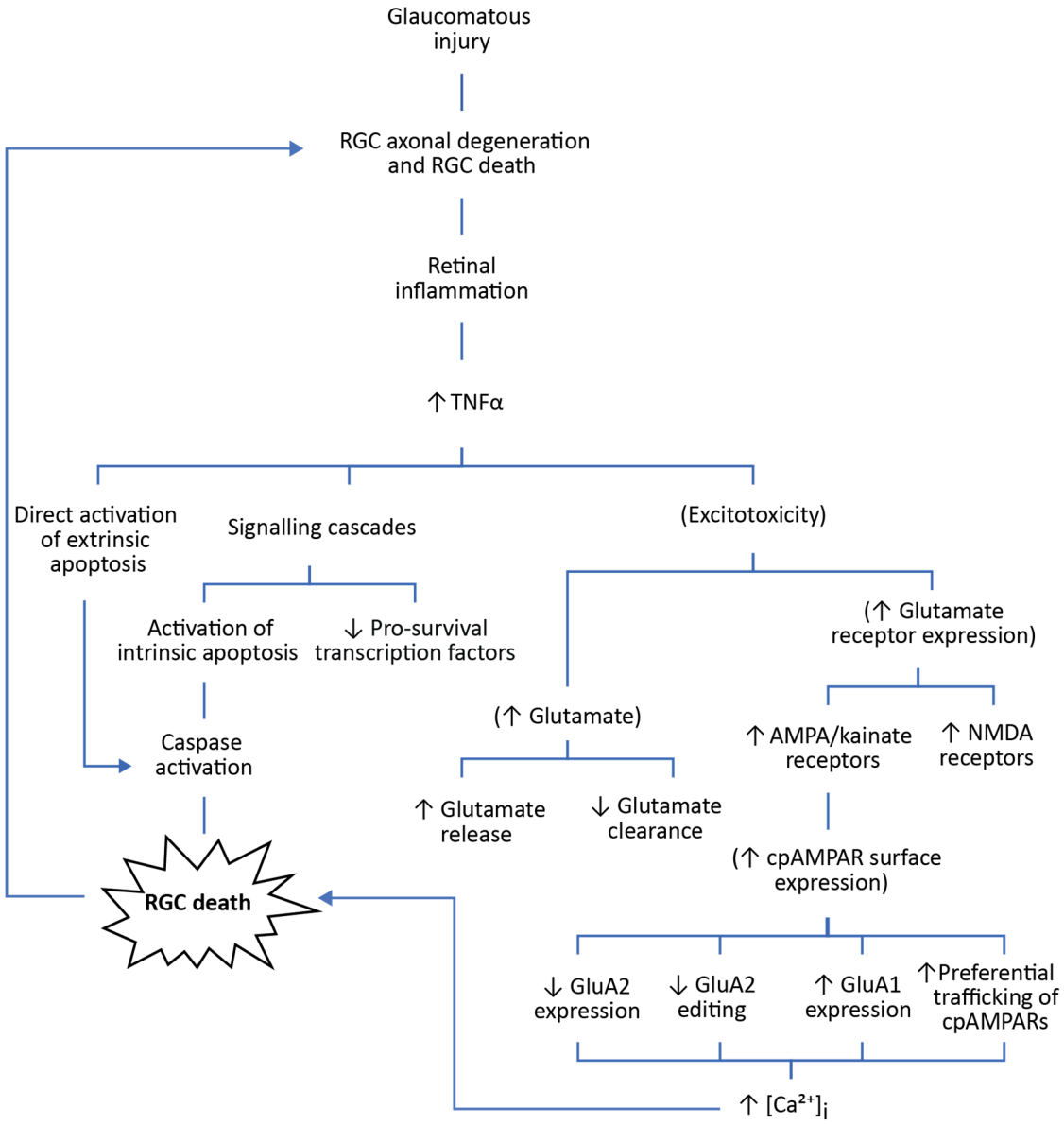

Figure 3.9 - Potential mechanisms of TNFα-induced glaucomatous RGC death.

Though cpAMPARs have been previously reported to be upregulated in models of glaucoma, to my knowledge, this is the first demonstration of the functional impact that glaucomatous alterations in cpAMPAR expression can have in isolated retina. Further, the demonstration of increased AMPA-induced calcium responses following TNFα administration was exciting. This data supports the hypothesis that TNFα can affect RGC calcium dynamics through changes in cpAMPAR expression, contributing to excitotoxic RGC death. The data provided in this thesis provides the first functional demonstration of support for this hypothesis within isolated retina.

3.4.1 The Role of TNFα

While there is evidence that TNFα contributes to RGC death, it has also been reported to increase RGC survival with repeated injection following ONT (Diem, Meyer, Weishaupt, & Bahr, 2001), or if injected prior to optic nerve crush (Mac Nair et al., 2014). Further, TNFα KO did not protect RGCs following ischemic injury (Fontaine et al., 2002), and was associated with increased damage following optic nerve crush (Mac Nair et al., 2014). Investigations of the contributions of TNFR1 versus TNFR2 also provided contradicting results. Oligodendrocyte loss resulting from TNFα injection was completely prevented in TNFR2 KO, but not in TNFR1 KO mice (Nakazawa et al., 2006). Likewise, Nakazawa et al. (2006) reported that TNFR2 KO had increased RGC soma and axon survival in a model of ocular hypertension, but that loss in TNFR1 KO was similar to ocular hypertensive wildtype. This suggests that TNFR1 was not involved in RGC death in this model (Nakazawa et al., 2006). However, increased RGC survival was reported in TNFR1 KO mice following optic nerve crush (Tezel & Yang, 2004), and ischemic injury (Fontaine et al., 2002). Administration of XPro1595, a dominant-negative TNF mutant that selectively inhibits soluble TNFα (which, as mentioned above, preferentially binds to TNFR1), also increased

RGC survival in a model of ocular hypertension (Cueva Vargas et al., 2015). This discrepancy in the effect of ocular TNFα on RGCs may be due to several variables; timing of interventions, as well as differences between models of glaucoma, leading to differences in TNFα receptor signalling favouring one pathway over another (Mac Nair & Nickells, 2015).

3.4.2 Expression Changes in cpAMPARs

The mechanism of cpAMPAR expression change observed in injury and disease has yet to be conclusively identified (Henley & Wilkinson, 2016; Weiss, 2011). Elucidating these mechanisms may lead to a better understanding of how TNFα may contribute to these changes. However, there are several hypotheses that have been investigated. These include: decreases in GluA2 editing; a decrease in expression of GluA2, and thus increasing non-GluA2 containing AMPARs; and/or an increase in preferential trafficking of cpAMPARs to the cell surface, potentially combined with the internalization of calcium-impermeable AMPARs (Henley & Wilkinson, 2016; Weiss, 2011). Even small changes in cpAMPAR expression by these mechanisms have been associated with significant outcomes. A mouse with an ~8% increased expression in unedited GluA2 was reported to have a 20% death rate, while knocking out an enzyme involved in the post-transcriptional editing of the GluA2 subunit (via adenosine deaminases acting on RNA 2 [ADAR2]) results in seizures and premature death (Wright & Vissel, 2012). Edited versus unedited GluA2 subunits also have different trafficking properties; where edited GluA2 subunits are pooled in the endoplasmic reticulum before being trafficked to the membrane, unedited GluA2 can be directly trafficked, not only requiring different proteins to achieve this, but means that insertion of new cpAMPARs can occur more quickly than calcium-impermeable AMPA receptors (Henley & Wilkinson, 2016). Targeting these specific mechanisms was neuroprotective at least in one model of amyotrophic lateral sclerosis (Mahajan & Ziff, 2007), and may be

important in regulating synaptic changes (Mahajan & Ziff, 2007). It is also possible that these mechanisms may vary by disease, with one mechanism playing a more important role in the pathology of one disease, but not another (Weiss, 2011; Wright & Vissel, 2012).

The cpAMPAR antagonist used in this study (IEM1460) is selective for only one type of cpAMPAR at the concentration used (Schlesinger, Tammena, Krampfl, & Bufler, 2005), and therefore, my results would suggest an increase in GluA2-lacking cpAMPARs, specifically, in nee mice. While increased cpAMPAR expression of unedited GluA2 is also possible, GluA2 expression and editing was not measured directly in this investigation.

Previous investigations of alterations cpAMPAR expression in ocular models, as measured through AMPA subunit mRNA and protein expression, have provided conflicting results. In a model of hypoxia, Sivakumar and colleagues (2013) reported that GluA1 and GluA2 AMPA subunit changes (as measured by mRNA and protein expression, as well as immunohistochemical studies) were transient, first increasing compared with baseline following insult, and then decreasing after day 7. In cultured RGCs exposed to hypoxia, GluA1 and GluA2 subunit expression was also increased when measured acutely (2-6 hours, Sivakumar et al., 2013). On the other hand, in a study of oxygen-glucose deprivation, Park and colleagues (2016) reported that GluA1-4 expression was decreased acutely. However, while subunit expression was decreased, this group also reported that cpAMPARs were instead increased, as demonstrated with the use of a cpAMPAR-selective fluorescent probe (Park et al., 2016).

Similarly, in a model of glutamate-induced excitotoxicity using cultured retinal RGCs, while GluA1 mRNA was decreased, GluA1 protein expression was reported as increased, with an acute rise in Ca^{2+} also reported, suggestive of an increase in cpAMPAR expression (Challenor et al., 2015). In an *in vivo* model of NMDA-induced excitotoxicity,

cpAMPAR expression was suggested to be increased in retinal cells, including amacrines and RGCs, as assessed by Co^{2+} stain (Lebrun-Julien et al., 2009). Co^{2+} staining is a technique that utilizes the permeability of cpAMPARs to pass divalent cations to assess expression. Since NMDA receptors are impermeable to Co^{2+}, staining is reported to be exclusive to cpAMPARs (Pourcho, Qin, Goebel, & Fyk-Kolodziej, 2002; Pruss, Akeson, Racke, & Wilburn, 1991).

The study of expression changes in chronic *in vivo* ocular hypertensive models has so far been limited. Membrane GluA2 was reported to be decreased in two different models of ocular hypertension (Cueva Vargas et al., 2015; Dong et al., 2015), though was not statistically different in another (A. L. Wang et al., 2014). Wang et al. (2014) also reported that ADAR2 expression was decreased, and suggested that increases in cpAMPAR expression may be due to a decrease in GluA2 editing. In contrast, while Cueva Vargas and colleagues (2015) found that cpAMPAR expression was upregulated in their model, as detected by Co^{2+} staining, GluA2 appeared fully edited (Cueva Vargas et al., 2015). On the other hand, phosphorylation of GluA2 was also increased with chronic ocular hypertension, suggesting increased internalization of, at least, GluA2-containing AMPARs. It is therefore possible that while ADAR2 expression may be decreased (Dong et al., 2015), GluA2 editing may remain intact, and any increase in cpAMPAR expression may be due to the insertion of new GluA2-lacking AMPARs into the cell membrane.

Despite the evidence to support that this TNFα-mediated increase in AMPA-induced calcium response is due to changes in cpAMPAR expression, based on the experimental protocol used in this work, contributions from other receptors cannot be conclusively ruled out. TNFα administration has also been demonstrated to affect calcium currents through interactions with other receptors, including L-type voltage-gated calcium channels (Cueva Vargas & Di Polo, 2016; Furukawa & Mattson, 1998; Pribiag & Stellwagen, 2014), which are

present on RGCs. As voltage-gated calcium channels were not blocked in the experimental protocol used, it is possible that an increase in these receptors may also be contributing to the observed changes. Upstream excitatory input may also be contributing to altered calcium responses, rather than directly on RGCs, and also cannot be ruled out in this experimental protocol. For example, TNFα may be inducing increased expression on upstream amacrine cells, thereby indirectly altering the AMPA-induced response in RGCs. Additionally, as electroporation is not selective for RGCs, and loads ganglion cell layer neurons which could include displaced amacrine cells, it is possible that some of my recordings also included amacrine cell responses. However, my data suggesting that the TNFα-mediated alterations in cpAMPAR expression occurs on RGCs is supported by studies using Co^{2+} staining in models where TNFα has also been upregulated (Cueva Vargas et al., 2015; Lebrun-Julien et al., 2009).

However, assessment of cpAMPAR expression with Co^{2+} staining may need to be interpreted with caution. The Co^{2+} staining protocol involves incubating tissues in a medium containing Co^{2+} during which AMPA receptors are stimulated to open. Once open, Co^{2+} passes through cpAMPARs into the cytosol, and then is precipitated by moving the tissue into a solution ammonium sulfide. Following fixation, the tissue is then developed with a silver stain. In the case of the retina, in order to properly visualize Co^{2+} staining within different cell types, the retina is sectioned before being silver enhanced (Leinders-Zufall, Rand, Waxman, & Kocsis, 1994). This can potentially increase non-specific staining due to cutting of tissue (Wigerblad et al., 2017), and therefore incorrect estimates of cpAMPAR expression. Thus, interpretation of studies solely using this technique must be cautious.

Collectively, the variability in previous reports of cpAMPAR expression, as measured by subunit expression and Co^{2+} stain, supports the importance of also investigating functional outcomes on cells, as reported in this chapter through Ca^{2+} imaging. Measuring

expression changes by non-functional techniques may not be sensitive enough to adequately represent the impact small changes in expression may have on cells. Until more cpAMPAR-selective tools and techniques become available, Ca^{2+} imaging therefore provides essential information about the function of cpAMPARs in cells, which may currently not be garnered through standard staining and protein quantification techniques.

The data presented in this chapter supports the hypothesis that TNFα could be contributing to glaucomatous RGC death through changes in cpAMPAR expression. This alteration in cpAMPAR may be contributing to damaging changes in calcium dynamics, enabling increased Ca^{2+} entry. Therefore, manipulation of this pathway may be a suitable target to reduce glaucomatous RGC loss.

Chapter 4: CB_1 Modulation as an IOP-Modifying and Neuroprotective Strategy in Glaucoma

Note: a portion of the data presented in this chapter was published in Cairns et al., 2017.

4.1 INTRODUCTION

It is now well established that the elements of the endocannabinoid system (ECS) including endocannabinoid ligands, cannabinoid receptors, and biosynthetic and degradative enzymes, are present in the eye. Here, the ECS can modulate aqueous humor turnover, intraocular pressure, blood flow, and synaptic signalling (Cairns et al., 2016a; Cairns et al., 2016b). Cumulative evidence has suggested that cannabinoids may have utility as pharmacotherapeutics in the treatment of glaucoma, given that in both animal models and humans cannabinoids reduce IOP, the principle modifiable risk factor, and are relatively safe when administered in humans (Cairns et al., 2016a; Cairns et al., 2016b; Ligresti, De Petrocellis, & Di Marzo, 2016). Additionally, several studies have also indicated the possibility of IOP-independent retinal neuroprotective effects of cannabinoids (Cairns et al., 2016a; Cairns et al., 2016b; Nucci et al., 2016). Cannabinoid-mediated mechanisms of neuroprotection may involve decreasing immune cell activation and migration (and therefore reducing release of pro-inflammatory mediators, notably tumor necrosis factor α [TNFα]), activation of pro-survival pathways, and modulation of neuronal excitability (Kendall & Yudowski, 2017; Ligresti et al., 2016; Xu & Chen, 2014; Yazulla, 2008). As IOP-modification is not always successful at preventing further RGC and vision loss, therapies which provide direct RGC neuroprotection may fulfill a current unmet need in the treatment of glaucoma (**Chapter 1**; Levin et al., 2017; Tamm et al., 2013). Therefore, a cannabinoid-based therapeutic may be advantageous as it could provide both IOP modulation, as well as IOP-independent modulation of mechanisms leading to RGC death.

4.1.1 THE ENDOCANNABINOID SYSTEM

The ECS is present throughout the body, and includes endogenous cannabinoids (endocannabinoids; such as 2-arachydonyl glycerol [2-AG] and *N*-arachidonoyl

ethanolamine [anandamide; AEA]), cannabinoid receptors (namely, cannabinoid receptor 1 and 2 [CB_1 and CB_2]), and the enzymes responsible for the formation and degradation of the endocannabinoids (Ligresti et al., 2016; Maccarrone et al., 2015). In the 50 years since the isolation and identification of the psychoactive active component in cannabis (delta-9-tetrahydrocannabinol; Δ^9-THC), the role of the ECS in the body has, and is, becoming more understood. The functions of the ECS are vast and tissue-dependent, but include roles in feeding, metabolism, intestinal motility, emesis, fertility, inflammation, and pain (Ligresti et al., 2016; Maccarrone et al., 2015). Aside from mammals, components of the ECS have also been identified in fish, birds, and reptiles (Howlett & Abood, 2017; Ligresti et al., 2016); however, for the purposes of this thesis, I will focus on the mammalian endocannabinoid system.

The two most extensively studied endocannabinoids are 2-AG and AEA, but several others have also been identified, including oleylethanolamide (OEA), palmitoylethanolamide (PEA), N-arachidonoyl dopamine (NADA), and 2-arachidonyl glyceryl ether (noladin ether; Fowler, Doherty, & Alexander, 2017). Elucidating the actions of the endocannabinoids are complicated in that some of their metabolites are also biologically active. Further, interactions between some endocannabinoids, metabolites, and other components of the ECS may have combined effects – dubbed the "entourage" effect (Murataeva et al., 2016). Endocannabinoids are made on demand, with no apparent storage, and so levels are regulated by the balance between synthesis and degradation (Fowler et al., 2017).

The synthesis of AEA and 2-AG are complex (**Fig. 4.1**), but in general, they are formed from phospholipid degradation by enzymes including diacyl glycerol lipase α (DAGLα) and β (DAGLβ), and *N*-acyl phosphatidylethanolamine-specific phospholipase D (NAPE-PLD). Enzymes responsible for the breakdown of endocannabinoids include fatty

Figure 4.1 - Components involved in the formation and degradation of the endocannabinoids 2-AG and AEA. Endocannabinoids are produced on demand, through breakdown of phospholipids. DAG, produced from membrane phospholipids, can be broken down by DAGLα or DAGLβ, producing 2-AG. 2-AG is broken down primarily by MAGL, but also ABHD6 and ABHD12, to arachidonic acid, or via COX-2 forming prostaglandin glyceryl esters (eicosanoids), which can be further broken down to prostaglandins. AEA is formed from its intermediary NAPE, through either NAPE-PLD-dependent or -independent pathways. However, AEA is quite unstable, and is rapidly broken down to arachidonic acid via FAAH or NAAA, or to a lesser extent, NAGly through a multistep process involving dehydrogenases or eicosanoid prostamides via COX-2. Aside from the eicosanoid production (i.e., prostaglandins via COX-2 metabolism), breakdown of arachidonic acid by FAAH can also produce NAGly, or be converted to a membrane phospholipid via a multistep pathway. Dashed line indicates indirect pathway. Figure adapted from Cairns, Baldridge, & Kelly, 2016a.

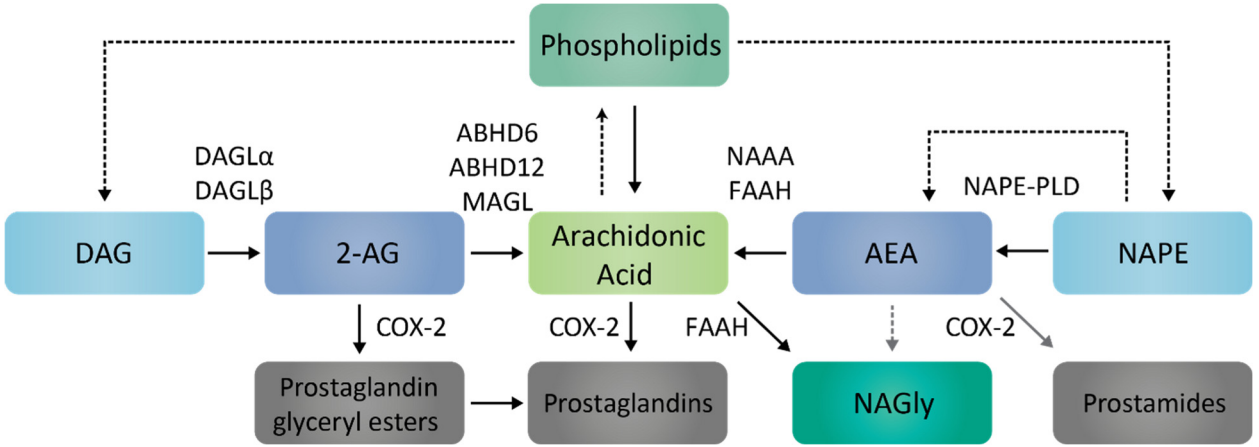
Phospholipids
DAGLα
DAGLβ
ABHD6
ABHD12
MAGL
NAAA
FAAH
NAPE-PLD
DAG
2-AG
Arachidonic Acid
AEA
NAPE
COX-2
COX-2
FAAH
COX-2
Prostaglandin glyceryl esters
Prostaglandins
NAGly
Prostamides

acid amide hydrolase (FAAH), monoacylglycerol lipase (MAGL), *N*-acylethanolamine-hydrolyzing acid amidase (NAAA), α/β-hydrolase domain 6 (ABHD6) and 12 (ABHD12), as well as cyclooxygenase 2 (COX-2; Di Marzo, 2011; Fowler et al., 2017). Additionally, some AEA may be broken down by alcohol and aldehyde dehydrogenase to form the active metabolite *N*-arachidonoyl glycine (NAGly; Bradshaw et al., 2009).

AEA and 2-AG are agonists at CB_1 and CB_2, but endocannabinoids can also have actions at the non-classical cannabinoid receptors GPR18, GPR55, GPR119 (Alexander & Kendall, 2007; Irving et al., 2017; Pertwee, 2015). Additionally, some endocannabinoids also have activity at non-cannabinoid receptors, including the transient vanilloid receptor 1 (TRPV1), a non-selective cation channel, and peroxisome proliferator activated receptors (PPARs; Alexander & Kendall, 2007; De Petrocellis, Nabissi, Santoni, & Ligresti, 2017; Pistis & O'Sullivan, 2017). Cannabinoid receptors are G protein-coupled receptors, typically coupling with G_i and G_o proteins; however, CB_1 can also couple to G_q, and in some cases G_s (Howlett & Abood, 2017; Ligresti et al., 2016; H. C. Lu & Mackie, 2016; Priestley, Glass, & Kendall, 2017).

CB_1 is expressed throughout the body, but primarily in the nervous system, while CB_2 expression is primarily in the periphery, with inducible expression following injury or inflammation (Howlett & Abood, 2017; Maccarrone et al., 2015). Neuronal expression of CB_1 appears to be both pre- and post-synaptic, with 2-AG appearing acting as a retrograde messenger, and both 2-AG and AEA acting post-synaptically (Ligresti et al., 2016; Maccarrone et al., 2015). Glia also express components of the ECS, and may contribute to effects on neuronal excitability; for example, through endocannabinoid-mediated release of gliotransmitters (Araque, Castillo, Manzoni, & Tonini, 2017; Howlett & Abood, 2017; Oliveira da Cruz, Robin, Drago, Marsicano, & Metna-Laurent, 2016). Therefore, it is no surprise that cannabinoid signalling is diverse, involving synaptic modulation of

excitation/inhibition, modulation of gene transcription through signalling cascades involving various protein kinases, and/or changes in cell motility (Howlett & Abood, 2017; Ligresti et al., 2016; H. C. Lu & Mackie, 2016).

There is also evidence that the ECS may be altered in disease; however, it is unclear if these alterations are contributing to the pathology, or are aiding to re-establish homeostasis. In several models of injury and disease, tissue levels of at least one endocannabinoid has been reported to be altered, either increased or decreased, though this varies widely (Di Marzo & Petrosino, 2007; Di Marzo, 2008; Pacher & Kunos, 2013; Skaper & Di Marzo, 2012).

The observation of the ocular effects of cannabis in the eye (Hepler & Frank, 1971) led to the investigation of the ocular ECS. For the most part, the ECS is present throughout ocular tissues, including the endocannabinoids (**Table 4.1**), synthesizing and degrading enzymes (**Table 4.2**), and cognate receptors (**Table 4.3**). There does appear to be some exceptions, the ECS appears to be absent in the lens, and non-pathological CB_2 expression is controversial (Cairns et al., 2016a; Cairns et al., 2016b). The presence of this system in ocular tissues suggests a role in the normal physiology of the eye, and consistent with this, administration of cannabinoids produces ocular effects such as reduction in IOP, hyperemia, and reduced tear production (Cairns et al., 2016a; Green, 1979; Schwitzer et al., 2016; Yazulla, 2008).

4.1.2 Cannabinoid Modulation of IOP

The IOP-lowering effects of cannabinoids were first described by Hepler and Frank (1971) using inhaled cannabis in humans. Since then, these effects have been replicated

Table 4.1 - Presence and Localization of Endocannabinoids in the Mammalian Eye

	Retina	TM	SC	CB	Choroid	Species	References
AEA	+	+		+	+	Cow, human, pig, rat	Matsuda et al., 1997; Bisogno et al., 1999; Stamer et al., 2001; Chen et al., 2005; but see Straiker et al., 1999b
2-AG	+			+	+	Cow, human, rat	Bisogno et al., 1999; Straiker et al., 1999b; Chen et al., 2005
PEA	+			+	+	Cow, human, rat	Bisogno et al., 1999; Straiker et al., 1999b; Chen et al., 2005
NAGly		*	*	*		Mouse	Caldwell et al, 2013

+: endocannabinoid is present in tissue. TM, trabecular meshwork; SC, Schlemm's canal; CB, ciliary body. *: measured from "anterior eye homogenates." Table modified from Cairns et al. (2016b).

Table 4.2 - Presence and Localization of Endocannabinoid Synthesizing and Degrading Enzymes in the Mammalian Eye

	Retina	TM	SC	CB	Choroid	Species	References
DAGLα/β	+[a]					Mouse, rat	Hu et al., 2010; Zabouri et al., 2011
NAPE-PLD	+					Mouse, rat	Zabouri et al., 2011; Cécyre et al., 2013
FAAH	+	+				Cow, monkey, mouse, rat	[b]Bisogno et al., 1999; Yazulla et al., 1999; Njie et al., 2008b; Yazulla, 2008; Hu et al., 2010; Bouskila et al., 2012
MAGL	+	+		+[c]		Mouse, rat	Njie et al., 2008a; Yazulla, 2008; Hu et al., 2010; Miller et al., 2016a
ABHD6	+					Rat	Hu et al., 2010

+, protein expression (ICH, western blotting). TM, trabecular meshwork; SC, Schlemm's canal; CB, ciliary body. [a]DGLβ was associated only with blood vessels in the retina**,** [b]Showed pharmacological evidence only, [c]MAGL was predominantly in pigmented epithelium, but not non-pigmented epithelium. Table modified from Cairns et al. (2016b).

Table 4.3 - Presence and Localization of Classical and Non-Classical Cannabinoid-Binding Receptors in the Mammalian Eye

	Retina	TM	SC	CB	Choroid	Species	References
CB1	+, ‡	+, ‡	+	+, ‡	‡	Guinea pig, human, mouse, monkey, pig, rat	Porcella et al., 1998; Straiker et al., 1999a; Straiker et al., 1999b; Yazulla et al., 1999; Porcella et al., 2000; Stamer et al., 2001
CB2	+, ‡	+				Monkey, pig, rat, human, cow	Lu et al., 2000; Zhong et al., 2005; [a]He et al., 2007; Lopez et al., 2011; Krishnan and Chatterjee, 2012; Cécyre et al., 2013; Krishan and Chatterjee, 2015; but see Porcella et al., 1998, and Bouskila et al., 2013a
GPR18	+, ‡	+		+	+	Mouse, rat	Caldwell et al., 2013; MacIntyre et al., 2014
GPR55	+[b]	‡				Monkey, pig	Kumar et al., 2012; Bouskila et al., 2013b
TRPV1	+, ‡					Cat, monkey, rat	Yazulla and Studholme, 2004; Nucci et al., 2007; Sappington et al., 2009
PPARα	‡					Cow, pig	Kumar et al., 2012, [c]Romano and Lograno, 2012

+, protein expression (ICH, western blotting); ‡, mRNA expression (RT-PCR). TM, trabecular meshwork; SC, Schlemm's canal; CB, ciliary body. [a]Pharmacological evidence only. [b]Staining exclusive to rods. [c]Pharmacological data from ophthalmic artery only. Table modified from Cairns et al. (2016b).

with several cannabinoids, including the main psychoactive component in cannabis Δ^9-THC (a partial CB_1/CB_2 agonist), and the synthetic non-selective CB_1/CB_2 agonists WIN55,212-2 (WIN) and CP55,940, in animal models, such as rodents (Hosseini et al., 2006; Hudson et al., 2011; Szczesniak, Kelly, Whynot, Shek, & Hung, 2006), rabbits (Green & Pederson, 1973; Green & Kim, 1977; Green, Bigger, Kim, & Bowman, 1977; Song & Slowey, 2000), and non-human primates (Chien, Wang, Mittag, & Podos, 2003; Green & Kim, 1977; Green et al., 1981). The cannabinoid-induced reduction in IOP does not appear to be limited by route of administration, as it has been demonstrated through topical, oral, and inhaled routes (Green & Pederson, 1973; Hepler & Frank, 1971; Levitt et al., 1981). The ability to maintain this effect with different modes of administration is not surprising given the lipophilic nature of cannabinoids and their ability to cross the blood-brain barrier (Cheng & Hitchcock, 2007; Samudre et al., 2008). However, these IOP-lowering actions appear to be local, rather than CNS- or systemically-induced (J. H. Liu & Dacus, 1987; Pate et al., 1996; Pate, Jarvinen, Urtti, Mahadevan, & Jarvinen, 1998).

Aqueous humor is produced through energy-dependent transfer of ions from the stroma of the pigmented epithelial cells in the ciliary body to the non-pigmented epithelial cells (see **Chapter 1, section 1.1**). From there, aqueous humor flows from the posterior chamber to the anterior chamber and exits through either the conventional pathway (through the trabecular meshwork to Schlemm's canal), or through the uveoscleral route from the irideocorneal angle to the ciliary body, draining to the supraciliary and suprachoroidal spaces (Civan, 2008; Toris, 2008). As stated above, components of the ECS are present throughout these tissues. Therefore, it is highly likely that the ECS plays an active role in aqueous humor dynamics. In support of this, i.p. or topical administration of the CB_1 inverse agonist SR141716A produces an increase in IOP (Pate et al., 1998; Song & Slowey, 2000).

The presence of cannabinoid receptors on the tissues involved with aqueous humor production and outflow would suggest that cannabinoids appear to be modifying IOP primarily by the direct interaction with these tissues. However, two studies have noted increased perfusion on ocular and retinal structures (Green, Wynn, & Padgett, 1978; Plange et al., 2007), though the contributions of these effects on IOP is unclear.

Additionally, since cannabinoids may provide an alternate mechanism of IOP-lowering, they may provide alternate therapeutic options, or additional IOP lowering when combined with other therapies. This approach was supported by a study in humans, where administration of WIN demonstrated IOP-lowering effect in otherwise treatment resistant ocular hypertension (Porcella, Maxia, Gessa, & Pani, 2001), and was supported by the demonstration of the added benefit of combining WIN and the prostaglandin analogue latanoprost in mice (Hudson et al., 2011).

Cannabinoid-mediated reductions in IOP appear to be predominantly due to actions at CB_1; however, depending on the ligand, may include some non-CB_1-mediated effects (Cairns et al., 2016a; Cairns et al., 2016b). The IOP-lowering actions of Δ^9-THC, CP55,940, WIN, and 2-AG appear to be CB_1 dependent, while the actions of AEA are more complex. IOP lowering by CP55,940 and WIN is blocked by the CB_1 inverse agonist SR141716A in rabbits and rats (Oltmanns et al., 2008; Pate et al., 1998; Song & Slowey, 2000), as are the actions of liposomal-encapsulated Δ^9-THC in rats (Szczesniak et al., 2006). Similarly, Szczesniak et al. (2011) found that the actions of WIN in rats were blocked by the CB_1 antagonist AM251, but not the CB_2 inverse agonist AM630, and that the CB_2-selective agonist HU308 had no effect on IOP. Additionally, WIN-mediated IOP reduction remained in CB_2 knockout mice, further suggestive of CB_1, rather than CB_2, -mediated actions on IOP (Hudson et al., 2011).

It is worth noting that the effects of WIN may also involve some non-CB_1/CB_2 activity. While administration of CP-55,940 or 2-AG had no effect in CB_1 knockout mice, as expected, administration of WIN actually increased IOP (Hudson et al., 2011; Miller et al., 2016a). This increase was not blocked with the CB_2 inverse agonist AM630, thus suggesting an alternate, yet to be determined, mechanism of IOP action which is otherwise masked by the effects at CB_1 (Hudson et al., 2011).

Oltmans et al. (2008), on the other hand, reported that the effects of topical WIN in rat were partially blocked by the CB_2 inverse agonist SR144528, while the administration of another CB_2 inverse agonist, AM630, decreased IOP in CB_1 knockout mice (Hudson et al., 2011). However, two different CB_2 agonists had no effect on IOP (Laine, Jarvinen, & Jarvinen, 2003; Szczesniak et al., 2011). To date, there is very little understanding of CB_2 and its potential role in IOP dynamics, as research in this area has been limited. But these findings may be relevant if CB_2 is upregulated in the eye under certain conditions (Cairns et al., 2016b).

The observed effects of 2-AG on IOP have varied depending on the animal model used. In rabbits, 2-AG produced a transient increase in IOP, followed by a slight, but not significant, decrease below baseline, which was not blocked with the CB_1 antagonist AM251 (Laine, Jarvinen, Pate, Urtti, & Jarvinen, 2002a; Laine, Jarvinen, Mechoulam, Breuer, & Jarvinen, 2002b). On the other hand, topical administration of 2-AG in mice produced a dose-dependent IOP-lowering effect which was absent in CB_1, but not CB_2, knockouts (Miller et al., 2016a). This 2-AG effect was maintained in mice in which MAGL, the enzyme responsible for 2-AG degradation, was pharmacologically inhibited; suggesting that 2-AG, rather than one of its metabolites, is responsible for the observed effect (Miller et al., 2016a).

The CB_1-mediated IOP lowering effect of cannabinoids appears dependent on β adrenergic receptors (Green et al., 1977; Hudson et al., 2011). CB_1 agonists did not produce IOP-lowering effects in β adrenergic receptor knockout mice, and the β blocker timolol, did not provide additive IOP-lowering effects when combined with CB_1 agonists (Hudson et al., 2011). Interestingly, there was also a loss of effect of β adrenergic ligands (both agonists and antagonists) in CB_1 knockout mice. This was suggested to be a result of desensitization of the β adrenergic receptor, due to loss of CB_1-induced suppression of norepinephrine release (Hudson et al., 2011).

The endocannabinoid AEA also produces IOP-modifying actions which are not exclusively CB_1-dependent (Laine et al., 2002a; Pate et al., 1996). This complexity is likely due to active metabolites, which are active at additional cannabinoid and non-cannabinoid receptors (Caldwell et al., 2013). Administration of AEA, similar to 2-AG, produces a characteristic biphasic response, with an initial IOP increase but followed by a significant decrease in pressure (Laine et al., 2002a; Pate et al., 1996). This effect appears to be due, at least in part, by prostaglandins derived from AEA degradation, as it can be blocked with the use of cyclooxygenase inhibitors (Pate et al., 1996). However, the AEA metabolite NAGly can also produce IOP-lowering, mediated through the non-classical cannabinoid receptor GPR18, which is independent of CB_1 or β adrenergic receptors (Caldwell et al., 2013). Consistent with this, when WIN was combined with a GPR18 agonist (abnormal cannabidiol), additional IOP-lowering is observed, suggesting separate mechanisms of IOP reduction (Szczesniak et al., 2011).

Recently, it has been suggested that NAGly, acting at GPR18, is involved in diurnal variation of IOP (Miller et al., 2016b). This finding was based on several observations. First, FAAH knockout mice altogether lack diurnal variation in IOP. Second, NAGly, but not AEA or 2-AG, was decreased at night in mice, where IOP is the highest, and was associated with an

increase in FAAH mRNA. Finally, blocking GPR18 during the night had no effect on IOP, while blocking during the day resulted in increased IOP (Miller et al., 2016b). Taken together these results suggest that tonic release of NAGly, acting at GPR18 during the day in mice, reduces IOP. As the diurnal pattern in humans compared with mice is opposite, it is presumed that the opposite pattern would be true in humans – NAGly would be released at night, contributing to nocturnal IOP-lowering (Miller et al., 2016b).

Some studies have also demonstrated IOP actions with the AEA analogue PEA (Costagliola et al., 2014; Kumar, Qiao, Kumar, & Song, 2012; Mikawa et al., 1997; Pescosolido, Librando, Puzzono, & Nebbioso, 2011). While PEA does not bind to CB_1 or CB_2, it binds to both GPR55 and PPARα, and is also broken down by FAAH. Therefore, any intervention targeting FAAH may also affect PEA, as well as AEA signalling. No IOP-lowering effect was observed with topical application of PEA in rabbits (Mikawa et al., 1997). However, pre-treatment with oral PEA successfully prevented iridectomy-induced increases in IOP in normotensive humans with narrow irideocorneal angles (Pescosolido et al., 2011), and resulted in significantly decreased IOP in patients with ocular hypertension and/or primary open angle glaucoma who had also been treated with timolol (Gagliano et al., 2011). In patients with normal-tension glaucoma, PEA decreased IOP and was associated with improved visual field outcomes on a 6 month follow up (Costagliola et al., 2014). At this time, the target(s) of these actions is/are unknown; however, PEA-induced effects on outflow facility in porcine anterior chamber segments were blocked by a PPARα antagonist as well as shRNA for GPR55 (Kumar et al., 2012).

There is evidence that cannabinoids can modify both IOP production as well as outflow, which is supported by the presence of the ECS in these tissues (**Tables 4.1-3;** Cairns et al., 2016a; Cairns et al., 2016b). In monkeys administered WIN, outflow facility was unchanged, yet the changes in aqueous humor production could not account for the

total IOP effect observed (Chien et al., 2003). Changes in aqueous humor formation were also suggested as a mechanism for the effect of topical Δ^9-THC administered to dog eyes (Merritt, Perry, Russell, & Jones, 1981). Conversely, Green and Kim (1976) reported that IOP reductions after intravenous Δ^9-THC administration in rabbits could be accounted for by the increase in total outflow facility. Further, Colasanti et al. (1985) reported an increase in outflow facility in cats administered Δ^9-THC with an osmotic minipump.

Studies using *ex vivo* models and cell culture have also supported a role for cannabinoid modulation of both aqueous humor production and outflow facility. THC administration reduced secretion in rabbit ciliary body (Green & Pederson, 1973), and outflow facility was increased with administration of cannabinoids in porcine anterior chamber (Kumar et al., 2012; Njie, Kumar, Qiao, Zhong, & Song, 2006; Njie, He, Qiao, & Song, 2008a; Njie, Qiao, Xiao, Wang, & Song, 2008b). CB_1 modulation also produced contractile responses in bovine ciliary muscle (Lograno & Romano, 2004), and relaxed primary and cultured human and porcine trabecular meshwork cells (Kumar & Song, 2006; McIntosh, Hudson, Yegorova, Jollimore, & Kelly, 2007; Njie et al., 2006; Stumpff et al., 2005). Contributions between conventional and uveoscleral pathways of outflow facility are dynamic, and vary widely between species (Fautsch & Johnson, 2006), and therefore, can create challenges when attempting to generalizing data between models.

While there have been a few investigations in ocular hypertensive models or humans, most studies investigating the IOP-lowering properties of cannabinoids have occurred in normotensive conditions. Therefore, depending on the drug and the model, findings in ocular hypertensive models may vary from results in normotensive investigation. These possible discrepancies could be due to anatomical differences in ocular tissues observed in ocular hypertension (Tamm et al., 2015), but also due to pathology-induced changes in the ECS. These potential differences are important to consider given that

changes in endocannabinoid signalling have been reported in various diseases, including endocannabinoid production, enzyme activity, and receptor expression. While early studies investigating these changes have so far been variable (Cairns et al., 2016a), it is likely that some part of the ECS is perturbed during glaucoma. Indeed, a study using human cadaveric tissue found decreased 2-AG and PEA in glaucomatous ciliary body, and decreased PEA in choroid (J. Chen et al., 2005). However, another study using a rat model of ischemia reperfusion injury reported that only retinal AEA was reduced, a finding which was associated with an increase in FAAH activity (Nucci et al., 2007). Interestingly, this group also reported that CB_1 was decreased in their model (Nucci et al., 2007). Njie and colleagues (2008b) also reported that while the FAAH inhibitor URB597 had no effect on outflow facility at normal pressures in a porcine anterior segment model, administration on its own significantly enhanced outflow facility at higher pressures, suggestive of an increase in AEA and/or FAAH activity. Thus, application of cannabinoid modulators may produce quite different effects in normotensive versus ocular hypertensive eyes, and further investigation in these conditions is warranted.

4.1.3 Altering the ECS as a Neuroprotective Strategy

Despite several decades of study, there is currently no drug designed specifically as a RGC neuroprotectant which has been approved for glaucoma therapy, let alone a drug designed to both modify IOP but also directly promote RGC survival (Tamm et al., 2013). However, aside from effects on IOP, there is significant evidence which suggests that ECS modulation could be neuroprotective, including reports of cannabinoid-mediated increases in RGC survival (Cairns et al., 2016a). Therefore, cannabinoid modulation may provide a novel strategy for glaucomatous pharmacotherapy.

Pinar-Sueiro et al. (2013) found that daily application of 1% WIN significantly improved RGC survival following induction of transient ischemia-reperfusion injury, findings also seen with daily administration of URB597 (i.p.), or the stable AEA analogue methanandamide (metAEA; intravitreally; Nucci et al., 2007). Additionally, Crandall and colleagues (2007) found that weekly i.p. administration of Δ^9-THC was sufficient to significantly reduce RGC death following episcleral vein cauterization. Models of pressure-independent RGC loss have also been used to investigate cannabinoid-induced neuroprotection. Early studies using a model of NMDA-induced excitotoxicity found that both THC and cannabidiol (CBD), the non-intoxicating component in cannabis, were neuroprotective (El-Remessy et al., 2003). Slusar and colleagues (2013) also reported that RGC survival was improved with URB597 administration after optic nerve transection (ONT) in rats. Furthermore, most of these studies also reported that these neuroprotective effects were CB_1-dependent (El-Remessy et al., 2003; Nucci et al., 2007; Slusar et al., 2013).

CB_1 modulation could promote RGC survival and reduce death in glaucoma by several possible mechanisms. These may include a reduction of inflammation, promotion of pro-survival pathways, or through alterations in neuronal excitability (Kendall & Yudowski, 2017; Ligresti et al., 2016; Xu & Chen, 2014; Yazulla, 2008). Given evidence that CB_1 can modulate these mechanisms *in vitro* (Kendall & Yudowski, 2017; Ligresti et al., 2016; Xu & Chen, 2014), including specific evidence in retinal cells (El-Remessy et al., 2003; Jo et al., 2017; Kokona & Thermos, 2015; Krishnan & Chatterjee, 2012; Krishnan & Chatterjee, 2015; Lalonde, Jollimore, Stevens, Barnes, & Kelly, 2006; Middleton & Protti, 2011; Opere et al., 2006; Qian et al., 2017; Slusar et al., 2013; Straiker et al., 1999b), it is therefore possible that more than one of these mechanisms could be involved in a CB_1-mediated neuroprotective effect on RGCs.

More recently, an additional possible mechanism by which CB_1 may mediate neuroprotection was proposed (Zhao et al., 2010). TNFα has been previously shown to increase calcium-permeable AMPA receptor (cpAMPAR) expression in several cell types, which may contribute to excitotoxic death (as reviewed in **Chapter 3**). Zhao et al. (2010), reported that in rat hippocampal cultures, TNFα-mediated increases in GluA1 cell surface expression (suggestive of an increase in cpAMPARs) were blocked by WIN, THC, AEA, or 2-AG. At least in the case of WIN, this block appeared to be by a CB_1-dependent mechanism. Further, WIN was neuroprotective against TNFα-exacerbated cell death induced by kainate (Zhao et al., 2010).

On the other hand, following global cerebral ischemia in mice, administration of WIN, 2-AG, and arachidonyl-2-chloroethylamide (ACEA) prevented transient decreases in hippocampal GluA2 expression, suggestive of an increase in GluA2-lacking cpAMPARs. This effect was determined to be CB_1, but not CB_2, dependent, at least in the case of 2-AG (Z. Liu et al., 2015). These findings are consistent with a transient increase in GluA2-lacking cpAMPARs, which was blocked by CB_1. In this model, reducing ischemia-induced GluA2 reductions were also associated with reducing neuronal death and improved motor function (Z. Liu et al., 2015). Whether or not CB_1 can manipulate cpAMPAR expression in retina has yet to be investigated, but presents an additional mechanism by which cannabinoids could provide IOP-independent RGC neuroprotection in glaucoma.

Taken together, modulation of RGC excitability, inflammation, and/or promotion of pro-survival pathways may contribute to cannabinoid-mediated neuroprotection in glaucoma models (Cairns et al., 2016a; Cairns et al., 2016b; Nucci et al., 2016). This multipronged modulation may be advantageous as a therapeutic approach over more direct pathway modulation, for example targeting TNFα directly, in that it may provide additive or synergistic opportunities to prevent or reduce RGC death.

4.1.4 ALTERNATE CB_1 MODULATION STRATEGIES

In order to capitalize on both IOP modification as well as potential neuroprotection, CB_1 is the most logical cannabinoid target. However, while CB_1 agonists have previously been explored as modulators of IOP as well as therapeutics for several other disorders, they have had limited clinical success (Ligresti et al., 2016). This is in part due to some of the disadvantages associated with direct CB_1 agonism, including short duration of action, desensitization with repeated administration, and systemic side effects (Pertwee, 2012). As glaucoma is a disease in which patients can require treatment over a number of decades, it requires a drug which is safe and efficacious when administered long-term (Levin et al., 2017).

The duration of reduction in IOP observed after acute administration of cannabinoids can be short, especially compared with currently available therapeutics. For example, acute topical administration of cannabinoids typically lasts only 1-3 hours (though longer durations have been noted; Chien et al., 2003; Hudson et al., 2011; Laine et al., 2002b; Oltmanns et al., 2008; Porcella et al., 2001; Song & Slowey, 2000), while the IOP lowering actions of prostaglandin analogues, the first line therapy for IOP lowering, are sufficient enough to only be administered once per day (Harasymowycz et al., 2016; Weinreb et al., 2014). Drugs with shorter durations of actions require more frequent administration to remain effective. However, frequent administration can reduce patient compliance, and so should be avoided if possible (J. C. Buchan, Siddiqui, & Gilmour, 2007; Hermann, Papaconstantinou, Muether, Georgopoulos, & Diestelhorst, 2011a; Hermann, Bron, Creuzot-Garcher, & Diestelhorst, 2011b; Reardon, Kotak, & Schwartz, 2011).

Furthermore, chronic cannabinoid modulation can lead to receptor desensitization and subsequent loss of effect. For example, repeated administration of high doses of an

inhibitor of 2-AG metabolism (JZL184) resulted in tolerance in a model of inflammatory nociception, likely due to chronically elevated 2-AG levels (Ghosh et al., 2013). However, this desensitization does not appear uniform across all settings and models, as MAGL knockout mice, which were reported to have significantly elevated ocular 2-AG and AEA, still had presumed CB_1-mediated IOP reductions (Miller et al., 2016a).

Finally, administration of cannabinoids is unfavorable due to the potential for side effects (Pertwee, 2009). Given the ubiquity of CB_1 receptor expression and the lipophilic nature of cannabinoids (Howlett & Abood, 2017; Ligresti et al., 2016), it is unsurprising that cannabinoid administration produces several on-target but off-site effects. These effects, including psychoactivity and cardiac effects, can significantly impact every day function, thus potentially affecting not only the tolerability of the drug, but the willingness to use the drug (Ligresti et al., 2016; Pertwee, 2009; Pertwee, 2012).

In recent years, modes of indirectly modulating CB_1 have been increasingly been explored as a means to circumvent or limit some of these undesirable effects. These include CB_1 allosteric modulation and the use of endocannabinoid enzyme inhibitors (Pacher & Kunos, 2013; Pertwee, 2009; Pertwee, 2012).

Inhibitors of endocannabinoid degradation, such as FAAH and MAGL inhibitors, have been extensively studied in the past few decades, and several have gone to clinical trials with varying degrees of success (though, none have successfully gone to market; Pacher & Kunos, 2013). Enzyme inhibitors are advantageous in that they do not alter endocannabinoid synthesis, but rather amplify or extend endocannabinoid action (K. Ahn, Johnson, & Cravatt, 2009; Mulvihill & Nomura, 2013). FAAH inhibitors have been safe in humans, even with approximately 96% FAAH inhibition (Huggins, Smart, Langman, Taylor, & Young, 2012). One drug that was reported to be a FAAH inhibitor produced substantial

toxic effects in humans, though was later found to have little selectivity for FAAH (Kerbrat et al., 2016). However, there appears to be some disadvantages associated with chronic MAGL inhibition, at least, resulting in both reduced CB_1 function and expression, but may be avoided at lower doses (Ghosh et al., 2013; Schlosburg et al., 2010; Schlosburg et al., 2014).

At least two studies have reported some efficacy of the FAAH inhibitor URB597, in models of glaucoma (Nucci et al., 2007; Slusar et al., 2013), as reported in the previous section, and in anterior chamber perfusion models, where co-administration with AEA extended its duration of enhancement on outflow facility (Njie et al., 2008). Additionally, as described previously, URB597 administration alone also increased outflow facility during elevated pressure, but not during normal pressure, highlighting a potential therapeutic targeting opportunity where AEA may be selectively regulated (Njie et al., 2008). However, administration of a non-selective enzyme inhibitor phenylmethylsulfonyl fluoride abolished the AEA-mediated IOP effect in rabbits (Laine et al., 2002a), suggesting importance of selectively inhibiting the enzymes.

There has not yet been any study investigating the chronic effects of DAGLα/β, MAGL, ABDH6, or ABHD12 inhibition in models of glaucoma; however, several other studies have reported protective effects in other neurodegenerative models, including Parkinson's (Fernandez-Suarez et al., 2014; Nomura et al., 2011), Alzheimer's (R. Chen et al., 2012), and traumatic brain injury (Katz et al., 2015; Tchantchou & Zhang, 2013). Additionally, administration of the non-selective enzyme FAAH/MAGL/ABHD6 inhibitor LY2183240 also increased the duration of effect on outflow facility enhancement when combined with 2-AG (Njie et al., 2008a).

With respect to receptor targets, allosteric ligands, and in particular allosteric modulators, have some significant therapeutic advantages to orthosteric ligands (Janero &

Thakur, 2016; Keov, Sexton, & Christopoulos, 2011; T. Nguyen et al., 2016; Ross, 2007; Wootten, Christopoulos, & Sexton, 2013). Allosteric ligands bind to receptors at distinct sites other than the orthosteric site, and either activate or inhibit the receptor directly (allosteric agonists/antagonists), or modify the function of the receptor, either by manipulating the affinity of the orthosteric ligand to the orthosteric site, or by modification of the efficacy of orthosteric binding (allosteric modulators; **Fig. 4.2**; Kenakin, 2016). Unlike orthosteric or allosteric agonists, allosteric modulators typically cannot activate the receptor on their own, and require the presence of an orthosteric ligand to exert their effects (Kenakin, 2016; Wootten et al., 2013). Allosteric modulators of CB_1 are a relatively new class of drug; the allosteric site only recently being described in 2005 (Price et al., 2005). Since then, several CB_1 allosteric modulators have been developed including both negative allosteric modulators and positive allosteric modulators (PAMs; Khurana et al., 2017; Morales, Goya, Jagerovic, & Hernandez-Folgado, 2016; T. Nguyen et al., 2016; Straiker, Mitjavila, Yin, Gibson, & Mackie, 2015).

The use of PAMs may permit fine-tuning of CB_1 signalling, but while minimizing the disadvantages accompanying direct orthosteric activation (Janero & Thakur, 2016). This could theoretically occur by stabilization of CB_1 in an alternate conformational state, extending disassociation time, or by decreasing receptor desensitization (Fay & Farrens, 2015; Janero & Thakur, 2016; Kenakin, 2016; Laprairie et al., 2017; T. Nguyen et al., 2016). Additionally, it is possible that the use of allosteric modulators may enable more selectivity, in that where there appears to be overlap between cannabinoid receptor orthosteric binding sites, the same may not be true for allosteric sites (Janero & Thakur, 2016; Ross, 2007).

Administration of cannabinoids activates CB_1 at supraphysiological levels and results in off-site effects (Volkow, Hampson, & Baler, 2017). The use of CB_1 PAMs, however,

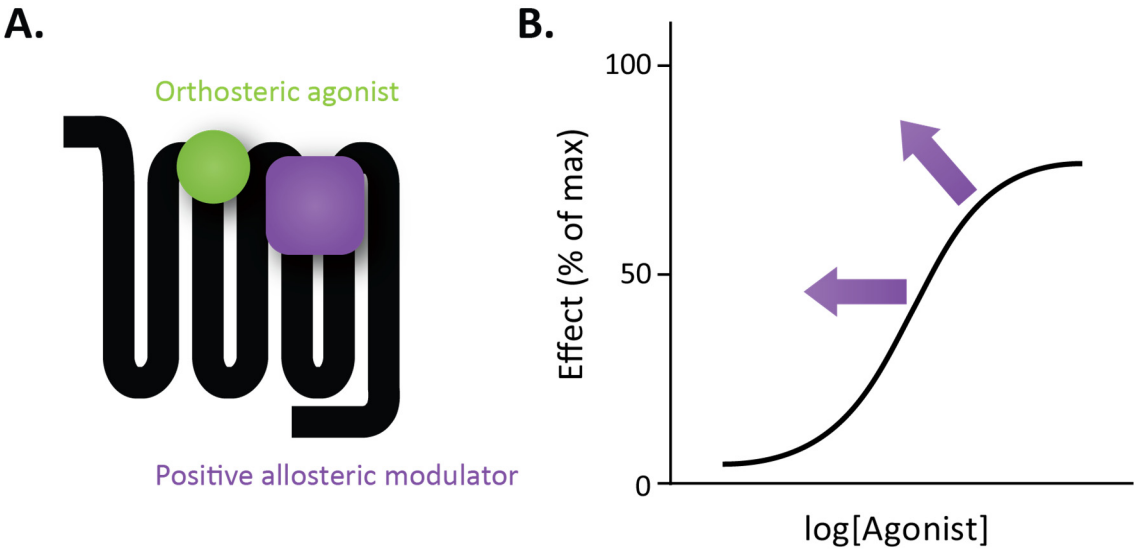

Figure 4.2 - Allosteric modulation of CB_1. (A) The GPCR CB_1 contains an allosteric site, which is separate from its orthosteric site, where ligands such as endocannabinoids bind. (B) A positive allosteric modulator in the presence of an orthosteric modulator can increase the affinity of the orthosteric ligand to the receptor, resulting in an increase in potency, and/or increase the response of the orthosteric ligand at the receptor, resulting in an increase in efficacy.

would not disrupt the tight spatial and temporal control of endocannabinoid activity as they cannot activate the receptor on their own (Fowler et al., 2017; Janero & Thakur, 2016; Kenakin, 2016; Ligresti et al., 2016; T. Nguyen et al., 2016; Volkow et al., 2017). This should result in fewer side effects with administration, all while maintaining the benefits of CB_1 activation (Janero & Thakur, 2016). For example, if endocannabinoids were increased at the site of pathology but not elsewhere, systemic administration of a CB_1 PAM should only produce effects at that target tissue, and therefore should not produce, or at least limit, off-site effects (Janero & Thakur, 2016). Alternatively, if CB_1 expression is reduced at the site of pathology, such as reported in a model transient high IOP (Nucci et al., 2007), PAM administration may enable enhancement of CB_1 activity, whereas administration of orthosteric ligands alone may be limited by receptor saturation (Janero & Thakur, 2016; Kenakin, 2016).

So far, only a small number of CB_1 PAMs and related compounds have been investigated: lipoxin A_4, ZCZ011, and GAT211 and its enantiomers GAT229 and GAT228. GAT211, while structurally similar to ZCZ011, it is a racemic mixture (approximately 50/50) of two pharmacologically distinct enantiomers: the "pure" PAM GAT229, and the partial allosteric agonist GAT228 (**Fig. 4.3;** Laprairie et al., 2017; Morales et al., 2016; T. Nguyen et al., 2016). GAT228 can activate CB_1 on its own from the allosteric site, unlike GAT229 – a true PAM ("pure" PAM), which shows no independent activity at CB_1 (Laprairie et al., 2017). GAT211, therefore, displays properties of both allosteric agonism, as well as positive allosteric modulation, making it an "ago-PAM" (Laprairie et al., 2017; Slivicki et al., 2017).

Systemic administration of ZCZ011 or GAT211 alone are antinociceptive in models of inflammatory and neuropathic pain, without producing tetrad effects, tolerance, physical

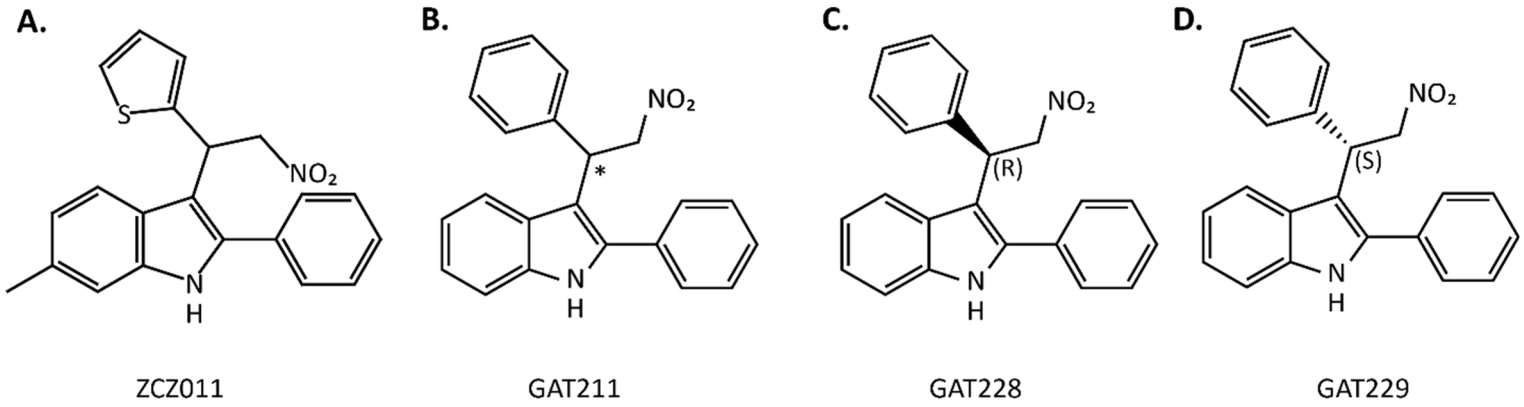

Figure 4.3 - Structure of CB_1 PAMs. (**B**) The ago-PAM GAT211is structurally similar to (**A**) CB_1 PAM ZCZ011. (**B**) GAT211 is a racemic mixture of the allosteric agonist GAT228 (the *R*-enantiomer, **C**) and the "pure" PAM GAT229 (the *S*-enantiomer, **D**). * indicates chiral center.

dependence, or place preference or aversion (Ignatowska-Jankowska et al., 2015; Slivicki et al., 2017). These data further support the hypothesis that PAM modulation of CB_1 may be favourable over direct CB_1 orthosteric activation for the long-term treatment of glaucoma. To date, however, there has been no study of the effects of CB_1 PAMs, either alone or in combination with other CB_1 modifying strategies, on IOP or RGC survival in a model of glaucoma.

4.1.5 OBJECTIVES

This cumulative data suggests that CB_1 modulation may provide a novel therapeutic for glaucoma, modifying not only IOP, but also acting independently from effects on IOP to protect RGCs from glaucomatous death. Further, CB_1 PAMs may provide an novel strategy to modulate CB_1 while avoiding some of the negative effects associated with direct orthosteric activation. So far, no glaucoma therapeutic has been developed specifically targeting both IOP and neuroprotection, and therefore, a CB_1 PAM could fulfill an unmet need. Therefore, I hypothesized that chronic administration of CB_1 PAMs could reduce IOP as well as provide IOP-independent neuroprotection against glaucomatous RGC death.

In order to investigate this hypothesis, my objectives were to: 1) investigate the IOP-lowering properties of CB_1 positive allosteric modulation, in both normotensive wildtype and ocular hypertensive mice, 2) investigate if CB_1 can modulate TNFα-induced cpAMPAR expression in RGCs, a potential additional mechanism of CB_1-mediated neuroprotection, and 3) investigate if CB_1 positive allosteric modulation is neuroprotective in two models of experimental glaucoma.

4.2 MATERIALS AND METHODS

4.2.1 DRUGS AND REAGENTS

All topical drugs were delivered by pipetting 5 μL of drug directly onto the cornea of the eye. GAT211 and GAT229 were synthesized and provided by Drs. Kulkarni and Thakur (Northeastern University, Cambridge, MA; (Kulkarni, Ranade, Garai, & Thakur, 2017; Laprairie et al., 2017). GAT211, GAT229, WIN (Bio-Techne, Abingdon, OX, UK), and KML29 (Bio-Techne, Minneapolis, MN), were topically delivered in a vehicle containing 2% dimethyl sulfoxide (DMSO, Sigma Aldrich, Oakville, ON) and 4% Tween-20 (Sigma Aldrich) in Tocrisolve (Bio-Techne, Minneapolis, MN). Δ^9-THC (Cayman Chemical, Ann Arbor, MI) was reconstituted in either soybean oil (Sigma Aldrich) for topical application, or in ethanol for i.p. administration. GAT211, GAT229, and Δ^9-THC were delivered i.p. in a vehicle containing 1:1:18 ethanol, Kolliphor EL (Sigma Aldrich), and saline at 1 mg/mL. URB597 (Cayman Chemical) was dissolved in a vehicle containing 1% DMSO and 1% Tween-80 (Sigma Aldrich), and delivered at 0.06 mg/mL.

4.2.2 Ca^{2+} IMAGING

Ca^{2+} imaging in mouse retina was carried out as described in **Chapter 3** (see **sections 3.2.2** and **3.3.4**).

4.2.3 IOP MEASUREMENTS

IOP measurements occurred as previously described (**Chapter 2**). Investigation of drug effects on IOP occurred as follows. Baseline recordings were taken from all mice prior to administration of either topical or i.p. delivery of drug. Follow up recordings were then taken 1, 6, and 12 hours later (unless otherwise indicated). All follow up IOP measurements

were normalized to the baseline IOP measurement, and are reported as change from baseline (**Fig. 4.4A**). Wherever possible, one eye received drug, and the contralateral eye received vehicle. This enabled paired analysis between eyes. In order to accommodate i.p. administration, some investigations required analysis between mice, and therefore unpaired analyses were used (**Fig 4.4B**).

4.2.4 RGC SURVIVAL

RGC densities were assessed as per **Chapter 2** (see **section 2.4**)

4.3 RESULTS

4.3.1 ACUTE EFFECTS OF CB_1 MODULATORS ON IOP

4.3.1.1 Acute Effects of CB_1 Modulators in Normotensive Mice

While WIN, a non-selective CB_1/CB_2 agonist, is known to produce a reduction in IOP at higher doses (1%), the reported effects at lower doses have been variable. Additionally, investigation of IOP effects beyond 2 hours has been limited. Before combining WIN with other drugs which may potentially have an extended duration of action, it was important to ensure lack of effect at these later time points. Therefore, the effects of topically administered 0.25%, 0.5%, and 1% WIN were investigated in normotensive C57Bl/6 mice on an extended time scale. Administration of 0.25% (**Fig. 4.5A**) nor 0.5% WIN (**Fig. 4.5B**) reduced IOP at either 1, 6, or 12 hours after administration when compared with vehicle (N = 4 in each group), and were considered subthreshold doses. As expected, 1% WIN reduced IOP compared with eyes treated with vehicle at 1 hour ($P < 0.05$, 0.4 ± 0.6 versus -1.6 ± 0.7 mmHg from baseline respectively, N = 9; **Fig 4.5C**), but this effect was no longer present at 6 or 12 hours.

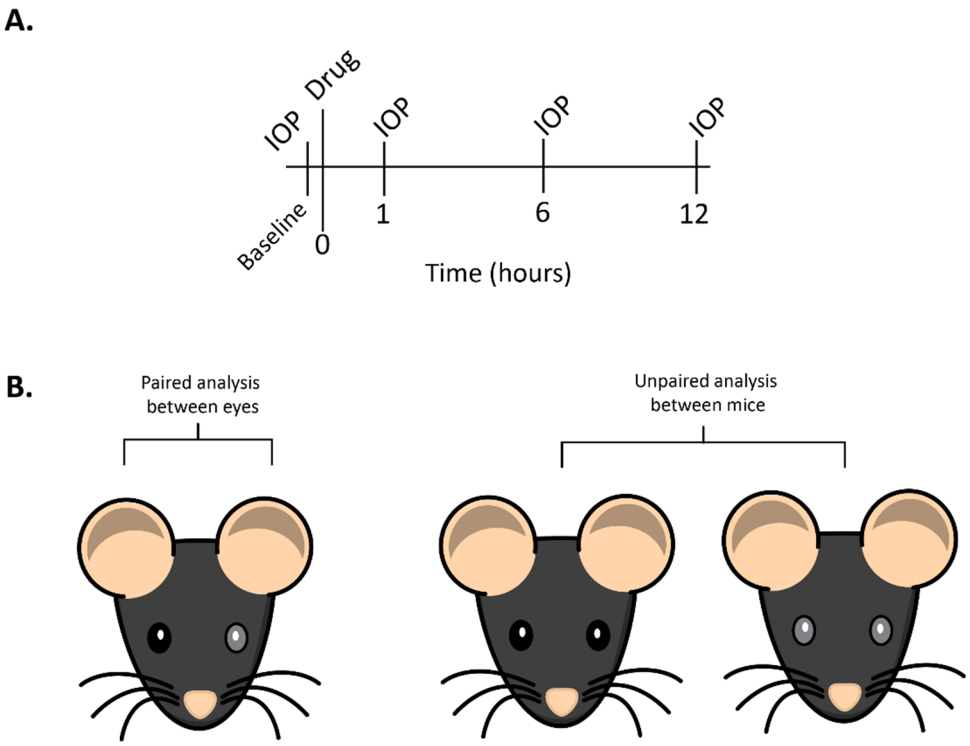

Figure 4.4 - IOP measurements. (**A**) IOPs in each eye were recorded prior to drug administration (baseline), and 1, 6, and 12 hours later, unless otherwise reported. In order to minimize variation from differences in starting IOP, all IOPs are reported as the change in IOP from baseline. (**B**) Where possible, analysis of topical drugs used paired analysis at each time point, with one eye receiving vehicle (black), and contralateral eye receiving drug (grey; left). However, in order to compare differences in drugs administered i.p., separate mice were used, and analysis at each time point was unpaired (right). In IOP studies, drug treatments are represented by grey bars, while vehicle treatments are indicated by black bars, unless otherwise indicated.

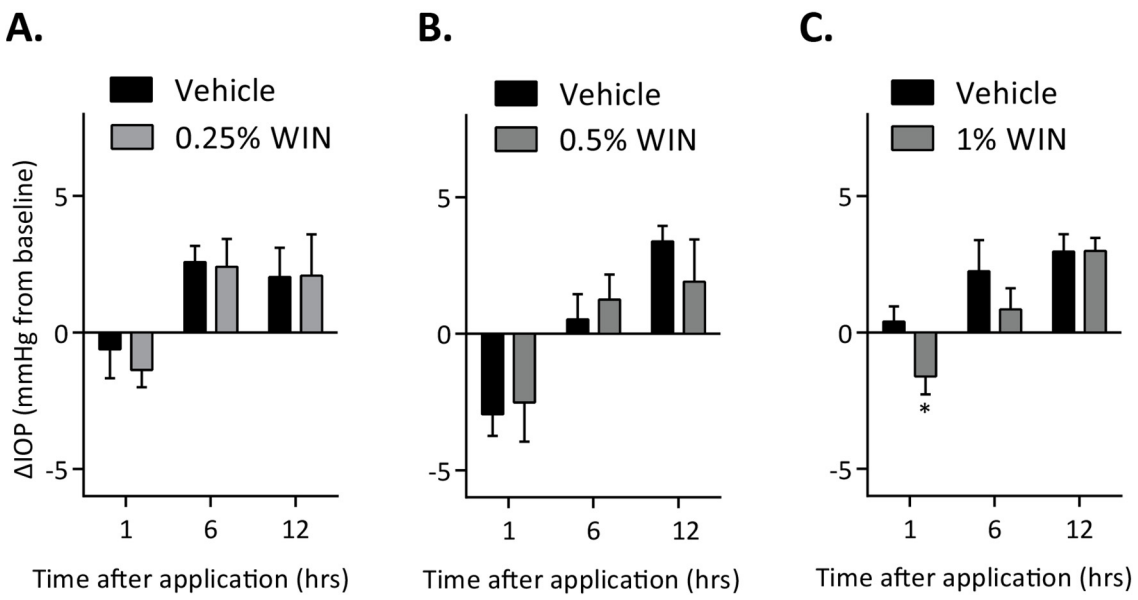

Figure 4.5 - Effects of the CB_1 orthosteric agonist WIN on IOP in normotensive C57Bl/6 mice over time. Topical administration of either (**A**) 0.25%, (**B**) 0.5% WIN did not significantly lower IOP compared with vehicle-treated eyes. (**C**) Administration of 1% WIN produced significant IOP-lowering effect at 1 hour compared with vehicle treatment, but was not significantly different at 6 or 12 hours following drug administration. *N* = 4-9 mice per group. Paired t-tests, * = $P < 0.05$.

As the possible effects of CB_1 positive allosteric modulation had yet to be investigated on IOP, it was unknown whether PAMs could alter IOP without additional administration of exogenous cannabinoids. That is, if basal endocannabinoid tone alone would be sufficient to potentiate an IOP-lowering effect. Both the ago-PAM GAT211 and the "pure" PAM GAT229 were investigated for their IOP-lowering properties in naïve mice and in mice with ocular hypertension. As allosteric modulation may result in IOP-lowering effects on a different time scale than CB_1 orthosteric ligands alone, IOPs were measured 1, 6, and 12 hours after administration (unless otherwise indicated).

In adult wildtype mice, administration of GAT211 alone at 0.2%, 2%, or 4% w/v did not reduce IOP at 1, 6, or 12 hours after administration compared with vehicle treated eyes (*N* = 5, 4, and 3, respectively; **Fig. 4.6 A-C**). Administration of 0.2% or 2% GAT211 with 0.25% WIN also did not reduce IOP compared with vehicle at 1, 6 or 12 hours following administration (*N* = 5 and 4, respectively; **Fig. 4.6 D-E**), suggesting that GAT211, at least at the doses investigated, does not potentiate the IOP-modulating effects of WIN.

Laprairie et al. (2017) demonstrated significant differences in *in vitro* studies in the effects of the allosteric agonist GAT228 compared with the "pure" PAM GAT229. In cell-based assays, GAT229 promoted CB_1-mediated cyclic adenosine monophosphate (cAMP) inhibition and β-arrestin recruitment consistent with PAM activity, while GAT228 effects in the same assays were consistent with allosteric agonist activity. It is therefore possible that while the racemic mixture of GAT211 did not produce IOP-lowering, that GAT229, in the absence of GAT228, could potentially have different effects. Administration of GAT229 alone at either 0.2% or 2% in normotensive wildtype mice did not produce IOP-lowering at 1, 6, or 12 hours after administration when compared with eyes receiving vehicle (*N* = 7 and 4, respectively; **Fig. 4.7 A-B**). However, the combination of 0.2% GAT229 with subthreshold

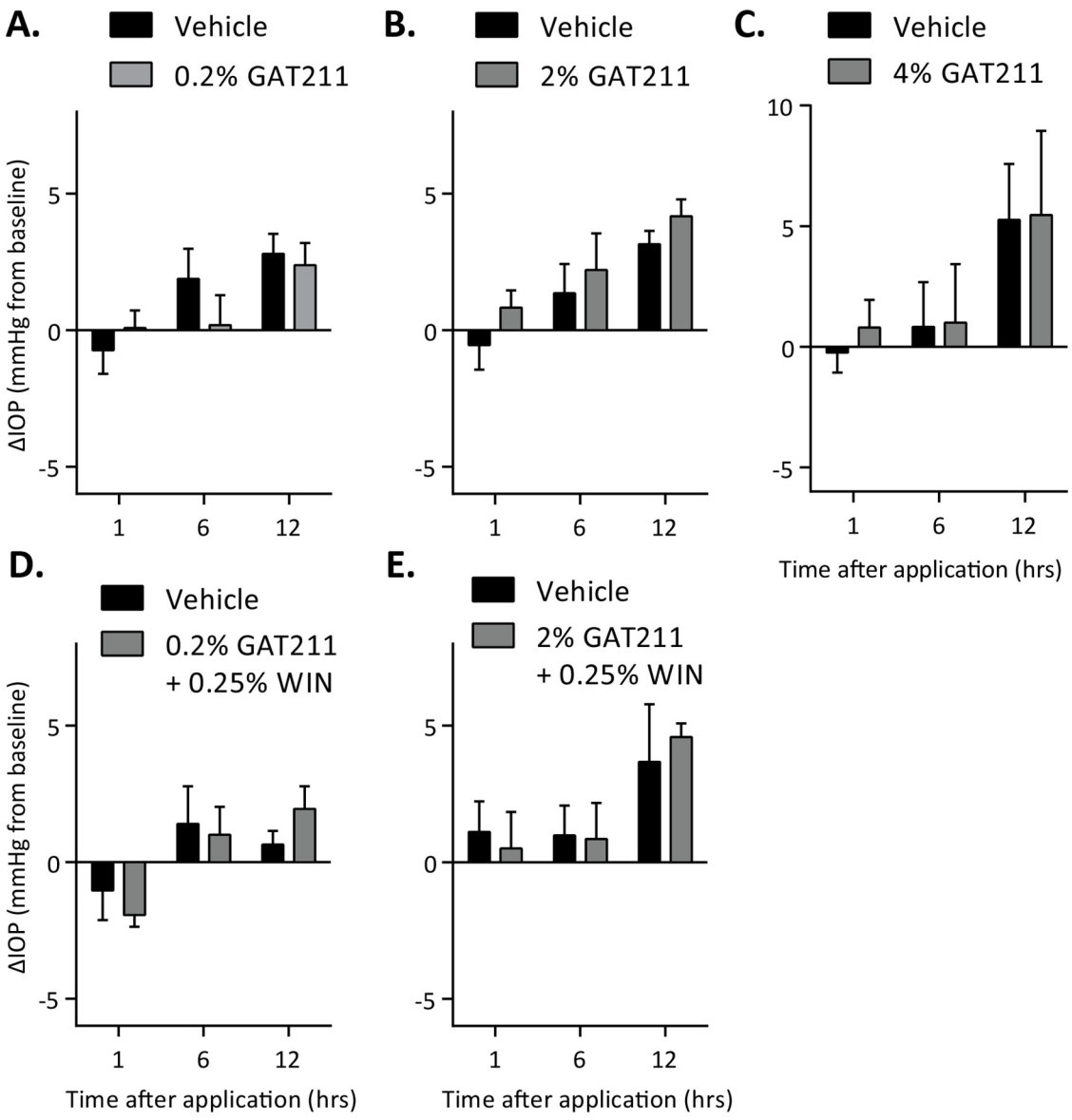

Figure 4.6 - Effects of the topical CB_1 ago-PAM GAT211, alone or in combination with WIN, on IOP in normotensive C57Bl/6 mice. (**A**) 0.2% (**B**) 2%, or (**C**) 4% of GAT211 administered alone did not reduce IOP compared with vehicle treated eyes. (**D,E**) Combination of GAT211 (0.2% or 2%) with topical 0.25% WIN had no effect on IOP. *N* = 3-5 mice per group. Paired t-tests.

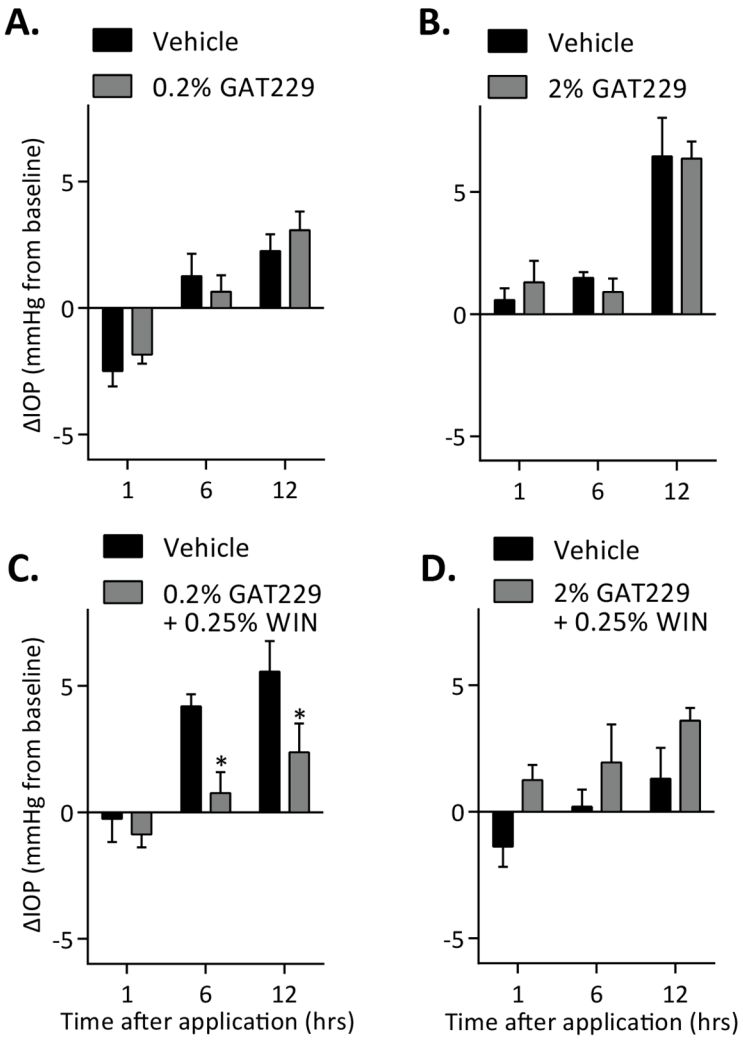

Figure 4.7 - Effects of the topical CB_1 PAM GAT229, alone or in combination with WIN, on IOP in normotensive C57Bl/6 mice. (**A**) Administration of 0.2%, or (**B**) 2% GAT229 alone did not significantly reduce IOP compared with vehicle treatment. (**C**) Combination of 0.2% GAT229 with 0.25% WIN resulted in significantly smaller changes in IOP from baseline compared with vehicle treatment at 6 and 12 hours following administration. (**D**) However, this effect was not present with the combination of 2% GAT229 and 0.25% WIN. N = 4-7 mice per group. Paired t-tests. * = $P < 0.05$

(0.25%) WIN produced significant IOP-lowering compared with eyes receiving vehicle at 6 and 12 hours (mean difference 3.4 ± 1.1 and 3.2 ± 0.9 mmHg, respectively, $P < 0.05$, $N = 5$; **Fig. 4.7C**), but not at 1 hour. This suggests that GAT229 potentiates the effect of subthreshold 0.25% WIN, but with a different time course than suprathreshold WIN alone (which produced an IOP-lowering effect at 1 hour only). The combination of 2% GAT229 with 0.25% WIN; however, did not reduce IOP compared with vehicle at either 1, 6, or 12 hours ($N = 4$; **Fig. 4.7D**).

To investigate if this allosteric effect was probe specific, another CB_1 agonist was investigated. Topical administration is preferred clinically as a route of administration due to ease of administration, and limited distribution producing fewer systemic side effects. Even though most reported data on the IOP effects of Δ^9-THC has been with i.p. delivery, Fischer et al. (2013) reported successful IOP-lowering with topical Δ^9-THC in dogs. Δ^9-THC is known to have a short duration of action (J. H. Liu & Dacus, 1987; Szczesniak et al., 2006); therefore, IOPs were investigated at 1 and 4 hours after topical administration. In wildtype normotensive mice, neither 0.5% nor 2% Δ^9-THC reduced IOP at 1 or 4 hours compared with eyes receiving vehicle ($N = 9$ and 4, respectively; **Fig. 4.8A-B**). Not surprisingly, the combination of 0.5% or 2% Δ^9-THC with 0.2% GAT229 also did not produce an IOP-lowering effect at 1 or 4 hours ($N = 5$ and 7, respectively; **Fig. 4.8C-D**).

Intraperitoneal administration of Δ^9-THC was then investigated. In congruence with previously reported literature (Szczesniak et al., 2006), 5 mg/kg Δ^9-THC produced greater IOP-lowering 1 hour following administration compared with mice receiving vehicle ($P < 0.01$, -2.3 ± 0.3 and -0.4 ± 0.4 mmHg from baseline, respectively, $N = 5$ mice in each group; **Fig. 4.9A**). However, this effect was no longer present at 6 or 12 hours. Administration 1 mg/kg Δ^9-THC ($N = 10$ mice) did not reduce IOP at 1, 6, or 12 hours following

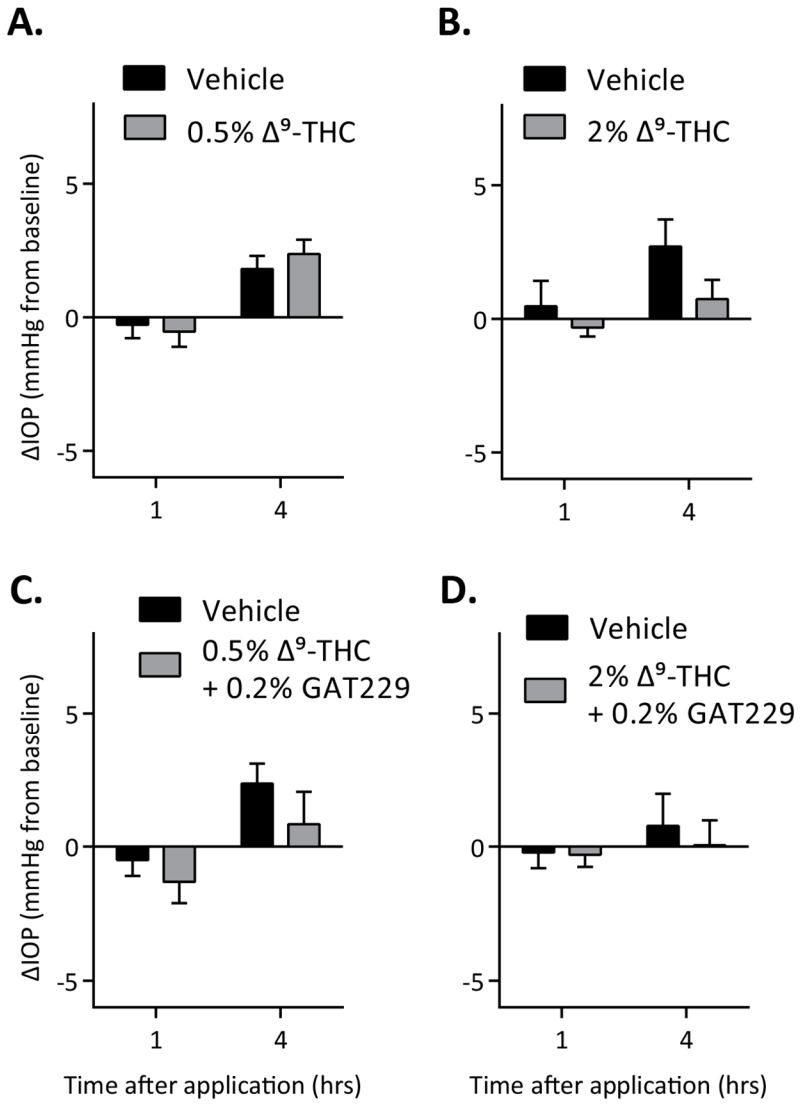

Figure 4.8 - Effects of topical Δ⁹-THC, alone or in combination with topical GAT229, on IOP in normotensive C57Bl/6 mice. The effects of the drugs were investigated at 1 and 4 hours. Administration of (**A**) 0.5% or (**B**) 2% Δ⁹-THC alone, did not lower IOP, as compared to vehicle treated eyes. Combination of Δ⁹-THC (0.5%) with topical (**C**) 0.2% GAT229, or (**D**) 2% GAT229 also had no effect on IOP. *N* = 4-9 mice per group. Paired t-tests.

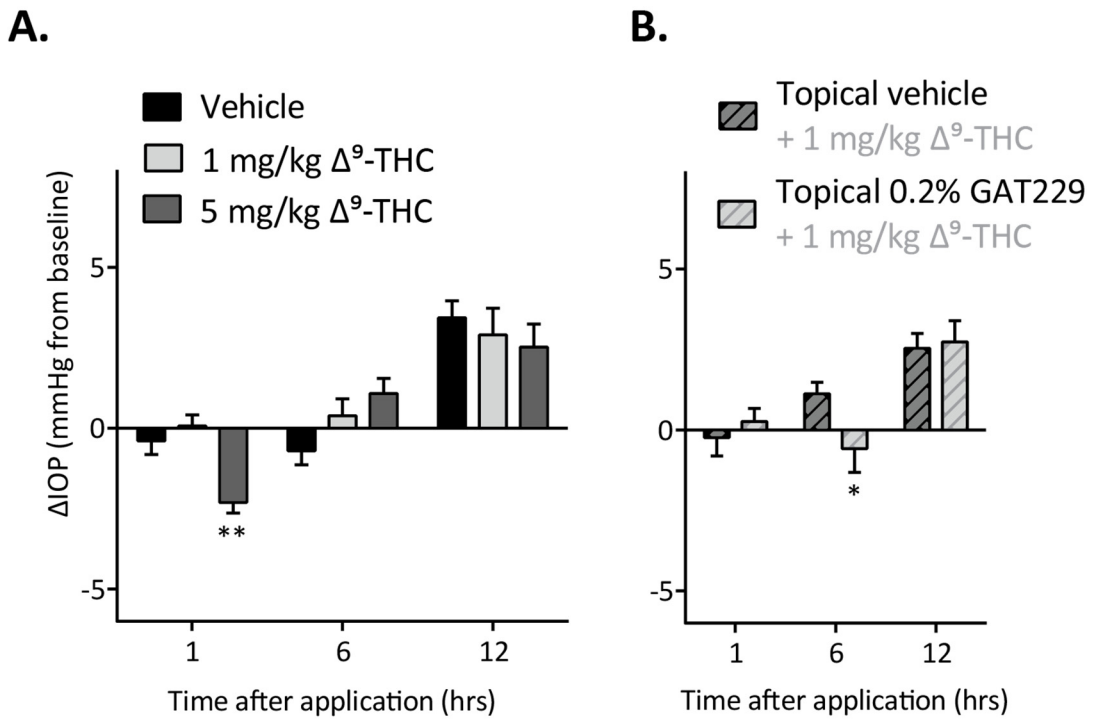

Figure 4.9 - Effects of the combination of i.p. Δ^9-THC with topical 0.2% GAT229 on IOP in normotensive C57Bl/6 mice. (**A**) Intraperitoneal administration of 5 mg/kg Δ^9-THC produced an IOP-lowering effect at 1 hour compared with vehicle-treated mice. However, i.p. administration of 1 mg/kg Δ^9-THC did not produce an IOP-lowering effect and was considered sub-threshold (Dunnett's one-way ANOVA compared with vehicle treatment, N = 5-10 eyes per group). (**B**) In mice receiving i.p. 1 mg/kg Δ^9-THC, there was a significant decrease in IOP in eyes receiving topical 0.2% GAT229 compared with contralateral eyes receiving vehicle at 6 hours, but not 1 or 12 hours post-administration, indicating potentiation of the subthreshold dose (paired t-test, N = 9 mice). * = $P < 0.05$, ** = $P < 0.01$.

administration compared with mice receiving vehicle (**Fig. 4.9A**), and was therefore considered a subthreshold dose.

Combination of subthreshold Δ^9-THC with GAT229 was then investigated for potential PAM-induced potentiation. For these experiments, mice were topically administered vehicle and 0.2% GAT229 in opposing eyes, alongside i.p. administration of 1 mg/kg Δ^9-THC. Like the topical co-administration of GAT229 with WIN (**Fig. 4.8C**), the combination of subthreshold i.p. Δ^9-THC and topical 0.2% GAT229 significantly reduced IOP at 6 hours compared with contralateral eyes receiving vehicle ($P < 0.05$, -0.6 ± 0.7 and 1.2 ± 0.4 mmHg from baseline, respectively, $N = 9$; **Fig. 4.9B**), but not at 1 or 12 hours. Thus, again, the potentiation of the orthosteric ligand with GAT229 produced an IOP-lowering effect, but with a different time course to the suprathreshold agonist alone.

Possible IOP-lowering effects through potentiation of endocannabinoids (e.g., AEA and 2-AG) by CB_1 allosteric modulation was also investigated in normotensive mice. As endocannabinoids are very unstable, they are difficult to administer in *in vivo* systems. Therefore, endocannabinoids were artificially increased by inhibiting endocannabinoid degrading enzymes. The FAAH inhibitor URB597 was used to increase AEA; URB597 injected i.p. increases brain AEA within 15 mins (and lasting at least 16 hours); therefore, likely increasing ocular AEA within a similar timeframe (Fegley et al., 2005; Piomelli et al., 2006). To facilitate time to reach ocular tissues and exert its effects, URB597 was injected i.p. 30 mins prior to topical administration of GAT229. IOP recordings were measured immediately prior to URB597 administration (-30 minutes), immediately prior to topical administration of GAT229 (0 minutes), and then 1, 6, and 12 hours thereafter. Mice receiving 0.3 mg/kg URB597 and 0.2% GAT229 exhibited a significant IOP-lowering effect compared with mice receiving i.p. and topical vehicle at 12 hours following topical administration ($P < 0.05$, mean difference 4.2 ± 1.3 mmHg, $N = 6$ in each group; **Fig. 4.10**).

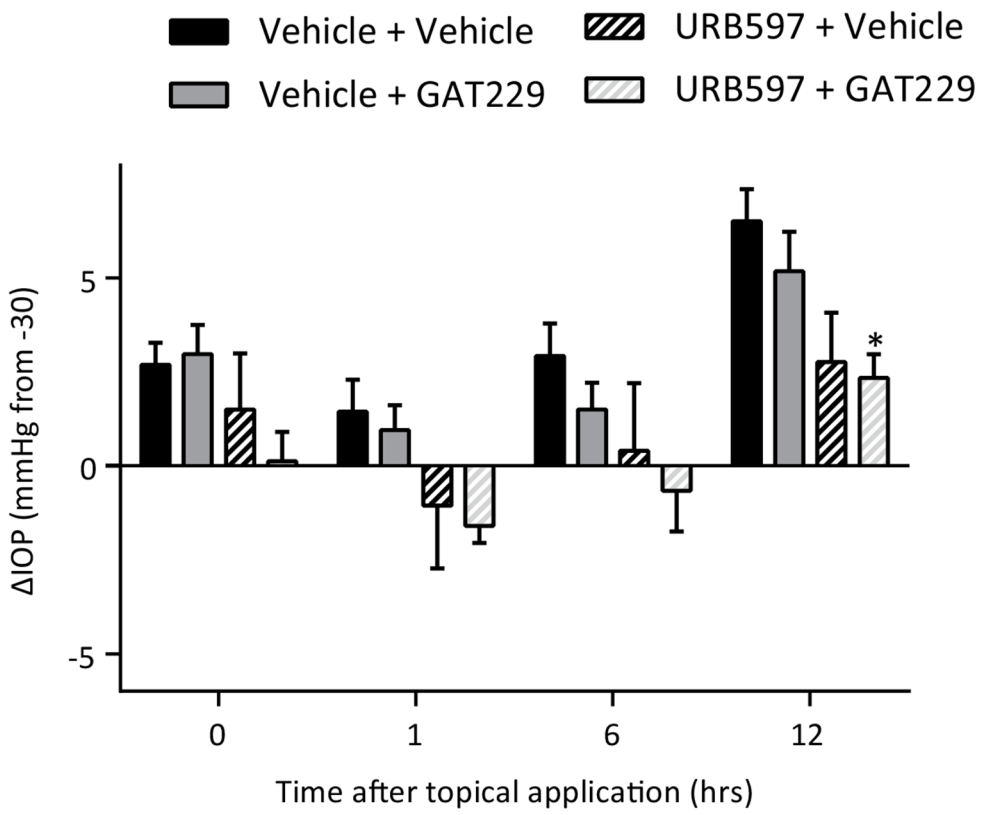

Figure 4.10 - Effects of the combination of the i.p. FAAH inhibitor URB597 with topical 0.2% GAT229 in normotensive C57Bl/6 mice. Intraperitoneal administration of either 0.3 mg/kg URB597 (hatched bars) or i.p. vehicle (solid bars) occurred 30 minutes prior to topical application (time 0) of either vehicle or 0.2% GAT229. Combination of either i.p. URB597 with topical vehicle (hatched black), or i.p. vehicle with topical 0.2% GAT229 (solid grey) did not produce an IOP-lowering effect compared with combined i.p. and topical vehicle treatments (solid black). However, combination of URB597 with 0.2% GAT229 (hatched grey) produced a significant IOP-lowering effect at 12 hours post topical administration compared with combined i.p. and topical vehicle treatments. N = 5-6 eyes per group. Dunnett's one-way ANOVA compared with combined vehicle treatments. * = $P < 0.05$.

Neither URB597 with topical vehicle, nor GAT229 with i.p. vehicle, reduced IOP significantly at any of the time points measured (N = 5 and 6, respectively).

Next, MAGL inhibition was explored to investigate potential CB_1 PAM potentiation of the endocannabinoid 2-AG. Topical administration of the MAGL inhibitor KML29 has previously been shown to lower IOP at 1 hour (Miller et al., 2016a). It was unknown if this effect could be potentiated by a CB_1 PAM. Similar to the previous report, topical administration of 1 mM KML29 significantly reduced IOP compared to eyes receiving vehicle 1 hour following administration (mean difference 1.6 ± 0.2 mmHg, $P < 0.01$, N = 5; **Fig. 4.11C**), but not at 4 hours. Neither 0.1 mM nor 0.2 mM produced significant IOP lowering at either 1 or 4 hours (N = 5 in each group; **Fig. 4.11A-B**), and were considered subthreshold doses. Unlike the combination of GAT229 with other orthosteric agonists, combination of 0.1 or 0.2 mM KML29 with 0.2% GAT229 did not produce an IOP-lowering effect at either 1 or 4 hours compared with contralateral eyes receiving vehicle (N = 6 and 9, respectively; **Fig. 4.11D-E**). Peculiarly, combination of 0.2% GAT229 and 1 mM KML29 resulted in no significant IOP-lowering effect when compared with eyes receiving vehicle at 1 or 4 hours (N = 5; **Fig. 4.11F**), unlike administration of 1 mM KML29 alone (**Fig. 4.11C**).

4.3.1.2 Acute Effects of CB_1 Modulators in Ocular Hypertensive Mice

The effects of ocular hypotensive drugs can vary in normotensive versus hypertensive settings; structural alterations in tissues associated with aqueous humor outflow have been reported in ocular hypertensive eyes, and may affect the functioning of certain drugs (Tamm et al., 2015). Additionally, endocannabinoid levels are altered in various disease states, which may alter how PAMs function (Di Marzo, 2008; Janero & Thakur, 2016; Pacher & Kunos, 2013). Ocular hypertensive adult nee mice (2-6 months) were used to investigate the effects of CB_1 modulators.

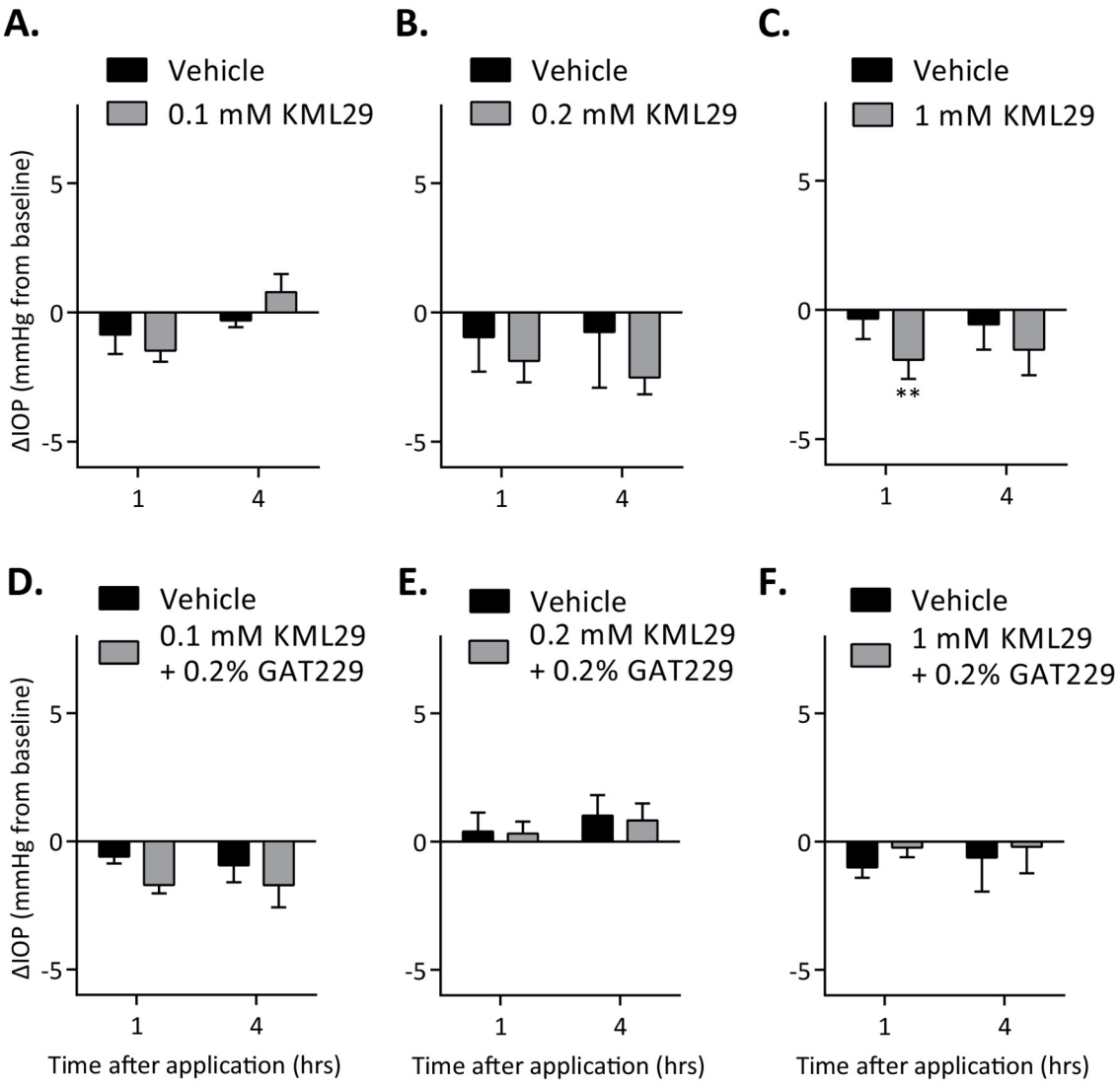

Figure 4.11 - Effects of the MAGL inhibitor KML29, alone or in combination with 0.2% GAT229, on IOP in normotensive C57Bl/6 mice. The effects of drugs were investigated at 1 and 4 hours following administration. Administration of (**A**) 0.1 mM and (**B**) 0.2 mM of KML229 had no effect on IOP. (**C**) Administration of 1 mM KML29 produced a significant IOP-lowering effect at 1 hour compared with vehicle treatment. Combined treatment of 0.2% GAT229 with topical (**D**) 0.1 mM, (**E**) 0.2 mM, or (**F**) 1 mM KML29 had no effect on IOP at either 1 or 4 hours compared to vehicle treated eyes. *N* = 5-9 mice per group. Paired t-tests. ** = $P < 0.01$.

Topical administration of 1% WIN in nee mice did not significantly reduce IOP compared with contralateral vehicle-treated eyes at 1, 6, or 12 hours (*N* = 6; **Fig. 4.12B**), unlike the IOP-lowering effect observed after administration in normotensive wildtype mice (**Fig 4.5C**). Similarly, 0.25% WIN did not produce an IOP-lowering effect (N = 4; **Fig. 4.12A**). As observed in normotensive mice (**Fig. 4.6**), administration of 0.2% or 2% GAT211 did not produce an IOP-lowering effect 1, 6, or 12 hours (*N* = 6 and 5, respectively; **Fig. 4.13A-B**), nor did combination of 0.2% or 2% GAT211 with 0.25% WIN (*N* = 6 and 4, respectively; **Fig. 4.13C-D**).

Unlike in normotensive mice (**Fig. 4.8A**), administration of 0.2% GAT229 alone produced a significant IOP-lowering effect compared with contralateral eyes receiving vehicle at 6 and 12 hours ($P < 0.05$, mean difference 4.10 ± 2.2 and 7.7 ± 3.0 mmHg, respectively, *N* = 6; **Fig. 4.14A**), but not at 1 hour. This effect was similar to that observed in normotensive mice receiving 0.2% GAT229 with 0.25% WIN (**Fig. 4.8C**). Interestingly, the combination of 0.2% GAT229 and 0.25% WIN did not produce a significant IOP-lowering effect in adult nee mice (*N* = 6; **Fig. 4.14C**), though the change in IOP from baseline tended to be greater in those eyes than in vehicle. In contrast to the IOP-lowering seen with 0.2% GAT229 alone at 6 and 12 hrs, administration of 2% GAT229 alone did not significantly produce an IOP- lowering effect at 1, 6, or 12 hours after administration (*N* = 5; **Fig. 4.14B**). However, the combination of 2% GAT229 with 0.25% WIN produced a significant IOP-lowering effect at 1 hour ($P < 0.05$, mean difference 11.7 ± 3.7 mmHg, *N* = 4; **Fig 4.14D**), but not 6 or 12, similar to the time course of the IOP-lowering effect of 1% WIN in normotensive mice (**Fig. 4.5C**).

To investigate if GAT229 could also produce an IOP-lowering effect using a different route of delivery, i.p. administration was also investigated. Twelve hours following i.p. administration of 10 mg/kg GAT229, changes in IOP from baseline were greater compared

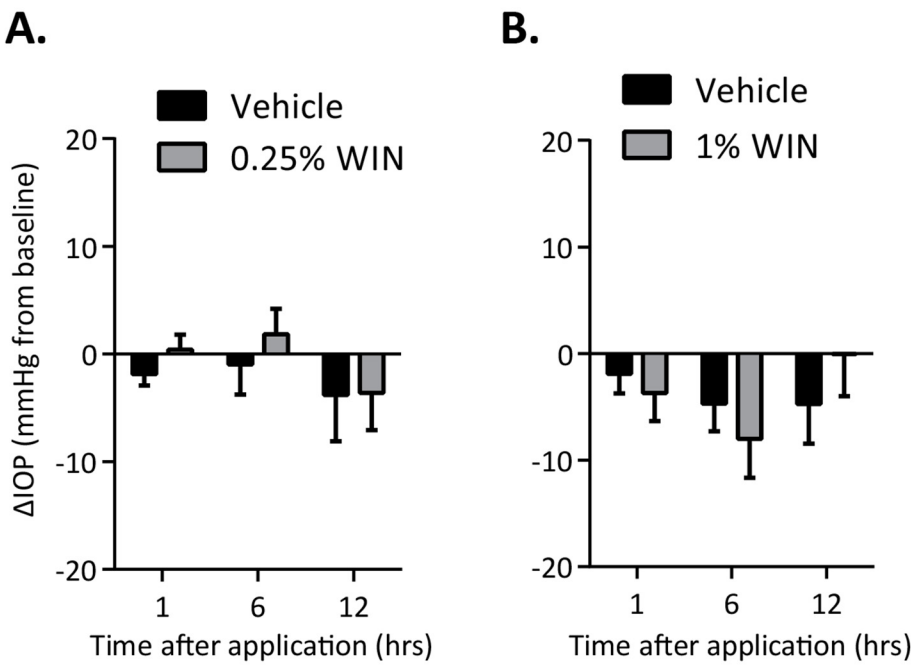

Figure 4.12 - Effects of topical WIN on IOP in ocular hypertensive adult nee mice. Administration of either (**A**) 0.25%, or (**B**) 1% topical WIN did not have significant effect on IOP compared with vehicle-treated eyes. *N* = 4-6 mice per group. Paired t-tests.

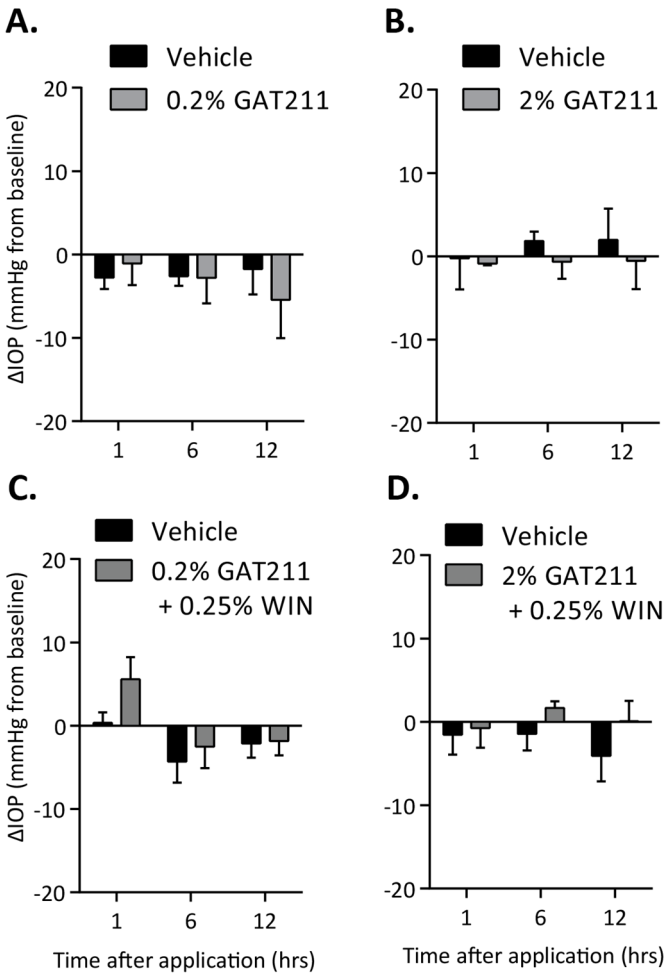

Figure 4.13 - Effects of the CB_1 ago-PAM GAT211, alone or in combination with WIN, on IOP in ocular hypertensive adult nee mice. Topical administration of GAT211 at (**A**) 0.2%, or (**B**) 2%, did not reduce IOP compared with vehicle-treated group. Combinations of (**C**) 0.2% GAT211, or (**D**) 2% GAT211, with 0.25% WIN also did not lower IOP compared with vehicle-treated eyes. *N* = 4-6 mice per group. Paired t-tests.

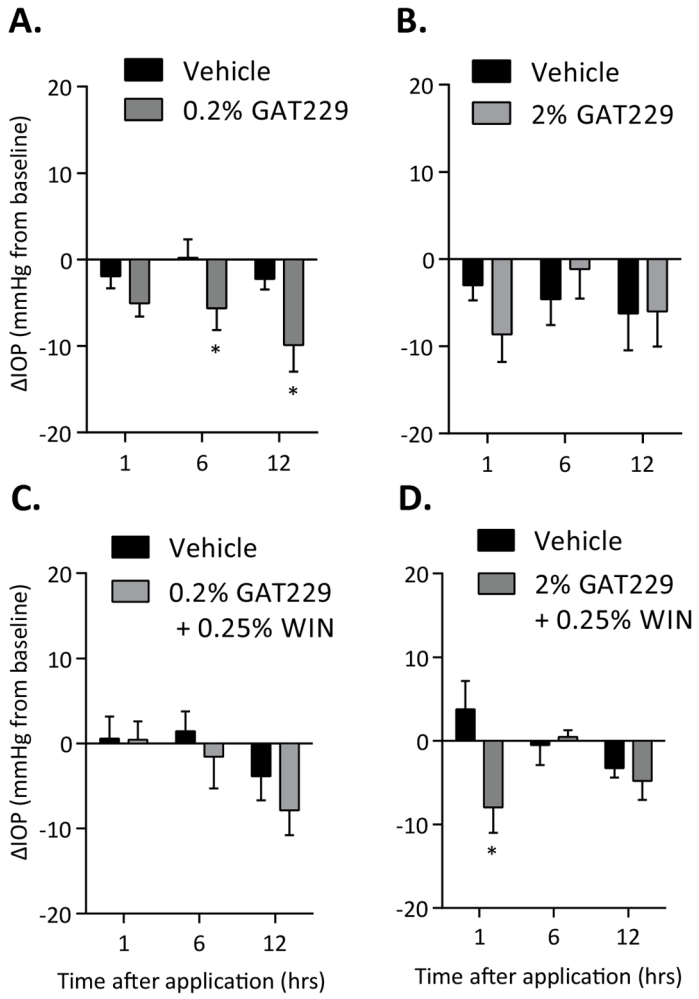

Figure 4.14 - Effects of topical administration of the CB_1 PAM GAT229, alone or in combination with WIN, on IOP in ocular hypertensive adult nee mice. (**A**) Topical administration of 0.2% GAT229 alone significantly reduced IOP at 6 and 12 hours following administration, as compared to contralateral vehicle-treated eye. (**B**) However, the administration of 2% GAT229 had no effect on IOP. (**C**) Co-administration of 0.2% GAT229with 0.25% WIN did not affect IOP, compared to vehicle, at 1, 6, or 12 hours following treatment. (**D**) Co-administration of 2% GAT229 with 0.25% WIN produced a significant IOP-lowering effect at 1 hour following administration, but not 6 or 12 hours. *N* = 4-6 mice per group. Paired t-tests. * = $P < 0.05$.

with adult nee mice receiving vehicle ($P < 0.01$, mean difference 8.7 ± 2.5 mmHg, $N = 4$ mice per group, t-test; **Fig. 4.15**), an effect which was similar to the effect of topical 0.2% GAT229 in nee mice (**Fig 4.14**).

4.3.2 The Effect of CB_1 Modulators on TNFα-Induced AMPA Responses and Neuroprotection

4.3.2.1 Cannabinoid-Mediated Modulation of TNFα-Induced cpAMPAR Expression

In the previous chapter (**Chapter 3**), I reported that one mechanism possibly contributing to glaucomatous RGC loss is via a TNFα-induced increase in cpAMPAR expression. In hippocampal neurons, WIN administration prevented TNFα-induced increases in surface GluA1 expression by a CB_1-dependent mechanism. This reduction was also associated with a reduction in excitotoxic death (Zhao et al., 2010). Therefore, it is possible that CB_1 activation in the retina could act similarly, and may be a mechanism by which CB_1 activation could provide IOP-independent neuroprotection.

To investigate this hypothesis, Ca^{2+} imaging was performed on *ex vivo* wildtype retinas as per **Chapter 4**, with the following additions. Following initial AMPA administration (10 μM) and recovery, retinas were subjected to either WIN (10 μM; Lalonde et al., 2006; Opere et al., 2006; Zhao et al., 2010) or vehicle for 30 minutes prior to the addition of 10^{-3} μg/μL TNFα or vehicle for 45 minutes. AMPA-induced calcium responses were then observed immediately following TNFα or vehicle, and then 15 and 30 minutes thereafter.

Compared with retinas receiving vehicle, AMPA-induced calcium responses immediately following incubation of TNFα alone were significantly larger ($P < 0.05$, mean difference 148.4 ± 38.9%, $N = 4$-5; **Fig. 4.16**). However, this response was not significant 15 or 30 minutes later. Exposure to WIN prior to TNFα significantly reduced the TNFα

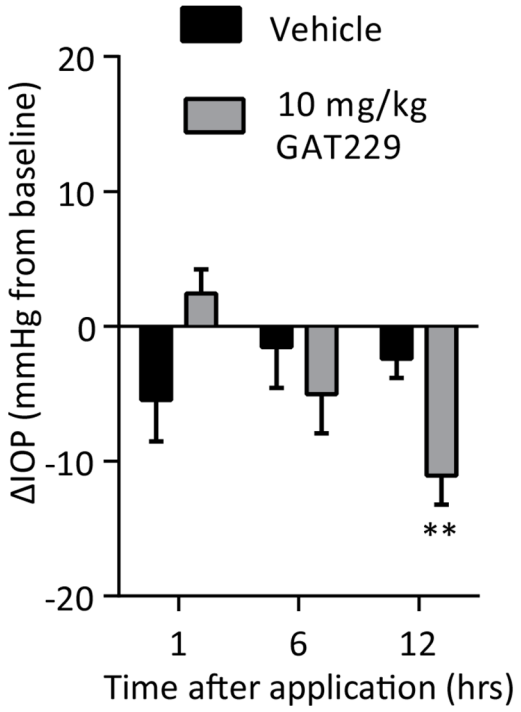

Figure 4.15 - Effects of i.p. administered GAT229 on IOP in ocular hypertensive adult nee mice. Intraperitoneal administration of 10 mg/kg GAT229 resulted in a significant decrease in IOP from baseline at 12 hours, but not 1 or 6 hours, following administration when compared with vehicle treated mice. *N* = 7-8 eyes per group. Unpaired t-test. ** = $P < 0.01$.

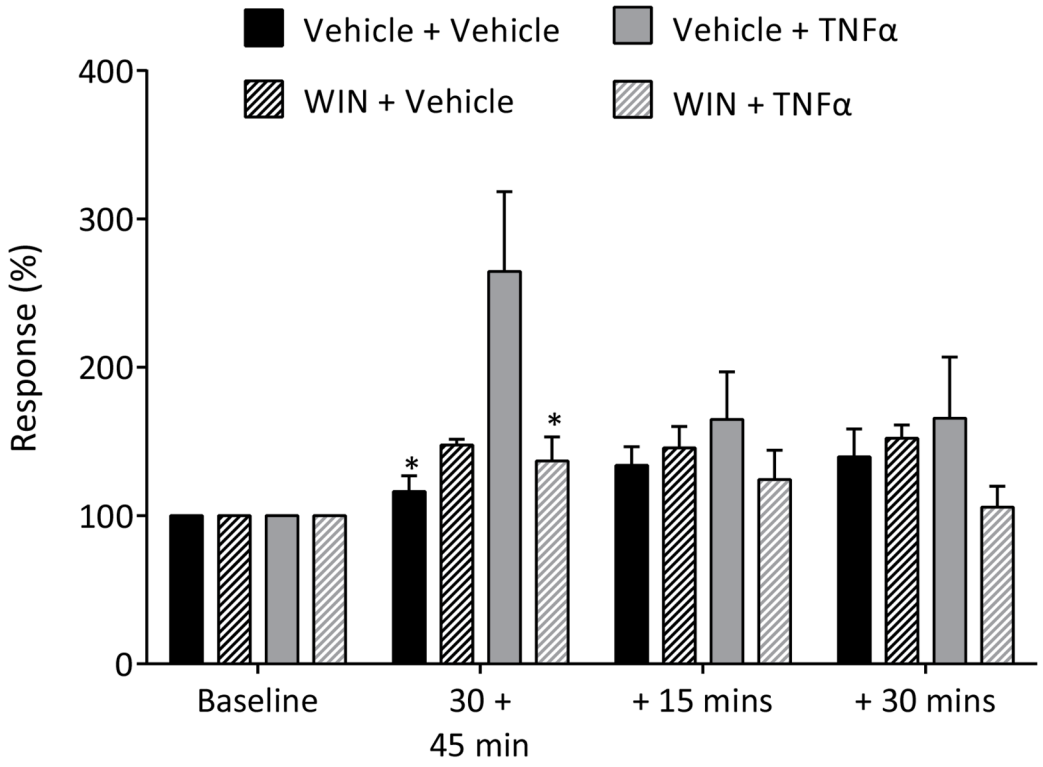

Figure 4.16 - Effects of WIN on TNFα-induced increase in AMPA response in naïve C57Bl/6 ganglion cell layer neurons. AMPA was administered alone (10 μM, baseline) prior to 30 minute incubation of either WIN (10 μM, hatched) or vehicle (solid bars), followed by a 45 minute incubation with either TNFα (10^{-3} μg/μL, grey) or vehicle (black). Responses in each cell were normalized to the initial AMPA response (100%) prior to analysis. Immediately following incubation, AMPA was administered again (30+45 min), and then 15 (+15 mins) and 30 minutes (+30 mins) thereafter. Immediately following incubation, bath application of TNFα alone resulted in significantly greater AMPA-induced calcium responses compared with vehicle treatment. While WIN administration in the absence of TNFα did not produce a significant effect compared with vehicle treatment, WIN administration in the presence of TNFα resulted in significantly lower AMPA-induced calcium responses immediately following incubation compared to TNFα treatment alone, but was not significantly different from vehicle treatment alone or WIN treatment in the absence of TNFα. *N* = 3-5 experiments per group. Tukey's one-way ANOVA. * = $P < 0.05$ (compared with vehicle + TNFα treatment).

response ($P < 0.05$, mean difference 127.7 ± 41.0%, $N = 4$), and was not significantly different from vehicle ($P > 0.05$). Administration of WIN in the absence of TNFα did not appear to have any effect on AMPA-induced Ca^{2+} responses at any time point ($P > 0.05$; $N = 3$). These results are consistent with the findings in hippocampal neurons (Zhao et al., 2010), and suggest that CB_1 modulation can inhibit TNFα-induced increases in cpAMPARs on RGCs, and may therefore be a possible mechanism of IOP-independent neuroprotection in glaucoma.

4.3.2.2 The Effect of Chronic CB_1 PAM Administration in Nee Mice

The effect of chronic CB_1 PAM administration on glaucomatous RGC death was then investigated in two models of glaucoma: in an ocular hypertensive model (nee), and an IOP-independent model (ONT). Nee mice were administered either topical or i.p. CB_1 modulators once per day for either 12 or 21 days beginning at p16 (**Fig. 4.17-19**). Daily topical administration of either 0.2% or 2% GAT211 or GAT229 alone for 12 days did not produce any effect on RGC density compared with the vehicle-treated group (N = 8-12 in each group; **Fig. 4.17B**). While RGC density tended to be greater in eyes receiving 0.25% WIN than in vehicle, there was no statistically significant effect, nor was there any difference in RGC density in eyes receiving 1% WIN ($N = 8$ in each WIN group; **Fig. 4.17B**). Administration of 0.25% WIN did increase the regional RGC density in the middle retina ($P < 0.05$, mean difference with vehicle treatment 170 ± 422 RGCs/mm^2; **Fig. 4.17C**), but not in the central or peripheral retina. This increase in RGC density was surprising, especially given that IOPs of nee mice before sacrifice (12 hours after administration of the drug; 9:30 pm) were significantly higher than nee mice receiving vehicle ($P < 0.05$, 32.2 ± 1.8 and 24.1 ± 1.5 mmHg, respectively; **Fig. 4.17A**). Topical co-administration of 0.2% GAT229 and 0.25% WIN for 12 days also did not produce an effect on RGC density ($N = 10$; **Fig. 4.17B**). Except for the previously mentioned 0.25% WIN treatment, IOPs taken from nee mice on

Figure 4.17 - IOP and RGC density after 12 days of daily topical administration of drugs in nee mice. Beginning at p16, nee mice received 12 days of consecutive topical treatment of either vehicle (grey), GAT211 (0.2 or 2%, blue), GAT229 (0.2 or 2%, red), WIN (0.25 or 1%, green), or the combination of 0.2% GAT229 and 0.25% WIN (purple). (**A**) Twelve hours following topical administration on the final day, absolute IOPs were significantly higher in nee mice receiving 0.25% WIN alone compared with vehicle-treated eyes. (**B**) Mean RGC densities did not significantly differ from vehicle treatment. (**C**) However, administration of 0.25% WIN alone resulted in significantly greater regional RGC density in the middle retina, but not central or peripheral retina, compared with vehicle treatment. No other drug treatment produced a significant effect on either mean RGC density, or regional RGC density per retina. N = 8-12 eyes per group. Dunnett's one way ANOVA compared with vehicle treatment. * = $P < 0.05$.

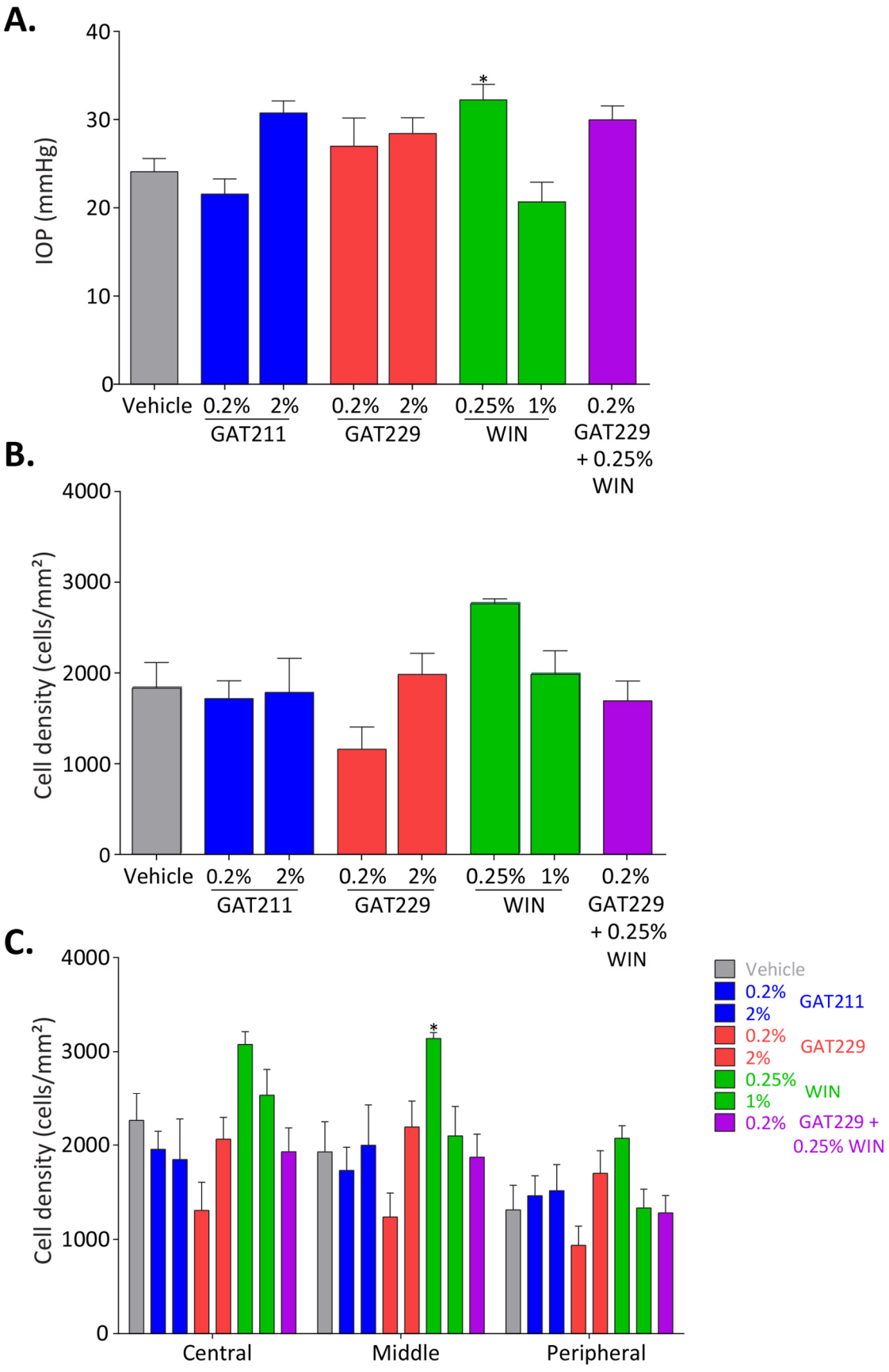
A.
IOP (mmHg)
40
30
20
10
0
*
Vehicle
0.2%
2%
GAT211
0.2%
2%
GAT229
0.25%
1%
WIN
0.2%
GAT229
+ 0.25%
WIN
B.
Cell density (cells/mm²)
4000
3000
2000
1000
0
Vehicle
0.2%
2%
GAT211
0.2%
2%
GAT229
0.25%
1%
WIN
0.2%
GAT229
+ 0.25%
WIN
C.
Cell density (cells/mm²)
4000
3000
2000
1000
0
*
Central
Middle
Peripheral
Vehicle
0.2%
2%
GAT211
0.2%
2%
GAT229
0.25%
1%
WIN
0.2%
GAT229 +
0.25% WIN

Figure 4.18 - IOP and RGC density after 21 days of daily topical administration of drugs in nee mice. Beginning at p16, nee mice received 21 days of consecutive topical treatment of either vehicle (grey), GAT211 (0.2 or 2%, blue), GAT229 (0.2 or 2%, red), WIN (0.25 or 1%, green), or the combination of GAT229 (0.2% or 2%) and 0.25% WIN (purple). (**A**) Twelve hours following topical administration on the 21st day, absolute IOPs were not significantly different compared with vehicle-treated eyes. (**B**) Mean RGC densities or (**C**) regional RGC densities per retina were not significantly different following 21 day drug treatments from vehicle-treated retinas. *N* = 8-12 eyes per group. Dunnett's one way ANOVA compared with vehicle treatment.

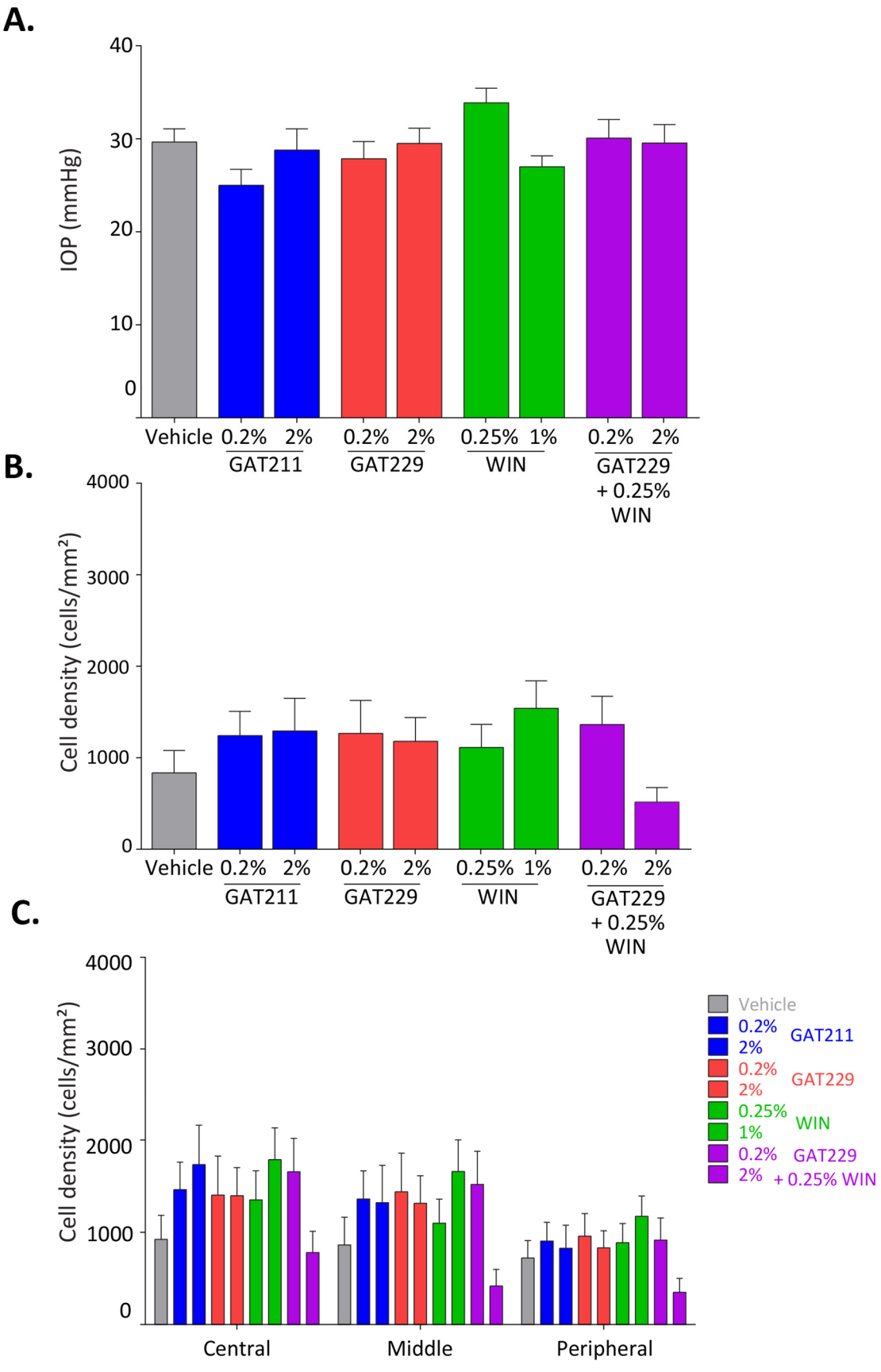
A.
IOP (mmHg)
40
30
20
10
0
Vehicle
0.2%
2%
GAT211
0.2%
2%
GAT229
0.25%
1%
WIN
0.2%
2%
GAT229
+ 0.25%
WIN
B.
Cell density (cells/mm²)
4000
3000
2000
1000
0
Vehicle
0.2%
2%
GAT211
0.2%
2%
GAT229
0.25%
1%
WIN
0.2%
2%
GAT229
+ 0.25%
WIN
C.
Cell density (cells/mm²)
4000
3000
2000
1000
0
Central
Middle
Peripheral
Vehicle
0.2%
2%
GAT211
0.2%
2%
GAT229
0.25%
1%
WIN
0.2%
2%
GAT229
+ 0.25% WIN

Figure 4.19 - IOP and RGC density after 21 days of daily i.p. administration in nee mice. Beginning at p16 nee mice were administered with either vehicle (grey), 10 mg/kg GAT211 (blue), or 10 mg/kg GAT229 (red). (**A**) Twelve hours following i.p. administration on the last day, IOP in nee mice receiving either GAT211 or GAT229 were not significantly different than vehicle-treated mice. (**B**) Additionally, GAT211 or GAT229 treatment did not result in significantly different mean, or (**C**) regional RGC densities compared to vehicle-treated eyes. *N* = 10-11 eyes per group. Dunnett's one way ANOVA compared with vehicle treatment.

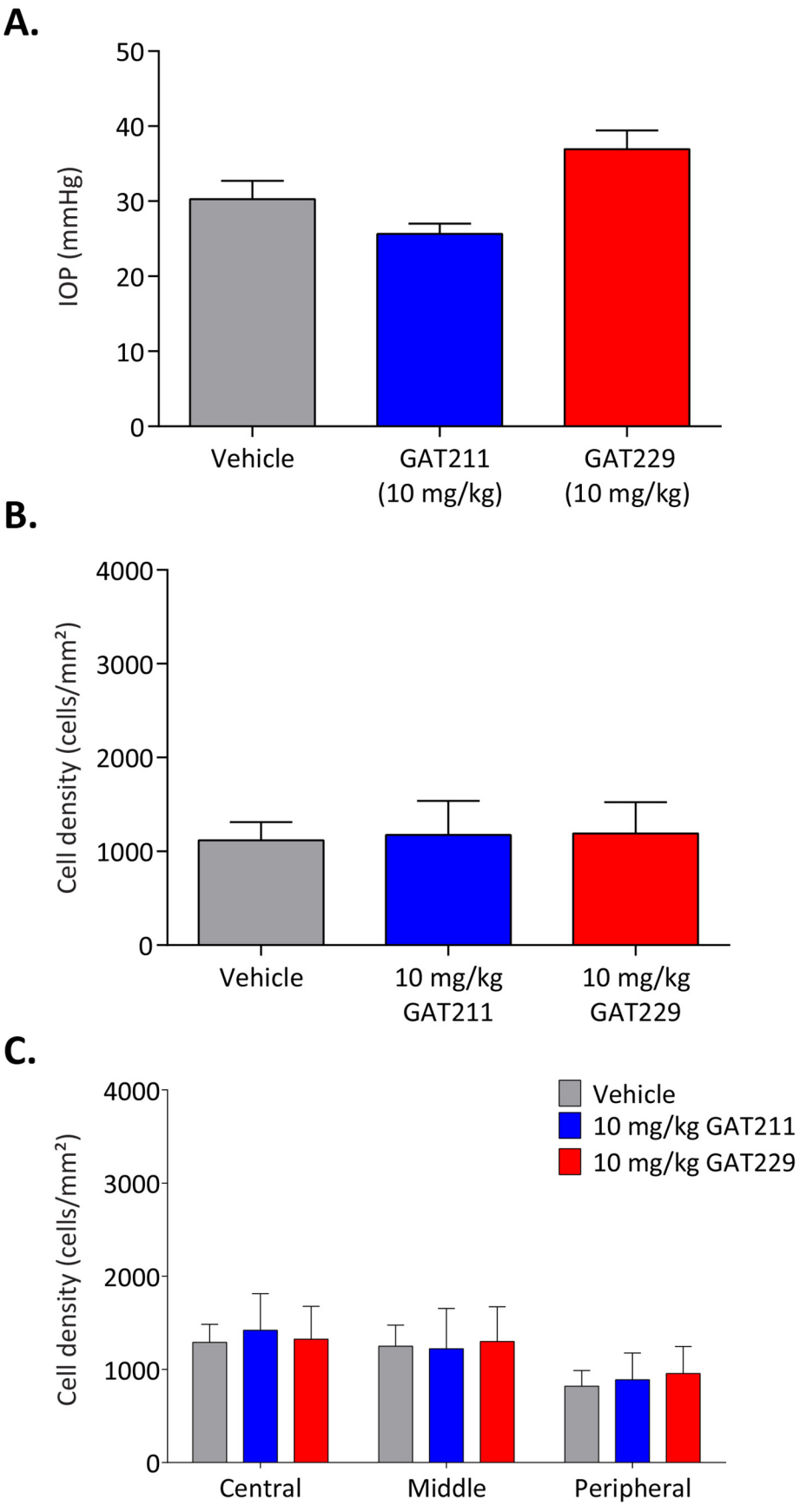
A.
IOP (mmHg)
50
40
30
20
10
0
Vehicle
GAT211
(10 mg/kg)
GAT229
(10 mg/kg)
B.
Cell density (cells/mm²)
4000
3000
2000
1000
0
Vehicle
10 mg/kg
GAT211
10 mg/kg
GAT229
C.
Cell density (cells/mm²)
4000
3000
2000
1000
0
Vehicle
10 mg/kg GAT211
10 mg/kg GAT229
Central
Middle
Peripheral

the last day of administration, 12 hours following the final administration, were not significantly different from nee mice eyes receiving vehicle treatment (**Fig. 4.17A**).

Following 21 days administration, compared with vehicle-treated eyes, RGC densities in nee mice receiving daily 0.2% or 2% GAT211 or GAT299 were not significantly different (*N* = 9-12; **Fig. 4.18B**). Unlike 12 day administration (**Fig. 4.17C**), RGC density in eyes receiving 0.25% WIN were not significantly different in any retinal sector (*N* = 10; **Fig. 4.18C**), as was the case following 1% WIN administration (*N* = 12). Combination of 0.25% WIN with 0.2% or 2% GAT229 also had no effect on RGC density (*N* = 10 and 8, respectively). None of the IOPs taken from each drug group were significantly different from eyes receiving vehicle on the final day, 12 hours after administration (**Fig. 4.18A**).

Efficacy using an alternate route of administration was also investigated. Daily i.p, injections of either GAT211 or GAT229 (10 mg/kg) for 21 days beginning at p16 had no effect on RGC density when compared with vehicle, or on IOP measured 12 hours after administration on the final day (*N* = 10-11 in each group; **Fig. 4.19**).

4.3.2.3 The Effect of Chronic CB_1 PAM Administration in Optic Nerve Transection

As RGC damage following ONT does not rely on IOP, ONT was also used to test for potential IOP-independent neuroprotection via CB_1 modulation. Axotomized eyes were treated topically for 7 days. Similar to 12 day administration in nee mice (**Fig. 4.17**), topical administration of either 0.2% or 2% GAT211 or GAT229 alone had no effect on average RGC density (*N* = 4-5 in each group; **Fig. 4.20A**); however, administration of 2% GAT229 did result in an increased regional RGC density in central retina ($P < 0.05$, mean difference 322 ± 105 RGCs/mm^2; **Fig. 4.20B**). Overall, axotomized eyes receiving daily topical administration of 0.25% WIN (*N* = 5) or 1% WIN (*N* = 5), did not have significantly greater

Figure 4.20 - RGC density after 7 days of daily topical administration in axotomized adult C57Bl/6 mice. Starting on the day of surgery, axotomized mice received 7 days of consecutive topical treatments of either vehicle (grey), GAT211 (0.2 or 2%, blue), GAT229 (0.2 or 2%, red), WIN (0.25 or 1%, green), or the combination of 0.2% GAT229 and 0.25% WIN (purple). (**A**) Mean RGC densities in drug-treated groups were not significantly different from the vehicle-treated group. (**B**) Administration of 0.25% WIN resulted in a significantly higher regional RGC density in middle retina compared with vehicle, while administration of 2% GAT229 resulted in a significantly higher RGC density in central retina No other drug treatment produced a significant effect on RGC density in central, middle, or peripheral retina compared with vehicle treatment. N = 4-7 eyes per group. Dunnett's one-way ANOVA compared with vehicle treatment. * = $P < 0.05$.

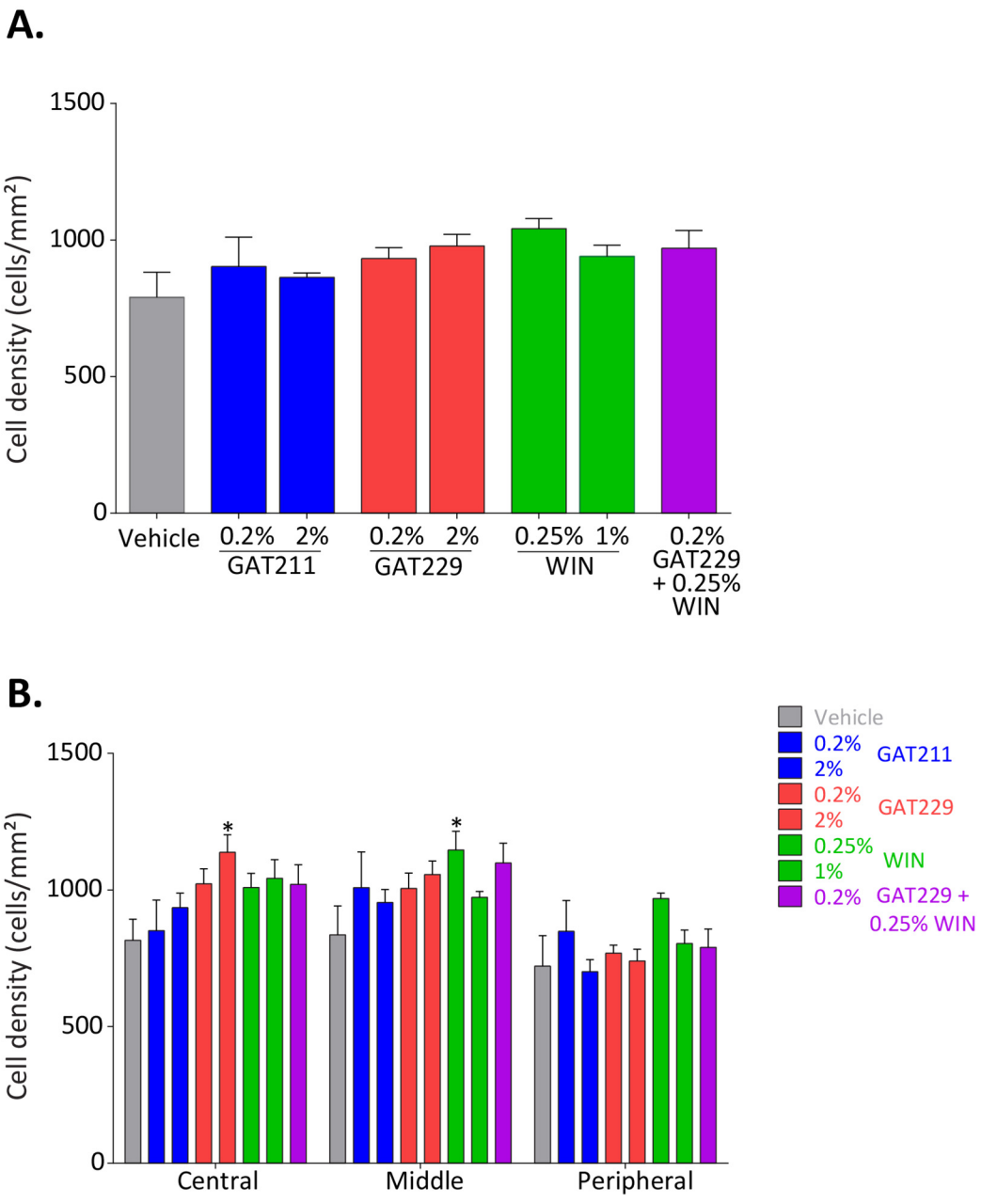
A.
1500
1000
500
0
Cell density (cells/mm²)
Vehicle
0.2%
2%
GAT211
0.2%
2%
GAT229
0.25%
1%
WIN
0.2%
GAT229
+ 0.25%
WIN
B.
1500
1000
500
0
Cell density (cells/mm²)
*
*
Central
Middle
Peripheral
Vehicle
0.2%
2%
GAT211
0.2%
2%
GAT229
0.25%
1%
WIN
0.2%
GAT229 +
0.25% WIN

RGC density than vehicle-treated axotomized eyes (N = 7), yet RGC density in the middle retina was significantly greater in retinas receiving 0.25% WIN (mean difference 311 ± 111 RGCs/mm^2; **Fig. 4.20B**). The combination of 0.2% GAT229 with 0.25% WIN had no effect on RGC density (N = 5).

To investigate if GAT229 could also potentiate endocannabinoid-mediated IOP-lowering, the FAAH inhibitor URB597 was administered i.p. daily, while GAT229 was administered topically. URB597 administration post-axotomy in rats was previously reported to increase retinal AEA and provide neuroprotection of RGCs (Slusar et al., 2013). In axotomized eyes, daily injection of 0.3 mg/kg URB597 either alone or in combination with topical 0.2% GAT229 did not result in overall changes in RGC density compared with vehicle (N = 4-7 in each group; **Fig 4.21A**). However, administration of URB597 alone significantly reduced regional RGC density in peripheral retina compared with vehicle (P < 0.05, mean difference 182 ± 52 cells/mm^2; **Fig. 4.21B**). Compared to URB597 treatment alone, co-administration with 0.2% GAT229 resulted in an increase in RGC density in both middle and peripheral retina (P < 0.05, mean difference 230 ± 85 and 190 ± 56 RGCs/mm^2, respectively; **Fig. 4.21B**).

4.4 DISCUSSION

The work in this chapter investigated the hypothesis that CB_1 PAMs may be a potential novel therapeutic for the treatment of glaucoma, through both IOP-modification as well as direct RGC neuroprotection. Administration of GAT229, but not GAT211 modified IOP, either alone in nee, or when combined with subthreshold CB_1 orthosteric agonists (0.25% WIN or 1 mg/kg Δ^9-THC) or an indirect CB_1 agonist (0.3 mg/kg URB597) in normotensive mice. However, while *ex vivo* CB_1 modulation via WIN was able to directly manipulate a mechanism which may contribute to glaucomatous RGC loss (TNFα-induced

Figure 4.21 - RGC density after 7 days of daily i.p. administration of URB597 (0.3 mg/kg), alone or in combination with topical administration of GAT229 (0.2%), in axotomized adult C57Bl/6 mice. (**A**) Mean RGC density did not significantly differ in either group compared with vehicle. (**B**) Regional RGC density in peripheral retina of URB597-treated mice was significantly lower than vehicle treated retinas. On the other hand, RGC densities in middle and peripheral retina in mice treated with URB597 and GAT229 were significantly higher than in URB597 treatment alone, but were not significantly different from vehicle-treated group. N = 4-7 eyes per group. Tukey's one-way ANOVA. * = $P < 0.05$.

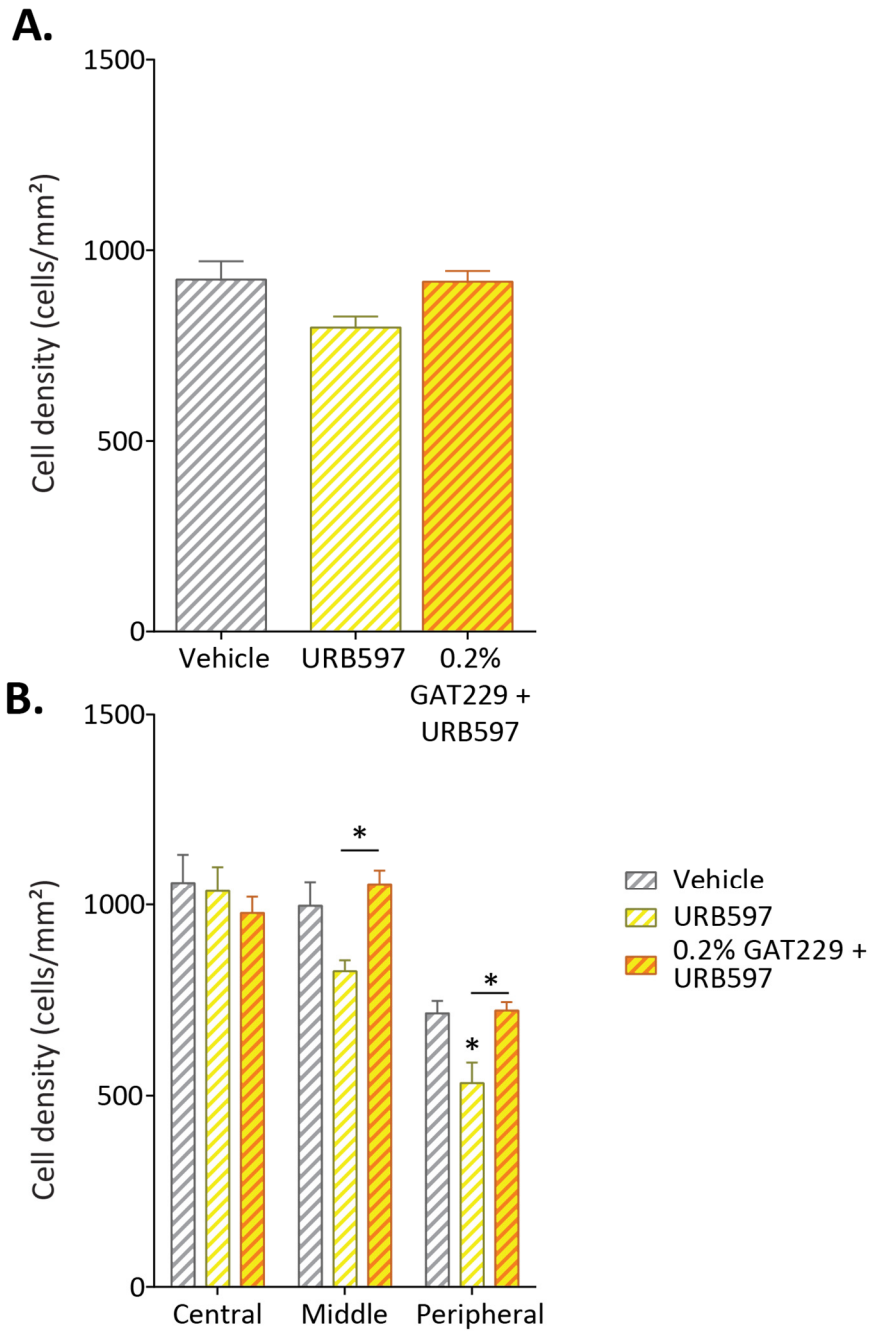
A.
1500
1000
500
0
Cell density (cells/mm²)
Vehicle
URB597
0.2% GAT229 + URB597
B.
1500
1000
500
0
Cell density (cells/mm²)
*
*
*
Central
Middle
Peripheral
Vehicle
URB597
0.2% GAT229 + URB597

changes in cpAMPAR expression), chronic administration of GAT211 or GAT229 did not provide significant neuroprotection in two models of experimental glaucoma.

4.4.1 CB_1 PAMs Can Modulate IOP

While CB_1 PAMs did not appear to deliver neuroprotection in the two models used, the finding that GAT229 could modify IOP was exciting, and is the first reported instance of CB_1 PAM-mediated IOP lowering. Typically, direct orthosteric activation of CB_1 results in an IOP-lowering effect in mice occurring within one hour of administration, as observed in normotensive mice receiving either topical 1% WIN (**Fig. 4.5**) or i.p. 5 mg/kg Δ^9-THC (**Fig. 4.9**), and typically lasts for 1-3 hours (Chien et al., 2003; Hudson et al., 2011; Laine et al., 2002b; Oltmanns et al., 2008; Porcella et al., 2001; Song & Slowey, 2000). In contrast, in both nee and normotensive mice, most GAT229-potentiated IOP effects were delayed, occurring most frequently approximately 6 hours after administration, and sometimes lasting for at least 6 hours, as measured 12 hours post-administration. This extended duration of action is important if CB_1 PAMs are to be considered for use as an IOP-modifying therapeutic, as this translates to less frequent administration. Medication requiring frequent administration has been associated with lack of compliance in glaucoma patients, and may lead to poor IOP control, and thus ineffective treatment (J. C. Buchan et al., 2007; Hermann et al., 2011a; Hermann et al., 2011b; Reardon et al., 2011).

The mechanism by which GAT229 would delay and/or extend the IOP-lowering actions of CB_1 is not yet known. Though, it does not appear to be probe specific, as combination of GAT229 with either 1 mg/kg Δ^9-THC or 0.25% WIN in normotensive mice, and presumed endocannabinoids in nee mice, produced the same delay in effect. Like other allosteric modulators, this delay could be due to stabilization of the receptor in an alternate conformational state (K. H. Ahn, Mahmoud, & Kendall, 2012; Fay & Farrens, 2015; Janero &

Thakur, 2016; Kenakin, 2016; T. Nguyen et al., 2016; Shore et al., 2014; Wootten et al., 2013). Consistently, three spatiotemporally distinct "waves" of CB_1 signalling following orthosteric agonism have been also previously reported, resulting from association with different effector proteins as the receptor moves from activation at the cell surface, to phosphorylation and recruitment of β-arrestins, to intracellular signalling following receptor internalization (Nogueras-Ortiz & Yudowski, 2016). Therefore, it may be possible that allosteric modulation of CB_1 may promote a receptor confirmation which may bias signalling towards a particular wave (Fay & Farrens, 2015; Janero & Thakur, 2016; Nogueras-Ortiz & Yudowski, 2016). Consistent with this, GAT211 decreased the rate of CP55,940 dissociation at CB_1 in mouse whole brain membranes (Laprairie et al., 2017). While the disassociation kinetics of GAT229 were not investigated, it is likely that they have similar effects to GAT211. GAT229 is also reported to have bias towards cAMP inhibition over β-arrestin2 recruitment (Laprairie et al., 2017); however, at this time, it is unclear what type of temporal outcome this may have on signalling (Nogueras-Ortiz & Yudowski, 2016).

Two CB_1 negative allosteric modulators, PSNCBAM-1 and ORG27569, also had delayed effects *in vitro* in human embryonic kidney 3HA-hCB_1 cells and Neuro-2A cells (Cawston et al., 2013). As CB_1 is G_i-coupled, administration of CP55,940 reduces forskolin-induced cAMP production (Pertwee, 2015). At doses corresponding to their respective EC_{50}, both PSNCBAM-1 and ORG27569 abolished CP55,940-mediated inhibition on cAMP production, but this effect was delayed by approximately 3 and 9 minutes, respectively. Furthermore, this effect appeared to be concentration-dependent, as higher doses did not experience a lag in effect, and produced actions that were consistent with stabilization of CB_1 in an inactive state (Cawston et al., 2013). Even though this lag in effect was within a matter of minutes, rather than the approximate 5 hour delay seen with GAT229 on IOP, it is

possible that these small *in vitro* delays may be additive, resulting in significantly amplified effects *in vivo*. These results suggest that allosteric modulation of CB_1, provides the capability of stabilization of receptors in different confirmations, which could promote altered signalling similar to other allosteric modulators at different GPCRs (Cawston et al., 2013; Janero & Thakur, 2016; T. Nguyen et al., 2016; Wootten et al., 2013). In fact, specific analysis of the effects of ORG27569 on CB_1 has revealed promotion of a receptor state which is different from both the inactive and active forms (Fay & Farrens, 2012; Fay & Farrens, 2015). Further analysis of the specific effects of GAT229 on CB_1, including changes over time, may reveal the specific mechanisms which lead to this *in vivo* delay.

As PAMs cannot activate the receptor in the absence of an orthosteric ligand, any PAM-mediated activity is dependent on the presence of an orthosteric ligand (Janero & Thakur, 2016; Kenakin, 2016). Therefore, the activity GAT229 on CB_1 is dependent either on the presence of an administered exogenous orthosteric ligand (e.g., WIN), or local production of endocannabinoids. In normotensive mice, the absence of any IOP-lowering effect of GAT229 when administered without addition of exogenous orthosteric ligands is suggestive of basal endocannabinoid levels which are insufficient to evoke CB_1-mediated IOP responses (Janero & Thakur, 2016; Laprairie et al., 2017). On the other hand, in nee mice, the IOP lowering observed with administration of either topical 0.2% GAT229 or 10 mg/kg GAT229 without addition of exogenous orthosteric ligands is suggestive of an increase in endocannabinoids compared to normotensive mice.

This finding is somewhat in contrast with previous reports investigating endocannabinoid levels in glaucoma. Nucci et al. (2007) reported decreased retinal AEA following ischemia reperfusion injury in rats (alongside increased FAAH activity, and decreased CB_1 expression). However, in ocular tissues from human cadavers with glaucoma, decreased 2-AG and palmitoylethanolamide (PEA) was reported in the ciliary body, and

decreased PEA was found in the choroid, with no reported change in AEA in any of the tissues measured. Studies investigating endocannabinoid profiles can be difficult to interpret given their labile nature (Angelini, Argueta, Piomelli, & DiPatrizio, 2017; Di Marzo, 2008). Endocannabinoids are degraded rapidly, thus technical differences in tissue acquisition or preparation can significantly affect the outcome of the study (Angelini et al., 2017; Piscitelli & Bradshaw, 2017). Nevertheless, the results demonstrated here indicate that further investigation is required specifically with respect to measurement of endocannabinoid levels. Lipid profiling in nee mice has yet to be performed but would provide valuable future insight into disease specific changes in these animals and the actions of CB_1 PAMs.

The hypothesis that IOP effects of GAT229 are due to potentiation of elevated endocannabinoids in nee mice are consistent with the IOP-lowering effect of GAT229 when combined with the FAAH inhibitor URB597 in normotensive mice (**Fig 4.10**). With this combination, although a slight reduction of IOP was present throughout each of the time points observed, this effect was only significant at 12 hours after GAT229 administration, similarly delayed as reported above.

The interpretation of these results is complicated by the multiplicity of actions of FAAH; FAAH metabolises not only AEA, but also contributes to the production of other cannabinoid-related lipids, including NAGly via arachidonic acid (Bradshaw et al., 2009; Fowler et al., 2017; Miller et al., 2016b). FAAH and NAGly, through actions at GPR18, have recently been demonstrated to play a role in diurnal changes of IOP in mice (Aihara et al., 2003; Hudson et al., 2011; Miller et al., 2016b). In both humans and mice, IOP changes throughout the day; depending on the light cycle, in mice, IOP is the lowest around 12-1 pm, while the highest around 9-10 pm (Aihara et al., 2003; Hudson et al., 2011). Miller et al. (2016b) reported increases in NAGly at noon (when IOP is the lowest), compared to

midnight. Blocking noontime increases in NAGly through FAAH inhibition, or directly blocking GPR18, was associated with an increase in IOP. Conversely, blocking GPR18 at night, when IOP is the highest, had no effect on IOP. These results suggest that NAGly is involved in daytime IOP lowering in mice (Miller et al., 2016b). As I began my experiments at 9:30 am, this noontime-effect would correspond to approximately 3 hours following topical application of GAT229. Therefore, blocking NAGly production via FAAH should prevent IOP lowering as a result of diurnal variation at 3 hours, which was a time point not measured in my study. Regardless, in my experiments, administration of 0.3 mg/kg URB597 alone at any time point did not produce an effect on IOP compared with vehicle, suggesting a lack of effect on diurnal variation of IOP at the time points measured. On the contrary, the potentiation of the URB597 response with GAT229 implies CB_1-mediated IOP lowering through AEA. Again, the observed IOP effect is consistent with endocannabinoid-mediated actions of GAT229 in nee mice.

On the other hand, the lack of effect of MAGL inhibition when combined with GAT229 in normotensive mice was surprising (**Fig. 4.9F**), especially given that on its own KML29 was able to produce an IOP-lowering effect (**Fig. 4.9C**), consistent with a previous report (Miller et al., 2016a). The cause of this apparent loss of effect is unknown, but could be a result of alterations in the response time of the IOP-lowering, which was not captured given the time points measured. As 1mM KML29 was already above threshold, it's possible that the enhancement of GAT229 at this dose may have resulted in rapid receptor activation, and desensitization, resulting in an early effect, that was also quickly lost, similar to the loss of time lag with higher doses of either ORG27569 and PSNCBAM-1 *in vitro* (Cawston et al., 2013; Cawston, Connor, Di Marzo, Silvestri, & Glass, 2015). Therefore, further investigation of the time course in IOP changes with the combination of these two drugs may be warranted.

Nevertheless, the ability of CB_1 PAMs to modulate CB_1 without administration of exogenous CB_1 direct orthosteric agonists during nee pathology is advantageous; especially if these findings extend to human glaucoma pathologies. One of the disadvantages of administration of CB_1 direct agonists is that global on-target, but off-site, receptor activation can result in side effects (Ligresti et al., 2016; Pertwee, 2012). In theory, a CB_1 PAM would only exert effects where endocannabinoids are being produced and released (Janero & Thakur, 2016), which is typically spatially and temporally restricted (Fowler et al., 2017), and in this case, is hypothesized to be increased in areas associated with aqueous humor dynamics. Because of this, administration of GAT229 on its own would not be expected to produce the same profile of side effects as a direct orthosteric agonist, including psychoactivity (Laprairie et al., 2017). This was true of the ago-PAM GAT211, as well as the chemically similar CB_1 PAM ZCZ011. Neither of these compounds when administered alone in WT mice resulted in tetrad activity (catalepsy, hypothermia, and antinocicpetion), typical hallmarks of global CB_1 activation (Ignatowska-Jankowska et al., 2015; Slivicki et al., 2017). However, when administered in models of pain, the same doses were sufficient to provide therapeutic efficacy (Ignatowska-Jankowska et al., 2015; Slivicki et al., 2017).

In both normotensive and nee mice, the absence of IOP-lowering effects by the racemic mixture GAT211 (**Figs. 4.5 and 4.13**), compared with the "pure" PAM GAT229 (**Figs. 4.6, 4.14, 4.15**), was surprising, but not completely unexpected. Laprairie et al. (2017), demonstrated significant differences between the actions of the "pure" PAM *S* enantiomer (GAT229) versus the allosteric agonist actions of the *R* enantiomer (GAT228). One explanation, though not directly tested, is that the allosteric agonist GAT228 does not produce any IOP-lowering effects. Therefore, as GAT229 and GAT228 most likely bind to the same, or overlapping, receptor binding sites, it is possible the two enantiomers antagonize, rather than potentiate, the effects of each other. However, that being said, one would expect

that with increasing concentrations of the racemic mixture, a larger population of CB_1 would be activated by GAT229, and an IOP effect would be apparent. However, if CB_1 expression is decreased during glaucoma, as suggested by Nucci et al. (2007), in nee mice it could be that there is insufficient CB_1 population in order to overcome this competition, explaining the complete lack of effect with and without the presence of WIN (**Fig. 4.13**). Therefore, in normotensive mice (with the combination of an subthreshold orthosteric ligand), and possibly in nee mice, a greater concentration of GAT211 may produce an IOP-lowering effect.

With respect to direct cannabinoid activation of CB_1, the lack of effect of 1% WIN alone in nee mice compared to wildtype mice was somewhat surprising, especially given that GAT229 alone was effective in nee mice. Additionally, the loss of effect of 0.2% GAT229 when combined with 0.25%WIN was also surprising. Since nee mice are a model of angle-closure glaucoma, the lack of effect with WIN may be due to an IOP modifying mechanisms which act predominantly by increasing aqueous humor outflow, the latter of which is restricted in nee. To the best of my knowledge, there does not appear to be any literature investigating the effects of WIN in an animal model of angle-closure glaucoma, and WIN, cannabis, or THC actions have been limited to investigation in either normotensive settings, or in models (or humans) with "heterogenous" glaucoma or open angle glaucoma (as reviewed in **section 4.1.2**). It is also possible that IOP lowering with 1% WIN in nee with did occur, but on a different time scale than in normotensive mice, but again, was not captured during the measurement periods in this protocol. Further investigation of additional time points, such as 2, 4, and 8 hours following administration, may clarify this hypothesis.

Co-administration of 2% GAT229 with 0.25% WIN in nee mice (**Fig 4.14D**), on the other hand, produced an IOP-lowering effect similar to suprathreshold administration of

WIN or Δ^9-THC alone in normotensive mice, with lowering present at 1 hour, but not 6 or 12 hours later. The reason for the difference in effect is unknown, but perhaps may reflect a dose-dependent stabilization of the receptor in a non-intermediate state, similar to orthosteric activation. Why this would occur only in nee mice where WIN was co-administered, but not with GAT229 administration alone is unknown.

Taken together, the results from these studies suggest that CB_1 PAMs can lower IOP, causing a delayed, yet sustained, reduction in IOP compared with traditional direct orthosteric CB_1 activation. This type of effect is advantageous in that it would require less frequent administration to achieve the desired effect, reducing potential for patient non-compliance (J. C. Buchan et al., 2007; Hermann et al., 2011a; Hermann et al., 2011b; Reardon et al., 2011). CB_1 PAMs may be administered without the addition of CB_1 agonists, which may result in fewer side effects associated with systemic CB_1 activation (Janero & Thakur, 2016; Ross, 2007). Furthermore, these data are also suggestive that endocannabinoids may be elevated in nee mice, at least in ocular tissues associated with IOP control. Future studies of cannabinoid receptor PAMs will require concurrent measurements of endocannabinoids in the experimental models tested, as well as extended IOP monitoring time with additional dose testing.

4.4.2 CB_1-Mediated Inhibition of Changes in TNFα-Induced cpAMPAR Expression as an Additional Mechanism of RGC Neuroprotection

Following establishment of CB_1 PAMs as modulators of IOP, I wanted to investigate if these compounds could also additionally provide direct neuroprotective effects on RGCs. While CB_1 has previously been reported to provide RGC neuroprotection in models of glaucoma (Crandall et al., 2007; El-Remessy et al., 2003; Nucci et al., 2007; Pinar-Sueiro et al., 2013; Slusar et al., 2013), the mechanisms underlying this neuroprotection in these

models are not yet fully understood. However, there is significant *in vitro* data to support direct RGC survival through several mechanisms, which may include modulation of RGC intracellular Ca^{2+} and excitability, activation of pro-survival pathways, and/or decreasing inflammation (**Fig 4.22**), as reviewed below.

Cannabinoid modulation of pro-survival pathways, for example through protein kinase B (Akt) and/or extracellular signal-related kinases (ERK) 1/2 modulation, has been demonstrated in several neuron types (Batista et al., 2016; Blazquez et al., 2015; Kendall & Yudowski, 2017). In rat retina, CB_1 activation through intravitreal injection of either AEA or the non-selective CB_1/CB_2/GPR55 agonist HU210 was protective against AMPA-induced excitotoxicity, in a CB_1-dependent manner. This was associated with activation of the pro-survival phosphoinositide 3-kinase (PI3K)/Akt pathway, as AEA and HU210 increased retinal phospho-Akt, but was blocked by an inhibitor of PI3K (wortmannin). Further, AEA, but not HU210, also significantly increased phosphor-ERK1/2 in these retinas, which was suggested to be involved in pro-survival pathway activation (Kokona & Thermos, 2015) However, applicability of these findings to RGCs is unknown, as the authors of the study state that this model induces amacrine, but not RGC, death (Kokona & Thermos, 2015).

Cannabinoid modulation of the immune response has been well documented in a variety of tissues, and may occur by decreasing immune cell activation and migration, and modulation of cytokine release (S. H. Kim, Won, Mao, Jin, & Greenberg, 2006; Krishnan & Chatterjee, 2012; Ligresti et al., 2016). As inflammation may play a significant role in the development of glaucomatous pathology (**Chapter 3**), reducing inflammation may aid in reducing glaucomatous RGC death. Consistent with this, in an ocular excitotoxic model, THC-induced promotion of RGC survival was associated with decreased with markers of inflammation, including nitrate and nitrotyrosine (El-Remessy et al., 2003).

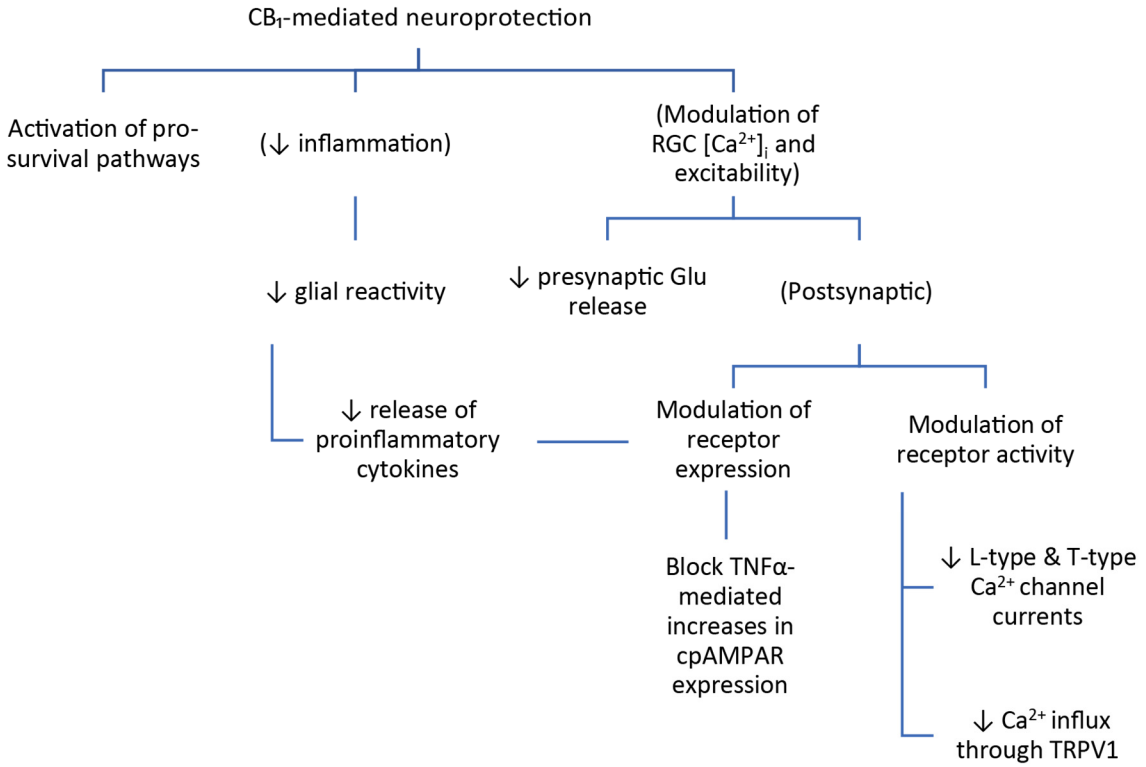

Figure 4.22 - Potential mechanisms of CB_1-mediated RGC neuroprotection.

Cannabinoid induced alterations in retinal Müller, astrocyte, and/or microglial reactivity during glaucomatous injury, may contribute to increased RGC survival. Increases observed in activated microglia one week following ONT were reduced with administration of URB597, in a CB_1-depentent manner (Slusar et al., 2013). Further, exposure of isolated Müller cells to lipopolysaccharide (LPS), a component of gram negative bacterial cell walls, induces gliosis, but is prevented with administration of either AEA or 2-AG (Krishnan & Chatterjee, 2012)

This cannabinoid modulation of reactivity and potential for associated neuronal survival may be a result of modulation of cytokine release. LPS-induced reactive Müller cells exposed AEA or 2-AG significantly decreased release of the pro-inflammatory cytokines interleukin (IL) -1β and TNFα, in a CB_1- and CB_2-dependent manner (Krishnan & Chatterjee, 2012). Additionally, the anti-inflammatory cytokines IL-10 and transforming growth factor β were also increased with cannabinoid exposure to LPS-exposed Müller cells in a CB_1- and CB_2-dependent manner (Krishnan & Chatterjee, 2012).

Finally, cannabinoid-mediated neuroprotection against excitotoxic injury in retina (El-Remessy et al., 2003; Kokona & Thermos, 2015), cerebral cortex (S. H. Kim et al., 2006), and hippocampal neurons (Karanian et al., 2007; Koch et al., 2011; Zhang & Chen, 2008) is consistent with evidence demonstrating that cannabinoids can alter neuronal excitability. Specifically, these mechanisms may include modulating pre-synaptic glutamate release, as well as postsynaptic alterations in receptor expression and/or activity (Jo et al., 2017; Lalonde et al., 2006; Middleton & Protti, 2011; Opere et al., 2006; Qian et al., 2017; Straiker et al., 1999b; X. H. Wang et al., 2016).

RGC excitability can be altered through cannabinoid modulation of presynaptic ion channels (Middleton & Protti, 2011; Opere et al., 2006; Straiker et al., 1999b; X. H. Wang et

al., 2016). WIN administration to isolated rat retina decreased the frequency of both excitatory and inhibitory postsynaptic currents, but not the amplitude or decay time of these currents, in RGCs, suggesting presynaptic, rather than postsynaptic, modulation (Middleton & Protti, 2011; X. H. Wang et al., 2016). Consistent with this, in bipolar cell terminals of tiger salamander, WIN reduced L-type Ca^{2+} channel currents (Straiker et al., 1999b). This modulation of presynaptic membrane potentials may affect glutamate release, and therefore, RGC excitability. In support of this, administration of metAEA, ACEA, and WIN in bovine retina decreased K^+- or ischemia-induced release of ^{3}[H]D-aspartate, a marker of glutamate release, which was blocked by AM251, consistent with a CB_1-dependent mechanism (Opere et al., 2006).

There is also evidence that cannabinoids may alter RGC excitability directly. In purified rat RGC cultures, WIN administration also reduced both L-type and T-type Ca^{2+} channel currents in a CB_1-dependent manner (Lalonde et al., 2006; Qian et al., 2017). Although not a synaptic receptor, TRPV1 may be involved in altering RGC excitability through sensing and responding to mechanical stress, such as during high IOP. Recently, CB_1 was reported to modulate capsaicin-induced TRPV1-mediated increases in intracellular Ca^{2+} in rat RGCs, through a G_i-mediated mediated mechanism (Jo et al., 2017). I have also demonstrated that CB_1 may be directly contributing to RGC neuroprotection via inhibition of TNFα-induced changes in cpAMPAR expression, consistent with previous reports of CB_1-mediated neuroprotection in a model of hippocampal excitotoxicity. This provides evidence of yet another potential mechanism of cannabinoid-mediated neuroprotection previously demonstrated in models of glaucoma, and is particularly relevant given the potential contribution of this pathway to glaucomatous RGC death (**Chapter 3**).

4.4.3 Chronic Treatment of CB_1 PAMs Did Not Provide Neuroprotection in Two Models of Experimental Glaucoma

My investigation of the effects of chronic CB_1 PAM modulation in two models of glaucoma, however, did not provide any significant evidence of mean RGC neuroprotection, apart from some protection in specific retinal regions. With respect to CB_1 orthosteric activation alone, with 12 days of administration, nee mice receiving 0.25% WIN had significantly higher RGC density in the middle retina; however, this effect was not present following 21 days of administration. The same effect was present in ONT, where following 7 days of administration, eyes receiving 0.25% WIN had greater RGC density in middle retina than vehicle. This was in contrast to previous reports, where topical administration of WIN provided significant neuroprotection in a model of ischemia reperfusion injury (Pinar-Sueiro et al., 2013). However, this paper used a transient injury model in rat, and RGCs were measured only 3 days later. This suggests that while WIN may have been efficacious in less severe models, this may not be the same given the severity of injury in nee and ONT.

Administration of topical GAT211 or GAT229 in nee, alone or in combination with WIN, did not produce any effect on mean RGC density, or in any specific area. This lack of effect did not appear to be due to route of administration, as i.p. administration of either GAT211 or GAT229 also did not produce a significant change in RGC density. In contrast, administration of 2% GAT229 for 7 days following ONT, resulted in significantly increased RGC density in the central retina compared with vehicle-treated eyes. Additionally, while not significantly different from vehicle, RGC densities in eyes administered topical 0.2% GAT229 with i.p. URB597 were significantly greater in the middle and peripheral retina compared with eyes receiving URB597 treatment alone. In contrast to a previous study in rats (Slusar et al., 2013), URB597 administration alone in ONT did not increase RGC density compared to vehicle, and in fact, RGC density was lower in peripheral retina than control.

This may be a result of the difference in animal used (mice vs. rat), or perhaps also the vehicle. In the experiments conducted by Slusar and colleagues (2013), URB597 was dissolved in a vehicle containing 33% DMSO. As DMSO can be cytotoxic in retinal cells, especially at such high quantities (Galvao et al., 2014), the vehicle in this study contained 1% DMSO and 1% Tween-80. However, DMSO itself is anti-inflammatory (Santos, Figueira-Coelho, Martins-Silva, & Saldanha, 2003), and therefore, the lack of neuroprotective effect of URB597 in this effect in this study may partially be due to a decrease "dose" of DMSO.

Although administration of at least GAT229 did produce effects on IOP at the chronically administered doses, it is possible that the dose of GAT211 and GAT229 was insufficient to produce neuroprotective effects. Thus, investigation of either higher doses, or repeated dosing throughout the day, may be warranted. Additionally, investigation of the ocular penetrance of these compounds may aid in optimizing dose quantity, but also vehicle delivery.

Additionally, unlike the IOP-lowering at 12 hours compared with vehicle in acute experiments, investigation of IOP at this time point following chronic administration did not show any significant differences between groups. The only exception was with nee mice administered 0.25% WIN for 12 days, where IOP was significantly higher than the rest, surprising given that these mice also had significantly greater RGC densities in middle retina. However, it is possible that while acute administration produced the largest effect on IOP at 12 hours, that with repeated dosing, this time course may have changed. Thus, without further exploring additional time points related with chronic administration, conclusions regarding effects on IOP, or lack there of, with chronic administration can not be made.

4.4.4 SUMMARY

In this chapter, I have demonstrated that while the CB_1 PAM GAT229 can modulate IOP acutely, GAT211 and GAT229, at least at the concentrations investigated, were not effective at promoting neuroprotection in either nee or ONT mice. However, I have also demonstrated that CB_1 orthosteric activation can reduce TNFα-induced increases in cpAMPAR expression, a possible mechanism contributing to glaucomatous RGC death. Taken together these finding support the hypothesis that CB_1 modulation does provide the capacity for both IOP modulation and IOP-independent neuroprotection, which may or may not be possible through the use of CB_1 positive allosteric modulators.

Chapter 5: DISCUSSION

5.1 SUMMARY OF FINDINGS

In this thesis, I have provided evidence to further support the hypothesis that CB_1 modulation may both decrease IOP, the primary modifiable risk factor in glaucoma, as well as provide direct IOP-independent protection of RGCs. However, while I proposed one possible mechanism of CB_1-mediated RGC neuroprotection (CB_1-mediated inhibition of TNFα-induced changes in cpAMPAR expression), and validated that CB_1 PAMs can reduce IOP, I found that chronic administration of the CB_1 PAMs GAT229 and GAT211 did not produce significant RGC neuroprotection when administered in two experimental models of glaucoma.

My thesis work expanded the characterization of a new mouse model of glaucoma. I confirmed that that the nee mouse is a good model for glaucoma; producing rapid and consistent IOP increases and RGC loss. Additionally, I investigated mechanisms of RGC death in these mice, and found a greater IEM1460-sensitive contribution to AMPA-induced calcium responses in nee mice compared with wildtype mice. I also found that administration of the proinflammatory cytokine TNFα to naïve retinas could alter AMPA-induced calcium responses, consistent with previous reports of increases in cpAMPAR expression in other neuronal types (Leonoudakis et al., 2008; Ogoshi et al., 2005). Given that TNFα is reported to be increased in both humans and animal models of glaucoma (Roh et al., 2012; Yang et al., 2011), my work suggests that increased TNFα in nee can contribute to these observed changes in calcium dynamics through increased expression of cpAMPARs. Further, building on evidence that activation of CB_1 can inhibit TNFα-mediated signalling in other neurons (Y. Liu et al., 2013; Zhao et al., 2010), I demonstrated that in naïve retinas, CB_1 activation can also block TNFα-induced increases in AMPA responses, suggestive of preventing TNFα-mediated increases in cpAMPAR expression. Taken together, these results

provide evidence of an additional mechanism of CB_1-mediated neuroprotection. Finally, I investigated the potential neuroprotective effects of chronic CB_1 allosteric modulation on glaucomatous RGC loss. CB_1 PAMs were proposed to provide several advantages over CB_1 orthosteric activation alone, including reduced potential for desensitization and psychoactivity (Ignatowska-Jankowska et al., 2015; Janero & Thakur, 2016; Slivicki et al., 2017). While CB_1 positive allosteric modulation could decrease IOP in nee mice in the absence of exogenous cannabinoids, or when combined with a subthreshold CB_1 orthosteric agonist in normotensive mice, I did not find any significant difference in RGC density over time in nee or ONT mice compared with vehicle-treated mice. Overall, my results show that while CB_1 PAMs show promise as modulators of IOP, the ability of CB_1 PAMs to modify mechanisms leading to RGC loss in glaucoma is not clear, but could involve decreasing proinflammatory cytokines, including TNFα, as well as decreasing TNFα-mediated changes in cpAMPAR expression.

5.2 The Nee Mouse as a Model of Glaucoma

The nee mouse had been previously proposed as a potential model of glaucoma (Iqbal et al., 2010; Mao et al., 2009; Mao et al., 2011); however, little information was reported about the development of ocular pathology in these mice. In my thesis, I have provided novel information validating this experimental model of glaucoma, including data describing the time course of development of ocular hypertension and RGC loss (**Fig. 2.5**). This data is relevant for future use of this mouse model to study glaucoma, as it highlights a major advantage over existing models: rapid and significant cell loss, with no surgical manipulation required.

In order to investigate pathological mechanisms and pharmacological therapies for glaucoma, consistency in pathology is key, both in terms of onset and severity (Fernandes et

al., 2015; T. V. Johnson & Tomarev, 2010; Morgan & Tribble, 2015; Morrison et al., 2011). Genetic models are typically advantageous over surgical-induced models in that have reproducible pathologies (T. V. Johnson & Tomarev, 2010; Morgan & Tribble, 2015). Overall, this appears to be the case in nee mice, IOPs are consistently elevated at p16 and beyond, and RGC loss at p28 and later was also significant and progressive. However, in this model there was a larger variability in RGC loss at p28, although this was reduced at p37, suggesting that the pathology is consistent across animals, though may vary slightly in onset. In contrast, the popular DBA/2J mouse model has reported to be variable, both in onset, and severity (Libby et al., 2005a). While IOP begins to increase in some DBA/2J mice around 8 months of age, only about 75% develop glaucomatous RGC loss by 12 months (Libby et al., 2005a). As such, experiments require a large number of eyes in order to account for variability (the authors of Libby et al. [2005a] recommend 40-60 eyes per experimental group), which is both expensive and very time-intensive to produce.

Ocular hypertension through surgical induction can be quite challenging to produce consistently, especially in mice, requiring significant technical skill which can vary between experimenters. Even still, variability in the development of ocular hypertension and/or RGC damage between animals of the same cohort has been noted (T. V. Johnson & Tomarev, 2010; Morrison et al., 2011). Surgical models typically involve obstructing the pathway of aqueous humor outflow in some way: by laser coagulation and subsequent scaring of the trabecular meshwork; by injection of saline into the episcleral veins, scarring the trabecular meshwork and the anterior chamber angle; by coagulation of the episcleral veins, reducing outflow from the trabecular meshwork; or through injection of particles, such as microbeads, obstructing aqueous flow through the trabecular meshwork (Fernandes et al., 2015; T. V. Johnson & Tomarev, 2010; Morgan & Tribble, 2015; Morrison et al., 2011). Other surgical models exist, including injection of excitotoxic substances into the eye, optic nerve

crush or ONT, or transient high IOP ischemia/reperfusion injury. However, apart from the brief period in ischemia-reperfusion injury, these models of injury are independent of IOP, and serve to investigate certain mechanisms of glaucomatous RGC death, rather than a holistic investigation (T. V. Johnson & Tomarev, 2010).

IOP increases in surgically-induced models are often transient, requiring multiple manipulations to sustain an ocular hypertensive state. As such, surgical models pose the increased risk for additional ocular inflammation and damage that can occur with surgical manipulation, which only further contributes to potential variability (T. V. Johnson & Tomarev, 2010; Morgan & Tribble, 2015).

Additionally, surgically-induced models typically produce an abrupt injury, leading to an almost immediate onset of pathology. While this is different from typical glaucomatous progression in humans and genetic models of glaucoma (e.g., DBA/2J and nee), it is advantageous in that it enables teasing out the time course of RGC injury with greater accuracy (Fernandes et al., 2015; T. V. Johnson & Tomarev, 2010; Morrison et al., 2011).

However, the reproducibility of pathology in the nee mouse was clearly advantageous in the investigation of mechanisms leading to RGC loss, as highlighted in studies comparing cpAMPAR expression in nee and bead rats. Consistently elevated IOP occurs in nee mice at p16, and as nee is a genetic model, significant numbers of animals can be generated by breeding. This is in contrast to surgical induction of ocular hypertension which requires time-consuming surgical manipulation, with sometimes inconsistent IOP elevation between animals (Fernandes et al., 2015; T. V. Johnson & Tomarev, 2010; Morgan & Tribble, 2015; Morrison et al., 2011). For example, while 18 rats underwent surgery to induce ocular hypertension with bead injection, only 10 of these had a successful sustained increase in

IOP. On the other hand, every nee mouse had a significant and sustained increase in IOP, with no manipulation required, other than colony management.

Additionally, aside from consistency and the non-invasive generation of ocular hypertension, there was less variability seen in IEM1460-sensitive calcium responses in nee mice compared to the rat ocular hypertensive model. Even though the increase in contributions to AMPA-induced calcium responses were similar in effect size in nee and bead rat compared with their respective controls (**Figs. 3.5, 3.7**), this effect was not significant in bead rats. While some of this variation can be attributed to the generalized reduced calcium responses in rat compared with mouse (**Fig. 3.2**), this might not be entirely the case. It is possible that this increased variability is due to inconsistencies in the induced pathology of the bead rat, as compared with nee mice. However, repeating these studies using a bead model in mouse may be useful, and may help to distinguish between species or model differences.

The severity of RGC loss in the nee is great, with an approximate 51.7 ± 9.6% loss at p28, which progresses to 71.2 ± 8.2% at p37, in comparison to wildtype littermates (**Fig. 2.5**). However, similar loss has been reported in other models of RGC injury (Nuschke et al., 2015; Smedowski, Pietrucha-Dutczak, Kaarniranta, & Lewin-Kowalik, 2014). In general, direct axon injury leads to greater RGC loss in a shorter amount of time. Kwong and colleagues (2011) reported 87% loss within 14 days of optic nerve crush in rats (Nuschke et al., 2015). In mice, Galindo-Romero (2011) reported 69 and 86% loss within 7 and 14 days, respectively, following ONT. However, in genetic models, the loss can also be severe. In DBA/2J mice, while delayed in onset, almost complete loss of RGCs has also been reported in some cases (McKinnon, Schlamp, & Nickells, 2009; Schlamp, Li, Dietz, Janssen, & Nickells, 2006), though at 12 months the average loss is approximately 38.6% (Libby et al., 2005a). On the other hand, severity of loss in bead models is typically more subdued, typically

approximately 35% in rats following 4-6 weeks of ocular hypertension (with IOP ranges from 29-31), and in mice 2-15% loss after 6-12 weeks of ocular hypertension (with IOP ranges from 11.8-16.4; Smedowski et al., 2014). The severity of this cell loss in nee mice, compared with the bead model in particular, is likely a result of the significant increase in IOP, which is consistently maintained at a greater level than in bead (Libby et al., 2005a; Smedowski et al., 2014).

Although nee mice are a model of angle-closure glaucoma, a far less common glaucoma in Canada and the rest of North America (Harasymowycz et al., 2016; Weinreb et al., 2016), the DBA2/J mouse is also a model of angle-closure glaucoma (John et al., 1998). While this may be a disadvantage in limiting the generalizability of findings to open-angle glaucoma (Weinreb et al., 2016), studies using the DBA/2J mouse have provided valuable information about the pathology of glaucoma in humans, both in terms of IOP modification, and in mechanisms leading to RGC loss (T. V. Johnson & Tomarev, 2010).

The measurable deficits in vision in nee mice are also advantageous, and may be used to investigate if novel therapeutics which can improve RGC survival can also improve visual outcomes. To ensure that this deficit is due to a loss in RGCs, and not because of issues relating to development, preferably, vision should also be tested in young nee, prior to significant RGC loss. However, because training and testing of mice takes 8 days for the visual water box, I did not measure vision in young mice. Although, retinas appeared normal at p16; therefore, it is likely that vision is still intact in these mice at this point, and that drug administration may be able to further preserve this. Had I identified a drug which had significantly improved RGC density, changes in visual outcomes could have also been investigated in this model.

Taken together, these data reinforce the usefulness of the nee mouse as a model of experimental glaucoma. Nee pathology, while severe, is consistent and rapid, and does not require manipulation to generate. As such, the nee mouse provides another opportunity to investigate potential of novel pharmacotherapeutics for the treatment of glaucoma; enabling measurements of effects on ocular hypertension, RGC survival, and protection against vision loss.

5.3 Dynamic Measurement of cpAMPAR Contributions to Calcium Dynamics

In **Chapter 3**, I reported a greater cpAMPAR contribution to AMPA-induced calcium responses in nee mice compared with wildtype. This was consistent with previous suggestions of increased cpAMPAR expression in a model of chronic ocular hypertension, as measured with Co^{2+} stain (Cueva Vargas et al., 2015). As TNFα is reported to be increased with ocular hypertension and glaucoma, the changes in calcium dynamics observed following incubation with TNFα reported in this thesis are consistent with a TNFα-mediated increase in cpAMPAR expression. I also reported for the first time in retina that CB_1 activation could manipulate this pathway, which was consistent with a previous report in hippocampal neurons (**Chapter 4**).

These results highlight advantages to using calcium imaging on *ex vivo* retinas - enabling dynamic manipulation within the same experiment. Calcium-permeable AMPA receptors have greater single channel conductance than their calcium-impermeable counterparts (Soto, Coombs, Gratacos-Batlle, Farrant, & Cull-Candy, 2014). Therefore, small changes in cpAMPAR expression can have dramatic effects on excitability (as evident in synaptic scaling; Henley & Wilkinson, 2016), and thus potentially on calcium dynamics leading to RGC death. Ca^{2+} imaging may present a sensitive method to demonstrate these

changes in calcium dynamics, which may be advantageous over other methods of quantifying cpAMPAR expression (i.e., AMPA receptor mRNA or protein), in that it provides a functional demonstration of the effect changes in plasma membrane cpAMPAR expression. Additionally, Ca^{2+} imaging enables investigation of multiple cells at once in contrast to single cell patching. In future, this technique may be used to elucidate the specific mechanisms of TNFα-induced changes in cpAMPAR in the retina, including investigation of whether these changes are due to increases in protein expression or receptor trafficking, and how potential therapies can modify such pathways.

IEM1460-sensitivity in the TNFα-induced change in calcium dynamics was not investigated in this thesis. However, the limitation of IEM1460 is that it is selective for GluA2-lacking cpAMPARs over unedited GluA2-containing cpAMPARs, and therefore may not be able to completely account for observed changes. As a selective agonist or antagonist for unedited GluA2-containing cpAMPARs does not exist, genetically-modified mice may be useful for further exploration of retinal TNFα-mediated changes. GluA2 knockouts, which results in complete expression of cpAMPARs, rather than calcium-impermeable AMPA receptors, are viable. Genetically modified mice where GluA2 is "forced" edited, where DNA coding for the GluA2 subunit is modified to produce GluA2(R) by default (Wright & Vissel, 2012), are also viable, and still contain GluA2-lacking cpAMPARs. If TNFα-mediated increases in AMPA-induced calcium dynamics are absent in GluA2 knockout mice, this would suggest that increased expression of unedited GluA2 is responsible, at least partially, for this response. Likewise, if TNFα-mediated changes were absent in forced edited GluA2 mice, this would suggest that this mechanism involves changes in GluA2-editing. Additionally, if changes in forced edited GluA2 mice persist, IEM1460 could be administered in these mice to verify that this change is due to GluA2-lacking cpAMPARs.

5.4 CB_1 Modulation as a Strategy for Reducing RGC Death in Glaucoma

The results reported in my thesis support the hypothesis that increases in TNFα following glaucomatous injury result in an increase in cpAMPAR expression, which may alter neuronal excitability, ultimately leading to RGC death. Therefore, targeting this mechanism should reduce RGC death. However, there are several disadvantages to directly targeting either cpAMPARs, TNFα, or the TNFα-mediated mechanisms altering cpAMPAR expression, including potential for significant CNS and ocular side effects, and immunosuppression (Gittis et al., 2011; Henley & Wilkinson, 2016; Jones et al., 2012; Michels, Becker, Wachtlin, & Binder, 2012; Shea et al., 2008; Sivaprasad & Oyetunde, 2016). Instead, targeting this mechanism through CB_1 modulation may be useful in that it may provide an opportunity to simultaneously modulate multiple pathways leading to RGC death in glaucoma (**Fig. 5.1**).

Direct block of cpAMPARs was neuroprotective in ocular models of excitotoxicity (Lebrun-Julien et al., 2009), an induced retinal damage model (Dong et al., 2015), and in a model of ocular hypertension (Cueva Vargas et al., 2015). However, chronic antagonism of cpAMPARs may result in unwanted side effects because of the important roles that cpAMPARs may play elsewhere in the retina and brain. *In vivo* blockade of cpAMPARs caused dyskinesias when injected into the sensorimotor striatum of mice (Gittis et al., 2011). Though in another study, intrathecal injection of IEM1460 in rats did not produce any changes in thermal or mechanical sensitivities, locomotion, or anxiety-like behaviour, but did alleviate behavioural responses produced by complete Freund's adjuvant-induced inflammatory pain (Gittis et al., 2011; Kopach, Krotov, Goncharenko, & Voitenko, 2016).

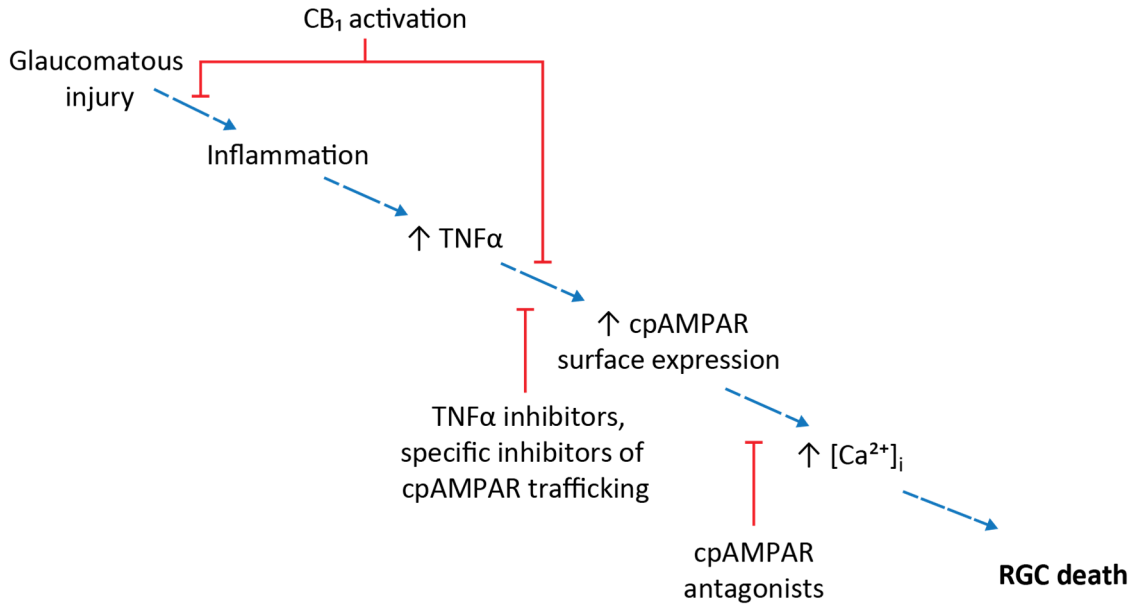

Figure 5.1 - Potential strategies to reduce RGC death in glaucoma.

Unfortunately, neither of these studies investigated possible effects of cpAMPAR antagonism on vision.

Calcium-permeable AMPA receptors contribute to retinal function under normal conditions. Rapid changes in cpAMPAR expression on RGCs in response to light in dark adapted retinas suggests a possible role in light adaptation (Jones et al., 2012; Xia et al., 2006; Xia et al., 2007). Additionally, cpAMPARs are also involved in the generation of long term potentiation in amacrine cells (M. H. Kim & von Gersdorff, 2016), and in the positive feedback from horizontal cells onto cones (Jackman, Babai, Chambers, Thoreson, & Kramer, 2011). Therefore, it's possible that cpAMPAR block could have significant effects on visual function, including loss of night vision. If this is the case, potential changes in visual function could deter patients from using direct cpAMPAR antagonists.

Upstream targeting of this pathway may be more appropriate. TNFα was previously reported to be upregulated in humans and animal models of glaucoma (Roh et al., 2012; Yang et al., 2011). Further, blocking TNFα, at least in some cases, was associated with increased RGC survival (Roh et al., 2012), potentially through blocking increases in cpAMPAR expression (Cueva Vargas et al., 2015). Chronic inhibition of TNFα is relatively safe, and TNFα inhibitors are currently used in the treatment of rheumatoid arthritis (Murdaca et al., 2015). However, current TNFα inhibitors pose several problems, which may limit usefulness as a glaucoma therapeutic. Inhibition of TNFα is immunosuppressive, and poses an increased risk of infection (Murdaca et al., 2015; Probert, 2015). Additionally, current TNFα inhibitors are biologics, and must be administered subcutaneously or intravenously. TNFα inhibitors could theoretically also be administered intravitreally, likely reducing systemic immunosuppression. However, this would require injection by medical professionals, which could add stress on the health care system, aside from potential issues

with patient compliance and cost (Michels et al., 2012; Shea et al., 2008; Sivaprasad & Oyetunde, 2016).

Direct targeting of TNFα-mediated changes in cpAMPAR expression may also be problematic. There is evidence that AMPA and cpAMPAR expression in certain neuronal populations is constitutively regulated by TNFα. This mechanism may be important in activity-dependent scaling at neuronal synapses, enabling synaptic feedback following prolonged changes in activity (Henley & Wilkinson, 2016; Pribiag & Stellwagen, 2014; Steinmetz & Turrigiano, 2010; Stellwagen & Malenka, 2006). Consistent with this, administration of a TNFα inhibitor alone reduced basal GluA1 surface expression in hippocampal neurons (Beattie et al., 2002; Stellwagen et al., 2005). Therefore, if mechanisms contributing to TNFα-induced increases in cpAMPARs in glaucomatous RGC death overlap with mechanisms which may provide homeostatic feedback in synapses, direct targeting at this level of the pathway may also not be appropriate.

On the other hand, upstream targeting via activation of CB_1 may be promising; CB_1 has previously shown to modulate various mechanisms which can contribute to RGC death in glaucoma (Cairns et al., 2016a; Cairns et al., 2016b), including the ability to reduce release of inflammatory cytokines, including TNFα (Krishnan & Chatterjee, 2012). Further, as demonstrated previously in hippocampal neurons (Zhao et al., 2010), and supported by findings presented here, CB_1 activation can also reduce TNFα-mediated increases in cpAMPAR expression. Additional CB_1-mediated actions which may directly contribute to a reduction in glaucomatous RGC death include reducing neuronal excitability (Howlett & Abood, 2017; Ligresti et al., 2016), and promoting activation of pro-survival pathways (Batista et al., 2016; Kendall & Yudowski, 2017). Finally, cannabinoids can also reduce IOP, the primary modifiable risk factor for glaucoma (Cairns et al., 2016a; Cairns et al., 2016b). Therefore, cannabinoid modulation may provide a multi-pronged approach to reduce

glaucomatous damage, targeting multiple point on the pathways leading to RGC death. Multi-target approaches often have improved outcomes over single-target approaches in complex pathologies, including inflammation (Csermely, Agoston, & Pongor, 2005; Koeberle & Werz, 2014; Medina-Franco, Giulianotti, Welmaker, & Houghten, 2013; Zimmermann, Lehar, & Keith, 2007).

CB_1 modulation provides the additional advantage over TNFα therapeutics in that some cannabinoid ligands can be administered topically, but are still able to reach the retina. Oltmanns and colleagues (2008) investigated the ocular penetrance of the non-selective CB_1/CB_2 agonist WIN following topical delivery in rat. They reported that while 15% of the drug was retained in the eyelids, by 60 minutes 1.5% had reached the retina and sclera, and was calculated to have an approximate half-life of 100 minutes (Oltmanns et al., 2008). Additionally, this group found that unlike systemic administration of cannabinoids, topical application of WIN did not produce a significant effect on heart rate or blood pressure, suggesting limited systemic activity when delivered in this manner (Oltmanns et al., 2008). However, repeated exposure was not investigated by this group.

While I showed that CB_1 activation by the cannabinoid WIN can decrease TNFα-induced mediated increases in AMPA-induced calcium responses, this inhibition did not translate to significant RGC neuroprotection when given chronically in either nee or ONT mice. Following 12 day administration in nee mice (p28), RGC density in middle retina was significantly increased with 0.25% WIN administration, but the overall mean RGC density was not significantly different. The increase in RGC density in middle retina following administration of 0.25% WIN at p28 (12 days administration) was surprising given that the IOPs measured in these mice were actually significantly higher than the other groups. Further, this dose of WIN was subthreshold for IOP reduction in wildtype mice. This suggests that perhaps the WIN-mediated effect on RGC density in middle retina is through

an IOP-independent mechanism, perhaps by modulation of inflammation in the retina. Following ONT, 7 day administration of 0.25% WIN also resulted in increased RGC survival in middle retina, but not overall. These data support the hypothesis that WIN-mediated increases in middle retina RGC density in nee were due to non-IOP-mediated mechanisms.

The reason for the lack of effect of WIN on overall mean RGC density reported here is unknown. These data vary from a previous report of increased RGC survival 48 hours following ischemia-reperfusion injury in rat when treated with topical 1% WIN (Pinar-Sueiro et al., 2013). However, there are significant differences in these models, including the shortened time course, and the severity of loss. RGC loss at 48 hours in injured control rats was only 12.33% (Pinar-Sueiro et al., 2013); whereas RGC loss was approximately 43.7 ± 8.7 and 73.9 ± 7.6% in vehicle treated p28 and p37 nee (12 and 21 day treatments), and 75.3 ± 7.6% 7 days post-ONT. WIN treatment in the ischemia-reperfusion injury model improved RGC survival by approximately 10% (Pinar-Sueiro et al., 2013). Given that secondary inflammation-induced RGC injury may be delayed in onset (Nakazawa et al., 2006), studies investigating effects at such an early time point (e.g., 48 hours), may not accurately portray possible neuroprotective effects. On the other hand, other models of RGC injury have also reported neuroprotection with cannabinoid modulation albeit through non-topical routes of administration (Crandall et al., 2007; El-Remessy et al., 2003; Nucci et al., 2007; Slusar et al., 2013). Taken together, these results suggest that while WIN may be able to reach the retina with acute exposure (Oltmanns et al., 2008), in order to effectively reduce RGC loss, either alternative routes of delivery must be used, or topical routes must be optimized to increase ocular penetrance.

Another possible reason for the lack of CB_1-mediated neuroprotection in nee and ONT presented in this thesis may be due to species differences. Studies of CB_1-mediated neuroprotection in experimental glaucoma so far have all occurred in rats, and not mice

(Crandall et al., 2007; El-Remessy et al., 2003; Nucci et al., 2007; Pinar-Sueiro et al., 2013; Slusar et al., 2013). Significant differences in endocannabinoid response to stress between rats and mice was previously reported. Acute restraint in rats and mice produces a decrease in AEA signalling, but in rats also produces an increase in 2-AG, which is absent in mice (Hill & McEwen, 2010). In a separate study investigating the effect of CB_1 modulation on anxiety, administration of WIN produced opposing effects on rats and mice (Haller et al., 2007). In both instances, these differences were speculated to be due to variable ECS expression between species, and therefore, similar differences could be possible in the eye, and may be contributing to the difference in observed effect (Haller et al., 2007; Hill & McEwen, 2010).

As outlined in **Chapter 4**, there are disadvantages associated with direct CB_1 orthosteric activation which may limit the usefulness of cannabinoids as long-term clinically-relevant therapeutics. Therefore, in this thesis I have explored an alternate strategy for CB_1 modulation – positive allosteric modulation, using the CB_1 PAM GAT229 and the CB_1 ago-PAM GAT211 (Laprairie et al., 2017). While the CB_1 PAM GAT229 could manipulate IOP in nee, at least acutely, neither GAT229 or GAT211, alone or in combination with an orthosteric agonist, provided significant neuroprotection. On the other hand, daily topical treatment of 2% GAT229 resulted in greater RGC density in central retina compared with vehicle-treatment in axotomized eyes. Daily administration 0.2% GAT229 combined with the FAAH inhibitor URB597 resulted in increased RGC densities in middle and peripheral retina compared with URB597 alone, but was not significantly different from vehicle treatment in ONT. Similar to WIN, the GAT229-mediated effects on RGC density in ONT would suggest an IOP-independent mechanism.

While topically or i.p. administered CB_1 PAMs did produce IOP-lowering effects, the ability of these compounds to reach the retina is unknown. Original dosing for the GAT compounds was based on other *in vivo* studies using experimental pain models (Slivicki et

al., 2017), through preliminary IOP studies (A. Straiker, personal communication), and through the IOP studies reported here. The increased RGC density observed in the central retina with topical administration of GAT229 in axotomized eyes would suggest that this compound is reaching the retina, though similarly to WIN, GAT229 concentration via the topical route may be insufficient to produce generalized effects on RGC survival (rather than limited to retinal area). Alternate routes of administration, such as intravitreal, or vehicles may therefore need to be considered. Further studies using autoradiography to investigate ocular absorption and distribution and pharmacokinetics of the GAT compounds would therefore be useful. Since ocular penetrance of the GAT compounds is unknown, it is difficult to conclude whether or not the lack of neuroprotective effects on mean RGC densities was due to insufficient dosing.

On the other hand, it is also possible that the dose and dosing regime used in my chronic experiments was too high/frequent, and resulted in receptor desensitization over time. This could explain why topical administration of 0.25% WIN resulted in increased RGC densities in middle retina at earlier time points (e.g., 7 day administration in ONT, and 12 day administration in nee), but not after longer periods (e.g., 21 day administration in nee). Cannabinoid receptor desensitization has been previously reported, particularly with chronic 2-AG administration (see **Chapter 4, section 4.1.4;** Ghosh et al., 2013; Kinsey et al., 2013; Schlosburg et al., 2010). Instead, the dose of the drugs may need to be lowered. Ghosh et al. (2013), reported that administration of the MAGL blocker JZL184 at 16 or 40 mg/kg, while effective acutely, resulted in loss of antinociceptive effects in a model of inflammatory pain when administered chronically. Yet, on the other hand, administration of a lower daily dose of 4 mg/kg of JZL184 retained therapeutic efficacy over the 6 days measured. Interestingly, in a rat model of chronic ocular hypertension induced through episcleral vein cauterization, Δ^9-THC that was delivered once weekly for twenty weeks resulted in a 40%

increase in RGC survival (Crandall et al., 2007), suggesting that reductions in frequency of administration may also help in preventing receptor desensitization.

When I initiated these studies, I had hoped that I would be able to use acute IOP modulation in nee and wildtype mice as an indicator of the effective drug dose required for chronic retinal neuroprotection. However, this was clearly not the case, as the only compound which provided some neuroprotection in two instances was at a dose which was subthreshold to IOP modification in wildtype (0.25% WIN).

Taking this into consideration, future screening of the CB_1 allosteric GAT compounds with Ca^{2+} imaging may serve two important purposes: confirmation that like WIN, GAT compounds can also directly modulate pathways which may contribute to glaucomatous RGC death; and as a way to estimate an effective dose that can reach the retina in order for these compounds to have an effect. For example, one could investigate if incubation of isolated retinas with GAT229 blocks TNFα-mediated increases in AMPA-induced calcium dynamics. Or, if GAT229 administration in nee mice could reduce IEM1460-sensitive changes in AMPA-induced calcium dynamics. From there, effectiveness of *in vivo* chronic dosing, in combination with drug pharmacokinetics, could be investigated by expanding investigation of RGC densities to include earlier time points. If optimized doses provide protection at earlier time points (for example, day 7 and 14) but not at later (for example, day 21), this might suggest that there is desensitization over time.

Until these additional experiments are done, it is difficult to conclude that CB_1 positive allosteric modulation is ineffective at reducing RGC death in experimental glaucoma. Instead, what can be concluded from these experiments is that given the doses, dosing frequency, and routes of delivery used, administration of GAT211 and GAT229 in these studies did not increase general RGC survival in nee or after ONT in wildtype mice.

5.5 CONCLUSIONS

There is a significant need for neuroprotective therapies in glaucoma. Modifying ocular hypertension alone is not always sufficient to prevent progressive blindness in this debilitating disease (Tamm et al., 2013). In order to develop new therapies, we must acquire a better understanding of the mechanisms leading to RGC death, as well as develop good tools for their study. In this thesis, I have provided additional evidence in support of the nee mouse as a new experimental mouse model of glaucoma. As I have found, this model may be useful in further describing mechanisms leading to RGC death, and in presenting opportunities to manipulate these pathways. Specifically, I have provided novel evidence in isolated retina to support the hypothesis that cpAMPARs may be upregulated in glaucoma, and that this can occur through TNFα-mediated signalling, which can be inhibited by CB_1 activation. Additionally, I have demonstrated for the first time the IOP-modulating abilities of a CB_1 positive allosteric modulator. This new class of compound has the potential to provide benefits over traditional CB_1 orthosteric agonists, while minimizing the associated disadvantages of CB_1 orthosteric ligands. As a whole, this work contributes to our understanding of cellular mechanisms underlying retinal neurodegenerative pathologies, and provides justification for further exploring CB_1 modulation as a potential therapeutic avenue for the treatment of glaucoma.

REFERENCES

Abu-Amero, K. K., Morales, J., & Bosley, T. M. (2006). Mitochondrial abnormalities in patients with primary open-angle glaucoma. *Investigative Ophthalmology & Visual Science, 47*(6), 2533-2541.

Agudo, M., Perez-Marin, M. C., Lonngren, U., Sobrado, P., Conesa, A., Canovas, I., . . . Vidal-Sanz, M. (2008). Time course profiling of the retinal transcriptome after optic nerve transection and optic nerve crush. *Molecular Vision, 14*, 1050-1063.

Agudo, M., Perez-Marin, M. C., Sobrado-Calvo, P., Lonngren, U., Salinas-Navarro, M., Canovas, I., . . . Vidal-Sanz, M. (2009). Immediate upregulation of proteins belonging to different branches of the apoptotic cascade in the retina after optic nerve transection and optic nerve crush. *Investigative Ophthalmology & Visual Science, 50*(1), 424-431.

Ahn, K., Johnson, D. S., & Cravatt, B. F. (2009). Fatty acid amide hydrolase as a potential therapeutic target for the treatment of pain and CNS disorders. *Expert Opinion on Drug Discovery, 4*(7), 763-784.

Ahn, K. H., Mahmoud, M. M., & Kendall, D. A. (2012). Allosteric modulator ORG27569 induces CB1 cannabinoid receptor high affinity agonist binding state, receptor internalization, and gi protein-independent ERK1/2 kinase activation. *The Journal of Biological Chemistry, 287*(15), 12070-12082.

Aihara, M., Lindsey, J. D., & Weinreb, R. N. (2003). Twenty-four-hour pattern of mouse intraocular pressure. *Experimental Eye Research, 77*(6), 681-686.

Aktas, Z., Karaca, E. E., Dogan, N., Çakmak, T., Unlu, M., Tok, L., & Hasanreisoglu, M. (2014). Congenital glaucoma as an ophthalmic manifestation of Frank–Ter haar syndrome. *International Ophthalmology, 34*(2), 351-354.

Alexander, S. P., & Kendall, D. A. (2007). The complications of promiscuity: Endocannabinoid action and metabolism. *British Journal of Pharmacology, 152*(5), 602-623.

Alm, A., & Nilsson, S. F. (2009). Uveoscleral outflow--a review. *Experimental Eye Research, 88*(4), 760-768.

Almasieh, M., Wilson, A. M., Morquette, B., Cueva Vargas, J. L., & Di Polo, A. (2012). The molecular basis of retinal ganglion cell death in glaucoma. *Progress in Retinal and Eye Research, 31*(2), 152-181.

Angelini, R., Argueta, D. A., Piomelli, D., & DiPatrizio, N. V. (2017). Identification of a widespread palmitoylethanolamide contamination in standard laboratory glassware. *Cannabis and Cannabinoid Research, 2*(1), 123-132.

Araque, A., Castillo, P. E., Manzoni, O. J., & Tonini, R. (2017). Synaptic functions of endocannabinoid signaling in health and disease. *Neuropharmacology, 124*, 13-24.

Aung, T., Ang, L. P., Chan, S. P., & Chew, P. T. (2001). Acute primary angle-closure: Long-term intraocular pressure outcome in asian eyes. *American Journal of Ophthalmology, 131*(1), 7-12.

Baptiste, D. C., Powell, K. J., Jollimore, C. A., Hamilton, C., LeVatte, T. L., Archibald, M. L., . . . Kelly, M. E. (2005). Effects of minocycline and tetracycline on retinal ganglion cell survival after axotomy. *Neuroscience, 134*(2), 575-582.

Batista, E. M., Doria, J. G., Ferreira-Vieira, T. H., Alves-Silva, J., Ferguson, S. S., Moreira, F. A., & Ribeiro, F. M. (2016). Orchestrated activation of mGluR5 and CB1 promotes neuroprotection. *Molecular Brain, 9*(1), 80-016-0259-6.

Beattie, E. C., Stellwagen, D., Morishita, W., Bresnahan, J. C., Ha, B. K., Von Zastrow, M., . . . Malenka, R. C. (2002). Control of synaptic strength by glial TNFalpha. *Science (New York, N.Y.), 295*(5563), 2282-2285.

Berger, S., Savitz, S. I., Nijhawan, S., Singh, M., David, J., Rosenbaum, P. S., & Rosenbaum, D. M. (2008). Deleterious role of TNF-alpha in retinal ischemia-reperfusion injury. *Investigative Ophthalmology & Visual Science, 49*(8), 3605-3610.

Berkelaar, M., Clarke, D. B., Wang, Y. C., Bray, G. M., & Aguayo, A. J. (1994). Axotomy results in delayed death and apoptosis of retinal ganglion cells in adult rats. *The Journal of Neuroscience, 14*(7), 4368-4374.

Bisogno, T., Delton-Vandenbroucke, I., Milone, A., Lagarde, M., & Di Marzo, V. (1999). Biosynthesis and inactivation of N-arachidonoylethanolamine (anandamide) and N-docosahexaenoylethanolamine in bovine retina. *Archives of Biochemistry and Biophysics, 370*(2), 300-307.

Blazquez, C., Chiarlone, A., Bellocchio, L., Resel, E., Pruunsild, P., Garcia-Rincon, D., . . . Guzman, M. (2015). The CB(1) cannabinoid receptor signals striatal neuroprotection via a PI3K/Akt/mTORC1/BDNF pathway. *Cell Death and Differentiation, 22*(10), 1618-1629.

Bosco, A., Steele, M. R., & Vetter, M. L. (2011). Early microglia activation in a mouse model of chronic glaucoma. *The Journal of Comparative Neurology, 519*(4), 599-620.

Bouskila, J., Burke, M. W., Zabouri, N., Casanova, C., Ptito, M., & Bouchard, J. F. (2012). Expression and localization of the cannabinoid receptor type 1 and the enzyme fatty acid amide hydrolase in the retina of vervet monkeys. *Neuroscience, 202*, 117-130.

Bouskila, J., Javadi, P., Casanova, C., Ptito, M., & Bouchard, J. F. (2013a). Muller cells express the cannabinoid CB2 receptor in the vervet monkey retina. *The Journal of Comparative Neurology, 521*(11), 2399-2415.

Bouskila, J., Javadi, P., Casanova, C., Ptito, M., & Bouchard, J. F. (2013b). Rod photoreceptors express GPR55 in the adult vervet monkey retina. *PloS One, 8*(11), e81080.

Bozkurt, B., Mesci, L., Irkec, M., Ozdag, B. B., Sanal, O., Arslan, U., . . . Tezcan, I. (2012). Association of tumour necrosis factor-alpha -308 G/A polymorphism with primary open-angle glaucoma. *Clinical & Experimental Ophthalmology, 40*(4), e156-62.

Bradshaw, H. B., Rimmerman, N., Hu, S. S., Benton, V. M., Stuart, J. M., Masuda, K., . . . Walker, J. M. (2009). The endocannabinoid anandamide is a precursor for the signaling lipid N-arachidonoyl glycine by two distinct pathways. *BMC Biochemistry, 10*, 14-2091-10-14.

Brandstatter, J. H., Koulen, P., & Wassle, H. (1998). Diversity of glutamate receptors in the mammalian retina. *Vision Research, 38*(10), 1385-1397.

Buchan, J. C., Siddiqui, S., & Gilmour, D. (2007). Simplification of eye drop regimes helps reduce involuntary non-compliance with glaucoma treatment. *Graefe's Archive for Clinical and Experimental Ophthalmology, 245*(2), 327-328.

Buchan, A. M., Lesiuk, H., Barnes, K. A., Li, H., Huang, Z. G., Smith, K. E., & Xue, D. (1993). AMPA antagonists: Do they hold more promise for clinical stroke trials than NMDA antagonists? *Stroke, 24*(12 Suppl), I148-52.

Burgoyne, C. (2015). The morphological difference between glaucoma and other optic neuropathies. *Journal of Neuro-Ophthalmology, 35 Suppl 1*, S8-S21.

Cairns, E. A., Baldridge, W. H., & Kelly, M. E. (2016a). The endocannabinoid system as a therapeutic target in glaucoma. *Neural Plasticity, 2016*, 9364091.

Cairns, E. A., Szczesniak, A. M., Straiker, A. J., Kulkarni, P. M., Pertwee, R. G., Thakur, G. A., . . . Kelly, M. E. M. (2017). The in vivo effects of the CB1-positive allosteric modulator GAT229 on intraocular pressure in ocular normotensive and hypertensive mice. *Journal of Ocular Pharmacology and Therapeutics, 33*(8), 582-590.

Cairns, E. A., Toguri, J. T., Porter, R. F., Szczesniak, A. M., & Kelly, M. E. (2016b). Seeing over the horizon - targeting the endocannabinoid system for the treatment of ocular disease. *Journal of Basic and Clinical Physiology and Pharmacology, 27*(3), 253-265.

Caldwell, M. D., Hu, S. S., Viswanathan, S., Bradshaw, H., Kelly, M. E., & Straiker, A. (2013). A GPR18-based signalling system regulates IOP in murine eye. *British Journal of Pharmacology, 169*(4), 834-843.

Canadian Ophthalmological Society Glaucoma Clinical Practice Guideline Expert Committee, & Canadian Ophthalmological Society. (2009). Canadian ophthalmological society evidence-based clinical practice guidelines for the management of glaucoma in the adult eye. *Canadian Journal of Ophthalmology.Journal Canadien d'Ophtalmologie, 44 Suppl 1*, S7-93.

Casson, R. J. (2006). Possible role of excitotoxicity in the pathogenesis of glaucoma. *Clinical & Experimental Ophthalmology, 34*(1), 54-63.

Cawston, E. E., Connor, M., Di Marzo, V., Silvestri, R., & Glass, M. (2015). Distinct temporal fingerprint for cyclic adenosine monophosphate (cAMP) signaling of indole-2-carboxamides as allosteric modulators of the cannabinoid receptors. *Journal of Medicinal Chemistry, 58*(15), 5979-5988.

Cawston, E. E., Redmond, W. J., Breen, C. M., Grimsey, N. L., Connor, M., & Glass, M. (2013). Real-time characterization of cannabinoid receptor 1 (CB1) allosteric modulators reveals novel mechanism of action. *British Journal of Pharmacology, 170*(4), 893-907.

Cecyre, B., Zabouri, N., Huppe-Gourgues, F., Bouchard, J. F., & Casanova, C. (2013). Roles of cannabinoid receptors type 1 and 2 on the retinal function of adult mice. *Investigative Ophthalmology & Visual Science, 54*(13), 8079-8090.

Challenor, M., O'Hare Doig, R., Fuller, P., Giacci, M., Bartlett, C., Wale, C. H., . . . Fitzgerald, M. (2015). Prolonged glutamate excitotoxicity increases GluR1 immunoreactivity but decreases mRNA of GluR1 and associated regulatory proteins in dissociated rat retinae in vitro. *Biochimie, 112*, 160-171.

Chauhan, B. C., Pan, J., Archibald, M. L., LeVatte, T. L., Kelly, M. E., & Tremblay, F. (2002). Effect of intraocular pressure on optic disc topography, electroretinography, and axonal loss in a chronic pressure-induced rat model of optic nerve damage. *Investigative Ophthalmology & Visual Science, 43*(9), 2969-2976.

Chen, J., Matias, I., Dinh, T., Lu, T., Venezia, S., Nieves, A., . . . Di Marzo, V. (2005). Finding of endocannabinoids in human eye tissues: Implications for glaucoma. *Biochemical and Biophysical Research Communications, 330*(4), 1062-1067.

Chen, R., Zhang, J., Wu, Y., Wang, D., Feng, G., Tang, Y. P., . . . Chen, C. (2012). Monoacylglycerol lipase is a therapeutic target for alzheimer's disease. *Cell Reports, 2*(5), 1329-1339.

Cheng, Y., & Hitchcock, S. A. (2007). Targeting cannabinoid agonists for inflammatory and neuropathic pain. *Expert Opinion on Investigational Drugs, 16*(7), 951-965.

Chien, F. Y., Wang, R. F., Mittag, T. W., & Podos, S. M. (2003). Effect of WIN 55212-2, a cannabinoid receptor agonist, on aqueous humor dynamics in monkeys. *Archives of Ophthalmology, 121*(1), 87-90.

Chong, R. S., & Martin, K. R. (2015). Glial cell interactions and glaucoma. *Current Opinion in Ophthalmology, 26*(2), 73-77.

Civan, M. M. (2008). Formation of the aqueous humor: Transport components and their integration. *Current Topics in Membranes, 62*(0), 1-45.

Colasanti, B. K., & Powell, S. R. (1985). Effect of delta 9-tetrahydrocannabinol on intraocular pressure after removal of autonomic input. *Journal of Ocular Pharmacology, 1*(1), 47-57.

Cone, F. E., Gelman, S. E., Son, J. L., Pease, M. E., & Quigley, H. A. (2010). Differential susceptibility to experimental glaucoma among 3 mouse strains using bead and viscoelastic injection. *Experimental Eye Research, 91*(3), 415-424.

Conrad, K. L., Tseng, K. Y., Uejima, J. L., Reimers, J. M., Heng, L. J., Shaham, Y., . . . Wolf, M. E. (2008). Formation of accumbens GluR2-lacking AMPA receptors mediates incubation of cocaine craving. *Nature, 454*(7200), 118-121.

Costagliola, C., Romano, M. R., dell'Omo, R., Russo, A., Mastropasqua, R., & Semeraro, F. (2014). Effect of palmitoylethanolamide on visual field damage progression in normal tension glaucoma patients: Results of an open-label six-month follow-up. *Journal of Medicinal Food, 17*(9), 949-954.

Crandall, J., Matragoon, S., Khalifa, Y. M., Borlongan, C., Tsai, N. T., Caldwell, R. B., & Liou, G. I. (2007). Neuroprotective and intraocular pressure-lowering effects of (-)Delta9-tetrahydrocannabinol in a rat model of glaucoma. *Ophthalmic Research, 39*(2), 69-75.

Csermely, P., Agoston, V., & Pongor, S. (2005). The efficiency of multi-target drugs: The network approach might help drug design. *Trends in Pharmacological Sciences, 26*(4), 178-182.

Cueva Vargas, J. L., Belforte, N., & Di Polo, A. (2016). The glial cell modulator ibudilast attenuates neuroinflammation and enhances retinal ganglion cell viability in glaucoma through protein kinase A signaling. *Neurobiology of Disease, 93*, 156-171.

Cueva Vargas, J. L., & Di Polo, A. (2016). Neuroinflammation in glaucoma: Soluble tumor necrosis factor alpha and the connection with excitotoxic damage. *Neural Regeneration Research, 11*(3), 424-426.

Cueva Vargas, J. L., Osswald, I. K., Unsain, N., Aurousseau, M. R., Barker, P. A., Bowie, D., & Di Polo, A. (2015). Soluble tumor necrosis factor alpha promotes retinal ganglion cell death in glaucoma via calcium-permeable AMPA receptor activation. *The Journal of Neuroscience, 35*(35), 12088-12102.

Dalvin, L. A., & Fautsch, M. P. (2015). Analysis of circadian rhythm gene expression with reference to diurnal pattern of intraocular pressure in mice. *Investigative Ophthalmology & Visual Science, 56*(4), 2657-2663.

Daniels, B. (2011). *Modulation of ionotropic glutamate receptors in retinal neurons by the amino acid D-serine* (doctoral dissertation). Dalhousie University, Halifax, NS.

De Petrocellis, L., Nabissi, M., Santoni, G., & Ligresti, A. (2017). In Kendall D., Alexander S. P. H.(Eds.), *Actions and regulation of ionotropic cannabinoid receptors.* Academic Press.

Di Marzo, V. (2008). Targeting the endocannabinoid system: To enhance or reduce? *Nature Reviews.Drug Discovery, 7*(5), 438-455.

Di Marzo, V. (2011). Endocannabinoid signaling in the brain: Biosynthetic mechanisms in the limelight. *Nature Neuroscience, 14*(1), 9-15.

Di Marzo, V., & Petrosino, S. (2007). Endocannabinoids and the regulation of their levels in health and disease. *Current Opinion in Lipidology, 18*(2), 129-140.

Diamond, J. S. (2011). Calcium-permeable AMPA receptors in the retina. *Frontiers in Molecular Neuroscience, 4*, 27.

Diem, R., Meyer, R., Weishaupt, J. H., & Bahr, M. (2001). Reduction of potassium currents and phosphatidylinositol 3-kinase-dependent AKT phosphorylation by tumor necrosis factor-(alpha) rescues axotomized retinal ganglion cells from retrograde cell death in vivo. *The Journal of Neuroscience, 21*(6), 2058-2066.

Dong, L. D., Gao, F., Wang, X. H., Miao, Y., Wang, S. Y., Wu, Y., . . . Wang, Z. (2015). GluA2 trafficking is involved in apoptosis of retinal ganglion cells induced by activation of EphB/EphrinB reverse signaling in a rat chronic ocular hypertension model. *The Journal of Neuroscience, 35*(13), 5409-5421.

Dvoriantchikova, G., & Ivanov, D. (2014). Tumor necrosis factor-alpha mediates activation of NF-kappaB and JNK signaling cascades in retinal ganglion cells and astrocytes in opposite ways. *The European Journal of Neuroscience, 40*(8), 3171-3178.

El-Remessy, A. B., Khalil, I. E., Matragoon, S., Abou-Mohamed, G., Tsai, N. J., Roon, P., . . . Liou, G. I. (2003). Neuroprotective effect of (-)Delta9-tetrahydrocannabinol and cannabidiol in N-methyl-D-aspartate-induced retinal neurotoxicity: Involvement of peroxynitrite. *The American Journal of Pathology, 163*(5), 1997-2008.

Euler, T., Haverkamp, S., Schubert, T., & Baden, T. (2014). Retinal bipolar cells: Elementary building blocks of vision. *Nature Reviews.Neuroscience, 15*(8), 507-519.

Fan, B. J., Liu, K., Wang, D. Y., Tham, C. C., Tam, P. O., Lam, D. S., & Pang, C. P. (2010). Association of polymorphisms of tumor necrosis factor and tumor protein p53 with primary open-angle glaucoma. *Investigative Ophthalmology & Visual Science, 51*(8), 4110-4116.

Fautsch, M. P., & Johnson, D. H. (2006). Aqueous humor outflow: What do we know? where will it lead us? *Investigative Ophthalmology & Visual Science, 47*(10), 4181-4187.

Fay, J. F., & Farrens, D. L. (2012). A key agonist-induced conformational change in the cannabinoid receptor CB1 is blocked by the allosteric ligand org 27569. *The Journal of Biological Chemistry, 287*(40), 33873-33882.

Fay, J. F., & Farrens, D. L. (2015). Structural dynamics and energetics underlying allosteric inactivation of the cannabinoid receptor CB1. *Proceedings of the National Academy of Sciences of the United States of America, 112*(27), 8469-8474.

Fegley, D., Gaetani, S., Duranti, A., Tontini, A., Mor, M., Tarzia, G., & Piomelli, D. (2005). Characterization of the fatty acid amide hydrolase inhibitor cyclohexyl carbamic acid 3'-carbamoyl-biphenyl-3-yl ester (URB597): Effects on anandamide and oleoylethanolamide deactivation. *The Journal of Pharmacology and Experimental Therapeutics, 313*(1), 352-358.

Ferguson, A. R., Christensen, R. N., Gensel, J. C., Miller, B. A., Sun, F., Beattie, E. C., . . . Beattie, M. S. (2008). Cell death after spinal cord injury is exacerbated by rapid TNF alpha-induced trafficking of GluR2-lacking AMPARs to the plasma membrane. *The Journal of Neuroscience, 28*(44), 11391-11400.

Fernandes, K. A., Harder, J. M., Williams, P. A., Rausch, R. L., Kiernan, A. E., Nair, K. S., . . . Libby, R. T. (2015). Using genetic mouse models to gain insight into glaucoma: Past results and future possibilities. *Experimental Eye Research, 141*, 42-56.

Fernandez-Suarez, D., Celorrio, M., Riezu-Boj, J. I., Ugarte, A., Pacheco, R., Gonzalez, H., . . . Aymerich, M. S. (2014). The monoacylglycerol lipase inhibitor JZL184 is neuroprotective and alters glial cell phenotype in the chronic MPTP mouse model. *Neurobiology of Aging, 35*(11), 2603-2616.

Fischer, K. M., Ward, D. A., & Hendrix, D. V. (2013). Effects of a topically applied 2% delta-9-tetrahydrocannabinol ophthalmic solution on intraocular pressure and aqueous humor flow rate in clinically normal dogs. *American Journal of Veterinary Research, 74*(2), 275-280.

Fitzgerald, M., Bartlett, C. A., Harvey, A. R., & Dunlop, S. A. (2010). Early events of secondary degeneration after partial optic nerve transection: An immunohistochemical study. *Journal of Neurotrauma, 27*(2), 439-452.

Fontaine, V., Mohand-Said, S., Hanoteau, N., Fuchs, C., Pfizenmaier, K., & Eisel, U. (2002). Neurodegenerative and neuroprotective effects of tumor necrosis factor (TNF) in retinal ischemia: Opposite roles of TNF receptor 1 and TNF receptor 2. *The Journal of Neuroscience, 22*(7), RC216.

Fowler, C. J., Doherty, P., & Alexander, S. P. H. (2017). In Kendall D., Alexander S. P. H.(Eds.), *Endocannabinoid turnover* Academic Press.

Furukawa, K., & Mattson, M. P. (1998). The transcription factor NF-kappaB mediates increases in calcium currents and decreases in NMDA- and AMPA/kainate-induced currents induced by tumor necrosis factor-alpha in hippocampal neurons. *Journal of Neurochemistry, 70*(5), 1876-1886.

Gagliano, C., Ortisi, E., Pulvirenti, L., Reibaldi, M., Scollo, D., Amato, R., . . . Longo, A. (2011). Ocular hypotensive effect of oral palmitoyl-ethanolamide: A clinical trial. *Investigative Ophthalmology & Visual Science, 52*(9), 6096-6100.

Galindo-Romero, C., Aviles-Trigueros, M., Jimenez-Lopez, M., Valiente-Soriano, F. J., Salinas-Navarro, M., Nadal-Nicolas, F., . . . Agudo-Barriuso, M. (2011). Axotomy-induced retinal ganglion cell death in adult mice: Quantitative and topographic time course analyses. *Experimental Eye Research, 92*(5), 377-387.

Galvao, J., Davis, B., Tilley, M., Normando, E., Duchen, M. R., & Cordeiro, M. F. (2014). Unexpected low-dose toxicity of the universal solvent DMSO. *FASEB Journal : Official Publication of the Federation of American Societies for Experimental Biology, 28*(3), 1317-1330.

Ganesh, B. S., & Chintala, S. K. (2011). Inhibition of reactive gliosis attenuates excitotoxicity-mediated death of retinal ganglion cells. *PloS One, 6*(3), e18305.

Gerace, E., Masi, A., Resta, F., Felici, R., Landucci, E., Mello, T., . . . Moroni, F. (2014). PARP-1 activation causes neuronal death in the hippocampal CA1 region by increasing the expression of ca(2+)-permeable AMPA receptors. *Neurobiology of Disease, 70*, 43-52.

Ghosh, S., Wise, L. E., Chen, Y., Gujjar, R., Mahadevan, A., Cravatt, B. F., & Lichtman, A. H. (2013). The monoacylglycerol lipase inhibitor JZL184 suppresses inflammatory pain in the mouse carrageenan model. *Life Sciences, 92*(8-9), 498-505.

Gittis, A. H., Leventhal, D. K., Fensterheim, B. A., Pettibone, J. R., Berke, J. D., & Kreitzer, A. C. (2011). Selective inhibition of striatal fast-spiking interneurons causes dyskinesias. *The Journal of Neuroscience, 31*(44), 15727-15731.

Green, K. (1979). Marihuana in ophthalmology-past, present and future. *Annals of Ophthalmology, 11*(2), 203-205.

Green, K., Bigger, J. F., Kim, K., & Bowman, K. (1977). Cannabinoid action on the eye as mediated through the central nervous system and local adrenergic activity. *Experimental Eye Research, 24*(2), 189-196.

Green, K., & Kim, K. (1976). Mediation of ocular tetrahydrocannabinol effects by adrenergic nervous system. *Experimental Eye Research, 23*(4), 443-448.

Green, K., & Kim, K. (1977). Acute dose response of intraocular pressure to topical and oral cannabinoids. *Proceedings of the Society for Experimental Biology and Medicine.Society for Experimental Biology and Medicine (New York, N.Y.), 154*(2), 228-231.

Green, K., & Pederson, J. E. (1973). Effect of 1 -tetrahydrocannabinol on aqueous dynamics and ciliary body permeability in the rabbit. *Experimental Eye Research, 15*(4), 499-507.

Green, K., Wynn, H., & Padgett, D. (1978). Effects of delta9-tetrahydrocannabinol on ocular blood flow and aqueous humor formation. *Experimental Eye Research, 26*(1), 65-69.

Green, K., Zalkow, L. H., Deutsch, H. M., Yablonski, M. E., Oliver, N., Symonds, C. M., & Elijah, R. D. (1981). Ocular and systemic responses to water soluble material derived from cannabis sativa (marihuana). *Current Eye Research, 1*(2), 65-75.

Gregory, M. S., Hackett, C. G., Abernathy, E. F., Lee, K. S., Saff, R. R., Hohlbaum, A. M., . . . Ksander, B. R. (2011). Opposing roles for membrane bound and soluble fas ligand in glaucoma-associated retinal ganglion cell death. *PloS One, 6*(3), e17659.

Haller, J., Matyas, F., Soproni, K., Varga, B., Barsy, B., Nemeth, B., . . . Hajos, N. (2007). Correlated species differences in the effects of cannabinoid ligands on anxiety and on GABAergic and glutamatergic synaptic transmission. *The European Journal of Neuroscience, 25*(8), 2445-2456.

Han, P., & Whelan, P. J. (2010). Tumor necrosis factor alpha enhances glutamatergic transmission onto spinal motoneurons. *Journal of Neurotrauma, 27*(1), 287-292.

Harada, C., Namekata, K., Guo, X., Yoshida, H., Mitamura, Y., Matsumoto, Y., . . . Harada, T. (2010). ASK1 deficiency attenuates neural cell death in GLAST-deficient mice, a model of normal tension glaucoma. *Cell Death and Differentiation, 17*(11), 1751-1759.

Harada, T., Harada, C., Nakamura, K., Quah, H. M., Okumura, A., Namekata, K., . . . Tanaka, K. (2007). The potential role of glutamate transporters in the pathogenesis of normal tension glaucoma. *The Journal of Clinical Investigation, 117*(7), 1763-1770.

Harasymowycz, P., Birt, C., Gooi, P., Heckler, L., Hutnik, C., Jinapriya, D., . . . Day, R. (2016). Medical management of glaucoma in the 21st century from a canadian perspective. *Journal of Ophthalmology, 2016*, 6509809.

Hartwick, A. T., Zhang, X., Chauhan, B. C., & Baldridge, W. H. (2005). Functional assessment of glutamate clearance mechanisms in a chronic rat glaucoma model using retinal ganglion cell calcium imaging. *Journal of Neurochemistry, 94*(3), 794-807.

He, F., & Song, Z. H. (2007). Molecular and cellular changes induced by the activation of CB2 cannabinoid receptors in trabecular meshwork cells. *Molecular Vision, 13*, 1348-1356.

Heijl, A., Leske, M. C., Bengtsson, B., Hyman, L., Bengtsson, B., Hussein, M., & Early Manifest Glaucoma Trial Group. (2002). Reduction of intraocular pressure and glaucoma progression: Results from the early manifest glaucoma trial. *Archives of Ophthalmology, 120*(10), 1268-1279.

Henley, J. M., & Wilkinson, K. A. (2016). Synaptic AMPA receptor composition in development, plasticity and disease. *Nature Reviews.Neuroscience, 17*(6), 337-350.

Hepler, R. S., & Frank, I. R. (1971). Marihuana smoking and intraocular pressure. *Journal of the American Medical Association, 217*(10), 1392.

Hermann, M. M., Papaconstantinou, D., Muether, P. S., Georgopoulos, G., & Diestelhorst, M. (2011a). Adherence with brimonidine in patients with glaucoma aware and not aware of electronic monitoring. *Acta Ophthalmologica, 89*(4), e300-e305.

Hermann, M. M., Bron, A. M., Creuzot-Garcher, C. P., & Diestelhorst, M. (2011b). Measurement of adherence to brimonidine therapy for glaucoma using electronic monitoring. *Journal of Glaucoma, 20*(8), 502-508.

Hill, M. N., & McEwen, B. S. (2010). Involvement of the endocannabinoid system in the neurobehavioural effects of stress and glucocorticoids. *Progress in Neuro-Psychopharmacology & Biological Psychiatry, 34*(5), 791-797.

Hosseini, A., Lattanzio, F. A., Williams, P. B., Tibbs, D., Samudre, S. S., & Allen, R. C. (2006). Chronic topical administration of WIN-55-212-2 maintains a reduction in IOP in a rat glaucoma model without adverse effects. *Experimental Eye Research, 82*(5), 753-759.

Howell, G. R., Soto, I., Libby, R. T., & John, S. W. (2013). Intrinsic axonal degeneration pathways are critical for glaucomatous damage. *Experimental Neurology, 246*, 54-61.

Howell, G. R., Soto, I., Zhu, X., Ryan, M., Macalinao, D. G., Sousa, G. L., . . . John, S. W. (2012). Radiation treatment inhibits monocyte entry into the optic nerve head and prevents neuronal damage in a mouse model of glaucoma. *The Journal of Clinical Investigation, 122*(4), 1246-1261.

Howlett, A. C., & Abood, M. E. (2017). In Kendall D., Alexander S. P. H.(Eds.), *CB1 and CB2 receptor pharmacology* Academic Press.

Hu, J. H., Park, J. M., Park, S., Xiao, B., Dehoff, M. H., Kim, S., . . . Worley, P. F. (2010). Homeostatic scaling requires group I mGluR activation mediated by Homer1a. *Neuron, 68*(6), 1128-1142.

Hu, S. S., Arnold, A., Hutchens, J. M., Radicke, J., Cravatt, B. F., Wager-Miller, J., . . . Straiker, A. (2010). Architecture of cannabinoid signaling in mouse retina. *The Journal of Comparative Neurology, 518*(18), 3848-3866.

Hudson, B. D., Beazley, M., Szczesniak, A. M., Straiker, A., & Kelly, M. E. (2011). Indirect sympatholytic actions at beta-adrenoceptors account for the ocular hypotensive actions of cannabinoid receptor agonists. *The Journal of Pharmacology and Experimental Therapeutics, 339*(3), 757-767.

Huggins, J. P., Smart, T. S., Langman, S., Taylor, L., & Young, T. (2012). An efficient randomised, placebo-controlled clinical trial with the irreversible fatty acid amide hydrolase-1 inhibitor PF-04457845, which modulates endocannabinoids but fails to induce effective analgesia in patients with pain due to osteoarthritis of the knee. *Pain, 153*(9), 1837-1846.

Hume, R. I., Dingledine, R., & Heinemann, S. F. (1991). Identification of a site in glutamate receptor subunits that controls calcium permeability. *Science (New York, N.Y.), 253*(5023), 1028-1031.

Ignatowska-Jankowska, B. M., Baillie, G. L., Kinsey, S., Crowe, M., Ghosh, S., Owens, R. A., . . . Ross, R. A. (2015). A cannabinoid CB1 receptor-positive allosteric modulator reduces neuropathic pain in the mouse with no psychoactive effects. *Neuropsychopharmacology, 40*(13), 2948-2959.

Iqbal, Z., Cejudo-Martin, P., de Brouwer, A., van der Zwaag, B., Ruiz-Lozano, P., Scimia, M. C., . . . van Bokhoven, H. (2010). Disruption of the podosome adaptor protein TKS4 (SH3PXD2B) causes the skeletal dysplasia, eye, and cardiac abnormalities of frank-ter haar syndrome. *The American Journal of Human Genetics, 86*(2), 254-261.

Irving, A., Abdulrazzaq, G., Chan, S. L. F., Penman, J., Harvey, J., & Alexander, S. P. H. (2017). In Kendall D., Alexander S. P. H.(Eds.), *Cannabinoid receptor-related orphan G protein-coupled receptors* Academic Press.

Ishimaru, Y., Sumino, A., Kajioka, D., Shibagaki, F., Yamamuro, A., Yoshioka, Y., & Maeda, S. (2017). Apelin protects against NMDA-induced retinal neuronal death via an APJ receptor by activating akt and ERK1/2, and suppressing TNF-alpha expression in mice. *Journal of Pharmacological Sciences, 133*(1), 34-41.

Jackman, S. L., Babai, N., Chambers, J. J., Thoreson, W. B., & Kramer, R. H. (2011). A positive feedback synapse from retinal horizontal cells to cone photoreceptors. *PLoS Biology, 9*(5), e1001057.

Janero, D. R., & Thakur, G. A. (2016). Leveraging allostery to improve G protein-coupled receptor (GPCR)-directed therapeutics: Cannabinoid receptor 1 as discovery target. *Expert Opinion on Drug Discovery, 11*(12), 1223-1237.

Jo, A. O., Noel, J. M., Lakk, M., Yarishkin, O., Ryskamp, D. A., Shibasaki, K., . . . Krizaj, D. (2017). Mouse retinal ganglion cell signalling is dynamically modulated through parallel anterograde activation of cannabinoid and vanilloid pathways. *The Journal of Physiology, 595*(20), 6499-6516.

John, S. W., Smith, R. S., Savinova, O. V., Hawes, N. L., Chang, B., Turnbull, D., . . . Heckenlively, J. R. (1998). Essential iris atrophy, pigment dispersion, and glaucoma in DBA/2J mice. *Investigative Ophthalmology & Visual Science, 39*(6), 951-962.

Johnson, M. (2006). 'What controls aqueous humour outflow resistance?'. *Experimental Eye Research, 82*(4), 545-557.

Johnson, T. V., & Tomarev, S. I. (2010). Rodent models of glaucoma. *Brain Research Bulletin, 81*(2-3), 349-358.

Jones, R. S., Carroll, R. C., & Nawy, S. (2012). Light-induced plasticity of synaptic AMPA receptor composition in retinal ganglion cells. *Neuron, 75*(3), 467-478.

Kapetanakis, V. V., Chan, M. P., Foster, P. J., Cook, D. G., Owen, C. G., & Rudnicka, A. R. (2016). Global variations and time trends in the prevalence of primary open angle glaucoma (POAG): A systematic review and meta-analysis. *The British Journal of Ophthalmology, 100*(1), 86-93.

Karanian, D. A., Karim, S. L., Wood, J. T., Williams, J. S., Lin, S., Makriyannis, A., & Bahr, B. A. (2007). Endocannabinoid enhancement protects against kainic acid-induced seizures and associated brain damage. *The Journal of Pharmacology and Experimental Therapeutics, 322*(3), 1059-1066.

Kass, M. A., Heuer, D. K., Higginbotham, E. J., Johnson, C. A., Keltner, J. L., Miller, J. P., . . . Gordon, M. O. (2002). The ocular hypertension treatment study: A randomized trial determines that topical ocular hypotensive medication delays or prevents the onset of primary open-angle glaucoma. *Archives of Ophthalmology (Chicago, Ill.: 1960), 120*(6), 701-13; discussion 829-30.

Katz, P. S., Sulzer, J. K., Impastato, R. A., Teng, S. X., Rogers, E. K., & Molina, P. E. (2015). Endocannabinoid degradation inhibition improves neurobehavioral function, blood-brain barrier integrity, and neuroinflammation following mild traumatic brain injury. *Journal of Neurotrauma, 32*(5), 297-306.

Kenakin, T. (2016). Theoretical aspects of GPCR–ligand complex pharmacology. *Chemical Reviews,*

Kendall, D. A., & Yudowski, G. A. (2017). Cannabinoid receptors in the central nervous system: Their signaling and roles in disease. *Frontiers in Cellular Neuroscience, 10*, 294.

Keov, P., Sexton, P. M., & Christopoulos, A. (2011). Allosteric modulation of G protein-coupled receptors: A pharmacological perspective. *Neuropharmacology, 60*(1), 24-35.

Kerbrat, A., Ferre, J. C., Fillatre, P., Ronziere, T., Vannier, S., Carsin-Nicol, B., . . . Edan, G. (2016). Acute neurologic disorder from an inhibitor of fatty acid amide hydrolase. *The New England Journal of Medicine, 375*(18), 1717-1725.

Khatib, T. Z., & Martin, K. R. (2017). Protecting retinal ganglion cells. *Eye, 31*(2), 218-224.

Khurana, L., Fu, B. Q., Duddupudi, A. L., Liao, Y. H., Immadi, S. S., Kendall, D. A., & Lu, D. (2017). Pyrimidinyl biphenylureas: Identification of new lead compounds as allosteric modulators of the cannabinoid receptor CB1. *Journal of Medicinal Chemistry, 60*(3), 1089-1104.

Kim, J. H., Lee, N. Y., Jung, S. W., & Park, C. K. (2007). Expression of N-methyl-d-aspartate receptor 1 in rats with chronic ocular hypertension. *Neuroscience, 149*(4), 908-916.

Kim, M. H., & von Gersdorff, H. (2016). Postsynaptic plasticity triggered by Ca(2)(+)-permeable AMPA receptor activation in retinal amacrine cells. *Neuron, 89*(3), 507-520.

Kim, S. H., Won, S. J., Mao, X. O., Jin, K., & Greenberg, D. A. (2006). Molecular mechanisms of cannabinoid protection from neuronal excitotoxicity. *Molecular Pharmacology, 69*(3), 691-696.

King, A., Azuara-Blanco, A., & Tuulonen, A. (2013). Glaucoma. *BMJ (Clinical Research Ed.), 346*, f3518.

Kinsey, S. G., Wise, L. E., Ramesh, D., Abdullah, R., Selley, D. E., Cravatt, B. F., & Lichtman, A. H. (2013). Repeated low-dose administration of the monoacylglycerol lipase inhibitor JZL184 retains cannabinoid receptor type 1-mediated antinociceptive and gastroprotective effects. *The Journal of Pharmacology and Experimental Therapeutics, 345*(3), 492-501.

Kitaoka, Y., Kitaoka, Y., Kwong, J. M., Ross-Cisneros, F. N., Wang, J., Tsai, R. K., . . . Lam, T. T. (2006). TNF-alpha-induced optic nerve degeneration and nuclear factor-kappaB p65. *Investigative Ophthalmology & Visual Science, 47*(4), 1448-1457.

Koch, M., Kreutz, S., Bottger, C., Grabiec, U., Ghadban, C., Korf, H. W., & Dehghani, F. (2011). The cannabinoid WIN 55,212-2-mediated protection of dentate gyrus granule cells is driven by CB1 receptors and modulated by TRPA1 and cav 2.2 channels. *Hippocampus, 21*(5), 554-564.

Koeberle, A., & Werz, O. (2014). Multi-target approach for natural products in inflammation. *Drug Discovery Today, 19*(12), 1871-1882.

Kokona, D., & Thermos, K. (2015). Synthetic and endogenous cannabinoids protect retinal neurons from AMPA excitotoxicity in vivo, via activation of CB1 receptors: Involvement of PI3K/Akt and MEK/ERK signaling pathways. *Experimental Eye Research, 136*, 45-58.

Kolb, H. (2003). How the retina works. *American Scientist, 91*(1), 28-35.

Konstas, A. G., Mantziris, D. A., Cate, E. A., & Stewart, W. C. (1997). Effect of timolol on the diurnal intraocular pressure in exfoliation and primary open-angle glaucoma. *Archives of Ophthalmology, 115*(8), 975-979.

Konstas, A. G., Quaranta, L., Bozkurt, B., Katsanos, A., Garcia-Feijoo, J., Rossetti, L., . . . Miglior, S. (2016). 24-h efficacy of glaucoma treatment options. *Advances in Therapy, 33*(4), 481-517.

Kopach, O., Krotov, V., Goncharenko, J., & Voitenko, N. (2016). Inhibition of spinal ca(2+)-permeable AMPA receptors with dicationic compounds alleviates persistent inflammatory pain without adverse effects. *Frontiers in Cellular Neuroscience, 10*, 50.

Krishnan, G., & Chatterjee, N. (2012). Endocannabinoids alleviate proinflammatory conditions by modulating innate immune response in muller glia during inflammation. *Glia, 60*(11), 1629-1645.

Krishnan, G., & Chatterjee, N. (2015). Anandamide rescues retinal barrier properties in muller glia through nitric oxide regulation. *Neuroscience, 284*, 536-545.

Krizaj, D., Ryskamp, D. A., Tian, N., Tezel, G., Mitchell, C. H., Slepak, V. Z., & Shestopalov, V. I. (2014). From mechanosensitivity to inflammatory responses: New players in the pathology of glaucoma. *Current Eye Research, 39*(2), 105-119.

Kulkarni, P. M., Ranade, A., Garai, S., & Thakur, G. A. (2017). Microwave-accelerated conjugate addition of 2-arylindoles to substituted β-nitrostyrenes in the presence of ammonium trifluoroacetate: An efficient approach for the synthesis of a novel class of CB1 cannabinoid receptor allosteric modulators. *J. Heterocyclic Chem,*

Kumar, A., Qiao, Z., Kumar, P., & Song, Z. H. (2012). Effects of palmitoylethanolamide on aqueous humor outflow. *Investigative Ophthalmology & Visual Science, 53*(8), 4416-4425.

Kumar, A., & Song, Z. H. (2006). CB1 cannabinoid receptor-mediated changes of trabecular meshwork cellular properties. *Molecular Vision, 12*, 290-297.

Kwak, S., & Weiss, J. H. (2006). Calcium-permeable AMPA channels in neurodegenerative disease and ischemia. *Current Opinion in Neurobiology, 16*(3), 281-287.

Kwong, J. M., Quan, A., Kyung, H., Piri, N., & Caprioli, J. (2011). Quantitative analysis of retinal ganglion cell survival with rbpms immunolabeling in animal models of optic neuropathies. *Investigative Ophthalmology & Visual Science, 52*(13), 9694-9702.

Laine, K., Jarvinen, K., Pate, D. W., Urtti, A., & Jarvinen, T. (2002a). Effect of the enzyme inhibitor, phenylmethylsulfonyl fluoride, on the IOP profiles of topical anandamides. *Investigative Ophthalmology & Visual Science, 43*(2), 393-397.

Laine, K., Jarvinen, K., & Jarvinen, T. (2003). Topically administered CB(2)-receptor agonist, JWH-133, does not decrease intraocular pressure (IOP) in normotensive rabbits. *Life Sciences, 72*(7), 837-842.

Laine, K., Jarvinen, K., Mechoulam, R., Breuer, A., & Jarvinen, T. (2002b). Comparison of the enzymatic stability and intraocular pressure effects of 2-arachidonylglycerol and noladin ether, a novel putative endocannabinoid. *Investigative Ophthalmology & Visual Science, 43*(10), 3216-3222.

Lalonde, M. R., Jollimore, C. A., Stevens, K., Barnes, S., & Kelly, M. E. (2006). Cannabinoid receptor-mediated inhibition of calcium signaling in rat retinal ganglion cells. *Molecular Vision, 12*, 1160-1166.

Landers, J., Martin, K., Sarkies, N., Bourne, R., & Watson, P. (2012). A twenty-year follow-up study of trabeculectomy: Risk factors and outcomes. *Ophthalmology, 119*(4), 694-702.

Laprairie, R. B., Kulkarni, P. M., Deschamps, J. R., Kelly, M. E., Janero, D. R., Cascio, M. G., . . . Denovan-Wright, E. M. (2017). Enantio-specific allosteric modulation of cannabinoid 1 receptor. *ACS Chemical Neuroscience,*

Lebrun-Julien, F., Bertrand, M. J., De Backer, O., Stellwagen, D., Morales, C. R., Di Polo, A., & Barker, P. A. (2010). ProNGF induces TNFalpha-dependent death of retinal ganglion cells through a p75NTR non-cell-autonomous signaling pathway. *Proceedings of the National Academy of Sciences of the United States of America, 107*(8), 3817-3822.

Lebrun-Julien, F., Duplan, L., Pernet, V., Osswald, I., Sapieha, P., Bourgeois, P., . . . Di Polo, A. (2009). Excitotoxic death of retinal neurons in vivo occurs via a non-cell-autonomous mechanism. *The Journal of Neuroscience, 29*(17), 5536-5545.

Leinders-Zufall, T., Rand, M. N., Waxman, S. G., & Kocsis, J. D. (1994). Differential role of two ca(2+)-permeable non-NMDA glutamate channels in rat retinal ganglion cells: Kainate-induced cytoplasmic and nuclear Ca2+ signals. *Journal of Neurophysiology, 72*(5), 2503-2516.

Leonoudakis, D., Braithwaite, S. P., Beattie, M. S., & Beattie, E. C. (2004). TNFalpha-induced AMPA-receptor trafficking in CNS neurons; relevance to excitotoxicity? *Neuron Glia Biology, 1*(3), 263-273.

Leonoudakis, D., Zhao, P., & Beattie, E. C. (2008). Rapid tumor necrosis factor alpha-induced exocytosis of glutamate receptor 2-lacking AMPA receptors to extrasynaptic plasma membrane potentiates excitotoxicity. *The Journal of Neuroscience, 28*(9), 2119-2130.

Levin, L. A., Crowe, M. E., Quigley, H. A., & Lasker/IRRF Initiative on Astrocytes and Glaucomatous Neurodegeneration Participants. (2017). Neuroprotection for glaucoma: Requirements for clinical translation. *Experimental Eye Research, 157*, 34-37.

Levitt, M., Wilson, A., Bowman, D., Kemel, S., Krepart, G., Marks, V., . . . Weinerman, R. (1981). Physiologic observations in a controlled clinical trial of the antiemetic effectiveness of 5, 10, and 15 mg of delta 9-tetrahydrocannabinol in cancer chemotherapy. ophthalmologic implications. *Journal of Clinical Pharmacology, 21*(8-9 Suppl), 103S-109S.

Levkovitch-Verbin, H. (2015). Retinal ganglion cell apoptotic pathway in glaucoma: Initiating and downstream mechanisms. *Progress in Brain Research, 220*, 37-57.

Levkovitch-Verbin, H., Kalev-Landoy, M., Habot-Wilner, Z., & Melamed, S. (2006). Minocycline delays death of retinal ganglion cells in experimental glaucoma and after optic nerve transection. *Archives of Ophthalmology (Chicago, Ill.: 1960), 124*(4), 520-526.

Levkovitch-Verbin, H., Quigley, H. A., Kerrigan-Baumrind, L. A., D'Anna, S. A., Kerrigan, D., & Pease, M. E. (2001). Optic nerve transection in monkeys may result in secondary degeneration of retinal ganglion cells. *Investigative Ophthalmology & Visual Science, 42*(5), 975-982.

Li, Y., Schlamp, C. L., Poulsen, K. P., & Nickells, R. W. (2000). Bax-dependent and independent pathways of retinal ganglion cell death induced by different damaging stimuli. *Experimental Eye Research, 71*(2), 209-213.

Libby, R. T., Anderson, M. G., Pang, I. H., Robinson, Z. H., Savinova, O. V., Cosma, I. M., . . . John, S. W. (2005a). Inherited glaucoma in DBA/2J mice: Pertinent disease features for studying the neurodegeneration. *Visual Neuroscience, 22*(5), 637-648.

Libby, R. T., Li, Y., Savinova, O. V., Barter, J., Smith, R. S., Nickells, R. W., & John, S. W. (2005b). Susceptibility to neurodegeneration in a glaucoma is modified by bax gene dosage. *PLoS Genetics, 1*(1), 17-26.

Ligresti, A., De Petrocellis, L., & Di Marzo, V. (2016). From phytocannabinoids to cannabinoid receptors and endocannabinoids: Pleiotropic physiological and pathological roles through complex pharmacology. *Physiological Reviews, 96*(4), 1593-1659.

Liu, J. H., & Dacus, A. C. (1987). Central nervous system and peripheral mechanisms in ocular hypotensive effect of cannabinoids. *Archives of Ophthalmology (Chicago, Ill.: 1960), 105*(2), 245-248.

Liu, Y., Wang, L., Long, Z. Y., Wu, Y. M., Wan, Q., Jiang, J. X., & Wang, Z. G. (2013). Inhibiting PTEN protects hippocampal neurons against stretch injury by decreasing membrane translocation of AMPA receptor GluR2 subunit. *PloS One, 8*(6), e65431.

Liu, Z., Chen, X., Gao, Y., Sun, S., Yang, L., Yang, Q., . . . Wang, Q. (2015). Involvement of GluR2 up-regulation in neuroprotection by electroacupuncture pretreatment via cannabinoid CB1 receptor in mice. *Scientific Reports, 5*, 9490.

Livne-Bar, I., Lam, S., Chan, D., Guo, X., Askar, I., Nahirnyj, A., . . . Sivak, J. M. (2016). Pharmacologic inhibition of reactive gliosis blocks TNF-alpha-mediated neuronal apoptosis. *Cell Death & Disease, 7*(9), e2386.

Lograno, M. D., & Romano, M. R. (2004). Cannabinoid agonists induce contractile responses through Gi/o-dependent activation of phospholipase C in the bovine ciliary muscle. *European Journal of Pharmacology, 494*(1), 55-62.

Lopez, E. M., Tagliaferro, P., Onaivi, E. S., & Lopez-Costa, J. J. (2011). Distribution of CB2 cannabinoid receptor in adult rat retina. *Synapse (New York, N.Y.), 65*(5), 388-392.

Lu, H. C., & Mackie, K. (2016). An introduction to the endogenous cannabinoid system. *Biological Psychiatry, 79*(7), 516-525.

Lu, Q., Straiker, A., Lu, Q., & Maguire, G. (2000). Expression of CB2 cannabinoid receptor mRNA in adult rat retina. *Visual Neuroscience, 17*(1), 91-95.

Mac Nair, C. E., Fernandes, K. A., Schlamp, C. L., Libby, R. T., & Nickells, R. W. (2014). Tumor necrosis factor alpha has an early protective effect on retinal ganglion cells after optic nerve crush. *Journal of Neuroinflammation, 11*, 194-014-0194-3.

Mac Nair, C. E., & Nickells, R. W. (2015). Neuroinflammation in glaucoma and optic nerve damage. *Progress in Molecular Biology and Translational Science, 134*, 343-363.

Mac Nair, C. E., Schlamp, C. L., Montgomery, A. D., Shestopalov, V. I., & Nickells, R. W. (2016). Retinal glial responses to optic nerve crush are attenuated in bax-deficient mice and modulated by purinergic signaling pathways. *Journal of Neuroinflammation, 13*(1), 93-016-0558-y.

Maccarrone, M., Bab, I., Biro, T., Cabral, G. A., Dey, S. K., Di Marzo, V., . . . Zimmer, A. (2015). Endocannabinoid signaling at the periphery: 50 years after THC. *Trends in Pharmacological Sciences, 36*(5), 277-296.

MacIntyre, J., Dong, A., Straiker, A., Zhu, J., Howlett, S. E., Bagher, A., . . . Kelly, M. E. (2014). Cannabinoid and lipid-mediated vasorelaxation in retinal microvasculature. *European Journal of Pharmacology, 735*, 105-114.

Maes, M. E., Schlamp, C. L., & Nickells, R. W. (2017). BAX to basics: How the BCL2 gene family controls the death of retinal ganglion cells. *Progress in Retinal and Eye Research, 57*, 1-25.

Mahajan, S. S., & Ziff, E. B. (2007). Novel toxicity of the unedited GluR2 AMPA receptor subunit dependent on surface trafficking and increased Ca2+-permeability. *Molecular and Cellular Neurosciences, 35*(3), 470-481.

Mao, M., Hedberg-Buenz, A., Koehn, D., John, S. W., & Anderson, M. G. (2011). Anterior segment dysgenesis and early-onset glaucoma in nee mice with mutation of Sh3pxd2b. *Investigative Ophthalmology & Visual Science, 52*(5), 2679-2688.

Mao, M., Thedens, D. R., Chang, B., Harris, B. S., Zheng, Q. Y., Johnson, K. R., . . . Anderson, M. G. (2009). The podosomal-adaptor protein SH3PXD2B is essential for normal postnatal development. *Mammalian Genome, 20*(8), 462-475.

Masland, R. H. (2012). The neuronal organization of the retina. *Neuron, 76*(2), 266-280.

Matsuda, S., Kanemitsu, N., Nakamura, A., Mimura, Y., Ueda, N., Kurahashi, Y., & Yamamoto, S. (1997). Metabolism of anandamide, an endogenous cannabinoid receptor ligand, in porcine ocular tissues. *Experimental Eye Research, 64*(5), 707-711.

McIntosh, B. T., Hudson, B., Yegorova, S., Jollimore, C. A., & Kelly, M. E. (2007). Agonist-dependent cannabinoid receptor signalling in human trabecular meshwork cells. *British Journal of Pharmacology, 152*(7), 1111-1120.

McKinnon, S. J., Schlamp, C. L., & Nickells, R. W. (2009). Mouse models of retinal ganglion cell death and glaucoma. *Experimental Eye Research, 88*(4), 816-824.

McLaren, J. W. (2010). Control of aqueous humor flow. In Editor-in-Chief: Darlene A. Dartt (Ed.), *Encyclopedia of the eye* (pp. 389-397). Oxford: Academic Press. doi:10.1016/B978-0-12-374203-2.00089-0

Medeiros, F. A., Gracitelli, C. P., Boer, E. R., Weinreb, R. N., Zangwill, L. M., & Rosen, P. N. (2015). Longitudinal changes in quality of life and rates of progressive visual field loss in glaucoma patients. *Ophthalmology, 122*(2), 293-301.

Medina-Franco, J. L., Giulianotti, M. A., Welmaker, G. S., & Houghten, R. A. (2013). Shifting from the single to the multitarget paradigm in drug discovery. *Drug Discovery Today, 18*(9-10), 495-501.

Merritt, J. C., Perry, D. D., Russell, D. N., & Jones, B. F. (1981). Topical delta 9-tetrahydrocannabinol and aqueous dynamics in glaucoma. *Journal of Clinical Pharmacology, 21*(8-9 Suppl), 467S-471S.

Michels, S., Becker, M., Wachtlin, J., & Binder, S. (2012). The intravitreal injection: Variations in regulations, cost and reimbursement in europe. *Spektrum Der Augenheilkunde, 26*(1), 2-6.

Middleton, T. P., & Protti, D. A. (2011). Cannabinoids modulate spontaneous synaptic activity in retinal ganglion cells. *Visual Neuroscience, 28*(5), 393-402.

Mikawa, Y., Matsuda, S., Kanagawa, T., Tajika, T., Ueda, N., & Mimura, Y. (1997). Ocular activity of topically administered anandamide in the rabbit. *Japanese Journal of Ophthalmology, 41*(4), 217-220.

Miller, S., Leishman, E., Hu, S. S., Elghouche, A., Daily, L., Murataeva, N., . . . Straiker, A. (2016a). Harnessing the endocannabinoid 2-arachidonoylglycerol to lower intraocular pressure in a murine model. *Investigative Ophthalmology & Visual Science, 57*(7), 3287-3296.

Miller, S., Leishman, E., Oehler, O., Daily, L., Murataeva, N., Wager-Miller, J., . . . Straiker, A. (2016b). Evidence for a GPR18 role in diurnal regulation of intraocular pressure. *Investigative Ophthalmology & Visual Science, 57*(14), 6419-6426.

Morales, P., Goya, P., Jagerovic, N., & Hernandez-Folgado, L. (2016). Allosteric modulators of the CB1 cannabinoid receptor: A structural update review. *Cannabis and Cannabinoid Research, 1*(1), 22-30.

Morgan, J. E., & Tribble, J. R. (2015). Microbead models in glaucoma. *Experimental Eye Research, 141*, 9-14.

Morrison, J. C., Cepurna Ying Guo, W. O., & Johnson, E. C. (2011). Pathophysiology of human glaucomatous optic nerve damage: Insights from rodent models of glaucoma. *Experimental Eye Research, 93*(2), 156-164.

Mulvihill, M. M., & Nomura, D. K. (2013). Therapeutic potential of monoacylglycerol lipase inhibitors. *Life Sciences, 92*(8-9), 492-497.

Murataeva, N., Dhopeshwarkar, A., Yin, D., Mitjavila, J., Bradshaw, H., Straiker, A., & Mackie, K. (2016). Where's my entourage? the curious case of 2-oleoylglycerol, 2-linolenoylglycerol, and 2-palmitoylglycerol. *Pharmacological Research, 110*, 173-180.

Murdaca, G., Spano, F., Contatore, M., Guastalla, A., Penza, E., Magnani, O., & Puppo, F. (2015). Infection risk associated with anti-TNF-alpha agents: A review. *Expert Opinion on Drug Safety, 14*(4), 571-582.

Nakazawa, T., Nakazawa, C., Matsubara, A., Noda, K., Hisatomi, T., She, H., . . . Benowitz, L. I. (2006). Tumor necrosis factor-alpha mediates oligodendrocyte death and delayed retinal ganglion cell loss in a mouse model of glaucoma. *The Journal of Neuroscience, 26*(49), 12633-12641.

Nguyen, T., Li, J. X., Thomas, B. F., Wiley, J. L., Kenakin, T. P., & Zhang, Y. (2016). Allosteric modulation: An alternate approach targeting the cannabinoid CB1 receptor. *Medicinal Research Reviews,*

Nguyen, T. D., & Ethier, C. R. (2015). Biomechanical assessment in models of glaucomatous optic neuropathy. *Experimental Eye Research, 141*, 125-138.

Nickells, R. W., Howell, G. R., Soto, I., & John, S. W. (2012). Under pressure: Cellular and molecular responses during glaucoma, a common neurodegeneration with axonopathy. *Annual Review of Neuroscience, 35*, 153-179.

Njie, Y. F., He, F., Qiao, Z., & Song, Z. H. (2008a). Aqueous humor outflow effects of 2-arachidonylglycerol. *Experimental Eye Research, 87*(2), 106-114.

Njie, Y. F., Kumar, A., Qiao, Z., Zhong, L., & Song, Z. H. (2006). Noladin ether acts on trabecular meshwork cannabinoid (CB1) receptors to enhance aqueous humor outflow facility. *Investigative Ophthalmology & Visual Science, 47*(5), 1999-2005.

Njie, Y. F., Qiao, Z., Xiao, Z., Wang, W., & Song, Z. H. (2008b). N-arachidonylethanolamide-induced increase in aqueous humor outflow facility. *Investigative Ophthalmology & Visual Science, 49*(10), 4528-4534.

Nogueras-Ortiz, C., & Yudowski, G. A. (2016). The multiple waves of cannabinoid 1 receptor signaling. *Molecular Pharmacology, 90*(5), 620-626.

Noh, K. M., Yokota, H., Mashiko, T., Castillo, P. E., Zukin, R. S., & Bennett, M. V. (2005). Blockade of calcium-permeable AMPA receptors protects hippocampal neurons against global ischemia-induced death. *Proceedings of the National Academy of Sciences of the United States of America, 102*(34), 12230-12235.

Nomura, D. K., Morrison, B. E., Blankman, J. L., Long, J. Z., Kinsey, S. G., Marcondes, M. C., . . . Cravatt, B. F. (2011). Endocannabinoid hydrolysis generates brain prostaglandins that promote neuroinflammation. *Science (New York, N.Y.), 334*(6057), 809-813.

Nucci, C., Gasperi, V., Tartaglione, R., Cerulli, A., Terrinoni, A., Bari, M., . . . Maccarrone, M. (2007). Involvement of the endocannabinoid system in retinal damage after high intraocular pressure-induced ischemia in rats. *Investigative Ophthalmology & Visual Science, 48*(7), 2997-3004.

Nucci, C., Russo, R., Martucci, A., Giannini, C., Garaci, F., Floris, R., . . . Morrone, L. A. (2016). New strategies for neuroprotection in glaucoma, a disease that affects the central nervous system. *European Journal of Pharmacology, 787*, 119-126.

Nuschke, A. C., Farrell, S. R., Levesque, J. M., & Chauhan, B. C. (2015). Assessment of retinal ganglion cell damage in glaucomatous optic neuropathy: Axon transport, injury and soma loss. *Experimental Eye Research, 141*, 111-124.

Ogoshi, F., Yin, H. Z., Kuppumbatti, Y., Song, B., Amindari, S., & Weiss, J. H. (2005). Tumor necrosis-factor-alpha (TNF-alpha) induces rapid insertion of Ca2+-permeable alpha-amino-3-hydroxyl-5-methyl-4-isoxazole-propionate (AMPA)/kainate (ca-A/K) channels in a subset of hippocampal pyramidal neurons. *Experimental Neurology, 193*(2), 384-393.

Oliveira da Cruz, J. F., Robin, L. M., Drago, F., Marsicano, G., & Metna-Laurent, M. (2016). Astroglial type-1 cannabinoid receptor (CB1): A new player in the tripartite synapse. *Neuroscience, 323*, 35-42.

Oltmanns, M. H., Samudre, S. S., Castillo, I. G., Hosseini, A., Lichtman, A. H., Allen, R. C., . . . Williams, P. B. (2008). Topical WIN55212-2 alleviates intraocular hypertension in rats through a CB1 receptor mediated mechanism of action. *Journal of Ocular Pharmacology and Therapeutics, 24*(1), 104-115.

Opere, C. A., Zheng, W. D., Zhao, M., Lee, J. S., Kulkarni, K. H., & Ohia, S. E. (2006). Inhibition of potassium- and ischemia-evoked [3H] D-aspartate release from isolated bovine retina by cannabinoids. *Current Eye Research, 31*(7-8), 645-653.

Osborne, N. N. (2009). Recent clinical findings with memantine should not mean that the idea of neuroprotection in glaucoma is abandoned. *Acta Ophthalmologica, 87*(4), 450-454.

Osswald, I. K., Galan, A., & Bowie, D. (2007). Light triggers expression of philanthotoxin-insensitive Ca2+-permeable AMPA receptors in the developing rat retina. *The Journal of Physiology, 582*(Pt 1), 95-111.

Pacher, P., & Kunos, G. (2013). Modulating the endocannabinoid system in human health and disease--successes and failures. *The FEBS Journal, 280*(9), 1918-1943.

Park, Y. H., Broyles, H. V., He, S., McGrady, N. R., Li, L., & Yorio, T. (2016). Involvement of AMPA receptor and its flip and flop isoforms in retinal ganglion cell death following Oxygen/Glucose deprivation. *Investigative Ophthalmology & Visual Science, 57*(2), 508-526.

Park, Y. H., Mueller, B. H.,2nd, McGrady, N. R., Ma, H. Y., & Yorio, T. (2015). AMPA receptor desensitization is the determinant of AMPA receptor mediated excitotoxicity in purified retinal ganglion cells. *Experimental Eye Research, 132*, 136-150.

Parrish, R. K.,2nd, Gedde, S. J., Scott, I. U., Feuer, W. J., Schiffman, J. C., Mangione, C. M., & Montenegro-Piniella, A. (1997). Visual function and quality of life among patients with glaucoma. *Archives of Ophthalmology (Chicago, Ill.: 1960), 115*(11), 1447-1455.

Pate, D. W., Jarvinen, K., Urtti, A., Jarho, P., Fich, M., Mahadevan, V., & Jarvinen, T. (1996). Effects of topical anandamides on intraocular pressure in normotensive rabbits. *Life Sciences, 58*(21), 1849-1860.

Pate, D. W., Jarvinen, K., Urtti, A., Mahadevan, V., & Jarvinen, T. (1998). Effect of the CB1 receptor antagonist, SR141716A, on cannabinoid-induced ocular hypotension in normotensive rabbits. *Life Sciences, 63*(24), 2181-2188.

Pertwee, R. G. (2009). Emerging strategies for exploiting cannabinoid receptor agonists as medicines. *British Journal of Pharmacology, 156*(3), 397-411.

Pertwee, R. G. (2012). Targeting the endocannabinoid system with cannabinoid receptor agonists: Pharmacological strategies and therapeutic possibilities. *Philosophical Transactions of the Royal Society of London.Series B, Biological Sciences, 367*(1607), 3353-3363.

Pertwee, R. G. (2015). Endocannabinoids and their pharmacological actions. *Handbook of Experimental Pharmacology, 231*, 1-37.

Pescosolido, N., Librando, A., Puzzono, M., & Nebbioso, M. (2011). Palmitoylethanolamide effects on intraocular pressure after nd:YAG laser iridotomy: An experimental clinical study. *Journal of Ocular Pharmacology and Therapeutics, 27*(6), 629-635.

Pinar-Sueiro, S., Zorrilla Hurtado, J. A., Veiga-Crespo, P., Sharma, S. C., & Vecino, E. (2013). Neuroprotective effects of topical CB1 agonist WIN 55212-2 on retinal ganglion cells after acute rise in intraocular pressure induced ischemia in rat. *Experimental Eye Research, 110*, 55-58.

Pinazo-Duran, M. D., Zanon-Moreno, V., Gallego-Pinazo, R., & Garcia-Medina, J. J. (2015). Oxidative stress and mitochondrial failure in the pathogenesis of glaucoma neurodegeneration. *Progress in Brain Research, 220*, 127-153.

Piomelli, D., Tarzia, G., Duranti, A., Tontini, A., Mor, M., Compton, T. R., . . . Putman, D. (2006). Pharmacological profile of the selective FAAH inhibitor KDS-4103 (URB597). *CNS Drug Reviews, 12*(1), 21-38.

Piscitelli, F., & Bradshaw, H. B. (2017). Endocannabinoid analytical methodologies: Techniques that drive discoveries that drive techniques. *Advances in Pharmacology (San Diego, Calif.), 80*, 1-30.

Pistis, M., & O'Sullivan, S. E. (2017). In Kendall D., Alexander S. P. H.(Eds.), *The role of nuclear hormone receptors in cannabinoid function* Academic Press.

Plange, N., Arend, K. O., Kaup, M., Doehmen, B., Adams, H., Hendricks, S., . . . Remky, A. (2007). Dronabinol and retinal hemodynamics in humans. *American Journal of Ophthalmology, 143*(1), 173-174.

Porcella, A., Casellas, P., Gessa, G. L., & Pani, L. (1998). Cannabinoid receptor CB1 mRNA is highly expressed in the rat ciliary body: Implications for the antiglaucoma properties of marihuana. *Brain Research.Molecular Brain Research, 58*(1-2), 240-245.

Porcella, A., Maxia, C., Gessa, G. L., & Pani, L. (2000). The human eye expresses high levels of CB1 cannabinoid receptor mRNA and protein. *The European Journal of Neuroscience, 12*(3), 1123-1127.

Porcella, A., Maxia, C., Gessa, G. L., & Pani, L. (2001). The synthetic cannabinoid WIN55212-2 decreases the intraocular pressure in human glaucoma resistant to conventional therapies. *The European Journal of Neuroscience, 13*(2), 409-412.

Pourcho, R. G., Qin, P., Goebel, D. J., & Fyk-Kolodziej, B. (2002). Agonist-stimulated cobalt uptake provides selective visualization of neurons expressing AMPA- or kainate-type glutamate receptors in the retina. *The Journal of Comparative Neurology, 454*(3), 341-349.

Pribiag, H., & Stellwagen, D. (2014). Neuroimmune regulation of homeostatic synaptic plasticity. *Neuropharmacology, 78*, 13-22.

Price, M. R., Baillie, G. L., Thomas, A., Stevenson, L. A., Easson, M., Goodwin, R., . . . Ross, R. A. (2005). Allosteric modulation of the cannabinoid CB1 receptor. *Molecular Pharmacology, 68*(5), 1484-1495.

Priestley, R., Glass, M., & Kendall, D. (2017). In Kendall D., Alexander S. P. H.(Eds.), *Functional selectivity at cannabinoid receptors* Academic Press.

Probert, L. (2015). TNF and its receptors in the CNS: The essential, the desirable and the deleterious effects. *Neuroscience, 302*, 2-22.

Prusky, G. T., West, P. W., & Douglas, R. M. (2000). Behavioral assessment of visual acuity in mice and rats. *Vision Research, 40*(16), 2201-2209.

Pruss, R. M., Akeson, R. L., Racke, M. M., & Wilburn, J. L. (1991). Agonist-activated cobalt uptake identifies divalent cation-permeable kainate receptors on neurons and glial cells. *Neuron, 7*(3), 509-518.

Qian, W. J., Yin, N., Gao, F., Miao, Y., Li, Q., Li, F., . . . Wang, Z. (2017). Cannabinoid CB1 and CB2 receptors differentially modulate L- and T-type Ca2+ channels in rat retinal ganglion cells. *Neuropharmacology, 124*, 143-156.

Qu, J., Wang, D., & Grosskreutz, C. L. (2010). Mechanisms of retinal ganglion cell injury and defense in glaucoma. *Experimental Eye Research, 91*(1), 48-53.

Quigley, H. A. (2012). Clinical trials for glaucoma neuroprotection are not impossible. *Current Opinion in Ophthalmology, 23*(2), 144-154.

Quigley, H. A., Nickells, R. W., Kerrigan, L. A., Pease, M. E., Thibault, D. J., & Zack, D. J. (1995). Retinal ganglion cell death in experimental glaucoma and after axotomy occurs by apoptosis. *Investigative Ophthalmology & Visual Science, 36*(5), 774-786.

Reardon, G., Kotak, S., & Schwartz, G. F. (2011). Objective assessment of compliance and persistence among patients treated for glaucoma and ocular hypertension: A systematic review. *Patient Prefer Adherence, 5*, 441-463.

Riordan-Eva, P. (2011). Chapter 1. anatomy & embryology of the eye. In P. Riordan-Eva, & E. T. Cunningham (Eds.), *Vaughan & asbury's general ophthalmology, 18e*. New York, NY: The McGraw-Hill Companies.

Roh, M., Zhang, Y., Murakami, Y., Thanos, A., Lee, S. C., Vavvas, D. G., . . . Miller, J. W. (2012). Etanercept, a widely used inhibitor of tumor necrosis factor-alpha (TNF-alpha), prevents retinal ganglion cell loss in a rat model of glaucoma. *PloS One, 7*(7), e40065.

Romano, M. R., & Lograno, M. D. (2012). Involvement of the peroxisome proliferator-activated receptor (PPAR) alpha in vascular response of endocannabinoids in the bovine ophthalmic artery. *European Journal of Pharmacology, 683*(1-3), 197-203.

Ross, R. A. (2007). Allosterism and cannabinoid CB(1) receptors: The shape of things to come. *Trends in Pharmacological Sciences, 28*(11), 567-572.

Sacca, S. C., Rolando, M., Marletta, A., Macri, A., Cerqueti, P., & Ciurlo, G. (1998). Fluctuations of intraocular pressure during the day in open-angle glaucoma, normal-tension glaucoma and normal subjects. *Ophthalmologica.Journal International d'Ophtalmologie.International Journal of Ophthalmology.Zeitschrift Fur Augenheilkunde, 212*(2), 115-119.

Salt, T. E., & Cordeiro, M. F. (2006). Glutamate excitotoxicity in glaucoma: Throwing the baby out with the bathwater? *Eye, 20*(6), 730-1; author reply 731-2.

Samudre, S. S., Schneider, J. L., Oltmanns, M. H., Hosseini, A., Pratap, K., Loose-Thurman, P., . . . Sheppard, J. D.,Jr. (2008). Comparison of topical and intravenous administration of WIN 55-212-2 in normotensive rabbits. *Current Eye Research, 33*(10), 857-863.

Sanes, J. R., & Zipursky, S. L. (2010). Design principles of insect and vertebrate visual systems. *Neuron, 66*(1), 15-36.

Santos, N. C., Figueira-Coelho, J., Martins-Silva, J., & Saldanha, C. (2003). Multidisciplinary utilization of dimethyl sulfoxide: Pharmacological, cellular, and molecular aspects. *Biochemical Pharmacology, 65*(7), 1035-1041.

Sappington, R. M., Carlson, B. J., Crish, S. D., & Calkins, D. J. (2010). The microbead occlusion model: A paradigm for induced ocular hypertension in rats and mice. *Investigative Ophthalmology & Visual Science, 51*(1), 207-216.

Sappington, R. M., Sidorova, T., Long, D. J., & Calkins, D. J. (2009). TRPV1: Contribution to retinal ganglion cell apoptosis and increased intracellular Ca2+ with exposure to hydrostatic pressure. *Investigative Ophthalmology & Visual Science, 50*(2), 717-728.

Scheyer, A. F., Loweth, J. A., Christian, D. T., Uejima, J., Rabei, R., Le, T., . . . Wolf, M. E. (2016). AMPA receptor plasticity in accumbens core contributes to incubation of methamphetamine craving. *Biological Psychiatry, 80*(9), 661-670.

Schlamp, C. L., Li, Y., Dietz, J. A., Janssen, K. T., & Nickells, R. W. (2006). Progressive ganglion cell loss and optic nerve degeneration in DBA/2J mice is variable and asymmetric. *BMC Neuroscience, 7*, 66.

Schlesinger, F., Tammena, D., Krampfl, K., & Bufler, J. (2005). Two mechanisms of action of the adamantane derivative IEM-1460 at human AMPA-type glutamate receptors. *British Journal of Pharmacology, 145*(5), 656-663.

Schlosburg, J. E., Blankman, J. L., Long, J. Z., Nomura, D. K., Pan, B., Kinsey, S. G., . . . Cravatt, B. F. (2010). Chronic monoacylglycerol lipase blockade causes functional antagonism of the endocannabinoid system. *Nature Neuroscience, 13*(9), 1113-1119.

Schlosburg, J. E., Kinsey, S. G., Ignatowska-Jankowska, B., Ramesh, D., Abdullah, R. A., Tao, Q., . . . Lichtman, A. H. (2014). Prolonged monoacylglycerol lipase blockade causes equivalent cannabinoid receptor type 1 receptor-mediated adaptations in fatty acid amide hydrolase wild-type and knockout mice. *The Journal of Pharmacology and Experimental Therapeutics, 350*(2), 196-204.

Schmidl, D., Schmetterer, L., Garhofer, G., & Popa-Cherecheanu, A. (2015). Pharmacotherapy of glaucoma. *Journal of Ocular Pharmacology and Therapeutics, 31*(2), 63-77.

Schwitzer, T., Schwan, R., Angioi-Duprez, K., Giersch, A., & Laprevote, V. (2016). The endocannabinoid system in the retina: From physiology to practical and therapeutic applications. *Neural Plasticity, 2016*, 2916732.

Sena, D. F., & Lindsley, K. (2017). Neuroprotection for treatment of glaucoma in adults. *The Cochrane Database of Systematic Reviews, 1*, CD006539.

Shea, A. M., Curtis, L. H., Hammill, B. G., Kowalski, J. W., Ravelo, A., Lee, P. P., . . . Schulman, K. A. (2008). Resource use and costs associated with diabetic macular edema in elderly persons. *Archives of Ophthalmology (Chicago, Ill.: 1960), 126*(12), 1748-1754.

Shih, G. C., & Calkins, D. J. (2012). Secondary neuroprotective effects of hypotensive drugs and potential mechanisms of action. *Expert Review of Ophthalmology, 7*(2), 161-175.

Shore, D. M., Baillie, G. L., Hurst, D. H., Navas, F.,3rd, Seltzman, H. H., Marcu, J. P., . . . Reggio, P. H. (2014). Allosteric modulation of a cannabinoid G protein-coupled receptor: Binding site elucidation and relationship to G protein signaling. *The Journal of Biological Chemistry, 289*(9), 5828-5845.

Sivakumar, V., Foulds, W. S., Luu, C. D., Ling, E. A., & Kaur, C. (2013). Hypoxia-induced retinal ganglion cell damage through activation of AMPA receptors and the neuroprotective effects of DNQX. *Experimental Eye Research, 109*, 83-97.

Sivaprasad, S., & Oyetunde, S. (2016). Impact of injection therapy on retinal patients with diabetic macular edema or retinal vein occlusion. *Clinical Ophthalmology (Auckland, N.Z.), 10*, 939-946.

Skaper, S. D., & Di Marzo, V. (2012). Endocannabinoids in nervous system health and disease: The big picture in a nutshell. *Philosophical Transactions of the Royal Society of London.Series B, Biological Sciences, 367*(1607), 3193-3200.

Slivicki, R. A., Xu, Z., Kulkarni, P. M., Pertwee, R. G., Mackie, K., Thakur, G. A., & Hohmann, A. G. (2017). Positive allosteric modulation of cannabinoid receptor type 1 suppresses pathological pain without producing tolerance or dependence. *Biological Psychiatry,*

Slusar, J. E., Cairns, E. A., Szczesniak, A. M., Bradshaw, H. B., Di Polo, A., & Kelly, M. E. (2013). The fatty acid amide hydrolase inhibitor, URB597, promotes retinal ganglion cell neuroprotection in a rat model of optic nerve axotomy. *Neuropharmacology, 72C*, 116-125.

Smedowski, A., Pietrucha-Dutczak, M., Kaarniranta, K., & Lewin-Kowalik, J. (2014). A rat experimental model of glaucoma incorporating rapid-onset elevation of intraocular pressure. *Scientific Reports, 4*, 5910.

Son, J. L., Soto, I., Oglesby, E., Lopez-Roca, T., Pease, M. E., Quigley, H. A., & Marsh-Armstrong, N. (2010). Glaucomatous optic nerve injury involves early astrocyte reactivity and late oligodendrocyte loss. *Glia, 58*(7), 780-789.

Song, Z. H., & Slowey, C. A. (2000). Involvement of cannabinoid receptors in the intraocular pressure-lowering effects of WIN55212-2. *The Journal of Pharmacology and Experimental Therapeutics, 292*(1), 136-139.

Soto, D., Coombs, I. D., Gratacos-Batlle, E., Farrant, M., & Cull-Candy, S. G. (2014). Molecular mechanisms contributing to TARP regulation of channel conductance and polyamine block of calcium-permeable AMPA receptors. *The Journal of Neuroscience, 34*(35), 11673-11683.

Stamer, W. D., Golightly, S. F., Hosohata, Y., Ryan, E. P., Porter, A. C., Varga, E., . . . Yamamura, H. I. (2001). Cannabinoid CB1 receptor expression, activation and detection of endogenous ligand in trabecular meshwork and ciliary process tissues. *European Journal of Pharmacology, 431*(3), 277-286.

Steinmetz, C. C., & Turrigiano, G. G. (2010). Tumor necrosis factor-alpha signaling maintains the ability of cortical synapses to express synaptic scaling. *The Journal of Neuroscience, 30*(44), 14685-14690.

Stellwagen, D., Beattie, E. C., Seo, J. Y., & Malenka, R. C. (2005). Differential regulation of AMPA receptor and GABA receptor trafficking by tumor necrosis factor-alpha. *The Journal of Neuroscience, 25*(12), 3219-3228.

Stellwagen, D., & Malenka, R. C. (2006). Synaptic scaling mediated by glial TNF-alpha. *Nature, 440*(7087), 1054-1059.

Straiker, A., Maguire, G., Mackie, K., & Lindsey, J. (1999). Localization of cannabinoid CB1 receptors in the human anterior eye and retina. *Investigative Ophthalmology & Visual Science, 40*(10), 2442-2448.

Straiker, A., Mitjavila, J., Yin, D., Gibson, A., & Mackie, K. (2015). Aiming for allosterism: Evaluation of allosteric modulators of CB1 in a neuronal model. *Pharmacological Research, 99*, 370-376.

Straiker, A., Stella, N., Piomelli, D., Mackie, K., Karten, H. J., & Maguire, G. (1999). Cannabinoid CB1 receptors and ligands in vertebrate retina: Localization and function of an endogenous signaling system. *Proceedings of the National Academy of Sciences of the United States of America, 96*(25), 14565-14570.

Stumpff, F., Boxberger, M., Krauss, A., Rosenthal, R., Meissner, S., Choritz, L., . . . Thieme, H. (2005). Stimulation of cannabinoid (CB1) and prostanoid (EP2) receptors opens BKCa channels and relaxes ocular trabecular meshwork. *Experimental Eye Research, 80*(5), 697-708.

Sun, X., Dai, Y., Chen, Y., Yu, D. Y., Cringle, S. J., Chen, J., . . . Jiang, C. (2017). Primary angle closure glaucoma: What we know and what we don't know. *Progress in Retinal and Eye Research, 57*, 26-45.

Szczesniak, A. M., Kelly, M. E., Whynot, S., Shek, P. N., & Hung, O. (2006). Ocular hypotensive effects of an intratracheally delivered liposomal delta9-tetrahydrocannabinol preparation in rats. *Journal of Ocular Pharmacology and Therapeutics, 22*(3), 160-167.

Szczesniak, A. M., Maor, Y., Robertson, H., Hung, O., & Kelly, M. E. (2011). Nonpsychotropic cannabinoids, abnormal cannabidiol and canabigerol-dimethyl heptyl, act at novel cannabinoid receptors to reduce intraocular pressure. *Journal of Ocular Pharmacology and Therapeutics, 27*(5), 427-435.

Tamm, E. R., Braunger, B. M., & Fuchshofer, R. (2015). Intraocular pressure and the mechanisms involved in resistance of the aqueous humor flow in the trabecular meshwork outflow pathways. *Progress in Molecular Biology and Translational Science, 134*, 301-314.

Tamm, E. R., Schmetterer, L., & Grehn, F. (2013). Status and perspectives of neuroprotective therapies in glaucoma: The european glaucoma society white paper. *Cell and Tissue Research, 353*(2), 347-354.

Tchantchou, F., & Zhang, Y. (2013). Selective inhibition of alpha/beta-hydrolase domain 6 attenuates neurodegeneration, alleviates blood brain barrier breakdown, and improves functional recovery in a mouse model of traumatic brain injury. *Journal of Neurotrauma, 30*(7), 565-579.

Tezel, G. (2008). TNF-alpha signaling in glaucomatous neurodegeneration. *Progress in Brain Research, 173*, 409-421.

Tezel, G., & Wax, M. B. (2000). Increased production of tumor necrosis factor-alpha by glial cells exposed to simulated ischemia or elevated hydrostatic pressure induces apoptosis in cocultured retinal ganglion cells. *The Journal of Neuroscience, 20*(23), 8693-8700.

Tezel, G., & Yang, X. (2004). Caspase-independent component of retinal ganglion cell death, in vitro. *Investigative Ophthalmology & Visual Science, 45*(11), 4049-4059.

Tham, Y. C., Li, X., Wong, T. Y., Quigley, H. A., Aung, T., & Cheng, C. Y. (2014). Global prevalence of glaucoma and projections of glaucoma burden through 2040: A systematic review and meta-analysis. *Ophthalmology, 121*(11), 2081-2090.

Thomas, C. N., Berry, M., Logan, A., Blanch, R. J., & Ahmed, Z. (2017). Caspases in retinal ganglion cell death and axon regeneration. *Cell Death Discovery, 3*, 17032.

Thoreson, W. B., & Witkovsky, P. (1999). Glutamate receptors and circuits in the vertebrate retina. *Progress in Retinal and Eye Research, 18*(6), 765-810.

Toris, C. B. (2008). *Aqueous humor dynamics I: Measurement methods and animal studies* Academic Press.

Vecino, E., Rodriguez, F. D., Ruzafa, N., Pereiro, X., & Sharma, S. C. (2016). Glia-neuron interactions in the mammalian retina. *Progress in Retinal and Eye Research, 51*, 1-40.

Vesce, S., Rossi, D., Brambilla, L., & Volterra, A. (2007). Glutamate release from astrocytes in physiological conditions and in neurodegenerative disorders characterized by neuroinflammation. *International Review of Neurobiology, 82*, 57-71.

Vohra, R., Tsai, J. C., & Kolko, M. (2013). The role of inflammation in the pathogenesis of glaucoma. *Survey of Ophthalmology, 58*(4), 311-320.

Volkow, N. D., Hampson, A. J., & Baler, R. D. (2017). Don't worry, be happy: Endocannabinoids and cannabis at the intersection of stress and reward. *Annual Review of Pharmacology and Toxicology, 57*, 285-308.

Vu, H. T. V., Keeffe, J. E., McCarty, C. A., & Taylor, H. R. (2005). Impact of unilateral and bilateral vision loss on quality of life. *British Journal of Ophthalmology, 89*(3), 360-363.

Wang, A. L., Carroll, R. C., & Nawy, S. (2014). Down-regulation of the RNA editing enzyme ADAR2 contributes to RGC death in a mouse model of glaucoma. *PloS One, 9*(3), e91288.

Wang, R., Seifert, P., & Jakobs, T. C. (2017). Astrocytes in the optic nerve head of glaucomatous mice display a characteristic reactive phenotype. *Investigative Ophthalmology & Visual Science, 58*(2), 924-932.

Wang, X. H., Wu, Y., Yang, X. F., Miao, Y., Zhang, C. Q., Dong, L. D., . . . Wang, Z. (2016). Cannabinoid CB1 receptor signaling dichotomously modulates inhibitory and excitatory synaptic transmission in rat inner retina. *Brain Structure & Function, 221*(1), 301-316.

Weber, A. J. (2013). Autocrine and paracrine interactions and neuroprotection in glaucoma. *Cell and Tissue Research, 353*(2), 219-230.

Weinreb, R. N., Aung, T., & Medeiros, F. A. (2014). The pathophysiology and treatment of glaucoma: A review. *Journal of the American Medical Association, 311*(18), 1901-1911.

Weinreb, R. N., Leung, C. K., Crowston, J. G., Medeiros, F. A., Friedman, D. S., Wiggs, J. L., & Martin, K. R. (2016). Primary open-angle glaucoma. *Nature Reviews.Disease Primers, 2*, 16067.

Weiss, J. H. (2011). Ca permeable AMPA channels in diseases of the nervous system. *Frontiers in Molecular Neuroscience, 4*, 42.

Werner, C. T., Murray, C. H., Reimers, J. M., Chauhan, N. M., Woo, K. K., Molla, H. M., . . . Wolf, M. E. (2017). Trafficking of calcium-permeable and calcium-impermeable AMPA receptors in nucleus accumbens medium spiny neurons co-cultured with prefrontal cortex neurons. *Neuropharmacology, 116*, 224-232.

Wigerblad, G., Huie, J. R., Yin, H. Z., Leinders, M., Pritchard, R. A., Koehrn, F. J., . . . Sorkin, L. S. (2017). Inflammation-induced GluA1 trafficking and membrane insertion of Ca2+ permeable AMPA receptors in dorsal horn neurons is dependent on spinal tumor necrosis factor, PI3 kinase and protein kinase A. *Experimental Neurology, 293*, 144-158.

Wolf, M. E., & Tseng, K. Y. (2012). Calcium-permeable AMPA receptors in the VTA and nucleus accumbens after cocaine exposure: When, how, and why? *Frontiers in Molecular Neuroscience, 5*, 72.

Wong, A. A., & Brown, R. E. (2006). Visual detection, pattern discrimination and visual acuity in 14 strains of mice. *Genes, Brain, and Behavior, 5*(5), 389-403.

Wong, A. A., & Brown, R. E. (2007). Age-related changes in visual acuity, learning and memory in C57BL/6J and DBA/2J mice. *Neurobiology of Aging, 28*(10), 1577-1593.

Wootten, D., Christopoulos, A., & Sexton, P. M. (2013). Emerging paradigms in GPCR allostery: Implications for drug discovery. *Nature Reviews.Drug Discovery, 12*(8), 630-644.

Wright, A., & Vissel, B. (2012). The essential role of AMPA receptor GluR2 subunit RNA editing in the normal and diseased brain. *Frontiers in Molecular Neuroscience, 5*, 34.

Xia, Y., Carroll, R. C., & Nawy, S. (2006). State-dependent AMPA receptor trafficking in the mammalian retina. *The Journal of Neuroscience, 26*(19), 5028-5036.

Xia, Y., Nawy, S., & Carroll, R. C. (2007). Activity-dependent synaptic plasticity in retinal ganglion cells. *The Journal of Neuroscience, 27*(45), 12221-12229.

Xin, X., Gao, L., Wu, T., & Sun, F. (2013). Roles of tumor necrosis factor alpha gene polymorphisms, tumor necrosis factor alpha level in aqueous humor, and the risks of open angle glaucoma: A meta-analysis. *Molecular Vision, 19*, 526-535.

Xu, J. Y., & Chen, C. (2014). Endocannabinoids in synaptic plasticity and neuroprotection. *The Neuroscientist, 21*(2), 152.168.

Yang, X., Luo, C., Cai, J., Powell, D. W., Yu, D., Kuehn, M. H., & Tezel, G. (2011). Neurodegenerative and inflammatory pathway components linked to TNF-alpha/TNFR1 signaling in the glaucomatous human retina. *Investigative Ophthalmology & Visual Science, 52*(11), 8442-8454.

Yasumura, R., Meguro, A., Ota, M., Nomura, E., Uemoto, R., Kashiwagi, K., . . . Mizuki, N. (2011). Investigation of the association between SLC1A3 gene polymorphisms and normal tension glaucoma. *Molecular Vision, 17*, 792-796.

Yazulla, S. (2008). Endocannabinoids in the retina: From marijuana to neuroprotection. *Progress in Retinal and Eye Research, 27*(5), 501-526.

Yazulla, S., & Studholme, K. M. (2004). Vanilloid receptor like 1 (VRL1) immunoreactivity in mammalian retina: Colocalization with somatostatin and purinergic P2X1 receptors. *The Journal of Comparative Neurology, 474*(3), 407-418.

Yazulla, S., Studholme, K. M., McIntosh, H. H., & Deutsch, D. G. (1999). Immunocytochemical localization of cannabinoid CB1 receptor and fatty acid amide hydrolase in rat retina. *The Journal of Comparative Neurology, 415*(1), 80-90.

Yin, H., Yin, H., Zhang, W., Miao, Q., Qin, Z., Guo, S., . . . Fang, X. (2016). Transcorneal electrical stimulation promotes survival of retinal ganglion cells after optic nerve transection in rats accompanied by reduced microglial activation and TNF-alpha expression. *Brain Research, 1650*, 10-20.

Yin, H. Z., Hsu, C. I., Yu, S., Rao, S. D., Sorkin, L. S., & Weiss, J. H. (2012). TNF-alpha triggers rapid membrane insertion of Ca(2+) permeable AMPA receptors into adult motor neurons and enhances their susceptibility to slow excitotoxic injury. *Experimental Neurology, 238*(2), 93-102.

Yucel, Y., & Gupta, N. (2015). Lymphatic drainage from the eye: A new target for therapy. *Progress in Brain Research, 220*, 185-198.

Zabouri, N., Bouchard, J. F., & Casanova, C. (2011). Cannabinoid receptor type 1 expression during postnatal development of the rat retina. *The Journal of Comparative Neurology, 519*(7), 1258-1280.

Zhang, J., & Chen, C. (2008). Endocannabinoid 2-arachidonoylglycerol protects neurons by limiting COX-2 elevation. *The Journal of Biological Chemistry, 283*(33), 22601-22611.

Zhao, P., Leonoudakis, D., Abood, M. E., & Beattie, E. C. (2010). Cannabinoid receptor activation reduces TNFalpha-induced surface localization of AMPAR-type glutamate receptors and excitotoxicity. *Neuropharmacology, 58*(2), 551-558.

Zhong, L., Geng, L., Njie, Y., Feng, W., & Song, Z. H. (2005). CB2 cannabinoid receptors in trabecular meshwork cells mediate JWH015-induced enhancement of aqueous humor outflow facility. *Investigative Ophthalmology & Visual Science, 46*(6), 1988-1992.

Zimmermann, G. R., Lehar, J., & Keith, C. T. (2007). Multi-target therapeutics: When the whole is greater than the sum of the parts. *Drug Discovery Today, 12*(1-2), 34-42.

APPENDIX: COPYRIGHT PERMISSIONS

Nature Publishing Group LICENSE TERMS AND CONDITIONS

Oct 30, 2017

This is a License Agreement between Ms. Elizabeth Cairns ("You") and Nature Publishing Group ("Nature Publishing Group") provided by Copyright Clearance Center ("CCC"). The license consists of your order details, the terms and conditions provided by Nature Publishing Group, and the payment terms and conditions.

All payments must be made in full to CCC. For payment instructions, please see information listed at the bottom of this form.

License Number	4218590472077
License date	Oct 30, 2017
Licensed content publisher	Nature Publishing Group
Licensed content title	Nature Reviews Neuroscience
Licensed content date	Jan 1, 2000
Type of Use	Thesis/Dissertation
Requestor type	Academic institution
Format	Print, Electronic
Portion	chart/graph/table/figure
Number of charts/graphs/tables/figures	1
The requesting person/organization is:	Elizabeth A. Cairns
Title or numeric reference of the portion(s)	Figure 1
Title of the article or chapter the portion is from	Retinal bipolar cells: elementary building blocks of vision
Editor of portion(s)	N/A
Author of portion(s)	Thomas Euler, Silke Haverkamp, Timm Schubert & Tom Baden
Volume of serial or monograph.	15
Page range of the portion	507-519
Publication date of portion	2014
Rights for	Main product

Duration of use	Life of current edition
Creation of copies for the disabled	no
With minor editing privileges	yes
For distribution to	Worldwide
In the following language(s)	Original language of publication
With incidental promotional use	no
The lifetime unit quantity of new product	Up to 499
Title	Strategies for Neuroprotection and IOP Modulation in Experimental Models of Glaucoma
Instructor name	Elizabeth A. Cairns
Institution name	Dalhousie University
Expected presentation date	Dec 2017
Total (may include CCC user fee)	0.00 USD

Walter de Gruyter and Company LICENSE TERMS AND CONDITIONS

Oct 30, 2017

This is a License Agreement between Ms. Elizabeth Cairns ("You") and Walter de Gruyter and Company ("Walter de Gruyter and Company") provided by Copyright Clearance Center ("CCC"). The license consists of your order details, the terms and conditions provided by Walter de Gruyter and Company, and the payment terms and conditions.

All payments must be made in full to CCC. For payment instructions, please see information listed at the bottom of this form.

License Number	4218590469256
License date	Oct 30, 2017
Licensed content publisher	Walter de Gruyter and Company
Licensed content title	Journal of Basic and Clinical Physiology and Pharmacology
Licensed content date	Dec 31, 1969
Type of Use	Thesis/Dissertation

Requestor type	Author of requested content
Format	Print, Electronic
Portion	chart/graph/table/figure
Number of charts/graphs/tables/figures	3
The requesting person/organization is:	Elizabeth A. Cairns
Title or numeric reference of the portion(s)	Tables 1-3
Title of the article or chapter the portion is from	Seeing over the horizon – targeting the endocannabinoid system for the treatment of ocular disease
Editor of portion(s)	N/A
Author of portion(s)	Elizabeth A. Cairns / J. Thomas Toguri / Richard F. Porter / Anna-Maria Szczesniak / Melanie E.M. Kelly
Volume of serial or monograph.	27
Issue, if republishing an article from a serial	3
Page range of the portion	253-266
Publication date of portion	2016
Rights for	Main product and any product related to main product
Duration of use	Life of current edition
Creation of copies for the disabled	no
With minor editing privileges	no
For distribution to	Worldwide
In the following language(s)	Original language of publication
With incidental promotional use	no
The lifetime unit quantity of new product	Up to 499
Title	Strategies for Neuroprotection and IOP Modulation in Experimental Models of Glaucoma
Instructor name	Elizabeth A. Cairns
Institution name	Dalhousie University
Expected presentation date	Dec 2017
Total (may include CCC user fee)	0.00 USD

Mary Ann Liebert Inc. LICENSE TERMS AND CONDITIONS

Oct 30, 2017

This is a License Agreement between Ms. Elizabeth Cairns ("You") and Mary Ann Liebert Inc. ("Mary Ann Liebert Inc.") provided by Copyright Clearance Center ("CCC"). The license consists of your order details, the terms and conditions provided by Mary Ann Liebert Inc., and the payment terms and conditions.

All payments must be made in full to CCC. For payment instructions, please see information listed at the bottom of this form.

License Number	4218590467211
License date	Oct 30, 2017
Licensed content publisher	Mary Ann Liebert Inc.
Licensed content title	Journal of ocular pharmacology and therapeutics
Licensed content date	Jan 1, 1995
Type of Use	Thesis/Dissertation
Requestor type	Author of requested content
Format	Print, Electronic
Portion	chart/graph/table/figure
Number of charts/graphs/tables/figures	6
The requesting person/organization is:	Elizabeth A. Cairns
Title or numeric reference of the portion(s)	Figures 1/6
Title of the article or chapter the portion is from	The In Vivo Effects of the CB1-Positive Allosteric Modulator GAT229 on Intraocular Pressure in Ocular Normotensive and Hypertensive Mice
Editor of portion(s)	N/A
Author of portion(s)	Elizabeth A. Cairns, Anna-Maria Szczesniak, Alex J. Straiker, Pushkar M. Kulkarni, Roger G. Pertwee, Ganesh A. Thakur, William H. Baldridge, and Melanie E.M. Kelly
Volume of serial or monograph.	33
Issue, if republishing an article from a serial	8
Page range of the portion	582-590
Publication date of portion	October 1, 2017

Rights for	Main product and any product related to main product
Duration of use	Life of current edition
Creation of copies for the disabled	no
With minor editing privileges	no
For distribution to	Worldwide
In the following language(s)	Original language of publication
With incidental promotional use	no
The lifetime unit quantity of new product	Up to 499
Title	Strategies for Neuroprotection and IOP Modulation in Experimental Models of Glaucoma
Instructor name	Elizabeth A. Cairns
Institution name	Dalhousie University
Expected presentation date	Dec 2017
Total (may include CCC user fee)	0.00 USD

Elsevier Science and Technology Journals LICENSE TERMS AND CONDITIONS

Nov 01, 2017

This is a License Agreement between Ms. Elizabeth Cairns ("You") and Elsevier Science and Technology Journals ("Elsevier Science and Technology Journals") provided by Copyright Clearance Center ("CCC"). The license consists of your order details, the terms and conditions provided by Elsevier Science and Technology Journals, and the payment terms and conditions.

All payments must be made in full to CCC. For payment instructions, please see information listed at the bottom of this form.

License Number	4220061091633
License date	Nov 01, 2017
Licensed content publisher	Elsevier Science and Technology Journals
Licensed content title	Neurobiology of aging
Licensed content date	Jan 1, 1980
Type of Use	Thesis/Dissertation
Requestor type	Academic institution

Format	Print, Electronic
Portion	chart/graph/table/figure
Number of charts/graphs/tables/figures	1
The requesting person/organization is:	Elizabeth A. Cairns
Title or numeric reference of the portion(s)	Figure 1 (A)
Title of the article or chapter the portion is from	Age-related changes in visual acuity, learning and memory in C57BL/6J and DBA/2J mice
Editor of portion(s)	N/A
Author of portion(s)	Aimee A. Wong, Richard E. Brown
Volume of serial or monograph.	28
Issue, if republishing an article from a serial	10
Page range of the portion	1577-1593
Publication date of portion	2007
Rights for	Main product
Duration of use	Life of current edition
Creation of copies for the disabled	no
With minor editing privileges	yes
For distribution to	Worldwide
In the following language(s)	Original language of publication
With incidental promotional use	no
The lifetime unit quantity of new product	Up to 499
Title	Strategies for Neuroprotection and IOP Modulation in Experimental Models of Glaucoma
Instructor name	Elizabeth A. Cairns
Institution name	Dalhousie University
Expected presentation date	Dec 2017
Total (may include CCC user fee)	0.00 USD

Elsevier Science and Technology Journals LICENSE TERMS AND CONDITIONS

Nov 01, 2017

This is a License Agreement between Ms. Elizabeth Cairns ("You") and Elsevier Science and Technology Journals ("Elsevier Science and Technology Journals") provided by Copyright Clearance Center ("CCC"). The license consists of your order details, the terms and conditions provided by Elsevier Science and Technology Journals, and the payment terms and conditions.

All payments must be made in full to CCC. For payment instructions, please see information listed at the bottom of this form.

License Number	4220061094010
License date	Nov 01, 2017
Licensed content publisher	Elsevier Science and Technology Journals
Licensed content title	Vision research
Licensed content date	Jan 1, 1961
Type of Use	Thesis/Dissertation
Requestor type	Academic institution
Format	Print, Electronic
Portion	chart/graph/table/figure
Number of charts/graphs/tables/figures	1
The requesting person/organization is:	Elizabeth A. Cairns
Title or numeric reference of the portion(s)	Figure 1B
Title of the article or chapter the portion is from	Behavioral assessment of visual acuity in mice and rats
Editor of portion(s)	N/A
Author of portion(s)	GT Prusky, PWR West, RM Douglas
Volume of serial or monograph.	40
Issue, if republishing an article from a serial	16
Page range of the portion	2201-2209
Publication date of portion	2000
Rights for	Main product
Duration of use	Life of current edition
Creation of copies for the disabled	no

With minor editing privileges	yes
For distribution to	Worldwide
In the following language(s)	Original language of publication
With incidental promotional use	no
The lifetime unit quantity of new product	Up to 499
Title	Strategies for Neuroprotection and IOP Modulation in Experimental Models of Glaucoma
Instructor name	Elizabeth A. Cairns
Institution name	Dalhousie University
Expected presentation date	Dec 2017
Total (may include CCC user fee)	0.00 USD

PERMISSION LICENSE: COMMERCIAL ELECTRONIC USE

Request ID/Invoice Number: ELI25721

Date: October 31, 2017

To: Elizabeth Cairns
Dalhousie University
15-B9 Sir Charles Tupper Building
5850 College St.
Halifax NS
Canada
"Licensee"

McGraw-Hill Education Material

Author: Riordan et al
Title: Vaughan & Ashbury's General Ophthalmology
ISBN: 9780071634205
Edition: 18
Copyright Year: 2011
Description of material: Figure 1-12 (1 Figure ONLY)

Fee: Waived

Licensee Work

Author: Carins, E.
Title: Strategies for Neuroprotection and IOP Modulation in Experimental Models of Glaucoma (Thesis)
Publisher: Dalhousie University
Print Run: 1
Format: Print/Electronic (Thesis)
Distribution/territory: Worldwide
Languages: English

McGraw-Hill Global Education Holdings, LLC (herein after known as "McGraw Hill Education") grants permission for the use described above under the following terms and conditions:

1. McGraw-Hill Education hereby grants Licensee the non-exclusive right to include the McGraw-Hill Education Material in the Licensee Work and to reproduce and distribute the McGraw-Hill Education Material as part of the Licensee Work. The McGraw-Hill Education Material may be used only in the Licensee Work. All use of the McGraw-Hill Education Material is subject to the terms and conditions of this Agreement.

2. No changes may be made to the McGraw-Hill Education Material without the prior written consent of McGraw-Hill Education.

3. Licensee will provide to McGraw-Hill Education the URL and password for the web site in which the McGraw-Hill Education Material appears (if applicable).

4. McGraw-Hill Education makes no representations or warranties as to the accuracy of any information contained in the McGraw-Hill Education Material, including any warranties of merchantability or fitness for a particular purpose. In no event shall McGraw-Hill Education have any liability to any party for special, incidental, tort, or consequential damages arising out of or in connection with the McGraw-Hill Education Material, even if McGraw-Hill Education has been advised of the possibility of such damages. All persons provided with the McGraw-Hill Education Material must be provided with written notice of this disclaimer and limitation liability, either in an end-user license and/or with an on-screen notice that is visible each time the end-user initiates access to the McGraw-Hill Education Material.

5. A credit to McGraw-Hill Education shall be visible each time the end-user initiates access to any screen or page containing any of the McGraw-Hill Education Material. Such credit shall include the title and author of the work and a copyright notice in the name of McGraw-Hill Education.

6. A SIGNED COPY OF THIS AGREEMENT should be sent to McGraw-Hill Global Education Holdings, LLC, Attn: Permissions Department, Wells Fargo Bank, Lockbox #6167, PO Box 8500, Philadelphia, Pa. 19178-6167.

7. This permission does not cover the use of any third-party copyrighted material, including but not limited to photographs and other illustrations, which appears in the McGraw-Hill Education Material with a credit to other sources. Written permission to use such material must be obtained from the cited source.

8. McGraw-Hill Education shall have the right to terminate this Agreement immediately upon written notice to Licensee if Licensee is in material breach of this Agreement.

9. Licensee shall indemnify McGraw-Hill Education from any damages, lawsuits, claims, liabilities, costs, charges, and expenses, including attorney's fees, relating to its use of the McGraw-Hill Education Material.

10. This Agreement incorporates the parties' entire agreement with respect to its subject matter. This Agreement may be amended only in writing and signed by both parties and shall be governed by the laws of New York. Licensee may not assign this Agreement or any rights granted hereunder to any third party.

Please sign and return one copy to the address above, as outlined in Clause 6 of this agreement.

For McGraw-Hill Education:

DocuSigned by:
C9E05569B1064E8...

Name Laura Connolly
Permissions Department

For Licensee:

DocuSigned by:
CF2490763CBC438...

Name

Title Graduate Student